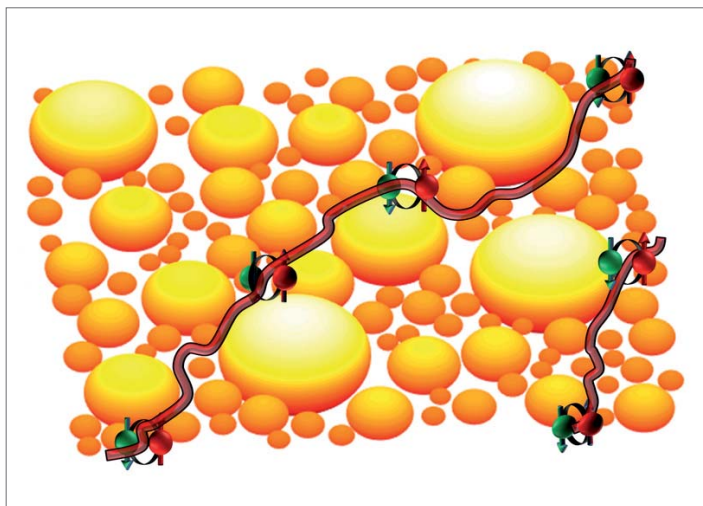

SUPERSTRIPES

2016



edited by
Antonio Bianconi

superstripes press



SUPERSTRIPES 2016

20th Anniversary of Stripes Conferences

Physics in Quantum Matter

Superconductivity, Magnetism & Ferroelectricity

edited by
Antonio Bianconi

superstripes press



science series

Science Series No.8

Title: Superstripes 2016

Published on June 2016
by Superstripes Press, Rome, Italy

<http://www.superstripes.net/science/science.htm>

© 2016 Superstripes Press
© 2016 Multiple authors

ISBN 978-88-6683-055-9
ISBN-A 10.978.886683/0559



This work is licensed under the Creative Commons Attribution-ShareAlike 4.0 International License. To view a copy of this license, visit <http://creativecommons.org/licenses/by-sa/4.0/> or send a letter to Creative Commons, PO Box 1866, Mountain View, CA 94042, USA.

Authors:

Adachi T., Aeppli G., Akashi R., Anahory Y., Andersen B. M., Annett J., Argyrou D. N., Arita R., Babaev E., Bachar N., Baeriswyl D., Balakirev F.F., Balicas L., Bao W., Barbiellini B., Barisic N., Baron A. Q. R., Baturina T., Bauch T., Berciu M., Bianconi A., Bill A., Billinge S.J.L., Bonca J., Borisenko S., Bothschafter E., Bourges P., Bovensiepen U., Bozin S., Brazovskii S., Brinkman A., Brzezicki W., Bussmann-Holder A., Capone M., Caprara S., Carbone F., Chavez I., Conradson S., Continentino M. A., Cren T., Ćwik J., De Llano M., de Mello E., De Padova P., Dean M., Degiorgi L., Dessau D., Devereaux T., Dobrosavljevic V., Doria M., Eckstein M., Efetov K., Efremov D., Egami T., Eremets M., Eremin I., Eremin M., Fatuzzo G., Felner I., Feng S., Fine B., Fink J., Freeman P.G., Freericks J., Fujimori A., Fujiwara N., Gajda D., Garcia-Garcia A. M., Gastiasoro M., Geck J., Giraldo-Gallo P., Glatz A., Goncharov A. F., Gray A., Greene L. H., Grinenko V., Haase J., Hackl R., Hardy F., Harrison N., He S., Hennel S., HonerCamp C., Huang Z., Iavarone M., Inoue I. H., Ishihara S., Iwasawa H., Jarlborg T., Johnson R. D., Joseph B., Kaindl A., Kanazawa I., Kanigel A., Kaptcia K. J., Kartsovnik M. V., Kataev V., Katrych S., Keller H., Keren A., Khalyavin D. D., Khomskii D. I., Kirova N., Kontani H., Korshunov M. M., Kristoffel N., Krüger F., Ksenofontov V., Kubozono Y., Kuzmicheva T., Lanzara A., Lawler M. J., LeBoeuf D., Lemberger T. R., Li W.H., Liarokapis E., Lichtenstein A., Linscheid A., Lorenzana J., Luetkens H., Machida K., Mackenzie, Madan I., Maggio-Aprile I., Maier T., Manske D., Manuel P., Markovic N., Marsiglio M., Massarotti D., Mazzoli C., Menushenkov A. P., Mertelj T., Micnas R., Mihailovic D., Miletto Granozio F., Mironov Y., Moewes A., Moreo A., Moroni M., Moskvina A.S., Mukhin S. I., Mustre de Leon J., Nakagawa K., Neilson D., Nishiyama S., Nissinen J., Oda M., Oles A.M., Ord T., Orgad D., Ovchinnikov S., Pan S. H., Pelc D., Pellicciari J., Perali A., Perfetti L., Perring T., Phillips P., Ponomarenko L. A., Popovic D., Prassides K., Pudalov V. M., Pupillo G., Purans J., Puzniak R., Qiu X.G., Quader K., Radzihovsky L., Renner Ch., Reznik D., Ricci A., Ronnow H. M., Salasnich L., Samuely P., Sanna S., Schneider W.D., Schopohl N., Seibold G, Shen Dawei, Shengelaya A., Shi Ming., Shimizu K., Simon P., Soh Y. A., Spivak B., Stojchevska L., Stornaiuolo D., Streltsov S., Strinati G., Sunko D., Sushkov P., Szabo P., Tabis W., Tagliacozzo A., Tajima S., Takahashi H., Tanner D. B., Teitelbaum G., Terashima, Tohyama T., Tokunaga Y., Tortello M., Tranquada J. M., Tsuchiya S., Turner P., Uemura Y., Vargunin A., Vinokurn V. M., Van der Marel D., Wang N. L., Watanabe T., Wirth S., Wu Shang-Yu, Wysokiński K., Yanagisawa T., Yukalov I., Zaikin A. D., Zheng G.Q., Zhigadlo N., Zhou Si., Zocco D

*These authors presented the scientific reports collected in this book at the Superstripes 2016 conference held in Ischia (It) on June 23-29, 2016

Papers presented at the international conference

Superstripes 2016

Ischia Italy June 23-29, 2016

Organized by

Non profit organization for scientific research Superstripes onlus

Rome International Center for Materials Science Superstripes - RICMASS

Chairman

Prof. Antonio Bianconi, RICMASS, Rome, I

Organizing Committee

Gabriel Aeppli, Paul Scherrer Institute, CH

Bernd Büchner, IFW Dresden, D

Takeshi Egami, University of Tennessee, USA

Alessandra Lanzara, University of California, USA

P.B. Littlewood, Argonne National Laboratory, UK

Andrea Perali, University of Camerino, I

Alessandro Ricci, Desy, D

Jan Zaanen, University of Leiden, NL

Superstripes 2016

Book of Abstracts

Table of Contents

A. P. Menushenkov: The europium valence state in EuCo_2As_2 at external and chemical pressure.....	13
L. Radzihovsky: Disorder-driven quantum phase transition and transport in Dirac semimetals and semiconductors	15
K. Prassides: Optimized Unconventional High- T_c Superconductivity in Fullerides. 16	
S. Conradson: Loss of the Mott Gap and Formation of a Superthermal Metal in the Coherent Polaronic Quantum Phase of O- and Photo-Doped $\text{UO}_{2(+x)}$	17
H. Keller: Isotope and pressure effects in cuprate high-temperature superconductors - recent results.....	19
A. Gray: Controlling electronic interactions and phase separation in VO_2 via strain, temperature and ultrafast electric fields	20
V. M. Vinokour: PT-symmetry mechanism of out-of-equilibrium phase transitions in superconducting and magnetic systems	21
S. Borisenko: Direct Observation of Spin-Orbit Coupling in Iron-Based Superconductors	23
A. Moreo: Multiorbital Hamiltonians for non-BCS superconductors.....	25
S. Ovchinnikov: Pressure effect on electronic structure, exchange interaction, and critical temperature of hole-doped cuprates	26
P. Phillips: Anomalous Dimensions and Unparticles in the Cuprate Superconductors	27
H. Kontani: Origins of the nematicity and superconductivity in FeSe and other Fe-based superconductors	28
G. Teitelbaum: Inhomogeneous state of the Mn doped topological insulator Bi_2Te_3	30
Y. Anahory: Superparamagnetism at oxide interfaces revealed by scanning SQUID-on-tip microscopy	31
E. Babaev: Metallic Superfluids and Superconducting Superfluids in	33
E. de Mello: Superconducting and pseudogap energy scales of cuprates intertwined by charge ordering	34
T. Perring: Spin excitations used to probe the nature of the magnetically ordered ground state of the CE-type phase of charge ordered manganites	36
S. Wirth: Structural and magnetic properties and phase transitions in the iron chalcogenides	38
D. Neilson: Novel Strongly-Correlated Ground States and Enhanced Multiband Electron-Hole Superfluidity in Graphene Structures	40
V. Ksenofontov: Role of local and itinerant magnetism in Fe-based superconductors	42

H. Luetkens: Magnetism in Fe-based Superconductors - The Various Ways to Coexist 44

J. Mustre de Leon: Resonant X-ray Inelastic Scattering and nanoscale inhomogeneity in $\text{FeSe}_{1-x}\text{Te}_x$ 46

S. Sanna: Why is Manganese a poison for superconductivity in $\text{LaFeAsO}_{0.89}\text{F}_{0.11}$? . 48

J. Pelliciari: Giant effect of isovalent doping on magnetism in $\text{BaFe}_2(\text{As}_{1-x}\text{P}_x)_2$.. 50

J. Geck:Orbital symmetry of charge density wave order and nematicity in $(\text{La},\text{M})_2\text{CuO}_4$ 52

H. M. Ronnow: Effective Hubbard Model of Spin Waves in Cuprates 54

T. Bauch: Macroscopic Quantum Tunneling in a Topological Josephson Junction . 55

D. van der Marel: Optical signatures of pair formation 57

D.LeBoeuf: Sound velocity study of charge order across the phase diagram of YBCO 58

M. Oda: STM/STSstudies for out-of-plane disorder effects on the charge orderand pseudogap in $\text{Bi}_2\text{Sr}_{1.7}\text{R}_{0.3}\text{CuO}_{6+\delta}$ (R = La and Eu) 59

E. Liarokapis:Local lattice distortions in $\text{NdFeAsO}_{1-x}\text{F}_x$ pnictide 60

A. Q. R. Baron:Extreme broadening of the bond-stretching phonon in $\text{YBaCuO}_{7-\delta}$ below T_c using a new x-ray spectrometer 62

M. Eremin: Temperature dependence of penetration depth in presence of momentum-dependent CDW and superconducting order parameters 64

K. Efetov:Charge and current modulations in a spin-fermion model withoverlapping hotspots 66

T. Tohyama:Enhanced charge excitations in electron-doped cuprates by resonant inelastic X-ray scattering..... 68

I. Kanazawa: Quantized Massive Gauge Fields and Hole-Induced Spin Glass Mechanism in Underdoped Cuprates 69

D. Mihailovic:Switching between hidden states of electronic matter under non-equilibrium conditions 70

U. Bovensiepen:Coupling of electronic excitations to boson modes in complex materials analyzed by femtosecond tr-ARPES..... 72

M. Eckstein: Nonthermal ultra-fast dynamics in excitonic condensates..... 74

J. Freericks: Pump/probe photoemission in charge-density-wave insulators 75

S. Ishihara:Ultrafast Optical Control of Correlated Electron System with Multi-degrees of Freedom..... 77

J. Lorenzana: Using Raman in real time to manipulation electronic states with light 79

A. M. Garcia-Garcia: Global critical temperature in disordered superconductors with weak multifractality	81
I. Madan: Ultrafast control of superconducting phase slips	83
T. Mertelj: All-optical femtosecond relaxation dynamics in iron based pnictides ...	85
L. Stojchevska: Ultrafast relaxation dynamics study in iron-based pnictides, cuprates and charge-density waves.....	87
L. Perfetti: High temperature superconductors far from equilibrium conditions.....	89
S. Tsuchiya: Quasiparticle dynamics in the organic superconductors investigated with polarized femtosecond spectroscopy.....	91
A. C. Komarek: Observation of multiferroicity in transition metal compounds with complex anionic lattice or complex magnetic structure.....	93
W.H. Li: Complex magnetic incommensurability and electronic charge transfer in type-II multiferroic Co_3TeO_6	94
J. Ćwik: High Field Dependence of the Magnetocaloric Effect in Laves Phase Compounds.....	96
N. Markovic: Designing Quantum Matter with Superconducting Nanowires	98
A. Zaikin: Shot Noise in Quantum Phase Slip Wires vibrations	100
P. Szabo: STM studies of the superconductor-insulator transition in MoC ultrathin films	101
N. A. S. Moskvina: Charge order-to-superfluid transition for 2D hard-core bosons and emergent domain structures.....	102
XG Qiu: Optical Study of the AFM state in electron doped CaNdFeAs	104
D. D. Khalyavin: Symmetry of C4 magnetic phase in hole-doped 122 iron based superconductors	105
P. Manuel: Antisymmetric exchange interactions tuning of the magnetic properties of La-substituted $\text{BiFe}_{0.5}\text{Sc}_{0.5}\text{O}_3$	106
R. D. Johnson: Modulated spin helicity stabilized by incommensurate orbital density waves in a quadruple perovskite manganite.....	108
T. Watanabe: Pseudogap phase diagram in cuprates studied by high field interlayer magnetotransport of overdoped Bi-2212.....	109
A. Fujimori: Competing orders/fluctuations in high-temperature superconductors revealed by ARPES	111
S. Tajima: Variety of Fermi surface nesting and the pairing mechanism beyond it in iron-based superconductors.....	113
D. B. Tanner: Infrared measurements of the superfluid and normal-fluid densities in the cuprate superconductors	115
G. Deutscher: MuSR detection of free spins in granular Al films near the Metal to Insulator transition.....	117

G. Strinati: Systematic investigation of the effects of disorder at the lowest order throughout the BCS-BEC crossover	118
Ch. Renner: Ubiquitous stripe charge order in low dimensional superconductors observed by scanning tunneling microscopy.....	119
D. Reznik:Finite wavevector nematic fluctuations in Fe-based Superconductors..	120
C. G. Fatuzzo:Synchrotron Spectroscopic Experiments on Ruthenates.....	122
F. F. Balakirev:High Magnetic Field Studies of Novel Superconductors	123
G. Seibold:Intrinsic Spin-Hall Effect in Systems with Striped Spin-Orbit Coupling	124
B. V. Fine: Fermi-surface in the presence of magnetic-vortex checkerboard	125
A. Brinkman:Topological superconductivity: from materials to topotronics	126
D. Zocco:Lattice dynamical properties of superconducting SrPt ₃ P studied via inelastic x-ray scattering and density functional perturbation theory	127
P. G. Freeman:Charge Ordered Structure of La _{2-x} Sr _x CoO ₄	129
N. L. Wang: Optical spectroscopy and pump-probe studies on charge density wave orders in LaAgSb ₂	130
A. Mackenzie:Delafossite metals: ultra high conductivity on two-dimensional triangular lattices	131
M. Shi:Camelback-shaped band reconciles heavy-electron behavior with weak electronic Coulomb correlations in superconducting TlNi ₂ Se ₂	132
H. Takahashi: Pressure-induced superconductivity in iron-based spin-ladder compound BaFe ₂ S ₃	133
Y. Kubozono: Superconductivity in two-dimensional layered materials through electron-doping by metal-intercalation and electrostatic technique.....	135
M. Capone: Why some iron-based compounds are more correlated than others?..	136
L. De Giorgi: Origin of the resistive anisotropy in the electronic nematic phase of BaFe ₂ As ₂ revealed by optical spectroscopy	138
C. Honer camp:Renormalization group study of nematic order in iron superconductors	140
S. Katrych: Single Crystals of Superconducting SmFeAsO _{1-x} H _x :Structure and Properties.....	141
B. M. Andersen:Quantitative description of disorder effects in iron-based superconductors: Correlated RKKY-exchange, impurity clusters and more	143
M. Gastiasoro: Nature, origin and detection of double-Q phases in Fe-pnictides ..	145
D. Efremov: Interplay of charge and spin degrees of freedom in pnictides and dichalcogenides	147
M.M. Korshunov:Cluster perturbation approach to iron-based superconductors...	148

Shang-Yu Wu: Holography without translational invariance.....	150
N. Kirova:Electronic ferroelectricity in carbon based materials.....	151
I. Yukalov: Nanoscale phase separation in ferroelectric materials	152
G. Gajda:The influence of 1 GPa isostatic pressure on J_c , B_{irr} , B_{c2} and T_c in MgB_2 wires and iron-based superconducting materials	153
J. Purans: Anharmonicity and Exafs Studies beyond the Quasiharmonic Approximation.....	155
S. Billinge:Magnetic pair distribution function (mPDF) analysis of short-range magnetism in strongly correlated materials.....	156
M. Dean: Orbital Polarization Driven by Anisotropic Hybridization in a NickelateHeterostructure determined by Resonant Inelastic X-Ray Scattering	158
E. S. Bozin:Local structural aspects of metal-metal transition in $IrTe_2$	160
J. Fink:Influence of Lifshitz transitions and correlation effects on the scattering rates and the effective mass of the charge carriers in ferropnictides and ferrochalcogenides	162
D. N. Argyrou: Solitonic lattice and Yukawa forces in the rare earth orthoferrite $TbFeO_3$	164
A. Glatz:Reentrance of superconductivity in parallel fields.....	166
N. Harrison:Towards a complete Fermi surface in underdoped high T_c superconductors	168
T. Egami:Quantum effect on atomic dynamics in superfluid 4He	170
Y. Uemura: Phase separation, first order transition and precursor states in unconventional superconductors, Mott insulators and Skyrmion systems --- analogy with 3-d and 2-d superfluid He --	172
S. H. Pan: Cooper Pairing and Phase Coherence in Iron-based Superconductor $Fe_{1+x}(Te,Se)$	173
V. M. Pudalov:Probing Energy Scale in the Interacting 2D Electron System by Transport and ThermodynamicMeasurements	174
A. Perali:Lifshitz transitions and BCS-BEC crossover in multigap superconductors as a root for room temperature superconductivity	176
T. Maier: Pairing in a dry Fermi sea	178
A. Linscheid: Sign changing pairing via spin-fluctuations of incipient bands close to the Fermi level	180
R. Micnas:Boson-Fermion resonant model for nonconventional superfluids	182
M. Doria:Kinetic origin of the Rashba interaction and of the Dirac cone from the Zero Helicity States.....	183
L. Salasnich:Vortex-Antivortex unbinding in the 2D BCS-BEC crossover.....	185

M. De Llano: A Generalized BEC Theory for Any Coupling.....	186
G. Pupillo: Cluster glass and superglass phases with cold atoms and 1.5 superconductors	188
T. Ord: Modification of spatial length-scales near the surface of a two-gap superconductor.....	189
T. Kuzmicheva: Anisotropic superconducting gaps in optimally doped $Ba_{1-x}K_xFe_2As_2$ and $BaFe_{2-x}Ni_xAs_2$ pnictides	190
M. Tortello: Nanoscale Characterization of the Thermal Conductivity of Supported Graphite Nanoplates, Graphene and Few-layer Graphene by Scanning Thermal Microscopy.....	192
A. Vargunin: Electric-field delocalization in multiband superconductors	194
J. Haase: New Perspective on the Cuprate Phase Diagram and the charge distribution in the copper-oxygen plane	195
K. Machida: Multiband superconductors with strong Pauli paramagnetic effect....	197
A. Shengelaya: Suppression of stripe order by nonmagnetic impurities in cuprates	199
S. Brazovskii: Recent identifications of microscopic solitons in quasi 1d electronic systems and generalisations to higher dimensions.....	200
R. Hackl: Fluctuations and Superconductivity in Fe-based Systems	202
N. Bachar: Competition between enhanced Cooper pairing and suppressed phase coherence in coupled aluminum nanograins	204
A. Bill: Pair Correlations in Superconducting-Magnetic Hybrid Systems.....	206
F. Hardy: Complex Phase Diagram of $Ba_{1-x}Na_xFe_2As_2$: A Multitude of Phases Striving for the Electronic Entropy.....	208
D. Manske: Higgs Spectroscopy of Superconductors in non-equilibrium	210
D. Sunko: Fundamental building blocks of strongly correlated wave functions	212
S. Streltsov: Covalent bonds against magnetism in transition metal compounds...	213
D. Dessau: Electron Self-energies in Cuprate Superconductors: Their Role in Setting T_c and Other Properties	214
M. Iavarone: Scanning Tunneling Microscopy and Spectroscopy of FeSe single crystals	215
S. Feng: Charge order driven by Fermi-arc instability and its connection with pseudogap in cuprate superconductors.....	216
J. Nissinen: Two-dimensional Quantum Liquid Crystals.....	217
T. Cren: Long range coherent magnetic bound states in superconductors	218
N. Fujiwara: NMR study on AF-SC-AF phase transition under a pressure of 3.0 GPa in $LaFeAsO_{1-x}H_x$: phase segregation around SC-AF phase boundary.....	220

I. H. Inoue: Negative charge-compressibility at the channel of SrTiO ₃ field-effect transistor	222
T. Adachi: Muon spin relaxation and transport studies in the electron-doped high- T_c T'-superconductors revealing the novel electronic state	224
T. Yanagisawa: Fluctuations and Nambu-Goldstone-Higgs Modes in Multi-Condensate superconductors	226
T. R. Lemberger: Quantum and Thermal Fluctuations in Strongly Underdoped Cuprates near the Super-to-Insulator Critical Point	228
Dawei Shen: Manipulating the electronic structure and magnetism of spin-orbit Mott insulator by tailoring superlattices.....	230
Y. A. Soh: Magnetic Force Microscopy of spin reorientation of iron tin	231
J. M. Tranquada: Intertwined Superconductivity and Antiferromagnetism in Cuprates	232
L. H. Greene: Topological surface states interacting with bulk spin excitons in the Kondo insulator SmB ₆ as revealed by planar tunneling spectroscopy	234
G. Aeppli: Statics and dynamics of crumpled graphene	235
Tom Devereaux : Induction & Dynamics of New States of Matter in 2D Materials	236
J. Annett: Time reversal symmetry breaking in multiband superconductors_	237
D.I.Khomskii: Novel effects in orbital physics D. I. Khomskii	238
M. J. Lawler: Commensurate features of cuprate charge density modulations	239
I. Maggio-Aprile: New twist on the vortex-core tunneling spectroscopy in YBa ₂ Cu ₃ O _{7-δ}	240
P. Giraldo-Gallo: Fermiology of hole-doped PbTe: Insights to understand superconductivity in a valence disproportionated compound	241
A. Ricci: Critical dynamics and inhomogeneity in complex materials.	243
A. Moewes: Adjacent Fe – vacancy interactions s the Origin of room temperature Ferromagnetism in (In _{1-x} Fe _x) ₂ O ₃	245
P. Orth: Frustrated spin polarons and percolation in the electrostatically and chemically doped complex oxide LaCoO ₃	246
D. Pelc: Superconducting percolation in the cuprates	247
B. Spivak: Macroscopic character of composite high temperature superconducting wires	248
N. Zhigadlo: Exploring multi-component superconducting compounds by high pressure method and combinatorial solid state chemistry	249
S. Hannel: Nonlocal Polarization Feedback in a Fractional Quantum Hall Ferromagnet	251

N. Schopohl : On the theory of surface superconductivity in high magnetic fields for s- and d-wave pairing superconductor films. 253

D. Popovic:Avalanches and hysteresis at the structural transition in stripe-ordered $\text{La}_{1.48}\text{Nd}_{0.4}\text{Sr}_{0.12}\text{CuO}_4$ 254

M. A. Continentino: Firstorderquantumphasetransitions 256

V. Dobrosavljevic:Bad-metal behavior and Mott quantum criticality 258

A. Lichtenstein:Plaquette Valence Bond Theory of Cuprate HTSC..... 260

N. Barišić:Scattering rate and carrier density throughout the phase diagram of the cuprates 261

F. Krüger: Fluctuation-driven helical magnetic order near criticality..... 262

Y. Tokunaga: Above-room-temperature formation of the magnetic skyrmion in β -Mn-type chiral magnets..... 264

V- Kataev:Possible magnetic field induced hidden order in the low-dimensional quantum magnet LiCuSbO_4 266

Zhao Huang: Fractional Flux Plateau in Magnetization Curve of Multiband Superconductor Loop 267

M. V. Kartsovnik:BETS-based organic conductors as archetypical antiferromagnetic/superconducting nanostructures..... 269

T. Terashima:FeSe under high pressure: phase diagram and electronic structure.. 271

Wojciech Tabis:Change of carrier density at the pseudogap critical pointof a cuprate superconductor..... 273

F. Carbone:Direct-space and real-time observation of quantum phenomena in plasmonic nanostructures 274

P. Samuely:Interplay between superconductivity and charge density waves in Cu_xTiSe_2 276

D. Massarotti:MacroscopicquantumphenomenainspinfilterferromagneticJosephsonjunctions..... 277

F. Miletto Granozio: Non-volatile electrical and optical resistive switching in 2D electron gases at oxide heterostructures 278

P. De Padova: $\sqrt{3}\times\sqrt{3}$ -Multilayer Silicene/Ag(111) or $\sqrt{3}\times\sqrt{3}$ -Ag/Si(111)7 \times 7? 279

S. He: Electronic Structure and Superconductivity of FeSe / SrTiO_3 Films and Related FeSe-Based Bulk Superconductors 280

D. Stornaiuolo:Tunable magnetism and superconductivity in an oxide heterostructure 281

W. D. Schneider:Electron transport in thin oxide films: From phonon-polariton excitations to changes in the quantum structure of oxide-supported Gold nanoparticles..... 283

P. Simon:New platforms for topological superconductivity: from Shiba to Majorana bound states	285
S. I. Mukhin: Gorkov's equations in the instantonic	286
M. Berciu:One-band vs. three-band models for weakly doped cuprates.....	288
V. Grinenko:Upper critical fields near the spin density wave transition of $\text{BaFe}_2(\text{As}_{1-x}\text{P}_x)_2$	289
M. Erements: High temperature superconductivity in hydrogen-rich materials.....	291
A. F. Goncharov: Hydrogen sulfide at high pressure: change in stoichiometry	293
K. Shimizu: 200-K superconductivity in compressed hydrogen sulfide systems ...	295
R. Arita:Fully non-empirical study on superconductivity in sulfur hydrides under high pressures	296
A. Bianconi : Multi-condensates in BCS and BEC-BCS crossover regime near Lifshitz transitions in H_3S as in all high T_c superconductors	298
A. Bussmann-Holder: Structure and composition of the 200 K-superconducting phase of H_2S under ultrahigh pressure: the perovskite $(\text{SH}^-)(\text{H}_3\text{S}^+)$	300
F. Marsiglio:Superconductivity in H_2S and in other superconductors; many band or band of many?	302
G-Q. Zheng: Electronic Orbital Order and Spin Nematicity in Iron-PnictideHigh-Temperature Superconductors as Revealed by NMR	303
S. Caprara:Dynamicalcharge density waves rule the phase diagram of cuprates ...	304
H. Iwasawa:Development of VUV-laser-based ARPES system for higher spatial resolution and its application to Fermiology on high- T_c cuprates	306
A. Kanigel:ARPES measurements of $\text{Bi}2212$ thin-films in the presence of electrical current	307
R. Akashi:Emergent Magnéli-type crystal phases and their mixture in pressurized sulfur hydride.....	308
J. Bonca: Relaxation and thermalization in many-body systems coupled to different bosonic degrees of freedom.....	310
P. Bourges:Q=0 Magnetic order in the pseudogap state of cuprates superconductors	312
D. Orga:Long-range order and pinning of charge-density waves incompetition with superconductivity.....	313
A.M. Oles:Exotic spin-orbital physics in hybrid d^4-d^3 and d^4-d^2 oxides	314
I. Felner: Superconductivity and unusual magnetic features in amorphous carbon and in other unrelated materials.....	316
I. Eremin:Spin-orbit coupling and spin excitations in Sr_2RuO_4 and iron-based superconductors	318

D. Baeriswyl: Variational results for the two-dimensional repulsive Hubbard model: The refined Gutzwiller ansatz.....	319
B. Barbiellini: X-ray studies of complex materials for energy applications	321
K. Quader: Zero and Finite-T Responses of 2D Dipolar Bosons at Non-zero Tilt Angles	323
E. M. Bothschafter: Time-resolved switching of magnetization in a multiferroic ..	325
P. Turner: A new approach to the growth of materials leading to macroscopic quantum coherence and high temperature superconductivity.....	327
W. Brzezicki: Charge - orbital order and topological effects in presence of zig-zag magnetic textures in 4d - 3d hybrid oxidespt.....	329
A. Kaindl: Stripes, phonons, and electronic dynamics: new views on ultrafast time scales	331
K. Nakagawa: Fluctuating Superconductivity in the Strongly Correlated Organic Superconductors in κ -(BEDT-TTF) ₂ X (X = Cu[N(CN) ₂]Br, Cu(NCS) ₂) Studied by Polarized Femtosecond Spectroscopy.....	333
B. Joseph: Temperature dependent structural modulation in Ca _{0.82} La _{0.18} FeAs ₂ pnictide superconductors	335
Wei Bao: Orbital ordering as the unifying mechanism for both the structural and antiferromagnetic transitions in the Fe-based superconductors.....	337
A. Keren: Opening a diagonal gap by a dynamic spin density wave in lightly doped La _{2-x} Sr _x CuO ₄	339
T. Baturina: Finite-temperature localized state in superconducting films.....	340
A. Y. Mironov: Effect of disorder on the vortex Mott transition in array of superconducting islands	342
L. A. Ponomarenko: Hydrodynamic transport in high mobility graphene.....	344
Si Zhou: 2D B-C-O alloy: a promising electronic material.....	346
A. Tagliacozzo: Incipient Berezinskii Kosterlitz and Thouless transition in two-dimensional coplanar Josephson junctions.....	348
C. Mazzoli: New evidences for in-plane entanglement of CDW in YBCO.....	350
R. Puzniak: Phase separation in single crystals of iron-based superconductors.....	351
L. Balicas: Interplanar coupling-dependent magnetoresistivity in high-purity layered metals	353
P. Sushkov: The amplitude and origin of charge density wave in YBCO	355
K. Wysokiński: Three-terminal system as a spin current source and heat to electricity converter.....	356
K. J. Kapcis: Various metallic and insulating phases and their phase separations in charge ordered systems	357

A. Lanzara: Mapping the spin-orbital texture of topological insulators in the energy, momentum spin and time domains. 359

N. Bachar: Detailed optical spectroscopy of the hybridization gap and the hidden order transition in high quality URu₂Si₂ single crystals..... 361

I. Chavez: BCS-Bose Crossover Extended with Hole Cooper Pairs 363

M. Doria: Onset of two-band superconductivity in superconducting-insulating superconducting tri-layer systems..... 365

T. Jarlborg: Charge transfers and band dispersions in magnetic Nd_{2-x}Ce_xCuO₄... 367

N. Kristoffel: The interplay of long range interactions and electron density distributions in polar and strongly correlated materials 368

M. Moroni: Effect of proton irradiation on the low-energy excitations of Ba(Fe_{1-x}Rh_x)₂As₂ superconductors 369

S. Nishiyama: Syntheses and characterization of superconducting metal-doped LaOBiS₂ 370

The europium valence state in EuCo_2As_2 at external and chemical pressure



A.P. Menushenkov^{1*}, A.A. Yaroslavtsev^{1,2},
A.Y. Geondzhian¹, R.V. Chernikov³, L. Nataf⁴, X. Tan⁵,
M. Shatruk⁵

¹*National Research Nuclear University "MEPhI" (Moscow Engineering Physics Institute), Moscow, 115409, Russia*

²*European XFEL GmbH, 22761, Hamburg, Germany*

³*DESY Photon Science, 22607, Hamburg, Germany*

⁴*Synchrotron SOLEIL, L'Orme des Merisiers, Saint-Aubin, France*

⁵*Department of Chemistry and Biochemistry, Florida State University, FL 32306, Tallahassee, USA*

Email: apmenushenkov@mephi.ru

Keywords: mixed valence state, XANES, ferromagnetism, antiferromagnetism, chemical pressure

The europium valence state was investigated in the series of EuCo_2As_2 -based samples by means of hard X-ray absorption near edge structure (XANES) spectroscopy at Eu $L_{2,3}$ edges. This compound crystallizes in the tetragonal ThCr_2Si_2 structure type famous for a plenty of fascinating physical phenomena such as unconventional superconductivity, heavy fermion state, valence fluctuations, quantum criticality, etc. Recently it was shown that the application of pressure can induce the ferromagnetism in initially antiferromagnetic EuCo_2As_2 ($T_N = 47\text{K}$) and the change of magnetic ordering correlates with the stabilization of mixed valence state of europium. Probably, the redistribution of electronic DOS under compression causes the fulfillment of Stoner criterion for cobalt states, which results in ferromagnetism. The similar behavior was previously observed for the isostructural EuCo_2P_2 phosphide with Pr- doping [1]. In order to obtain the more comprehensive picture of europium valence behavior in EuCo_2As_2 in different environments we tested the series of samples with various Ca and La doping to study the effect chemical pressure, isoelectronic and non-isoelectronic substitution. The measurements at high applied pressure (up to 40 GPa) in a broad temperature range (4.5-300 K) have been performed as well. The low temperature X-ray absorption measurements have been carried out at beamlines mySpot of BESSY-II (HZB, Berlin) and i811 of MAX-lab (Lund, Sweden). The high pressure experiment with sample in diamond anvil cell has been performed at the energy dispersive beamline ODE of synchrotron SOLEIL (Paris, France).

According to our recent study, the Eu valence in parent compound EuCo_2As_2 is close to +2 which is in agreement with the results obtained by other methods and is typical for europium transition metal pnictides. Here we convinced that the applied pressure

has the strongest effect on valence. The experiment on compound $\text{Eu}_{0.5}\text{Ca}_{0.5}\text{Co}_2\text{As}_2$ (Fig. 1) has shown that in a broad pressure range the valence changes almost linearly and does not show hysteresis. The chemical pressure induced by Ca^{2+} inclusion also results in quite considerable valence change while the temperature has a rather weak effect. Thus the modification of electronic band structure near Fermi level in EuCo_2As_2 under impact is uniform and reversal, and requires quite high energy cost because the only effective way to change the valence is the applied pressure. But even in this case, $\text{Eu}_{0.5}\text{Ca}_{0.5}\text{Co}_2\text{As}_2$ at a strong compression of 38.6 GPa shows the valence +2.65, which is much smaller than the almost +3 value reached in EuCo_2P_2 -based compounds. Summing up, the valence instability in EuCo_2As_2 -based materials increases under external or internal compression. It can cause the further perturbation of electronic structure and the change of magnetic state, which is currently under investigation.

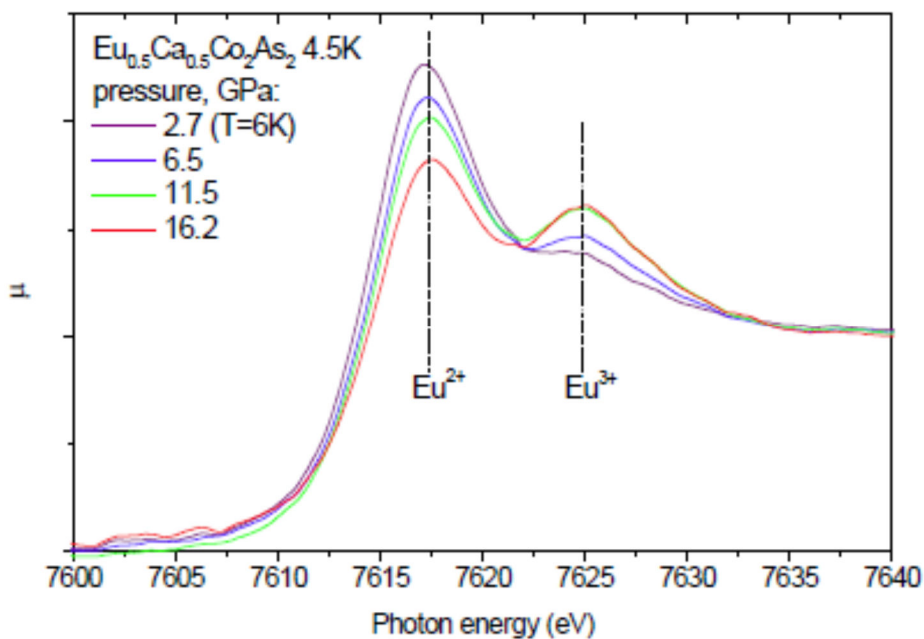


Figure 1. Pressure dependence of L_2 -Eu XANES spectrum of $\text{Eu}_{0.5}\text{Ca}_{0.5}\text{Co}_2\text{As}_2$ at 4.5 K.

References

1. K. Kovnir, W.M. Reiff, A.P. Menushenkov, et al., Chem. Mater. **23**(12), 3021 (2011)

Disorder-driven quantum phase transition and transport in Dirac semimetals and semiconductors



Leo Radzihovsky

¹University of Colorado at Boulder

Email: radzihov@colorado.edu

Keywords: disorder, quantum criticality, Dirac semimetals

Motivated by Weyl semimetals and weakly doped semiconductors, I will discuss recent work on weakly disordered materials with a power-law quasiparticle dispersion. Above a critical dimensions at low-electron density the system exhibits a novel disorder-driven quantum phase transition that manifests itself in the critical behavior of single-particle density of states and of electrical transport. Utilizing a controlled renormalization-group analysis I will describe our predictions for the low-temperature conductivity and density of states in Weyl semimetals and weakly doped semiconductors near and below the critical disorder point.

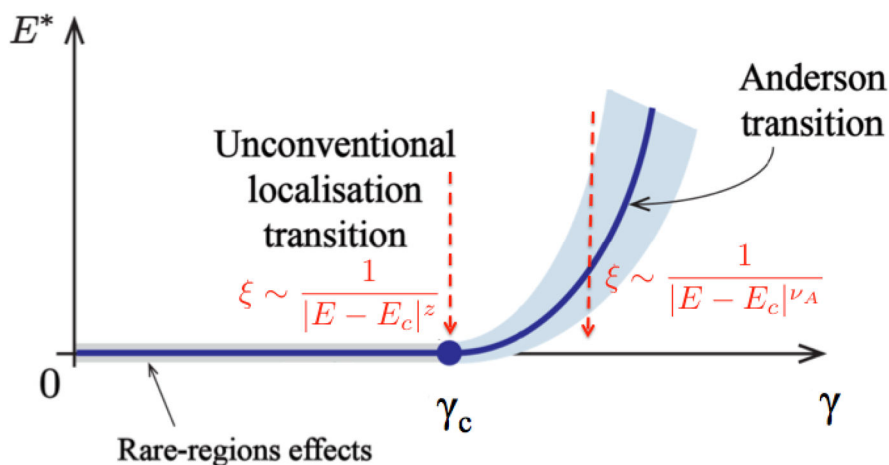
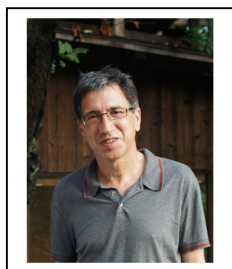


Figure 1: Mobility threshold nonanalyticity as a function of disorder gamma.

References

1. S. Syzranov, L. Radzihovsky, V. Gurarie, Phys. Rev. Lett. 114, 166601 (2015).
2. S. Syzranov, V. Gurarie, L. Radzihovsky, Phys. Rev. B 91, 035133 (2015).

Optimized Unconventional High- T_c Superconductivity in Fullerides



Kosmas Prassides

WPI-AIMR, Tohoku University, Sendai, Japan

Email: k.prassides@wpi-aimr.tohoku.ac.jp

Keywords: fullerenes, strong correlations, Mott insulator, Jahn-Teller effect

Understanding the relationship between the superconducting, the neighbouring insulating, and the normal metallic state above T_c is a major challenge for all unconventional superconductors. The molecular A_3C_{60} fulleride superconductors have a parent antiferromagnetic insulator in common with the atom-based cuprates, but here the C_{60}^{3-} electronic structure controls the geometry and spin state of the structural building unit *via* the on-molecule Jahn-Teller effect. We have recently identified [1] the Jahn-Teller metal as a fluctuating microscopically-heterogeneous coexistence of both localized Jahn-Teller-active and itinerant electrons that connects the insulating and superconducting states of fullerides. The balance between these molecular and extended lattice features of the electrons at the Fermi level gives a dome-shaped variation of T_c with interfulleride separation, demonstrating molecular electronic structure control of superconductivity.

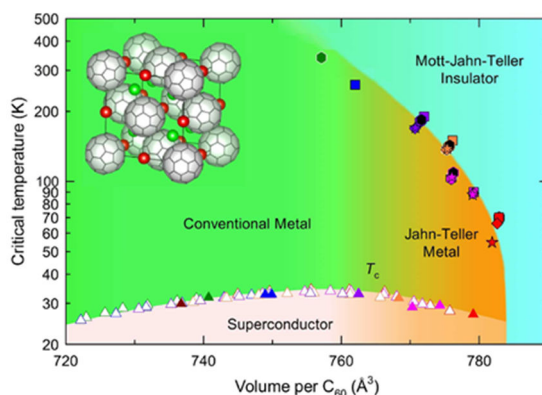


Figure 1: Electronic phase diagram of fcc A_3C_{60} fullerides showing the evolution of T_c (superconductivity dome) and the Mott-Jahn-Teller insulator to Jahn-Teller metal crossover temperature, T as a function of volume per C_{60} . The inset shows the A_3C_{60} crystal structure.

References

1. R. H. Zadik *et al.*, *Science Adv.* *1*, e1500059 (2015). doi: 10.1126/sciadv.1500059

Loss of the Mott Gap and Formation of a Superthermal Metal in the Coherent Polaronic Quantum Phase of O- and Photo-Doped $\text{UO}_{2(+x)}$



Steven D. Conradson
Institut Josef Stefan
Department of Complex Matter

Email: * st3v3n.c0nrads0n@icloud.com

Keywords: tunneling polarons, feshbach resonance, phonon-mediated coherence, multiband superconductivity

The tunneling polarons in $\text{UO}_{2(+x)}$ self-organize into a quantum phase whose properties provide strong evidence for its condensation [1,2]. Numerous experimental results imply a novel, chemistry-based condensation mechanism that we have postulated is a disproportionation excitation synchronized throughout the domain and enhanced by the solid state equivalent of a Fano-Feshbach type resonance[3,4] connecting the two nondegenerate valence states. This would be the extreme case of condensation promoted by an anharmonic phonon strongly coupled to the charge distribution[5]. An outstanding question is the nature of the electronic structure and its consistency with this scenario. Measurements of the densities-of-states across the Mott gap in O-doped and photoexcited UO_{2+x} show that both cause it to fill, the former by an exceptionally large reduction in the energy of the lower edge of unoccupied states of the upper Hubbard band, whereas for the latter optical pumping into the $5f$ states effects a relatively flat density-of-states (DOS) extending continuously from the edge of the lower Hubbard band throughout the entire gap to emulate the effects of O-doping that gives the dynamical quantum phase structure, whereas high energy excitation promotes electrons across the gap into the unoccupied states calculated for the static structure of UO_2 . This latter result is surprising because of the unpredicted sensitivity of the immediate excitation process to the wavelength that contradicts current assumptions about the response to the photon impulse [6], possibly because of a combination of the wide Mott gap, absence of a metal-insulator transition, the quantum phase in UO_2 , and the coupling of the quantum phase to a specific phonon that may be activated only by certain excitations. This energy dependence was, however, previously observed in time-resolved reflectivity of UO_2 [1]. These results corroborate the conjectures that quantum phases produced by O- and photo-doping are closely related but not small perturbations of the UO_2 structure and the postulated importance of mixing with states above the Fermi level, where the already observed dynamical characteristics would contribute to this broad and featureless DOS. They also demonstrate that the quantum phase possesses unusual stability that we attribute to the formation of the condensate. In addition to the possibilities this exotic configuration provides for Bardeen-Cooper-Schrieffer – Bose-Einstein condensate crossover[7] and multiband exchange scenarios[8], these current experiments couple the observed coherence to a metallic phase at ambient temperature.

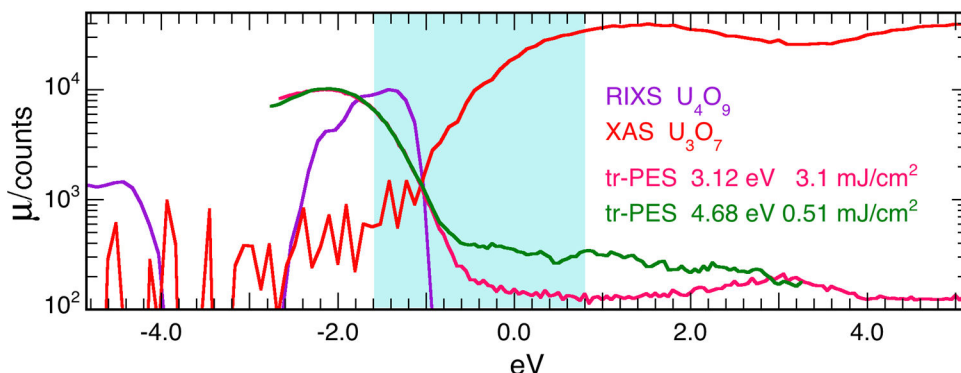


Figure 1: DOS of $\text{UO}_{2(+x)}$, with the O-doped states extrapolated from the RIXS, and XAS and the photo-doped states of the static (4.68 eV excitation, magenta) and dynamic (3.12 eV excitation, green) structures determined by time-resolved photoemission. The amplitudes were scaled to match those determined by LDA+U calculations. The blue band is the optical gap of UO_2 . The LHB is intersected by the tail of the unoccupied states to give an overlap of a few percent at the edge at a constricted point. The DOS of the photodoped states passes near this same point, with those with 3.12 eV excitation forming a superthermal metal as in the dynamic structure but conserving the Mott gap in the static one.

References

1. S. D. Conradson, et al. *Phys. Rev. B* 88, 115135 (2013).
2. S. D. Conradson, et al. *Sci. Rep.* 5, 15278 (2015).
3. E. A. Donley, N. R. Claussen, S. T. Thompson, C. E. Wieman. *Nature* 417, 529 (2002).
4. A. Bianconi. *Nature Phys.* 9, 536 (2013).
5. R. Mankowsky, et al. *Nature* 516, 71 (2014).
6. L. Perfetti, et al. *New J. Phys.* 10, 053019 (2008).
7. K. Okazaki, et al. *Sci. Rep.* 4, 4109 (2014).
8. A. Guidini, A. Perali. *Supercon. Sci. Tech.* 27, 124002 (2014).

Isotope and pressure effects in cuprate high-temperature superconductors - recent results



H. Keller*
Physik-Institut der Universität Zürich
CH-8057 Zürich, Switzerland

Email: [*keller@physik.uzh.ch](mailto:keller@physik.uzh.ch)

Keywords: isotope effects in cuprates, pressure effects in cuprates, pseudogap phase in cuprates, stripes in cuprates, lattice effects in cuprates

Cuprate high-temperature superconductors (HTSs) have some essential features 1) They have unusually high transition temperatures T_c which are beyond BCS theory. 2) They have a layered structures with strongly anisotropic normal state and superconducting properties. 3) They exhibit a rich doping dependent phase diagram with partially coexisting magnetic and superconducting phases, including a pseudogap and stripe-order phase. 4) They are multi-band superconductors with mixed order parameters. 5) They exhibit unconventional isotope effects on various quantities (e.g. the superconducting transition temperature T_c , the in-plane magnetic penetration depth $\lambda_{ab}(0)$, the spin-stripe order temperature T_{so} , the pseudogap order temperature T^*). 6) They show interesting pressure effects on various magnetic and superconducting properties. All the isotope and pressure effects observed in HTSs clearly demonstrate that lattice effects which in most theoretical models are neglected play an essential role in cuprates.

In this talk recent results of oxygen-isotope ($^{16}\text{O}/^{18}\text{O}$) effect (OIE) and pressure effect studies of the cuprate system $\text{La}_{2-x}\text{Ba}_x\text{CuO}_4$ are presented:

1) The doping dependence of the OIE on the pseudogap temperature T^* in $\text{La}_{2-x}\text{Ba}_x\text{CuO}_4$

($0.06 \leq x \leq 0.15$) has been studied by means of x-ray near edge structure (XANES) experiments. A substantial x dependent and sign reversed OIE on T^* is observed which is most pronounced at low doping.

2) The simultaneous occurrence of static magnetism and superconductivity in the stripe phase of $\text{La}_{2-x}\text{Ba}_x\text{CuO}_4$ ($x = 0.155$) has been investigated by muon-spin rotation (μSR) and magnetization experiments under hydrostatic pressure up to $p = 2.2$ GPa. The results provide new insight into the complex interplay between magnetism and superconductivity in the stripe phase of cuprates.

Controlling electronic interactions and phase separation in VO₂ via strain, temperature and ultrafast electric fields



Alexander X. Gray^{1**},

¹*Department of Physics, Temple University, Philadelphia, Pennsylvania 19122, USA*

Email: * axgray@temple.edu

Keywords: strongly-correlated oxides, metal-insulator transition

Ultrafast electric-field control of fundamental physical interactions in strongly-correlated oxides is currently considered to be one of the most promising avenues towards realizing new generations of energy-efficient devices. Yet, our ability to manipulate the underlying degrees of freedom leading to the emergent behavior and phase transitions in these highly-functional electronic systems is still in its infancy. In this talk I will present the results of several recent x-ray spectroscopic studies aimed at establishing pathways towards the control of metal-insulator transition in an archetypal strongly-correlated oxide VO₂. Using polarization- and temperature-dependent x-ray absorption spectroscopy, in combination with x-ray diffraction and electronic transport measurements, we demonstrate that the metal-insulator transition temperature can be tuned continuously with strain [1]. We then show that both the collapse of the insulating gap and the change in crystal symmetry in homogeneously strained single-crystalline VO₂ films are preceded by the purely-electronic softening of Coulomb correlations within V-V singlet dimers [2]. Finally, we demonstrate that the purely-electronic and purely-structural transitions in VO₂ can be decoupled from each other in time domain using intense THz electric-field pulses [3]. Future applications and experiments will be discussed.

References

1. N. B. Aetukuri *et al.*, Control of the metal–insulator transition in vanadium dioxide by modifying orbital occupancy, *Nature Physics* **9**, 661 (2013).
2. A. X. Gray *et al.*, Correlation-driven insulator-metal transition in near-ideal vanadium dioxide films, *Phys. Rev.Lett.*, *in print* (2016). arXiv:1503.07892
3. A. X. Gray *et al.*, Ultrafast THz field control of electronic and structural interactions in vanadium dioxide, arXiv:1601.07490 (2016)

PT-symmetry mechanism of out-of-equilibrium phase transitions in superconducting and magnetic systems



V. M. Vinokur^{1*}, Nicola Poccia^{2,3}, Martijn Lankhorst², Martin P. Stehno², Alexey Galda¹, Vikram Tripathi^{1,4}, Francesco Coneri², Ginestra Bianconi⁵, Tatyana I. Baturina^{1,6,7}, Hans Hilgenkamp², Alexander Brinkman², Alexander A. Golubov^{2,8}

¹*Materials Science Division, Argonne National Laboratory, 9700 S. Cass Avenue, Argonne, IL 60637, USA*

²*MESA+ Institute for Nanotechnology, University of Twente, 7500 AE Enschede, The Netherlands*

³*NEST Istituto Nanoscienze-CNR & Scuola Normale*

Superiore, Pisa, Italy

⁴*Department of Theoretical Physics, Tata Institute of Fundamental Research, Homi Bhabha Road, Mumbai 400005, India*

⁵*School of Mathematical Sciences, Queen Mary University of London, London E1 4NS, United Kingdom*

⁶*Institut für experimentelle und angewandte Physik, Universität Regensburg, D-93025 Regensburg, Germany*

⁷*A.V.Rzhanov Institute of Semiconductor Physics SB RAS, 13 Lavrentjev Avenue, Novosibirsk 630090, Russia*

⁸*Moscow Institute of Physics and Technology, Dolgoprudnyi, Moscow district, Russia*

*vinokour@anl.gov

Keywords: out-of-equilibrium physics, out-of-equilibrium phase transitions, Mott transition, dynamic Mott transition, spin dynamics, Landau-Lifshitz equation, Landau-Lifshitz-Slonezewski dynamics

We posit a non-Hermitian Hamiltonian approach as a general technique for description of out-of-equilibrium phase transitions. We apply our theory to dissipative non-equilibrium dynamics of an open quantum spin system and dynamic vortex Mott transition. In spin system the imaginary part of the proposed Hamiltonian describes effects of damping and the applied Slonezewski spin-transfer torque (STT). In the classical limit, our approach reproduces Landau-Lifshitz-Slonezewski dynamics of a large macrospin. We reveal the STT-driven *parity-time* (PT) symmetry-breaking transition corresponding to a phase transition from precessional magnetization dynamics to controlled switching. We further describe the critical behavior of current-driven dynamic vortex Mott insulator-to-metal transition [1] in terms of non-Hermitian Hamiltonians invariant under simultaneous parity and time-reversal operations. The dynamic Mott transition is identified as a PT symmetry-breaking phase transition, where the Mott insulating state corresponds to the regime of unbroken PT symmetry with the real energy spectrum. We establish that the imaginary part of the Hamiltonian arises from the combined effects of the driving field and inherent dissipation. We

derive the renormalization and collapse of the Mott gap at the dielectric breakdown and describe the resulting critical behavior of transport characteristics.

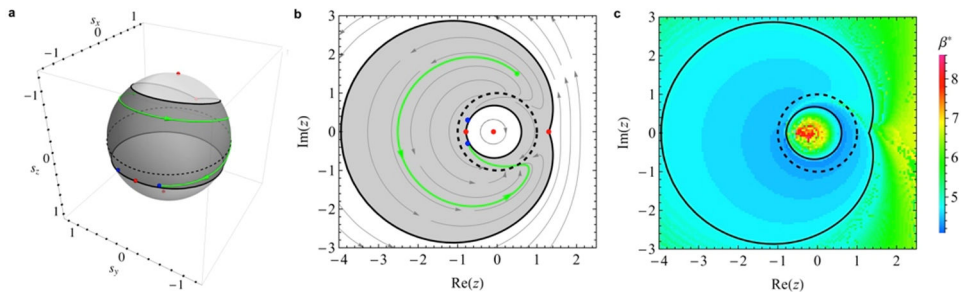
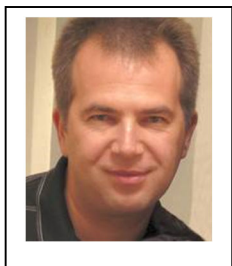


Figure 1: **a-b**: Spin dynamics described by the non-Hermitian modification of the Landau-Lifshitz-Slonczewski Hamiltonian. Parity-time reversal symmetry is broken in the shaded region around the easy plane $|z|=1$ (dashed line), encompassing two fixed points, $z_{1,2}$ (blue dots), appearing as source and sink nodes. The green line depicts a typical non-oscillatory spin trajectory in the region of broken PT symmetry. Red dots represent fixed points. **c**: Results of micromagnetic simulations as a function of stereographic projection of the initial spin direction. In the blue region the PT symmetry is broken and spin in less than 0.5 ns saturates in the direction z_1 in a full agreement with the analytical result.

References

1. N. Poccia, T. I. Baturina, F. Coneri, C. G. Molenaar, X. R. Wang, G. Bianconi, A. Brinkman, H. Hilgenkamp, A. A. Golubov, and V. M. Vinokur, Critical behavior at a dynamic vortex insulator-to-metal transition, *Science*, **349**, 1202 (2015).

Direct Observation of Spin–Orbit Coupling in Iron-Based Superconductors



Sergey Borisenko

¹*IFW-Dresden, Dresden, Germany*

Email: *S.Borisenko@ifw-dresden.de*

Keywords: iron-based superconductors, ARPES

Spin–orbit coupling is a fundamental interaction in solids that can induce a broad range of unusual physical properties, from topologically non-trivial insulating states to unconventional pairing in superconductors. In iron-based superconductors its role has, so far, not been considered of primary importance, with models based on spin- or orbital fluctuations pairing being used most widely. Using angle-resolved photoemission spectroscopy, we directly observe a sizeable spin–orbit splitting in all the main members of the iron-based superconductors. We demonstrate that its impact on the low-energy electronic structure and details of the Fermi surface topology is stronger than that of possible nematic ordering. The largest pairing gap is supported exactly by spin–orbit-coupling-induced Fermi surfaces, implying a direct relation between this interaction and the mechanism of high-temperature superconductivity.

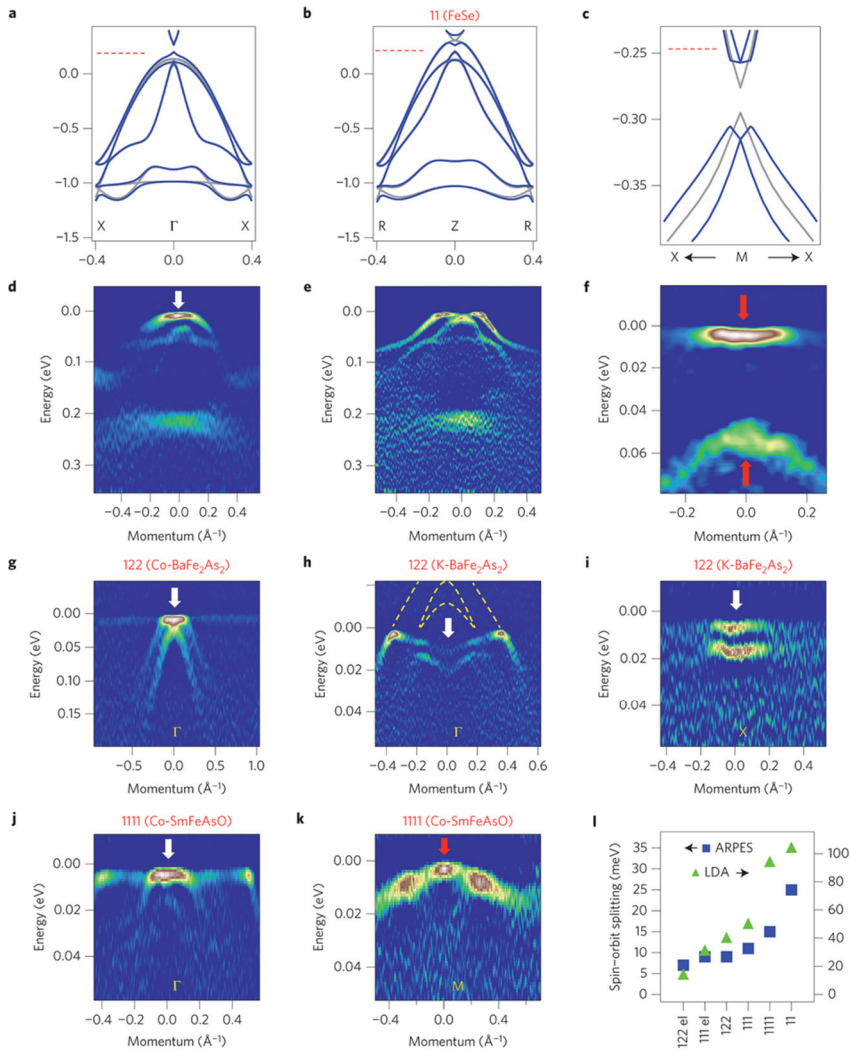


Figure 1: a–c, Results of the band-structure calculations of FeSe excluding SOC (grey lines) and including SOC (blue lines) along the high-symmetry directions. d–f, Corresponding experimental data, shown as second derivatives of the raw data. Note that in c two single features are observed at the M-point, contrary to the expected two double features in the nematic scenario. g–i, Same for 122 materials. Dashed lines in h show the expected dispersions in the unoccupied part of the spectrum. j,k, Same for Co-SmFeAsO. l, Comparison of the experimental values for SOC obtained by reading the peak positions from the corresponding EDCs shown in Supplementary Fig. 3, with the theoretical values. ‘el’ means electron pocket.

References

1. S. Borisenko et al. NaturePhysics (2015) doi:10.1038/nphys3594

Multiorbital Hamiltonians for non-BCS superconductors



Adriana Moreo^{1,2*}

¹University of Tennessee

²Oak Ridge National Laboratory

Email: * amoreo@utk.edu

Keywords: high T_c, multiorbitals, multiple degrees of freedom

Non-BCS superconductors are characterized by multi-orbital Fermi surfaces and by the simultaneous interaction of charge, spin, orbital, and lattice degrees of freedom. An on-site attractive multiorbital Hamiltonian for d-wave superconductivity will be presented.[1] Via a canonical mean-field procedure similar to the one applied to the well-known negative-U Hubbard model, it will be shown that the new model develops d-wave superconductivity with nodes along the diagonal of the Brillouin zone. This result is also supported by the exact diagonalization of a small cluster. It will be shown that the pairing state of the model phenomenologically reproduces several properties of the high T_c cuprates. In addition a multiorbital spin-fermion model [2] with electron- and spin-lattice coupling for the study of FeTe will be introduced and its transport properties will be presented.

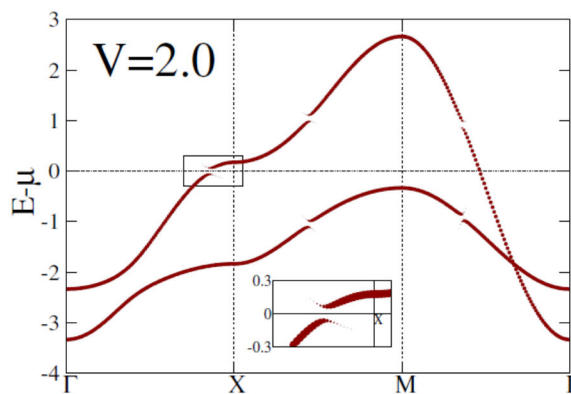


Figure 1: The spectral function $A(k, \omega)$ in the mean-field approximation for the H_{MD} model, working at $V=2$. The inset highlights the weak intensity “shadow” spectral weight below and above the gaps opened by the attraction V . Note the node along the diagonal of the Brillouin zone.

References

1. C. Bishop et al., arXiv : 1602.02420.
2. S. Liang et al., Phys. Rev. Lett. **109**, 047001 (2012).

Pressure effect on electronic structure, exchange interaction, and critical temperature of hole-doped cuprates



Sergei Ovchinnikov^{1,2*}, Vladimir Gavrichkov¹, Sergei Nikolaev², Kirill Sidorov², Zlata Pchelkina³
¹*Kirensky Institute of Physics*
²*Siberian Federal University*
³*Mikheev Institute of Physics of Metals*

Email: * sgo@iph.krasn.ru

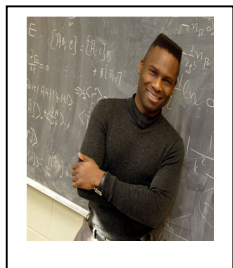
Keywords: high T_c , t-J model, magnetic pairing, external pressure, Lifshitz transitions

The pressure effects on the normal state electronic structure, the superexchange interaction, and the critical temperature of d-type superconductivity mediated by magnetic pairing have been studied within the multielectron hybrid scheme LDA+GTB that takes into account electron correlations in CuO_2 planes[1]. From ab initio LDA calculations we have found the changes of the multiband p-d model parameters at 3% compression of different symmetry: a) hydrostatic, b) along the c-axis, c) in (a,b) plane. We have studied the changes of the Fermi surface under external pressure for different hole doping concentration x . In general this effect is too small except two critical concentrations $x_{c1} \approx 0.16$ and $x_{c2} = 0.24$ where the Lifshitz transitions occur with the change of the Fermi surface topology. The exchange coupling increases when the CuO_4 placket area is decreasing and vice versa. The effects of pressure on the antiferromagnetic coupling J and the baric derivative of relative mean-field value of T_c , $d\text{Ln}T_c/dP$ are obtained in a good agreement to experimental data for isotropic pressure[2] and in qualitative agreement for anisotropic compression. Chemical pressure due to different lattice parameters in thin film results in T_c increasing [3].

References

1. K.A., Sidorov, et al. *Phys.Stat.Solidi B*, (2015), DOI 10.1002/pssb.201552465.
2. F. Hardy et al., *Phys. Rev. Lett.* **105**, 167002 (2010).
3. I. Bozovic, et al., *Phys. Rev. Lett.* **89**, 107001 (2002)

Anomalous Dimensions and Unparticles in the Cuprate Superconductors



Professor Philip Phillips*,
¹*University of Illinois*

Email: *dimer@illinois.edu*

Keywords: high T_c , nano-clusters, shell structure,

High-temperature superconductivity in the cuprates remains an unsolved problem because no knock-down experiment has revealed unambiguously the nature of the charge carriers in the normal state. I will show here that what is strange about the normal state is that the current for the underlying charge carriers possess an anomalous dimension. To show this, I will focus on the optical conductivity. Two features are problematic: 1) violation of the f-sum rule and 2) power-law scaling in the mid-infrared. So befuddling is the latter that even high-energy theorists have written papers on the puzzling $\omega^{-2/3}$ scaling law in the cuprates. The key claim here is that the observed power law is a universal consequence of gravity in the presence of translational symmetry breaking. I will explain this claim and report on a calculation that tests it. I will show that the general claim is not true. As an alternative, I will show how unparticles or a scale invariant sector in the mid-infrared can account for the experimentally observed power law and a violation of the f-sum rule. A feature of the unparticle construction is that they admit an anomalous dimension for the current. I will show how an anomalous dimension can be constructed from massive gravity. I will also show how anomalous dimensions can be experimentally probed by the fractional Aharonov-Bohm effect in the normal state of the cuprates.

Origins of the nematicity and superconductivity in FeSe and other Fe-based superconductors



Hiroshi Kontani^{1*}, Youichi Yamakawa¹, Seiichiro Onari²,
¹*Nagoya University, Japan*
²*Okayama University, Japan*

Email: * kon@slab.phys.nagoya-u.ac.jp

Keywords: orbital fluctuations, vertex correction, FeSe

The origins of the nematicity and the pairing mechanism are the central unsolved problems in Fe-based superconductors. To understand these issues, we study the first-principles multiorbital Hubbard model for FeSe by applying the self-consistent vertex correction (SC-VC) method [1-3]. Strong orbital fluctuations are induced by weak spin fluctuations by including the Aslamazov-Larkin (AL) vertex correction, which is dropped in the mean-field-level approximations. Above the structure transition temperature T_S , the strong ferro-orbital susceptibility due to the AL-VC well explains the experimental large nematic susceptibility [4]. Below T_S , we find that the orbital polarization ($\Delta E_{xz}(\mathbf{k})$, $\Delta E_{yz}(\mathbf{k})$) has drastic \mathbf{k} -dependence, and the relations $\Delta E_{xz}(\Gamma) - \Delta E_{yz}(\Gamma) > 0$ and $\Delta E_{xz}(Y) - \Delta E_{yz}(X) < 0$ are satisfied in the FeSe model [5]. This result well explains the "sign-reversing orbital polarization" reported by ARPES studies. Thus, fundamental electronic properties of the nematicity without magnetization in FeSe are well explained by the SC-VC method, and the origin of the nematicity is the orbital order.

We stress that the mechanism of the spin-fluctuation-driven orbital order due to the AL vertex correction is universal in multiorbital systems. For example, the p -orbital CDW order in cuprate superconductors is well explained by the SC-VC theory [6]. The validity of the SC-VC theory and the significance of the AL vertex correction is confirmed by the functional renormalization-group (fRG) method [7,8].

Next, we study the pairing mechanism in FeSe families by formulating the gap equation beyond the Migdal-Eliashberg (ME) approximation [9]. We calculate the vertex corrections for effective Coulomb interaction for the spin- and charge-channels $\Gamma^{c,s}(\mathbf{p};\mathbf{q})$, and apply them into both the susceptibilities $\chi^{c,s}(\mathbf{q})$ and the electron-boson couplings. In the electron-doped FeSe model without the hole-pocket (Fig. 1 (a)), moderate spin and orbital fluctuations emerge due to the AL vertex correction for $\chi^{c,s}(\mathbf{q})$. The attractive interaction due to orbital fluctuations, $\Gamma^c(\mathbf{p};\mathbf{q})\chi^c(\mathbf{q})\Gamma^c(-\mathbf{p};-\mathbf{q})$, is strongly enlarged since $\Gamma^c(\mathbf{p};\mathbf{q})$ is much larger than the bare Coulomb interaction U due to the AL vertex correction. In addition, the crossing fluctuation term, which is dropped in the ME approximation, also produces the attractive interaction. For these reasons, the s_{++} -wave state is obtained in the electron-doped FeSe in the present study [9,10].

The obtained gap anisotropy shown in Fig. 1 (b) is consistent with the recent ARPES studies. In contrast, the d-wave state due to the spin fluctuations, shown in Fig. 1 (c), is not realized since its eigenvalue is just $\lambda_E = 0.02$. The obtained nodal gap structure due to the spin-orbit interaction $\lambda_{SOI}=0.1\text{eV}$ is inconsistent with the ARPES studies. In summary, the fully-gapped s_{++} -wave state in the electron-doped FeSe is satisfactorily reproduced by the attractive interaction due to the orbital fluctuations, by going beyond the ME theory. We also discuss the superconducting state in undoped FeSe.

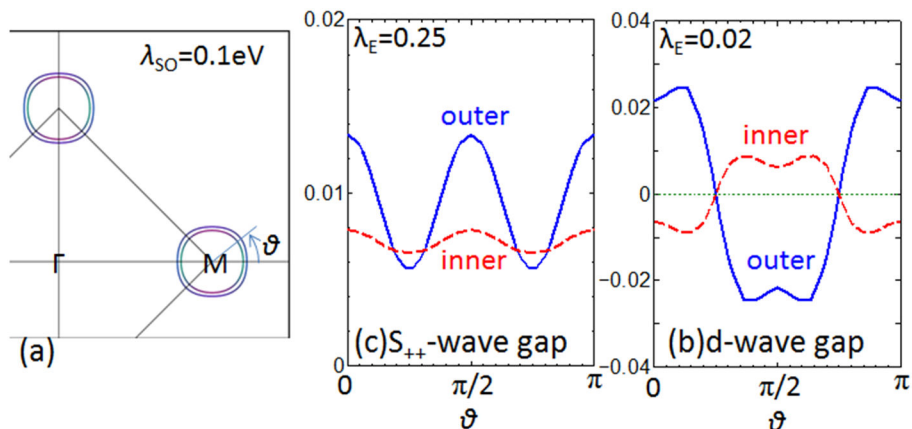
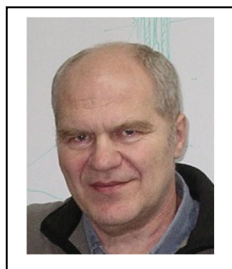


Figure 1: (a) Fermi surfaces for the 15% electron-doped FeSe model (2-Fe unit cell) for the spin-orbit interaction $\lambda_{SOI}=0.1\text{eV}$. (b) The fully-gapped s_{++} -wave gap structure due to orbital fluctuations. The obtained gap anisotropy is consistent with the reports by ARPES studies. (c) The nodal d-wave gap structure due to spin fluctuations, which is not realized since the eigenvalue is just $\lambda_E=0.02$.

References

1. S. Onari and H. Kontani, Phys. Rev. Lett. 109, 137001 (2012)
2. S. Onari, Y. Yamakawa and H. Kontani, Phys. Rev. Lett. 112, 187001 (2014)
3. H. Kontani and Y. Yamakawa, Phys. Rev. Lett. 113, 047001 (2014).
4. Y. Yamakawa, S. Onari and H. Kontani, arXiv:1509.01161
5. S. Onari, Y. Yamakawa and H. Kontani, arXiv:1509.01172.
6. Y. Yamakawa and H. Kontani, Phys. Rev. Lett. 114, 257001 (2015).
7. M. Tsuchiizu, Y. Yamakawa and H. Kontani, arXiv:1508.07218.
8. M. Tsuchiizu et al, Phys. Rev. Lett. 111, 057003 (2013)
9. Y. Yamakawa, S. Onari and H. Kontani, in preparation.
10. H. Kontani and S. Onari, Phys. Rev. Lett. 104, 157001 (2010).

Inhomogeneous state of the Mn doped topological insulator Bi_2Te_3



V. Sakhin, E. Kukovitskii, N. Garif'yanov, Yu. Talanov and
G. Teitel'baum^{*,*},
E.K. Zavoiskii Institute for Technical Physics, Kazan, Russia

Email: **grteit@kfti.knc.ru*

Keywords: topological insulators, magnetic impurities, ESR

The evolution of topological insulators properties upon doping by the magnetic ions is one of the hot topics at their studies. While at low doping the topological insulators remain stable to such perturbations at higher doping a kind of ferromagnetic ordering takes place [1]. The important details of such ordering such as possibility of different textures existence together with their characteristic space and time scales are still unknown.

We report the results of ESR studies of Mn doped single crystals Bi_2Te_3 which reveal the strong changes of the resonance line depending on the dopants' concentration. The characteristic behavior of the Mn resonance gives evidence of the ferromagnetic ordering for 5% amount of Mn ions with the Curie temperature $T_c \sim 11$ K (additional confirmation follows from the parallel SQUID measurements of susceptibility). Interestingly that the corresponding signal typical for ferromagnetic resonance was observable also at temperatures much higher than T_c (at least up to 45 K). Such a behavior may be due to the phase separation to coexisting ferromagnetic and nonmagnetic microscopic sub-phases. The signal intensity was considerably decreasing upon heating from T_c up to 45 K revealing that the relative fraction of the ferromagnetic-like sub-phase experiences suppression in this temperature interval. Given that the electrons scattering by the ordered Mn ions is weaker than by disordered ones the coexistence of the magnetically disordered and ferromagnetic phases was also documented by the behavior of resistivity which increased gradually in the same temperature range.

It is worth noting that the problem of different magnetic structures coexisting with the surface topological phases is a matter of intense discussions [2]. Its solution may open the possibility of the topological currents processing via the pumping of the doped ions spin resonance.

This work is supported by RFBR through the Grant № 15-42-02477.

References

1. Y. S. Hor et al., Phys. Rev., B 81 (2010) 195203
2. J. Henk et al., Phys. Rev. Lett., 108, 206801 (2012).

Superparamagnetism at oxide interfaces revealed by scanning SQUID-on-tip microscopy



Y. Anahory¹, L. Embon¹, C. J. Li², S. Banerjee¹, A. Meltzer¹,
H. R. Naren¹, A. Yakovenko¹, J. Cuppens¹, Y. Myasoedov¹,
M. L. Rappaport¹, M. E. Huber³, K. Michaeli¹
T. Venkatesan², Ariando² and E. Zeldov¹

¹Weizmann Institute of Science

²National University of Singapore

³University of Colorado Denver

Email: y.anahory@gmail.com

Keywords: Complex oxide interfaces, magnetism, Scanning SQUID microscopy

NanoSQUIDs residing on the apex of a quartz tip (SOT), suitable for scanning probe microscopy with record size, spin sensitivity, and operating magnetic fields, are presented[1]. We have developed SOT made of Pb with an effective diameter of 46 nm and flux noise of $\Phi_n = 50 \text{ n}\Phi_0/\text{Hz}^{1/2}$ at 4.2 K that is operational up to unprecedented high fields of 1 T[1]. The corresponding spin sensitivity of the device is $S_n = 0.38 \mu_B/\text{Hz}^{1/2}$, which is about two orders of magnitude more sensitive than any other SQUID to date.

This technique is used to study nanoscale magnetism present in systems such as atomically sharp oxide heterostructures (Figure 1a). These systems exhibit a range of novel physical phenomena that do not occur in the parent bulk compounds. The most prominent example is the appearance of highly conducting and superconducting states at the interface between the band insulators LaAlO₃ and SrTiO₃. Here we report a new emergent phenomenon at the LaMnO₃/SrTiO₃ interface in which an antiferromagnetic insulator abruptly transforms into a magnetic state that exhibits unexpected nanoscale superparamagnetic dynamics. Upon increasing the thickness of LaMnO₃ above five unit cells, our scanning nanoSQUID-on-tip microscopy shows spontaneous formation of isolated magnetic islands of 10 to 50 nm diameter, which display random moment reversals by thermal activation or in response to an in-plane magnetic field[2]. Our charge reconstruction model of the polar LaMnO₃/SrTiO₃ heterostructure describes the sharp emergence of thermodynamic phase separation leading to nucleation of metallic ferromagnetic islands embedded in an insulating antiferromagnetic matrix (Figure 2a). The model further suggests that the nearby superparamagnetic-ferromagnetic transition can be gate tuned, holding potential for applications in magnetic storage and spintronics.

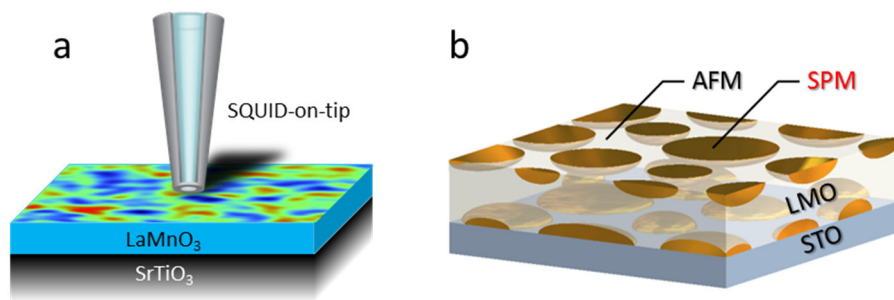


Figure 1: (a) Scanning SQUID-on-tip microscopy setup (b) Schematic representation of hole-doped and electron-doped SPM islands in the case of electron transfer from Mn^{3+} orbitals at the top surface of LMO.

References

1. D. Vasyukov, Y. Anahory, L. Embon, D. Halbertal, J. Cuppens, L. Neeman, A. Finkler, Y. Segev, Y. Myasoedov, M. L. Rappaport, M. E. Huber, and E. Zeldov, *Nature Nanotech.* 8, 639 (2013)
2. Y. Anahory, L. Embon, C. J. Li, S. Banerjee, A. Meltzer, H. R. Naren, A. Yakovenko, J. Cuppens, Y. Myasoedov, M. L. Rappaport, M. E. Huber, K. Michaeli, T. Venkatesan, Ariando and E. Zeldov, arXiv:1509.01895

Metallic Superfluids and Superconducting Superfluids in “metallic hydrogen”-type systems



Egor Babaev¹

¹*Department of Theoretical Physics the Royal Institute of Technology Stockholm, Sweden*

Email: babaevgor@kth.se

Keywords: Metallic Hydrogen, superconducting hydrogen alloys

Currently known super states of matter are classified as superfluid liquids, gases superconductors and supersolids. I will discuss, that “liquid metallic hydrogen-type” systems (i.e. metallic states of hydrogen or deuterium or their alloys with potential Cooper pairing instabilities for protons or condensation of deuterons) can allow states that cannot be categorized exclusively as a superconductor or superfluid but rather represent different “super” state of matter [1]. Also they can form states that combine superconductivity and superfluidity, while violating their common properties such as Onsager's superfluid velocity quantization [2], London's electrodynamics [3]

References

1. E Babaev, A Sudbø, NW Ashcroft Nature 431 (7009), 666-668
2. E Babaev, NW Ashcroft Nature Physics 3 (8), 530-533
3. Egor Babaev, Ludvig D Faddeev, Antti J Niemi Phys. Rev. B 65, 100512(R) (2002)

Superconducting and pseudogap energy scales of cuprates intertwined by charge ordering



E.V.L. de Mello^{1,*}, J.E. Sonier²

¹*Universidade Federal Fluminense, Niterói, Brazil*

²*Simon Fraser University, Burnaby, British Columbia V5A 1S6, Canada,* ³*Canadian Institute for Advanced Research, Toronto, Ontario M5G 1Z8, Canada.*

Email: * evandro@if.uff.br

Keywords: high T_c , nano-clusters, shell structure, [Times 11]

The electronic states of cuprate high-temperature superconductors are influenced by distinct energy gaps associated with superconducting (SC) and normal-state pseudogap (PG) phases. The exact connection between charge ordering (CO) and the superconductivity is one of the most important problem of high temperature superconducting physics. We have developed a phenomenological model that links the two distinct energy scales of the SC and PG phases via CO. We show that simulated static "checkerboard" charge-order modulations resembling those observed in $\text{Bi}_{2-y}\text{Pb}_y\text{Sr}_{2-z}\text{La}_z\text{CuO}_{6+x}$ [(Pb, La)-Bi2201]¹ yield free energy density modulations that intertwine the SC and charge orders by localizing charge and providing the energy scale for the SC attractive potential. Our model reproduces the values of the PG onset temperature T^* , and with the inclusion of Josephson coupling between the segregated nanoscale SC domains², the SC transition temperature T_c of underdoped (Pb, La)-Bi2201 samples.

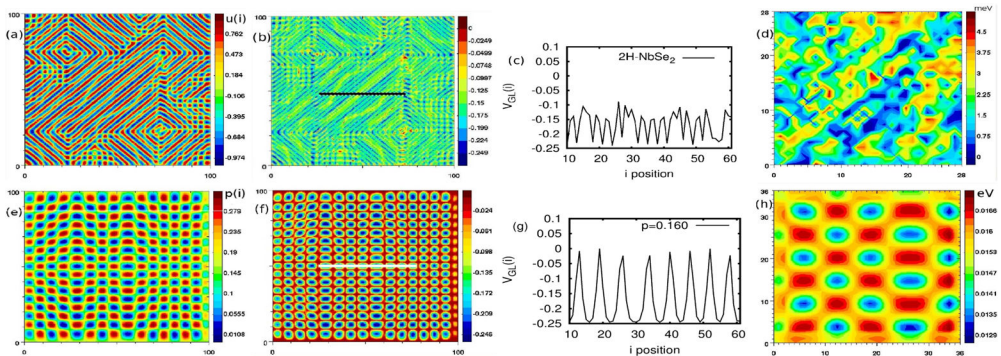


Figure 1: Top panels are simulations of 2H-NbSe₂: a) the order parameter $u(i)$ map with uniaxial stripe ordering on a 100×100 square lattice. b) The $V_{GL}(i)$ map with the same ordering on the same location and in (c) along the black straight line drawn to clarify the modulations. d) The local SC amplitudes $\Delta_s(i)$ on a 28×28 square in the middle of panel a) with the constraint $\langle \Delta_s(T \approx 0 \text{ K}) \rangle \sim 2.5$ meV from ARPES. Low panels are the simulations for $p = 0.16$ (Pb, La)-Bi2201. e) is similar to a) but instead of $u(i)$ we plot the equivalent local doping $p(i)$. The related local $V_{GL}(i)$ with the same ordering is plotted in g) and again panel g) has $V_{GL}(i)$ along the white line along seven “tiles”. On panel h) the local SC amplitudes $\Delta_d(i)$ on a 36×36 square in the middle of panel e) with the average $\langle \Delta_d(T \approx 0 \text{ K}) \rangle \sim 15$ meV according with the STM data.¹

References

- 1.W. D. Wise *et al.*, Nat. Phys. **4**, 696 (2008).
- 2.E.V.L. de Mello, Europhys. Lett. **98**, 57008 (2012)

Spin excitations used to probe the nature of the magnetically ordered ground state of the CE-type phase of charge ordered manganites



Toby Perring^{1,2*}, *, Russell Ewings¹, Graeme Johnstone³, Olga Sikora⁴, Doug Abernathy⁵, D. Prabhakaran³, Alexander Komarek⁶, Y. Tomioka⁷, Andrew Boothroyd³, Yoshi Tokura⁸
¹*ISIS Facility, STFC Rutherford Appleton Laboratory, UK*
²*London Centre for Nanotechnology, UCL, London, UK*
³*Department of Physics, University of Oxford, UK*
⁴*Department of Physics, University of Bristol, UK*
⁵*SNS, Oak Ridge National Laboratory, USA*
⁶*Max Planck Institute CPfS, Dresden, Germany*

⁷*Electronics and Photonic Research Institute, AIST, Tsukuba, Japan*

⁸*Department of Applied Physics, University of Tokyo, Japan*

Email: * toby.perring@stfc.ac.uk

Keywords: Colossal magnetoresistance, manganites, CE order

There has been a debate in recent years as to the true electronic ground state in the CE-type antiferromagnetic phase in materials related to the colossal magnetoresistive manganites. The widely assumed picture is the Goodenough model of a checkerboard lattice of nominal Mn^{3+} and Mn^{4+} ions, with the CE-type antiferromagnetic order arising from the Goodenough-Kanamori rules, and which receives support from model calculations on the doubly degenerate exchange (DDEX) model [1]. The possibility of dimerisation, where pairs of Mn ions form Mn_2^{7+} units has also been proposed, and can arise in extensions to the DDEX model that include interactions with the lattice [2], as well as the DDEX model itself away from half-doping i.e. nominal $\text{Mn}^{3.5+}$ valence. We will report the results of inelastic neutron scattering measurements throughout the Brillouin zone on the single layer, bilayer, and (pseudo-)cubic manganites $\text{Pr}_{0.5}\text{Ca}_{1.5}\text{MnO}_4$ [3], $\text{Pr}(\text{Sr}_{0.1}\text{Ca}_{0.9})_2\text{Mn}_2\text{O}_7$ [4] and $\text{Pr}_{0.5}\text{Ca}_{0.5}\text{MnO}_3$ [5]. We find that in all cases the Goodenough model provides the best description of the spin wave excitations, so long as further neighbour interactions along the weakly interacting quasi-one-dimensional ferromagnetic chains that make up the CE-type structure are included. The limiting case of strongly bound Mn ions, that is, the Zener polaron picture, can be eliminated on the basis of gross features in the spin wave spectra. A more realistic model of weak dimerisation can describe the spin wave dispersion in these materials, but is incompatible with the wavevector dependency of the spin wave structure factors. The results are consistent with the DDEX model, and the analysis provides a recipe for how to interpret future measurements away from half-doping, where DDEX models predict more complex ground states.

References

1. D.V. Efremov et al., Nature Materials 3 853 (2004)
2. P. Barone et al., Phys Rev B 83 233103 (2011)
3. T.G. Perring et al., unpublished
4. G.E. Johnstone et al., Phys Rev Lett 109 237202 (2012)
5. R.A. Ewings et al., submitted to Phys Rev B

Structural and magnetic properties and phase transitions in the iron chalcogenides



S. Wirth^{*}, ^{*}S. Rößler¹, C. Koz¹, L. Jiao¹, P. Materne², H. H. Klauss², D. Cherian³, S. Elizabeth³, U. K. Rößler⁴, and U. Schwarz¹

¹MPI Chemical Physics of Solids Dresden, Germany

²Department of Physics, TU Dresden, Germany

³Department of Physics, Indian Institute of Science, Bengaluru, India

⁴IFW Dresden, Germany

Email * wirth@cpfs.mpg.de

Keywords : phase transitions – phase diagrams –precursor state

The so called 11 family of materials is the structurally simplest version of the iron-based super-conductors. Nonetheless, many physical properties are strongly influenced by subtle changes in the crystal structure and stoichiometry. In particular, the interstitial Fe plays a crucial role.

FeSe, a superconductor with a critical temperature $T_c \approx 8.5$ K, displays a structural transition at $T_s \approx 87$ K below which the fourfold rotational symmetry is broken. We combine investigations of its electronic properties through scanning tunneling microscopy/spectroscopy (STM/STS), magnetization, and electrical transport measurements [1]. Our results indicate the existence of two energy scales. At a temperature $T^* \approx 75$ K we observed an onset of electron-hole asymmetry in STS, enhanced spin fluctuations, and increased positive magnetoresistance. At a lower temperature $T_0 \approx 22 - 30$ K a partial gap of about 8 meV opens up in STS and Kohler's rule is recovered. We interpret these results as the onset of an incipient ordering mode at T^* and its nucleation below T_0 . This ordering mode is observed in the spin and charge channel, suggesting a coupling between the spins with charge or orbital degrees of freedom.

Instead of superconductivity, Fe_{1+y}Te exhibit a complex interplay of magnetic and structural phase transitions in dependence on the excess amount of Fe. Detailed structural, thermodynamic and magnetic measurements resulted in a complex temperature-composition phase diagram [2] to which the temperature-pressure phase diagram shows several similarities [3]. A detailed analysis of the second-order phase transition for $y \geq 0.11$ within Landau theory reveals a violation of the Lifshitz condition, which calls for the occurrence of a precursor state [4]. Such precursor phenomena have been observed by Mössbauer spectroscopy [4].

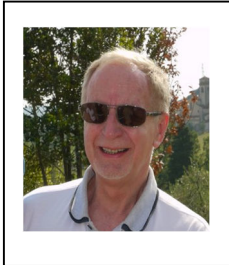
In addition to the end members, the interplay of structure, magnetism and superconductivity in $\text{Fe}_{1+y}\text{Te}_{1-x}\text{Se}_x$ has been investigated [5] and the resulting phase diagram will be discussed. We also investigate the influence of Co and Ni doping in

Fe_{1+y}Te on its physical properties [6].

References

1. S. Röbber, C. Koz, L. Jiao, U. K. Röbber, F. Steglich, U. Schwarz, and S. Wirth, *Phys. Rev. B* **92**, 060505(R) (2015).
2. C. Koz, S. Röbber, A. A. Tsirlin, S. Wirth, and U. Schwarz, *Phys. Rev. B* **88**, 094509 (2013).
3. C. Koz, S. Röbber, A. A. Tsirlin, D. Kasinathan, C. Börrnert, M. Hanfland, H. Rosner, S. Wirth, and U. Schwarz, *Phys. Rev. B* **86**, 094505 (2012).
4. P. Materne, C. Koz, U. K. Röbber, M. Doerr, T. Goltz, H. H. Klauss, U. Schwarz, S. Wirth, and S. Röbber, *Phys. Rev. Lett.* **115**, 177203 (2015).
5. D. Cherian, S. Röbber, S. Wirth, and S. Elizabeth, *J. Phys.: Condens. Matter* **27**, 205702 (2015).
6. C. Koz, S. Röbber, A. A. Tsirlin, C. Zor, G. Armagan, S. Wirth, and U. Schwarz, *Phys. Rev. B* **93**, 024504 (2016).

Novel Strongly-Correlated Ground States and Enhanced Multiband Electron-Hole Superfluidity in Graphene Structures



David Neilson
University of Camerino, Italy

Email: *david.neilson@unicam.it

Keywords: Graphene, High T_c Superfluid, Nanoribbons, Multiband superfluidity, BCS - BEC crossover

With graphene and related atomically thin crystals, we are at an exciting many-body threshold to realise and exploit novel quantum phases with tuneable properties. High quality, atomically flat two-dimensional electron graphene sheets and quasi-one-dimensional electron graphene nanoribbons, both with tuneable electron densities and band gaps, can exhibit novel phenomena that are driven by strong many-body correlations. These phenomena switch in when average Coulomb interactions between the electrons become dominant over their Fermi energies. Certain configurations of double graphene sheets[1-4] or double nanoribbons[5], one doped with electrons and the other with holes, should generate new strongly-correlated ground states, including a high density Wigner crystal[6], density-modulated charge density waves[6], as well as electron-hole superfluid states characterised by large superfluid energy gaps >100 meV. Such a superfluid is multiband, and it will exhibit novel BCS - BEC crossover effects[7].

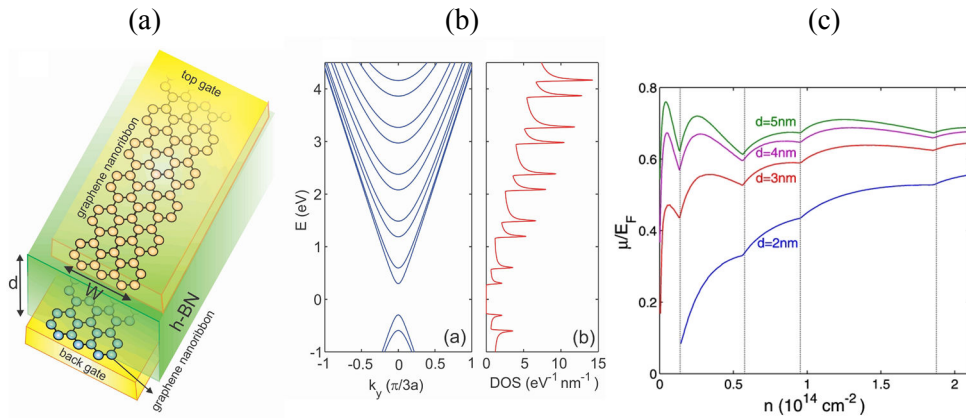


Figure 1: (a) Upper electron-doped and lower hole-doped armchair-edge terminated graphene nanoribbons separated by hexagonal-Boron Nitride insulator. (b) The low-lying single-particle energy subbands $\varepsilon_j(k_y)$, $j = 1, 2, \dots$ in an armchair graphene nanoribbon of width 2 nm, and the corresponding density of states. The van Hove singularities are visible at bottom of each subband. (c) The ratio of chemical potential μ to Fermi energy E_F as function of density n . d is thickness of insulating barrier separating the nanoribbons. The width of the nanoribbon is 2 nm. Note the shape resonance effects whenever E_F enters the bottom of a subband (vertical lines).

References.

1. A. Perali, D. Neilson and A. R. Hamilton, *High-Temperature Superfluidity in Double-Bilayer Graphene*, Phys. Rev. Letters **110**, 146803 (2013)
2. D. Neilson, A. Perali and A.R. Hamilton, *Excitonic superfluidity and screening in electron-hole bilayer systems*, Phys. Rev. B Rapid Comm. **89**, 060502(R) (2014)
3. M. Zarenia, A. Perali, D. Neilson, and F. M. Peeters, *Enhancement of electron-hole superfluidity in double few-layer graphene*, Sci. Reports **4**, 7319 (2014)
4. Luca Dell'Anna, Andrea Perali, Lucian Covaci, and David Neilson, *Using magnetic stripes to stabilize superfluidity in electron-hole double monolayer graphene*, Phys. Rev. B Rapid Comm. **92**, 220502(R) (2015)
5. M. Zarenia, A. Perali, F. M. Peeters, and D. Neilson, *Large gap electron-hole superfluidity and shape resonances in coupled graphene nanoribbons*, Sci. Reports (to appear)
6. David Neilson, Andrea Perali, and Mohammad Zarenia, *Many-body electron correlations in graphene*, J. Phys.: Conf. Series (to appear)
7. S. Conti, D. Neilson, and A. Perali (in preparation)

Role of local and itinerant magnetism in Fe-based superconductors



V. Ksenofontov^{1*}, S. Shylin¹, S. A. Medvedev², P. Naumov²,
G. Wortmann³, C. Felser²

¹*Institut für Anorganische und Analytische Chemie, Johannes
Gutenberg-Universität, Mainz, Germany*

²*Max-Planck-Institut für Chemische Physik fester Stoffe,
Dresden, Germany*

³*Department Physik, Universität Paderborn, Paderborn,
Germany*

Email: * v.ksenofontov@uni-mainz.de

Keywords: pairing mechanism, iron-based superconductors, Mössbauer effect, pressure

Many experimental facts provide evidence that antiferromagnetic spin fluctuations can mediate superconductivity acting as “glue” for Cooper pairs in Fe-based superconductors [1,2]. Our Mössbauer studies of FeSe intercalated with Li/NH₃ spacer layers with a superconducting transition temperature of $T_C = 43$ K support this idea [3]. They demonstrate that simultaneously with superconducting transition in ⁵⁷Fe Mössbauer spectra appears a magnetic subspectrum of dynamic nature. In this regard, this novel superconductor with its high T_C could be considered as a clue compound for the understanding of the principal mechanisms of superconductivity in Fe-based superconductors. From Mössbauer measurements follows that the intensity of the magnetic fraction scales with a transition curve when passing to the superconducting state. From other hand, conductivity measurements demonstrate that T_C decreases with increasing pressure. Taking into account this fact, a detailed Mössbauer study of FeSe intercalated with Li/NH₃ under pressure was performed using the ⁵⁷Fe-Synchrotron Mössbauer Source (SMS) at measuring line ID18 at ESRF. Pressure measurements with SMS revealed that both the amount of magnetic fraction and the frequency of the hyperfine magnetic field fluctuations do follow the variation of T_C with pressure. Pressure experiment confirmed that the superconducting pairing in FeSe-based superconductors is mediated by the antiferromagnetic spin fluctuations.

From other hand, existence of static non-compensated magnetic moments is incompatible with superconductivity. In the series of ⁵⁷Fe-SMS we performed also pressure studies of Cu-doped FeSe superconductor (20% ⁵⁷Fe-enriched Fe_{0.97}Cu_{0.04}Se). Doping of small amounts of Cu into the FeSe matrix suppresses superconductivity and introduces local static moments at the Fe sites, evidenced by glassy magnetic interactions [4]. Application of pressure leads to restoration of superconductivity in Cu-doped FeSe [5]. High-pressure studies of non-superconductive Fe_{0.97}Cu_{0.04}Se using the SMS revealed that this occurs because of the suppression of the static spin-glass state. Only nano-scale phase separation [6,7] of insulating vacancy-ordered antiferromagnetic and metallic non-magnetic FeSe-similar domains provides conditions for coexistence of static magnetism and superconductivity [8,9].

References

1. D. J. Scalapino, Rev. Mod. Phys. 84, 1383 (2012).
2. Y. Imai, et al., Phys. Rev. Lett. 102, 177005 (2009).
3. S. I. Shylin, et al., Europhys. Lett. 109, 67004 (2015).
4. A. Williams, et al., J. Phys.: Condens. Matter 21, 305701 (2009).
5. L. M. Schoop, et al., Phys. Rev. B. 84, 174505 (2011).
6. A. Ricci et al., Phys. Rev. B 84, 060511(R) (2011).
7. A. Ricci, et al., Supercond. Sci. Technol. 24, 082002 (2011).
8. V. Ksenofontov et al., Phys. Rev. B 84, 180508(R) (2011).
9. V. Ksenofontov et al., Phys. Rev. B 85, 214519 (2012).

Magnetism in Fe-based Superconductors - The Various Ways to Coexist



Hubertus Luetkens^{1*}

¹*Laboratory for Muon-Spin Spectroscopy, Paul Scherrer Institut, Villigen PSI, Switzerland*

Email: *hubertus.luetkens@psi.ch

Keywords: Fe-base superconductors, magnetism, coexistence

Magnetism and superconductivity are key elements in the electronic phase diagram of all unconventional superconductors, such as the high-T_c cuprates, heavy-fermion, organic and Fe-based superconductors. Muon spin rotation (μ SR) is a powerful tool for studying the exact nature of the transition from the antiferromagnetic to the superconducting phase in high-T_c superconductors as a function of a control parameter such as doping or pressure. In this context, it is of special advantage that μ SR, as a local probe, is sensitive to both the superconducting and magnetic volume fractions and to the respective order parameters, that fundamental microscopic parameters such as the magnetic penetration depth can be determined absolutely, and that μ SR is extremely sensitive to small-moment and short-range magnetic order.

From the very beginning of research on Fe-based superconductors in 2008, μ SR has contributed important information. It is widely recognized as one of the key techniques for investigating fundamental magnetic and superconducting properties, as well as testing for microscopic competition or coexistence of the magnetic and superconducting ground states.

Interestingly, in the electronic phase diagrams of Fe-based superconductors we find various ways of how the magnetic and superconducting order can coexist, namely in i) an electronically and structurally phase separated way, ii) with a competition about the volume, iii) with a competition about the magnetic moment, iv) a coexistence without competition, v) with magnetism as a necessary prerequisite for superconductivity and vi) with no coexistence at all.

In this talk, after a short introduction to μ SR, we will review our μ SR results [1-16] on the magnetic and superconducting properties of various families of Fe-based superconductors.

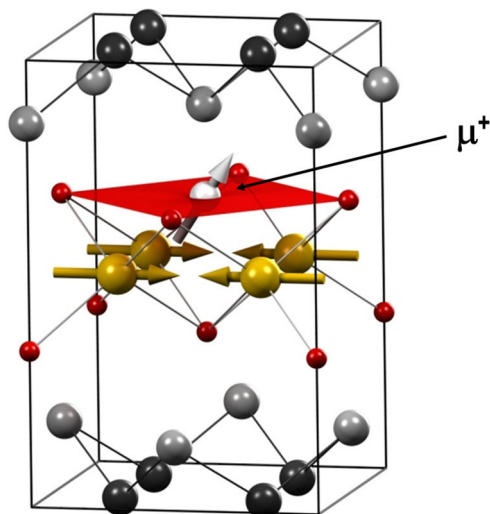
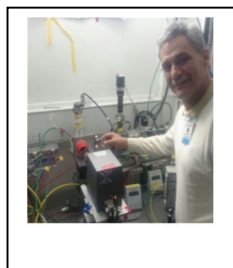


Figure 1: Schematic view of the muon acting as a local probe in a magnetic material (LaOFeAs). Muon spin rotation (μ SR) is based on the observation of the time evolution of the spin polarization of an ensemble of initially polarized muons implanted in a sample. The muon spins interact with the local magnetic field making it possible to extract information about its magnetic environment. μ SR is an extremely sensitive magnetic probe which can detect magnetic moments as low as $10^{-4}\mu_B$. Due to the local character of the measurement the method is sensitive to long range, short range and disordered magnetism as well as to the volume fractions in phase separated specimens.

References

1. H. Luetkens et al., Phys. Rev. Lett. 101, 097009 (2008).
2. H.-H. Klauss et al., Phys. Rev. Lett. 101, 077005 (2008).
3. H. Luetkens et al., Nature Materials 8, 305 (2009).
4. R. Khasanov et al., Phys. Rev. Lett. 102, 187005 (2009).
5. R. Khasanov et al., Phys. Rev. Lett. 103, 067010 (2009).
6. R. Khasanov et al., Phys. Rev. Lett. 104, 087004 (2010).
7. M. Bendele et al., Phys. Rev. Lett. 104, 087003 (2010).
8. Z. Shermadini et al., Phys. Rev. Lett. 106, 117602 (2011).
9. E. Wiesenmayer et al., Phys. Rev. Lett. **107**, 237001 (2011).
10. R. Khasanov et al., Phys. Rev. B **84**, 100501(R) (2011)
11. Z. Shermadini et al., Phys. Rev. B 85, 100501(R) (2012).
12. A. Jesche et al., Phys. Rev. B 86, 020501 (2012).
13. R. Frankovsky et al., Phys. Rev. B **87**, 174515 (2013).
14. T. Goltz et al., J. Phys.: Conf. Ser. 551 012025 (2014).
15. U. Pachmayr et al., Angew. Chem. Int. Ed. Engl. **54**, 293 (2015).
16. P. Materne et al., Phys. Rev. B **92**, 134511 (2015)

Resonant X-ray Inelastic Scattering and nanoscale inhomogeneity in $\text{FeSe}_{1-x}\text{Te}_x$



Jose Mustre de León Author^{1*}, Diego Mulato¹, Joshua Kaas², John Rehr²

¹ *Departamento de Física Aplicada, Cinvestav-Mérida, Mérida, Yucatán, México*

² *Physics Department, University of Washington, Seattle, Washington, USA.*

Email: * jmustre@cinvestav.mx

Keywords: Fe-based chalcogenide superconductors, x-ray inelastic scattering, x-ray absorption, x-ray emission

The evolution of the superconducting transition temperature, T_c , in the $\text{FeSe}_x\text{Te}_{1-x}$ system, under Te substitution presents a maximum for intermediate Te content. This observation suggests phase separation between FeSe and FeTe.[1] X-ray absorption near edge spectroscopy (XANES) results are consistent with an inhomogeneous electronic structure resulting from nanoscale phase separation of coexisting magnetic ordered region of FeTe and nonmagnetic FeSe.[1] However, details of electronic structure reflected in XANES are masked by core hole lifetime effects that broaden peaks related with those states. Resonant Inelastic X-ray Scattering (RIXS) can provide richer information about the electronic structure as it probes both unoccupied states above the Fermi level, and occupied states below. Thus it provides, more stringent tests of electronic structure inhomogeneity. However, until recently the interpretation of RIXS spectra could be done only in a rough qualitative approach [2]. We present calculations of RIXS spectra in $\text{FeSe}_x\text{Te}_{1-x}$ for $x=1, 0.75, 0.50, 0$. For these calculations we use a Density Functional Theory approach, based on a one-electron approximation that expresses the cross section as a result of the convolution of the x-ray absorption spectra and x-ray emission spectra. We have used structural models previously used in XANES interpretations, based on nanoscale phase separation between FeSe and FeTe.[2] These calculations show the same trends observed in experimental RIXS spectra (see figure 1). [3] We thus conclude that the electronic structure resulting from nanoscale phase separation is reflected both for excited states above the Fermi level and occupied valence band states.

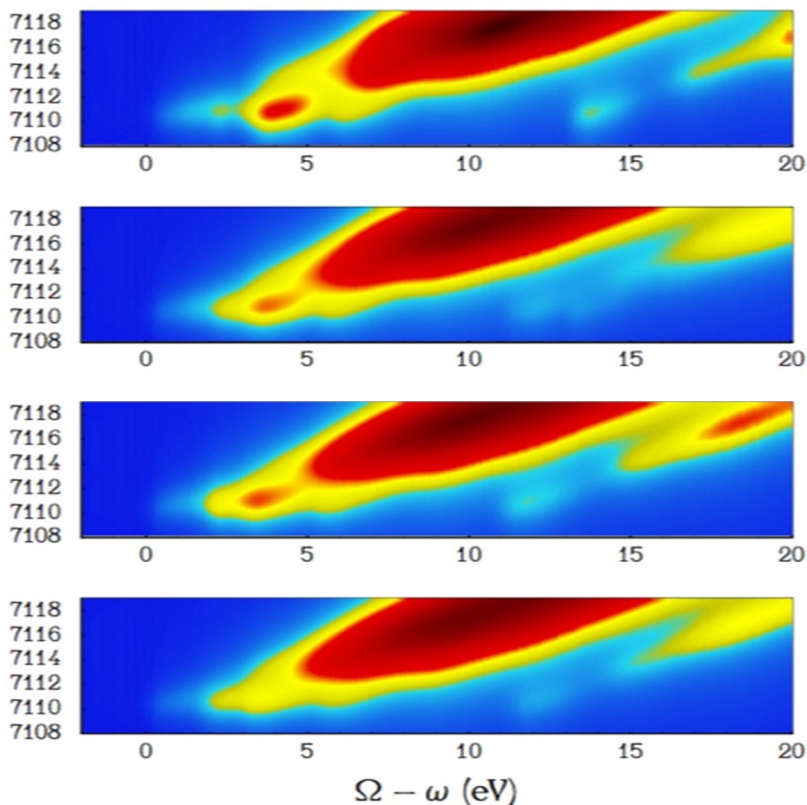


Figure 1: Calculated Spectra using a Density Functional Theory approach, compare with Figure 4 in Ref. 3.

References

1. D.C. Johnston, *Advances in Physics*, 59 803 (2010). DOI: 10.1080/00018732.2010.513480
2. A. Vega-Flick, J. Mustre de Leon, N.L. Saini, *Journal of Superconductivity and Novel Magnetism* 28, 1355 (2015). DOI: 10.1007/s10948-015-2955-3.
3. L. Simonelli, N. Saini, Y. Mizuguchi, Y. Takano, T. Mizokawa, G. Baldi, et al, *Journal of Physics: Condensed Matter* 24 415501(2012). DOI: 10.1088/0953-8984/24/41/415501.

Why is Manganese a poison for superconductivity in $\text{LaFeAsO}_{0.89}\text{F}_{0.11}$?



Samuele Sanna^{1*}, Matteo Moroni¹, Pietro Carretta,¹ Franziska Hammerath,^{1,2} Roberto De Renzi³, Gianrico Lamura⁴, Toni Shiroka,^{5,6} Rhea Kappenberger,² Sabine Wurmehl,² Mesfin A. Afrassa,² Anja U. B. Wolter,² Bernd Büchner²

¹ *Department of Physics, Pavia University, Pavia, Italy*

² *IFW-Dresden, Institute for Solid State Research, Dresden, Germany*

³ *Department of Physics and Earth Sciences, University of Parma*

⁴ *CNR-SPIN and University of Genova, Genova, Italy*

⁵ *Laboratorium für Festkörperphysik, ETH-Honggerberg, Zurich, Switzerland*

⁶ *Paul Scherrer Institut, CH-5232 Villigen PSI, Switzerland*

**Samuele.Sanna@unipv.it*

Keywords: interplay of Magnetism and Superconductivity, effect of magnetic impurities, effect of chemical pressure and strain effects

Superconductivity in the optimally electron doped $\text{LaFeAsO}_{0.89}\text{F}_{0.11}$ is fully destroyed by substituting Fe with a very tiny amount of 0.2% of Mn. Such an effect cannot be accounted for by charge doping, disorder or by a change of the band structure. This behaviour indicates that the mechanism here involved is directly and intrinsically linked to the puzzling mechanism driving unconventional superconductivity in the pnictides.

Here we study the evolution of the superconducting and magnetic state of $(\text{La}_{1-y}\text{Y}_y)(\text{Fe}_{1-x}\text{Mn}_x)\text{AsO}_{0.89}\text{F}_{0.11}$ by muon spin spectroscopy and nuclear magnetic and quadrupolar resonance (NMR/NQR) by combining the poisoning effect of Mn and the beneficial effect on T_c of the chemical pressure/strain via the La/Y substitution. The results show that as soon as superconductivity is destroyed by Mn an ordered magnetic state is established and the system is driven across a Quantum Critical Point [1, 2]. Conversely, the magnetic state is gradually destroyed by substituting La with the smaller Y and the corresponding changes in the band structure cause the recovery of superconductivity [2, 3]. NMR/NQR measurements and the comparison to DFT calculations [4, 5] indicate that the Fe/Mn substitution stabilizes a new type of magnetic state (possibly of Néel type) which competes with the $Q=(\pi, 0)$ stripe order. Here we argue that the superconducting pairing is assisted by stripe magnetic fluctuations which are progressively suppressed by Mn.

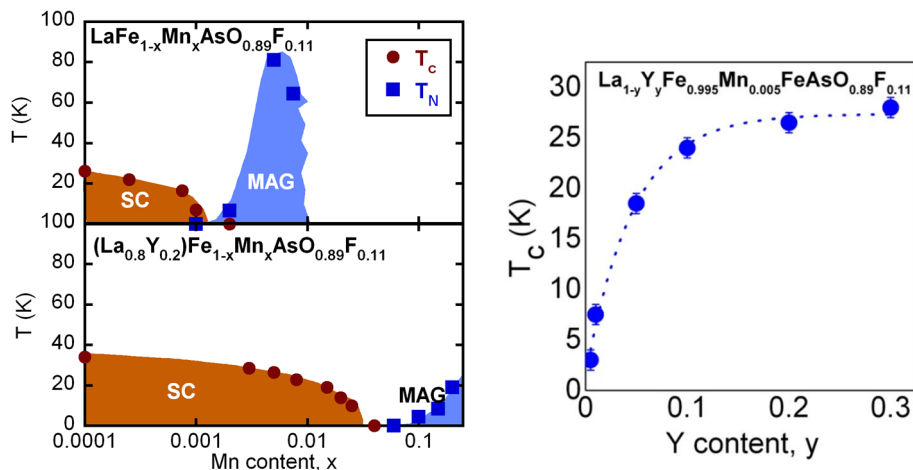


Figure 1: (left) Phase diagrams as a function of Mn content for $Ln\text{Fe}_{1-x}\text{Mn}_x\text{AsO}_{0.89}\text{F}_{0.11}$ for $Ln = \text{La}$ and $\text{La}_{0.8}\text{Y}_{0.2}$; (right) Superconducting transition T_c as a function of chemical pressure/strain via La/Y substitution. The Mn suppresses superconductivity (at 0.2% for $Ln=\text{La}$!) while La/Y substitution fully recovers it.

References

1. F. Hammerath, P. Bonfà, S. Sanna, G. Prando, R. De Renzi, Y. Kobayashi, M. Sato, and P. Carretta, Phys. Rev. B 89, 134503 (2014).
2. F. Hammerath, M. Moroni, L. Bossoni, S. Sanna, R. Kappenberger, S. Wurmehl, A. U. B. Wolter, M. A. Afrassa, Y. Kobayashi, M. Sato, B. B. uchner, and P. Carretta, Phys. Rev. B 92, 020505(R) (2015).
3. M. Moroni, et al. in preparation.
4. G. Giovannetti, C. Ortix, M. Marsman, M. Capone, J. van den Brink, and J. Lorenzana, Nat. Commun. 2, 398 (2011).
5. M. N. Gastiasoro and B. M. Andersen, Phys. Rev. Lett. 113, 067002 (2014).

Giant effect of isovalent doping on magnetism in $\text{BaFe}_2(\text{As}_{1-x}\text{P}_x)_2$



J. Pellicciari^{1*}, Y. Huang^{1,2}, K. Ishii³, M. Dantz¹, V. Strocov¹, X. Wang², L. Xing², C. Q. Jin², X. Lu¹, T. Watahige⁴, S. Kasahara⁴, T. Shibauchi^{4,5}, T. Das⁶, and T. Schmitt¹

¹Swiss Light Source, Paul Scherrer Institut, Switzerland

²Beijing National Lab for Condensed Matter Physics, Institute of Physics, China

³Spring-8, Japan Atomic Energy Agency, Japan

⁴Department of Physics, Kyoto University, Japan

⁵Department of Advanced Materials Science, Tokyo University, Japan

⁶Department of Physics, Indian Institute of Science, India

Email: *jonathan.pellicciari@psi.ch

Keywords: iron pnictides, magnetism, scattering, unconventional superconductivity

Superconductivity (SC) in iron pnictides was discovered in 2008 [1], and since then, a lot of effort has been devoted in order to explain their unconventionality. As in other high temperature superconductors (HTSCs), magnetism and SC exhibit proximity, competition and / or coexistence along the phase diagram, indicating strong connections between them [2, 3, 4]. In this context, the experimental characterization of static and dynamic magnetism is of vital importance in constraining advanced theoretical models. The $\text{BaFe}_2(\text{As}_{1-x}\text{P}_x)_2$ series is an interesting case because SC appears with isovalent doping without changing the number of carriers [2,4].

We present a combined Fe- L_3 Resonant Inelastic X-Ray Scattering (RIXS) and Fe- K_β X-rays emission spectroscopy (XES) study of parent and doped $\text{BaFe}_2(\text{As}_{1-x}\text{P}_x)_2$ spanning a large portion of the phase diagram as shown in Fig. 1a. RIXS measurements (sketch of the RIXS process in Fig.1b) reveal the persistence of broad dispersive magnetic excitations for all doping levels. Remarkably, the energy of such modes is strongly hardened by doping, contrasting with the case of hole-doped BaFe_2As_2 [6]. Moreover, their spectral weight is conserved along the phase diagram. Additional XES experiments (sketch of the XES process in Fig.1b) show, unexpectedly, a gradual quenching of the local magnetic moment. Employing theoretical calculations, we explain the trend observed for the magnetic moment as just partially arising from a deterioration of the Fermi surface nesting. On the other hand, the hardening trend observed for spin excitations originates from a gradual decrease of electronic correlation. We link this unconventional evolution of magnetism to the shift from 2- to 3-dimensional topology of the Fermi surface, manifested in the warping of the Fermi surface. The conservation of the spin excitations weight is confirmed in our calculations, showing a reshaping of the spin modes to higher energy.

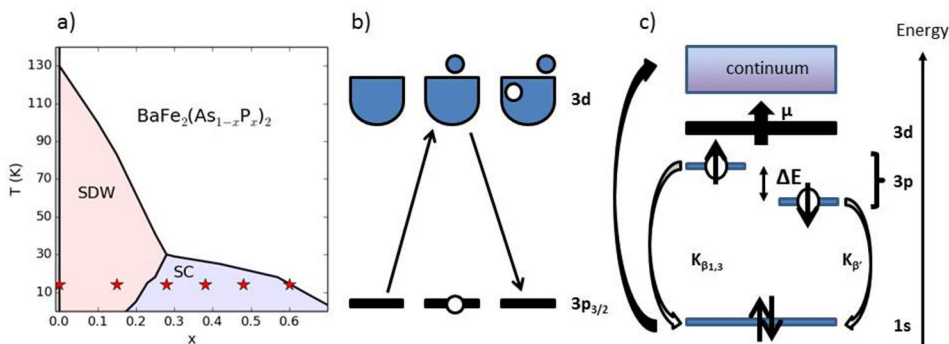


Figure 1: a) Phase diagram of $\text{BaFe}_2(\text{As}_{1-x}\text{P}_x)_2$. The stars represent the doping levels measured. b) Sketch of Resonant Inelastic X-Ray Scattering process. c) Sketch of K_β X-rays emission spectroscopy

References

1. Y. Kamihara et al, J. Am. Chem. Soc. 130, 3296 (2008)
2. G. R. Stewart, Rev. Mod. Phys., 83, 1589 (2011)
3. D. J. Scalapino, Rev. Mod. Phys., 84, 1383 (2012)
4. D. C. Johnston, Advances in Physics Vol. 59, No. 6, 803 (2010)
5. L. J. P. Ament et al, Rev. Mod. Phys. 83, 705 (2011)
6. K. J. Zhou et al, Nat. Comm., 4, 1470 (2013)

Orbital symmetry of charge density wave order and nematicity in $(\text{La},\text{M})_2\text{CuO}_4$



A. J. Achkar¹, M. Zwiebler², C. McMahon¹, F. He³,
R. Sutarto³, I. Djianto¹, Z. Hao¹, M. J. P. Gingras^{1,4,5},
M. Hücker⁶, G. D. Gu⁶, A. Revcolevschi⁷, H. Zhang⁸,
Y.-J. Kim⁸, J. Geck^{9*}, D. G. Hawthorn^{1,4}

¹*Department of Physics and Astronomy, University of Waterloo, Waterloo, Ontario N2L 3G1, Canada.*

²*Leibniz Institute for Solid State and Materials Research IFW Dresden, Helmholtzstrasse 20, 01069 Dresden, Germany.*

³*Canadian Light Source, Saskatoon, Saskatchewan, S7N 2V3, Canada.*

⁴*Canadian Institute for Advanced Research, Toronto, Ontario M5G 1Z8, Canada.*

⁵*Perimeter Institute for Theoretical Physics, 31 Caroline Street North, Waterloo, Ontario N2L 2Y5, Canada.*

⁶*Condensed Matter Physics and Materials Science Department, Brookhaven National Laboratory, Upton, NY 11973, USA.*

⁷*Synthèse Propriétés et Modélisation des Matériaux (SP2M), UMR 8182, Université Paris-Sud, 91405 Orsay Cedex, France.*

⁸*Department of Physics, University of Toronto, Toronto, Ontario M5S 1A7, Canada.*

⁹*Paris Lodron University Salzburg, Chemistry and Physics of Materials, Hellbrunner Strasse 34, 5020 Salzburg, Austria.*

Email: * jochen.geck@sbg.ac.at

Keywords: charge density wave, stripe order, high T_c , resonant scattering

The rich competition between superconductivity and spatial electronic order is an ubiquitous feature of the high-temperature superconducting cuprates. An important step towards a better understanding of these materials is therefore a detailed characterization of their inherent electronic ordering instabilities on the microscopic quantum level; a point that poses significant challenges and currently attracts large interest. Here we present a detailed study of the electronic order in prototypical $(\text{La},\text{M})_2\text{CuO}_4$ by means of resonant elastic x-ray scattering (REXS).

Exploiting the polarization dependence of REXS, we show that the charge density wave (CDW) order in $\text{La}_{1.875}\text{Ba}_{0.125}\text{CuO}_4$ has a predominant s'-symmetry, in contrast to the d-symmetry recently reported in other cuprate materials [1]. This identifies the CDW-symmetry as a key parameter, which distinguishes different cuprate families and may be directly related to the absence or presence of static spin order.

We also exploit the site-selectivity of REXS to probe the relation between the electronic nematicity in the CuO_2 -planes and structural distortions of the $(\text{La},\text{M})_2\text{O}_2$ -layers [2]. The experiments show that the structural distortions and the electronic nematicity display distinct temperature dependences, with only the latter being coupled

to the CDW order. The electronic nematicity is therefore distinct from a purely structural order parameter. In fact, our results together with previous reports clearly indicate that electronic nematicity may be a generic and intrinsic feature of underdoped cuprates.

References

1. *Orbital symmetry of charge-density-wave order in $La_{1.875}Ba_{0.125}CuO_4$ and $YBa_2Cu_3O_{6.67}$* , A. J. Achkar, F. He, R. Sutarto, Christopher McMahon, M. Zwiebler, M. Hucker, G. D. Gu, Ruixing Liang, D. A. Bonn, W. N. Hardy, J. Geck, and D. G. Hawthorn, Nature Materials, advance online publication (2016)
2. *Nematicity in stripe-ordered cuprates probed via resonant x-ray scattering*, A. J. Achkar, M. Zwiebler, Christopher McMahon, F. He, R. Sutarto, Isaiah Djianto, Zhihao Hao, Michel J. P. Gingras, M. Hucker, G. D. Gu, A. Revcolevschi, H. Zhang, Y.-J. Kim, J. Geck, and D. G. Hawthorn, Science **351**, 576 (2016)

Effective Hubbard Model of Spin Waves in Cuprates



Henrik M. Ronnow^{1*}, Noore Elahi Shaik¹, Bastien Dalla Piazza¹
¹Laboratory for Quantum Magnetism, Institute of Physics,
 EPFL, Switzerland

Email: * henrik.ronnow@epfl.ch

Keywords: cuprates, Hubbard model, spin waves

The arrival of high-resolution resonant inelastic X-ray scattering has made it possible to measure spin wave excitations in more families of cuprates than had been achieved with neutron scattering due to the required sample size and instrument time of the latter. To provide a unified parameterization of dispersions we employ an effective one-band Hubbard model with U , t , t' and t'' and project it to 4th order in hopping to produce a spin-Hamiltonian, from which spin-wave dispersions are calculated. The model is applied to describe dispersions in several undoped cuprates, including the stuffed CuO_2 lattice of tetragonal CuO and the half-stuffed lattice of $\text{Ba}_2\text{Cu}_3\text{O}_4\text{Cl}_2$. Finally I shall discuss the consequence of ionic motion and isotope effect on electronic hopping and magnetic interactions.

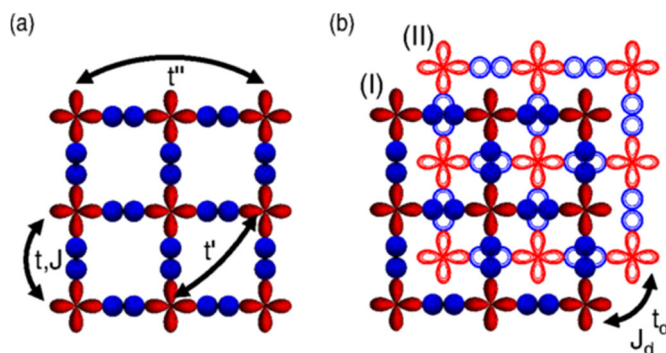


Figure 1: Hopping paths in CuO_2 lattice and the stuffed lattice of tetragonal CuO

References

1. M. Guarise *et al.*, Phys. Rev. Lett. **105**, 157006 (2010)
2. B. Dalla Piazza *et al.*, Phys. Rev. B **85**, 100508 (2012)
3. P. S. Haefliger *et al.*, Phys. Rev. B **89**, 085113 (2014)
4. S. Moser *et al.*, Phys. Rev. B **92**, 140404(R) (2015)

Macroscopic Quantum Tunneling in a Topological Josephson Junction



Thilo Bauch¹, Luca Galletti¹, Sophie Charpentier¹, Marco Arzeo¹, Gunta Kunakova¹, Dmitry Golubev², Floriana Lombardi¹

¹*Chalmers University of Technology, Department of Microtechnology and Nanoscience, 41296 Göteborg, Sweden*

²*Aalto University, Low Temperature Laboratory, 00076 Aalto, Finland*

Email: thilo.bauch@chalmers.se

Keywords: Topological Insulator, hybrid device, Josephson junction, Macroscopic Quantum Tunneling, Majorana Fermion

Abstract text here made of about 2500 characters including spaces (times new roman 11pt - normal) .

All material should fit in a maximum of 2 pages with format ISO B5.

Do not alter the fonts or size/color of the text. Such changes will be ignored and replaced with the standard.

References in square bracket [1] in the text.

Novel flavors on the superconducting proximity effect are recently coming from the integration of nanowires, or quasi-bi-dimensional systems, such as the surface states of topological insulators (TIs) [1,2], as the normal conductor in superconductor-normal conductor-superconductor (SNS) Josephson junctions. This is the case of the proximity effect through the conducting surface of a TI, where the transport through topologically protected states leads to a completely novel Josephson phenomenology, which should manifest neat fingerprints of Majorana fermions. These particles, which are their own antiparticles, are indeed expected to emerge in hybrid structures, involving the interface between a superconductor and a TI [1], or between a superconductor and a nanowire with strong spin-orbit interaction [2]. Superconducting hybrid structures are also considered a crucial step towards a topological quantum computer, which would be exceptionally well protected from errors, thanks to the non-Abelian statistics of Majorana fermions [3]. Therefore the realization of a topological quantum computer architecture based on S-TI-S Josephson junctions requires a thorough understanding of such junctions in the quantum limit.

However, up to now only the classical dynamics of S-TI-S Josephson junction has been investigated experimentally [4]. In this contribution we present measurements of the escape rate of the fictitious Josephson phase particle in Al-Bi₂Te₃-Al Josephson junctions as a function of temperature. For low enough temperatures we observe Macroscopic Quantum Tunneling (MQT) of the fictitious phase particle with a very pronounce temperature dependence of the MQT escape rate. Indeed, a highly transparent TI channel and S-TI interfaces can account for this at first contradictive

sounding phenomenon. We model our experimental findings using a generic expression of the current phase relation and standard expressions for the thermal and quantum limit of the phase dynamics. The fitted transmission probabilities clearly show that the TI surface states are highly transparent. This is the first fundamental step towards the understanding of Majorana physics in the quantum limit.

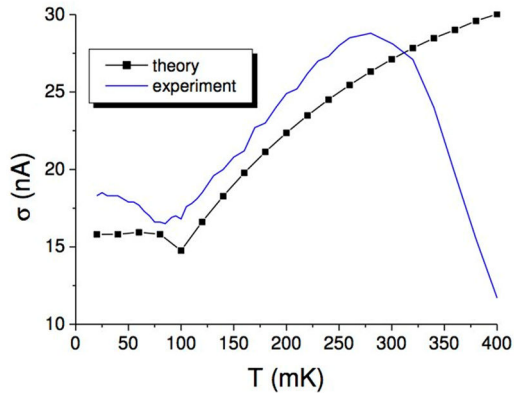


Figure 1: Width of the switching current distribution as a function of temperature. Solid blue line: experimental data. Squares: theoretical fit.

References

1. L. Fu and C. L. Kane, Phys. Rev. Lett. 100, 096407 (2008).
2. Y. Oreg, G. Rafael, and F. von Oppen, Phys. Rev. Lett. 105, 177002 (2010).
3. C. Nayak, S. H. Simon, A. Stern, M. Freedman, and S. Das Sarma, Rev. Mod. Phys 80, 1083 (2008).
4. L. Galletti et al., Phys. Rev. B 89, 134512, (2014).

Optical signatures of pair formation



J. Levallois¹, M. K. Tran¹, D. Pouliot², C. N. Presura³, L. H. Greene³, J. Eckstein², J. Uccelli¹, E. Giannini¹, G. D. Gu⁴, A. J. Leggett², and D. van der Marel^{1*},

¹*Université de Genève, Switzerland*

²*University of Illinois at Urbana-Champaign, USA*

³*Philips Research, Eindhoven, The Netherlands*

⁴*Brookhaven National Laboratory, USA*

Email: * dirk.vandermarel@unige.ch

Keywords: high T_c, Coulomb energy, optics

The basic understanding of pair formation in the conventional (i.e. BCS) model of superconductivity is, that electrons form pairs as a result of an attractive interaction. On general grounds one than expects the interaction energy to become reduced when the electrons form pairs, while at the same their kinetic energy increases. In this talk I will demonstrate that these two effects can be observed in the cuprate superconductors, that behave according to aforementioned trends for strongly overdoped cuprates, but that the observed effects have the opposite sign for underdoped and optimally doped cuprates. These observations compare favorably with published numerical calculations based on models of strong electron-electron correlation, not involving the vibrations of the lattice, and where the electron-electron interaction is purely repulsive.

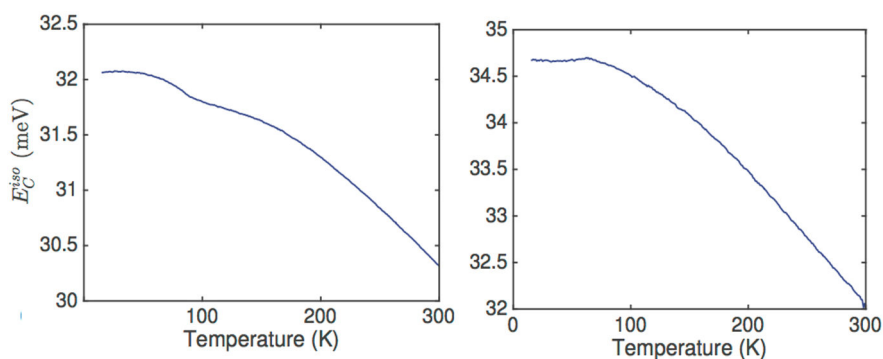


Figure 1: Partial Coulomb energy of underdoped (left) and overdoped (right) Bi2212 measured using spectroscopic ellipsometry.

References

1. J. Levallois, M.K. Tran, D. Pouliot, C.N. Presura, L.H. Greene, J.N. Eckstein, J. Uccelli, E. Giannini, G.D. Gu, A.J. Leggett & D. van der Marel; arXiv:1512.00672.

Sound velocity study of charge order across the phase diagram of YBCO



D. LeBoeuf^{1,*}, C. Proust¹, F. Laliberté¹, B. Borgnic¹, M. Frachet¹, J. Porras², T. Loew², M. Le Tacon², B. Keimer²

¹Laboratoire National de Champs Magnétiques Intense, CNRS, EMFL, France

²Max Planck Institut, Stuttgart, Germany

Email: * david.leboeuf@lncmi.cnrs.fr

Keywords: high T_c , charge order

In underdoped YBCO, short range charge density wave correlations appear well above the critical temperature T_c ^{1,2}. The charge modulations are mostly bidimensional. Below T_c , the application of a magnetic field causes change in the charge order and reveal a three dimensional and rather long range order, as seen by NMR³, sound velocity⁴ and x-ray measurements^{5,6}. Here we report a doping dependence of high fields ultrasonic measurements in underdoped YBCO to determine the phase diagram and the critical doping where charge order disappears.

References

1. G. Ghinringhelli *et al.*, Science 337 6096 (2012)
2. J. Chang *et al.*, Nat. Phys. 8 12 (2012)
3. T. Wu *et al.*, Nature 477 191 (2011)
4. D. LeBoeuf *et al.*, Nat. Phys. 9 79 (2013)
5. S. Gerber *et al.*, Science 350 949 (2015)
6. J. Chang *et al.*, preprint at arXiv :1511.06092 .

STM/STS studies for out-of-plane disorder effects on the charge order and pseudogap in $\text{Bi}_2\text{Sr}_{1.7}\text{R}_{0.3}\text{CuO}_{6+\delta}$ (R = La and Eu)

M. Oda,^{1*} T. Kurosawa,¹ K. Takeyama,² S. Baar,³ M. Kataoka,¹ S. Katsumata,¹ A. Kishi,¹ Y. Yonekawa,¹ S. Mizuta,¹ H. Yoshida,¹ N. Momono,³ and M. Ido¹

¹*Department of Physics, Hokkaido University*

²*Department of Physics, Asahikawa Medical University*

³*Department of Applied Sciences, Muroran Institute of Technology*

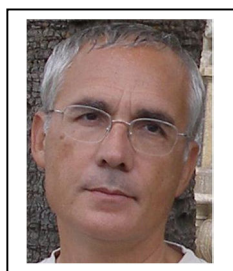
Email: *moda@sci.hokudai.ac.jp

Keywords: high T_c , charge order, pseudogap

STM/STS experiments were performed at 8 K in $\text{Bi}_2\text{Sr}_{1.7}\text{R}_{0.3}\text{CuO}_{6+\delta}$ (R-Bi2201) systems that had nearly optimal (OP) hole-doping levels ($p \sim 0.17$) but different T_c values, 35 K for R=La and 20 K for R=Eu, and examined out-of-plane disorder effects on the electronic charge order (CO) and energy gaps. The present results on the energy gaps are consistent with the following findings obtained by ARPES in OP R-Bi2201: as out-of-plane disorders, caused by the substitution of R^{3+} ions for Sr^{2+} sites, are strengthened by replacing La^{3+} with Eu^{3+} , the antinodal region on the Fermi surface (FS), mainly responsible for the pseudogap (PG), extends, while the nodal region or the so-called “Fermi arc” (FA), mainly responsible for the SC gap, shrinks, leading to the reduction in T_c .¹ For the CO, it has been demonstrated that the period \square remains unchanged with the strengthening of out-of-plane disorders, which strongly affect the electronic system of the Cu-O plane while maintaining the hole-doping level; $\square \sim 5a$ for nearly OP and $4a$ for $p \sim 0.1$ (a : the lattice constant along the Cu-O bond directions).² This finding suggests that the hole-doping level may be an essential factor for determining the period of the CO. We have also demonstrated some other interesting features of the CO such as the bias (energy) dependence of its intensity, the bias-polarity dependence of its intensity and phase, and the relation between \mathbf{Q}_{CO} and \mathbf{Q}_{AN} or \mathbf{Q}_{FAT} , which are the wavevectors for the CO, the antinodal nesting of the FS and the connection between the nearest neighbor tips of the FA, respectively.² On the basis of these findings, we will discuss the origin of the CO.

References

1. Y. Okada *et al.*, Phys. Rev. B **83**, 104502 (2011).
2. T. Kurosawa *et al.*, J. Phys. Soc. Jpn., in press (2016).

Local lattice distortions in NdFeAsO_{1-x}F_x pnictide

E. Liarokapis^{1*}, M. Calamiotou², N. D. Zhigadlo³, S. Katrysh³⁺, and J. Karpinski³⁺

¹*Department of Physics, National Technical University of Athens, GR15780, Athens, Greece*

²*Solid State Physics Department, Faculty of Physics, University of Athens, GR-15784 Athens, Greece*

³*Laboratory for Solid State Physics, ETH Zurich, 8093 Zurich, Switzerland*

+ *Present address: Institute of Condensed Matter Physics, EPFL, 1015 Lausanne, Switzerland*

Email: * eliaro@central.ntua.gr

Keywords: oxypnictides, phase transitions, synchrotron xrd, Raman spectroscopy

In a recent study of Sm1111 oxypnictides, a slight broadening of the (110) peak was found and attributed to an orthorhombic phase that is stable even in the near optimally doped system [1]. Anomalous behavior above T_c has been already found in some other studies; phonon and lattice modifications in oxygen deficient Nd1111 compound [2], [3], resistivity anomalies in the parent 1111 compounds [4], in NMR studies of SmFeAsO_{1-x}F_x [5], and in the photoexcited carriers of superconducting SmFe_{0.93}Co_{0.07}AsO single crystal that revealed an electronic nematicity around 170 K [6]. All these data show that even in the optimally doped 1111 compounds the electron-lattice system is modified at relatively high temperatures. Based on our previous findings of lattice anomalies at 180 K in NdFeAsO_{0.8} [3] and the assumption of a structural phase transition for the analogous superconducting compound SmFeAsO_{1-x}F_x [1], we have carried out detailed low temperature high resolution synchrotron diffraction and micro-Raman measurements on two samples of NdFeAsO_{1-x}F_x ($x=0.05$ and 0.25) looking for a possible structural phase transition that may occur in the optimally doped superconducting sample. No increase of the width of the (220) or (322) tetragonal diffraction peaks and microstrains could be found in the superconducting sample from the synchrotron XRD measurements. On the other hand, the atomic displacement parameters seem to deviate from the expected behavior, in agreement with modifications in the phonon width, as obtained by Raman scattering. These deviations occur around 150 K for both F doping levels, with distinct differences among the two compounds. The absence of magnetic effect in this temperature range for the superconducting compound does not support the association of the observed effect with spin ordering, but rather hints at the presence of lattice effects. We attribute the observed lattice anomalies to the formation of local lattice distortions that, being screened by the carriers, can only acquire long-range coherence by means of a structural phase transition at low doping levels. The similarities of the Raman spectra

in the Nd₁₁₁₁ and Sm₁₁₁₁ compounds, indicate that a similar effect happens in both systems and the hypothesis of a structural phase transition in the optimally doping oxypnictides requires further verification.

References

1. A. Martinelli et al., Phys. Rev. Lett. **106**, 227001 (2001).
2. E. Siranidi et al., J. Alloys Compd. **487**, 430 (2009).
3. M. Calamiotou et al., EPL **91**, 57005 (2010).
4. P. Chen et al, Phys. Rev. B **78**, 134508 (2008).
5. M. Majumder et al., J. Phys. Condens. Matter **25**, 025701 (2013).
6. T. Mertelj et al., Phys. Rev. B **87**, 174525 (2013).

Extreme broadening of the bond-stretching phonon in $\text{YBaCuO}_{7.8}$ below T_c using a new x-ray spectrometer



Alfred Q.R. Baron
Materials Dynamics Laboratory
RIKEN SPring-8 Center
1-1-1 Kouto, Sayou, Hyogo 679-5148

Email: baron@spring8.or.jp

Keywords: Phonons, Cuprate high-temperature superconductors, YBCO, electron-phonon coupling

High-resolution inelastic x-ray scattering (IXS) can be used to measure atomic motions at THz frequencies over angstrom-scale correlation lengths. While the required instrumentation is difficult to set up, dedicated facilities make the method available to the broader scientific community, and potentially of interest for anyone studying lattice dynamics, electron-phonon coupling, superconductivity, ferro-electricity/multi-ferroicity, phase transformations, magneto-elastic coupling, elasticity, or the dynamics of liquids or glasses. In particular, IXS allows access to tiny (~ 0.01 mm) samples so phonon measurements are possible on newly discovered materials, or in extreme conditions (e.g. $P > 100$ GPa, $T > 2000$ K). The speaker has been responsible for the design, construction, commissioning and operation of two IXS beamlines [1][2] at SPring-8 - introducing high-resolution IXS within Japan. A overview of IXS may be found in [3].

The main difficulty for IXS measurements of heavy materials is that they are badly flux limited. Whereas with neutrons, the absorption is very low so one can use large sample thickness (\sim cm) to increase rates, the rather short (~ 0.001 cm) penetration of x-rays means that signal rates from, say, cuprates are very low, especially for optical modes. For the past several years we have been making a new and extremely powerful IXS spectrometer based on a tailored 15m insertion device, which provides uniquely high flux ($\sim 2 \times 10^{10}$ /sec/0.8 meV) onto the sample. This has enabled us [4] to obtain clear temperature dependent measurements of the bond-stretching mode of optimally doped $\text{YBa}_2\text{Cu}_3\text{O}_{7.8}$ for the first time.

We find the bond-stretching phonon mode responds very strongly to the onset of superconductivity, beginning to broaden at T_c , and getting increasingly broader as the temperature is reduced - with an increase, at one momentum transfer, from a width ~ 7 meV at 100K, above $T_c \sim 93$ K, to a width of ~ 20 meV at 20K [4]. The momentum transfer where the line-width increases coincides with that where charge density wave (CDW) order appears in under-doped materials. This suggests a common origin that

evolves, with doping, from static competition with superconductivity into dynamical synergy.

References

1. A.Q.R. Baron, *et al.*, J. Phys. Chem. Solids **61**, 461 (2000)
2. A.Q.R. Baron, SPring-8 Inf. Newsl. **15**, 14 (2010), <http://user.spring8.or.jp/sp8info/?p=3138>
3. A.Q.R. Baron, in *Synchrotron Light Sources and Free Electron Lasers*, edited by E. Jaeschke, *et al.* (Springer Publishing, 2015)<http://arxiv.org/abs/1504.01098>
4. A. Q.R. Baron, D. Ishikawa, H. Uchiyama, T. Fukuda, T. Masui, R. Heid, K.-P. Bohnen, S. Miyasaka and S. Tajima, In Preparation.

Temperature dependence of penetration depth in presence of momentum-dependent CDW and superconducting order parameters



Eremin M.V., Sunyaev D.A.

Institute of Physics, Kazan Federal University, Russia.

meremin@kpfu.ru

Keywords: High-temperature superconductivity-charge density waves-magnetic penetration depth.

We derived an analytical expression for the temperature dependence of the penetration depth in the presence of external magnetic field in the regime of coexistence between charge density wave (CDW) and superconductivity (SC) beyond the effective mass approximation. In contrast to the previous studies, we included the momentum dependence of both CDW and superconducting order parameters. In particular, it was found that if the CDW gap depends on the momentum, the magnetic penetration depth is finite even above T_c , i.e., within the interval $T_c < T < T_{CDW}$.

The equation for the temperature dependence of the magnetic penetration depth (λ) was derived by computing the “current-current” Green’s function

$$\frac{1}{4\pi\lambda^2} = \left(\frac{e}{c\hbar}\right)^2 \left[\sum_{k,\sigma} \frac{\partial^2 \varepsilon_k}{\partial (k_x)^2} \langle a_{k,\sigma}^+ a_{k,\sigma} \rangle - 2\pi i \left(\frac{\hbar}{e}\right)^2 \langle \langle j_\alpha(-q) | j_\alpha(q) \rangle \rangle_{\omega \rightarrow 0, q \rightarrow 0} \right] \quad (1)$$

Here $\varepsilon_k = \sum_j t_{ij} \exp(ikR_{il})$ is the tight-binding quasiparticle energy dispersion,

$a_{k,\sigma}^+$, $a_{k,\sigma}$ are creation and annihilation operators, $j_\alpha(q)$ is the current density operator given by

$$j_x(q) = -\frac{e}{2\hbar} \sum_{k,\sigma} \left[\frac{\partial \varepsilon_k}{\partial k_x} + \frac{\partial \varepsilon_k}{\partial (k_x + q_x)} \right] a_{k,\sigma}^+ a_{k+q,\sigma}. \quad (2)$$

In general, CDWs suppress the superfluid density in the SC state. This tendency is in qualitative agreement with experimental data. Unexpectedly, CDW with the k-dependent order parameter yields relatively small but finite superfluid density even above T_c . This result can be seen analytically from Eq (1), when one assumes $\Delta_k = 0$. Indeed, doing integration by part of the first term in (1) one gets:

$$\frac{1}{4\pi\lambda^2}\Big|_{\Delta_k=0} = \left(\frac{e}{c\hbar}\right)^2 \frac{1}{E_{1k} - E_{2k}} \left\{ - \left(\frac{\partial \varepsilon_k}{\partial k_x} - \frac{\partial \varepsilon_{k+Q}}{\partial k_x} \right) \frac{f(E_{1k}) - f(E_{2k})}{(E_{1k} - E_{2k})} \frac{(\varepsilon_k - \varepsilon_{k+Q})}{(E_{1k} - E_{2k})} \right. \\ \left. + \left[\left(u_k^2 \frac{\partial \varepsilon_k}{\partial k_x} + v_k^2 \frac{\partial \varepsilon_{k+Q}}{\partial k_x} \right) \frac{\partial f(E_{1k})}{\partial E} - \left(v_k^2 \frac{\partial \varepsilon_k}{\partial k_x} + u_k^2 \frac{\partial \varepsilon_{k+Q}}{\partial k_x} \right) \frac{\partial f(E_{2k})}{\partial E} \right] \right\} \left(\frac{\partial |D_k|^2}{\partial k_x} \right) \quad (3)$$

The superfluid density does not drops down to zero, when $\Delta_k = 0$, and its value

is proportional to the derivative $\frac{\partial |D_k|^2}{\partial k}$. This term originates from the

diamagnetic component of the current (first term in Eq. (1). In this particular case

$$u_k^2 = \frac{1}{2} \left[1 + \frac{\varepsilon_k - \varepsilon_{k+Q}}{E_{1k} - E_{2k}} \right], v_k^2 = \frac{1}{2} \left[1 - \frac{\varepsilon_k - \varepsilon_{k+Q}}{E_{1k} - E_{2k}} \right], \quad (4)$$

$$E_{1k,2k} = \frac{\varepsilon_k + \varepsilon_{k+Q}}{2} \pm \frac{1}{2} \sqrt{(\varepsilon_k - \varepsilon_{k+Q})^2 + 4|D_k|^2}.$$

The results of numerical calculations are discussed in the context of available experimental data for underdoped cuprates.

M.V.E. supported by the PPK Program of Kazan Federal University, No.1053_r.

Charge and current modulations in a spin-fermion model with overlapping hotspots



Konstantin Efetov^{1,2,3*}, Pavel Volkov¹

¹*Ruhr University Bochum, Germany*

²*National University of Science and Technology MISIS, Moscow Russia*

³*International Institute of Physics, Natal, Brazil*

Email: * Konstantin.B.Efetov@ruhr-uni-bochum.de

Keywords: high T_c , charge density waves, orbital currents, Pomeranchuk instability.

Several well-known phenomena in the hole-doped cuprates like breaking of the rotational invariance, appearance of the pseudogap, charge modulation and d-wave superconductivity occur on a low energy scale of hundreds Kelvin. As it is not quite clear how to obtain these phases in an unified way from microscopic models of cuprates, we consider a low-energy model of fermions interacting with close to critical antiferromagnetic excitations. In contrast to a standard spin-fermion model, we assume, in agreement with ARPES data, that the fermion spectrum in the antinodal region is shallow, such that the 8 hotspots merge at not very weak interaction into 2 antinodal hot regions. In addition to the interaction via antiferromagnetic fluctuations, a long range part of the Coulomb interaction reducing the superconducting transition temperature is taken into the consideration.

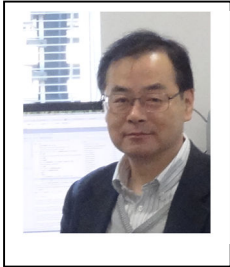
It is demonstrated in the mean field approximation that the strongest instability in this situation is a Pomeranchuk instability leading at temperatures $T < T_{\text{Pom}}$, where T_{Pom} is a critical temperature, to a deformation of the Fermi surface and breaking of the rotational symmetry. As a result, at $T < T_{\text{Pom}}$ the charges on the “vertical” and “horizontal” O-atoms of the CuO lattice are different from each other. Below T_{Pom} the Fermi surface remains ungapped and further phase transitions are possible.

Indeed, it turns out that a second critical temperature $T^* < T_{\text{Pom}}$ exists below which a d-wave excitonic insulator state with a gap in the antinodal region forms. It is characterized by orbital currents modulated with wave vectors $(\pm\pi/a_0, \pm\pi/a_0, \pm\pi/c_0)$, where a_0 and c_0 are lattice constants in the CuO plane and perpendicular to it, respectively, thus forming a 3D antiferromagnetic structure. This state is rather similar to the DDW-state but, in contrast to the latter, the orbital currents are modulated also in the c-direction. We identify this state with the pseudogap state in the cuprates. The gap in the fermionic spectrum of the pseudogap state is localized in the antinodal region and other instabilities of the ungapped parts of the Fermi surface are still possible.

We show that, in addition to the d-wave excitonic insulator, superconductivity and a charge density wave (CDW) can appear at temperatures $T_c, T_{\text{CDW}} < T^*$. Both the superconductivity and CDW have the d-wave symmetry. The d-wave symmetry of

CDW is enforced by the long range part of the Coulomb interaction. The modulation vector of CDW is directed along the direction of the nematicity and is incommensurate with both the spin modulation of the parent antiferromagnet and with the modulation of the orbital currents. The obtained symmetry corresponds to a stripe charge modulation on the O atoms along the bonds, while the charge on the Cu atoms is not modulated. Applying a magnetic field suppresses the superconductivity but stabilizes CDW. The results of our theory can serve as an explanation of recent experiments on cuprates performed with the help of STM, NMR, hard and resonant soft X-ray scattering, neutron scattering, sound propagation, and with some other techniques.

Enhanced charge excitations in electron-doped cuprates by resonant inelastic X-ray scattering



Takami Tohyama

Department of Applied Physics, Tokyo University of Science

Email: * tohyama@rs.tus.ac.jp

Keywords: high T_c , charge excitations, RIXS

Resonant inelastic x-ray scattering (RIXS) tuned for Cu L edge is a possible tool to detect momentum-dependent intra-orbital charge excitations in cuprate superconductors [1]. We theoretically investigate the possibility for observing the low-energy charge excitation with the same energy scale as spin excitation by RIXS [2]. We find that the core-hole Coulomb potential enhances the spectral weight of the charge excitation in electron-doped systems. Furthermore, from a large scale density-matrix renormalization group (DMRG) calculation, we find that the electron-doped system enhances small-momentum low-energy dynamical charge structure factor, whose energy is lower than that of spin excitation. This indicates a nontrivial mechanism of charge-spin coupling and superconductivity in electron-doped cuprates.

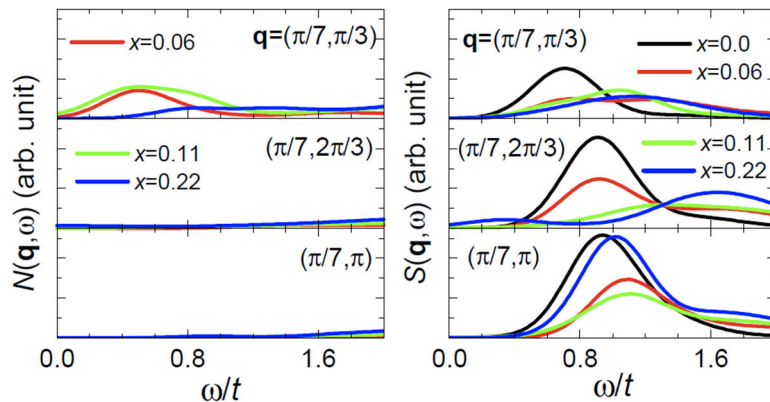


Figure 1: DMRG calculations of dynamical charge and spin structure factors of doped Hubbard model corresponding to electron-doped cuprates.

References

1. K. Ishii, M. Fujita, T. Sasaki, M. Minola, G. Dellea, C. Mazzoli, K. Kummer, G. Ghiringhelli, L. Braicovich, T. Tohyama, K. Tsutsumi, K. Sato, R. Kajimoto, K. Ikeuchi, K. Yamada, M. Yoshida, M. Kurooka and J. Mizuki, *Nat. Commun.* **5**, 3714 (2014).
2. T. Tohyama, K. Tsutsui, M. Mori, S. Sota, and S. Yunoki, *Phys. Rev. B* **92**, 014515 (2015)

Quantized Massive Gauge Fields and Hole-Induced Spin Glass Mechanism in Underdoped Cuprates

I. Kanazawa^{1*}, Takami Tohyama

T. Sasaki¹, R. Maeda¹

¹*Department of Physics, Tokyo Gakugei University*

Email: kanazawa@u-gakugei.ac.jp

Keywords: high T_c, massive gauge fields, freezing mechanism

Neutron scattering, muon spin relaxation, and nuclear magnetic-resonance experiments show that exists the phenomenon, generally interpreted in terms of glass spin freezing, in underdoped cuprates. Niedemayer et al. [1] found a very important result that the spin freezing temperature exhibits the same linear dependence on the planar hole content for LaSrCuO and YCaBaCuO in lightly doped system. Recently the present authors can introduce angle-resolved photoemission of the single- and double-layered Bi family [2] and Bi2201 [3] high-T_c superconductors, using quantized massive gauge fields, which might contain effects of spin fluctuations, charge fluctuations, and phonons. In this study, by using quantized massive gauge fields, we shall consider the freezing mechanism of the string-like aggregation of hole-induced hedgehog-like solitons in undoped high-T_c cuprates.

References

1. Ch. Niedemayer et al., Phys. Rev. Lett. **80**, 3843 (1998).
2. I. Kanazawa and T. Sasaki, Phys. Scr. **T165**, 014038 (2015).
3. I. Kanazawa and T. Sasaki, JPS Conf. Proc. **3**, 015016 (2014).

Switching between hidden states of electronic matter under non-equilibrium conditions



I.Vaskivskiy¹, L.Stojchevska¹, S.Brazovskii^{1,3}, M.Borovsak¹, V.Nesretinova¹, P.Kirchmann², D.Svetin¹, I.A. Mihailovic¹, J. Gospodaric¹, I. Fisher² and D.Mihailovic^{1*},
¹*Jozef Stefan Institute, Jamova 39, Ljubljana, Slovenia*
²*SLAC, Stanford University, California, USA*
³*Universite Paris Sud, Orsay, France*

Email: * dragan.mihailovic@ijs.si

Keywords: New states of matter, charge density waves, hidden states, ultrafast phenomena, complex matter.

The application of pressure, doping or external fields to complex materials under equilibrium conditions leads to familiar phase diagrams with intertwined ordered phases of matter. However, in such complex systems with competing interactions, completely new states of matter can be created under non-equilibrium conditions in areas of the free energy landscape that are not accessible under equilibrium conditions. Such non-equilibrium conditions are created by ultrafast quench with carefully tuned resonant femtosecond laser pulse excitation. Destruction-Pump-probe (DPP) spectroscopy is particularly useful for exploring different materials which potentially display such hidden states.

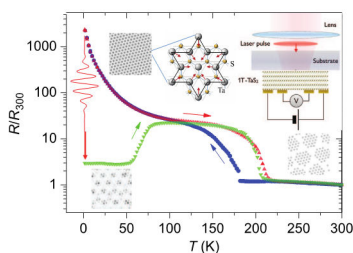


Fig. 1 The insulator-metal transition in 1T-TaS₂ caused by a single 35 fs laser pulse. The inserts show the schematic charge-density wave structure before and after switching and the sample configuration for measurement of optical switching and relaxation measurements [1,5].

Time-resolved DPP spectroscopy, STM, ARPES and XRD reveal common features of metastable hidden states created by short pulsed laser excitation. The most representative dichalcogenide TaS₂, with its exceptionally stable low-temperature state, has given us the most detailed information on the origin of hidden charge-density-wave states¹ and the ensuing mixing between localized and itinerant states (Fig.1). Both in-plane and out-of-plane ordering are found to be important. However other oxides, nitrides² and layered tri-chalcogenides³ also reveal dynamically broken symmetry states⁴, suggesting that such phenomena may be more common than previously imagined.

Of particular fundamental interest is the origin of the electronic metastability in these states, their control and relaxation mechanisms⁵, which can be controlled externally, by electrical pulses, strain, temperature or light pulses. The emerging mechanism is highly non-trivial, as shown by ultrafast (ps) electronic switching measurements which indicate a “running conversion” from localized to itinerant states as shown schematically in Fig. 3.

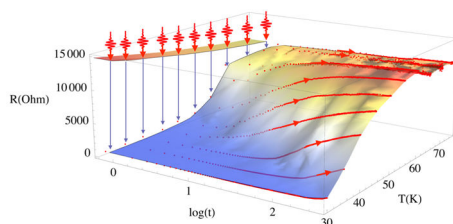


Fig. 2 The spontaneous metal-insulator transition in 1T-TaS₂ at different temperatures after switching by a single 35 fs laser pulse. The relaxation time is measured in seconds [5]. Relaxation can be enhanced or controlled by light [1], electrical pulses [6] or strain [5].

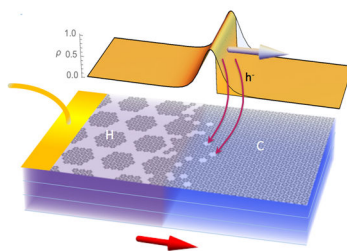


Fig.3 A schematic diagram of the switching mechanism by running conversion from from one CDW state to another.

These studies open new a dimension in the non-equilibrium landscape leading to entirely new states of hidden matter of general significance from cosmology to elementary particle physics. They have also raised interest in the applied community because of possible applications for ultrafast record-breaking low-temperature memristive memory devices⁶.

References

1. Stojchevska, L. *et al. Science***344**, 177–180 (2014).
2. Buh, J. *et al. Nat Comms***6**, 10250 (2015).
3. Yusupov, R. *et al. Nature Phys***6**, 681–684 (2010).
4. Mertelj, T. *et al. Phys Rev Lett***110**, 156401 (2013).
5. Vaskivskiy, I. *et al. Science Adv.* **1**, e1500168 (2015).
6. Vaskivskiy, I. *et al. arXiv:1409.3794* (2014), *ibid.*, *Nature Comms.* **7**, (2016).

Coupling of electronic excitations to boson modes in complex materials analyzed by femtosecond tr-ARPES



Uwe Bovensiepen^{1*}

¹University Duisburg-Essen, Faculty of Physics,
47048 Duisburg, Germany

Email: * uwe.bovensiepen@uni-due.de

Keywords: ultrafast dynamics, electronic and bosonic excitations, charge density wave materials

Pump-probe experiments using femtosecond laser pulses offer by now almost routine means to analyse electronic and bosonic excitations in the time domain. The current development aims on the one hand at specific pump excitations, e. g. in the mid infrared spectral regime. On the other hand quantitative methods are essential for probing the transient state in order (i) to obtain insight into the optically excited, non-equilibrium situation and (ii) to develop means to analyse the coupling of electronic and bosonic excitations in the time domain.

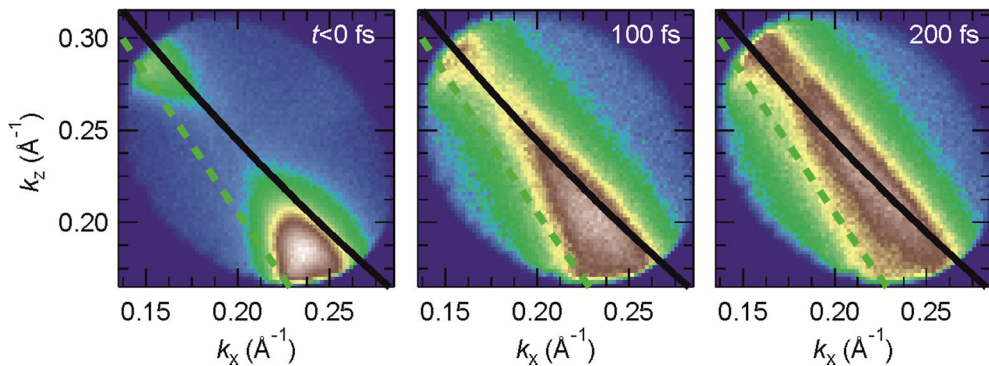


Figure 1: Time-dependent Fermi surface of DyTe₃ obtained by femtosecond time- and angle-resolved photoemission spectroscopy for various pump-probe delays in the CDW phase. The gapped Fermi surface ($t < 0$ fs) transforms within 200 fs into a continuous one, indicative of a metallic state. The black line indicates the Fermi surface predicted by tight binding calculations, the dashed green line includes back folding leading to shadow bands.

In this talk recent results of femtosecond tr-ARPES on charge density waves like tritellurides and dichalcogenides will be presented. As shown in Fig. 1 optical excitation using 800 nm femtosecond laser pulses results in closing of the charge density wave energy gap at the Fermi surface within 200 fs indicating dominant electron phonon interaction in the mechanism of charge density wave formation, see Ref. [1] for details. This finding is in good agreement with the time domain classification of charge density wave insulators [2] as well as the conclusions from static ARPES and tight binding modelling [3].

The results obtained for various pump excitation density indicate different regimes of dynamic charge density wave response. At rather low absorbed fluence of 0.1 mJ/cm^2 we find a harmonic oscillation of the gap in the electronic structure due to excitation of the amplitudon mode, which turns into a strongly non-harmonic variation for higher excitation density up to 0.4 mJ/cm^2 . The latter regime exhibits a persisting electronic gap which is explained by a competition between fluctuations in the electronically excited state, which tend to reduce order, and transiently enhanced Fermi surface nesting stabilizing the charge density wave order. The potential for manipulating the electronic structure by optical excitation in the non-equilibrium state will be discussed.

References

1. L. Rettig et al., Nat. Commun. **7**, 10459 (2016).
2. S. Hellmann et al., Nat. Commun. **3**, 1069 (2012).
3. R. Moore et al., Phys. Rev. B **81**, 073102 (2010).

Nonthermal ultra-fast dynamics in excitonic condensates



Martin Eckstein^{1*}

¹*Max Planck Research Department for Structural Dynamics,
University of Hamburg-CFEL, 22761 Hamburg, Germany*

Email: * martin.eckstein@mpsdcfel.de

Keywords: Ultra-fast dynamics, Exciton condensates

Ultra-fast laser pump-probe experiments allow to impulsively excite correlated materials and monitor the time-evolving state with femtosecond resolution. An important aspect of this is the dynamics of long-range order: Laser excitation can quench long-range order in an ultra-fast way, or impulsively stimulate collective oscillations such as the Higgs modes of the superconducting condensate. Even more intriguing possibility is that non-thermal distributions generated by a laser can possibly enhance long-range order. Excitonic condensates [1] provide an ideal test-bed to explore these possibilities, as long-range order is predominantly of electronic origin, making a theoretical description feasible. Here we report on the theoretical investigation of ultra-fast laser induced dynamics within a two-band model simulation of an excitonic insulator, using a fully self-consistent nonequilibrium GW simulations on the Keldysh contour. We identify two dynamical transition points where the relaxation behavior qualitatively changes, with both are characterized by a slow-down of the dynamics: one corresponds to the thermal phase transition due to the energy deposited by the pulse, and the other is connected to the existence of transient nonthermal long-range order in systems with effective temperature above the thermal critical temperature. This resembles the finding of non-thermal criticality predicted earlier for quenches in superconductors [2].

References

1. T. Rohwer et al., Nature 471, 490 (2011)
2. N. Tsuji, M. Eckstein, and Ph. Werner, Phys. Rev. Lett. 110, 136404 (2013Z)

Pump/probe photoemission in charge-density-wave insulators



James Freericks^{1*}, Oleg Matveev^{1,2}, Andrij Shvaika², and Tom Devereaux^{3,4}

¹*Georgetown University*

²*Institute of Condensed Matter Physics, Lviv, Ukraine*

³*Stanford University*

⁴*Stanford Institute for Materials and Energy Sciences*

Email: *james.freericks@georgetown.edu

Keywords: ultrafast nonequilibrium dynamics, charge density wave insulator, photoemission

In this work, we describe time-resolved photoemission for charge-density-wave insulators described either by a simple noninteracting two-sublattice bandstructure [1] or by the ordered CDW phase of the spinless Falicov-Kimball model [2,3]. The former is solved exactly by employing a direct calculation of the evolution operator employing the Trotter formula, while the latter is solved exactly by employing nonequilibrium dynamical mean-field theory within an ordered phase. We focus on two different physical phenomena. The first involves the transient closing of the gap during and shortly after the pump (which commonly occurs while the system still has charge-order) and the second involves the excitation of electrons from the lower to upper band and their subsequent relaxation.

Experiments have already established a decoupling between the gap induced in the density of states and the order parameter given by the charge modulation on the different sublattices of the charge-density wave. We see similar behavior here. In addition, we examine how the correlations (which bring in subgap states at finite temperature in equilibrium) affect this behavior.

We show a false color image of preliminary work on the correlated charge-density wave insulator in Fig. 1. Throughout the talk we will make connections between the results of the theory on model systems and experiments on real materials.

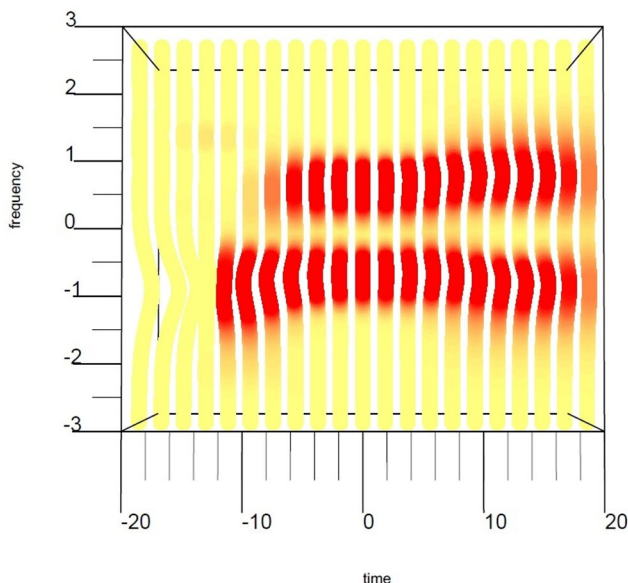


Figure 1: False color image of preliminary results for the time-resolved photoemission of a strongly correlated charge-density-wave insulator at a critical coupling strength. One can see how the initially occupied lower band gets excited to the upper, and how the system appears to be generating long-time oscillations of the photoemission spectra.

References

1. Wen Shen, Yizhi Ge, A. Y. Liu, H. R. Krishnamurthy, T. P. Devereaux, and J. K. Freericks, Phys. Rev. Lett. **112**, 176404 (2014). <http://dx.doi.org/10.1103/PhysRevLett.112.176404> .
2. O. P. Matveev, A. M. Shvaika, T. P. Devereaux, and J. K. Freericks. Journal of Superconductivity and Novel Magnetism, *to appear* (2016). <http://dx.doi.org/10.1007/s10948-015-3304-2> .
3. O. P. Matveev, A.M. Shvaika, T. P. Devereaux, and J. K. Freericks, Phys. Rev. B **93**, 045110 (2016). <http://dx.doi.org/10.1103/PhysRevB.93.045110>

Ultrafast Optical Control of Correlated Electron System with Multi-degrees of Freedom

Sumio Ishihara*, Atsushi Ono, Hiroshi Hashimoto, Hiroaki Matsueda, and Hitoshi Seo

¹*Department of Physics, Tohoku University, Sendai* ²*Sendai National College of Technology, Sendai Japan*

³*Condensed Matter Theory Laboratory, RIKEN, Wako, Japan*

⁴*RIKEN Center for Emergent Matter Science, Wako,,Japan*

Email: * ishihara@cmpt.phys.tohoku.ac.jp

Keywords: Ultrafast dynamics, Spin-charge coupling, Theory

Ultrafast photo-induced electron dynamics in strongly correlated electron systems have significantly attracted much attention, since a number of time-resolved experimental techniques and theoretical calculation methods for non-equilibrium states are rapidly developed in the last decade. In particular, a number of exotic phenomena have been observed in correlated electron systems with multi-degrees of freedom, e.g. spin, charge, orbital, lattice and so on. In this talk, I introduce recent our theoretical studies in the photo-induced transient electron dynamics in correlated electron systems with multi degrees of freedom.

- 1) The photo-excited real time dynamics in the two-leg ladder Hubbard model are studied [1,2]. Real-time evolutions of photoexcited electronic states are examined by the exact-diagonalization method in finite size clusters. In a doped metallic phase, low-energy optical responses are remarkably suppressed by photo-irradiation, in contrast to the photoexcitation in insulating states. After photo-irradiation, the hole pair-field correlation, which is known to play crucial roles on the electronic structure in ladder system, becomes to be short range, being similar to the insulating phase. We also examine the double-pulse excitations, and propose the optical control of the pair coherence. The results show good agreements with the recent pump-probe experiments in ladder cuprates.
- 2) Photo-excited charge dynamics of interacting charge-frustrated systems are studied in an interacting electron model on a two dimensional triangular lattice coupled with the lattice vibrations [3, 4]. We find that not only the transition from the charge ordered (CO) insulator to the metal but also the transition from the CO to another CO phase. There is an intermediate time domain, in which the electron and lattice degrees of freedom are evolving cooperatively. This characteristic time dependence is attributed to the charge frustration effect which decreases the electronic energy scale and induces the non-adiabatic lattice vibration.

- 3) Coherent optical control of correlated electron systems are examined. It is well known that the effective electron motion is suppressed under the CW light. This is known as “Dynamical Localization” (DL) phenomena. We examine this phenomena in one dimensional Hubbard model by using the infinite time-evolving block decimation (iTEBD) method, by which transient electronic states are examined without finite size effect. It is shown that the DL strongly depends on the on-site Coulomb interaction and electron density. The numerical results are interpreted by the Floquet theory

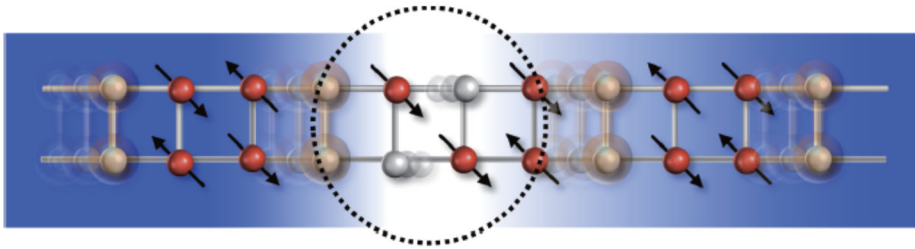


Figure 1: A schematic photoinduced excited state in the ladder system, suggested from the numerical analyses of the two-leg Hubbard model and the optical pump-probe experiments in ladder cuprates [1,2].

References

1. R. Fukaya, Y. Okimoto, M. Kunitomo, K. Onda, T. Ishikawa, S. Koshihara, H. Hashimoto, S. Ishihara, A. Isayama, and T. Sasagawa, *Nat. Comm.* **6**, 8519 (2015).
2. H. Hashimoto and S. Ishihara, arXiv:1511.00365.
3. H. Hashimoto, H. Matsueda, H. Seo, and S. Ishihara, *J. Phys. Soc. Jpn.* **83**, 123703 (2014).
4. H. Hashimoto, H. Matsueda, H. Seo, and S. Ishihara, *J. Phys. Soc. Jpn.* **84**, 113702 (2015).
5. A. Ono, H. Hashimoto and S. Ishihara (in preparation).

Using Raman in real time to manipulation electronic states with light



S. Borroni¹, E. Baldini^{1,2}, A. Mann¹, C. Arrell²,
F. van Mourik², J. Teyssier³, J. Lorenzana^{4*}, F. Carbone¹

¹Laboratory for Ultrafast Microscopy and Electron Scattering, ICMP, École Polytechnique Fédérale de Lausanne, CH-1015 Lausanne, Switzerland.

²Laboratory for Ultrafast Spectroscopy, ISIC, École Polytechnique Fédérale de Lausanne, CH-1015 Lausanne, Switzerland.

³Department of Quantum Matter Physics, University of Geneva, CH-1211 Geneva, Switzerland.

⁴Institute for Complex System – CNR, and Physics Department, University of Rome “La Sapienza”, I-00185 Rome, Italy.

Email: *jose.lorenzana@uniroma1.it

Keywords: high-T_c, magnetite, pump-probe spectroscopy, Landau Theory

I will review recent theory and experiments in which the electronic state of a material is controlled with light pulses. In the case of a superconductor[1], I will show that an impulsive stimulated Raman mechanism allows putting the superconductor in a nonequilibrium state in which the condensate oscillates in time, allowing to detect excitations which are coupled to it and which may be involved in the pairing. In the case of magnetite [2], which has a metal-insulator transition which, as first proposed by Verwey is attributed to charge ordering, I will show a Raman mechanism by which the disordered charges, above the ordering temperature, can transiently be induced to order opposing common expectations that a laser pulse should heat the material and promote disorder. Both cases illustrate the formidable flexibility of Raman processes as a tool for ultrafast manipulation of condensed matter.

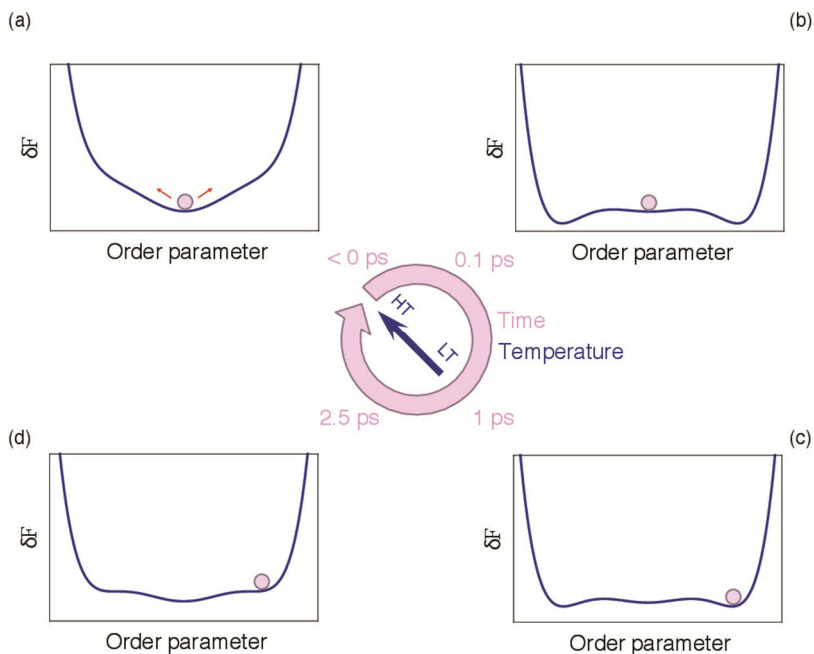


Figure 1: Schematic representation of the evolution of the local Landau free energy (blue line) and order parameter (violet dot) as a function of pump-probe time-delay slightly above the Verwey transition temperature T_v in magnetite. Panel (a) is the equilibrium state, above T_v . Panel (c) represents both the equilibrium Landau free energy below T_v and a light induced transient state that can be obtained above T_v . Panels (b) and (d) are intermediate transient states above T_v .

References

1. B.Mansart et al., Proc. Nat. Acad. Sci. 110, 4539 (2013)
2. S. Borroni et al., arXiv:1507.07193

Global critical temperature in disordered superconductors with weak multifractality



Antonio M. Garcia Garcia^{1*}, James Mayoh¹
¹ *Cavendish Laboratory, JJ Thomson Avenue, Cambridge, CB3 0HE, UK*

Email: * amg73@cam.ac.uk

Keywords: enhancement of superconductivity, disorder, superconductor-insulator transition

There is growing evidence that a key feature of sufficiently disordered superconductors is the spatial inhomogeneity of the order parameter. However, not much is known analytically about the impact of the inhomogeneity on the global critical temperature that signals the onset of resistance in the superconductor. Here [1] we address this problem in the experimentally relevant case of disordered conventional superconductors characterized by weak multifractality such as quasi-two-dimensional thin films. We compute analytically the superconducting energy gap, the temperature at which it vanishes, and the energy dependence and spatial distribution of the order parameter. The latter is found to be log normal. The global critical temperature, computed by percolation techniques, is much smaller than the temperature at which the energy gap vanishes. We show that disorder might enhance superconductivity but only for very weakly coupled superconductors, such as Al, and for relatively weak phase fluctuations. These results are consistent with experiments where enhancement of the critical temperature is observed in Al thin films but not in more strongly coupled materials.

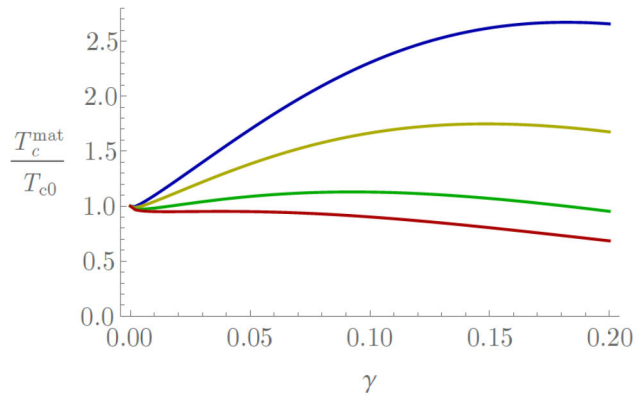


Figure 1: The global critical temperature T_c^{mat} obtained as the temperature at which the percolation transition occurs in units of the critical temperature in the non disordered limit as a function of the degree of multifractality γ for different values of the electron-phonon coupling $\lambda = 0.25$ (Blue), 0.3 (Yellow), 0.4 (Green), 0.5 (Red). Except in the case of small λ no or very modest enhancement of the critical temperature is observed.

References

1. J. Mayoh and A. M. Garcia-Garcia, Phys. Rev. B 92, 174526 (2015).

Ultrafast control of superconducting phase slips



Ivan Madan*, Jože Buh, Vladimir Baranov, Aleš Mrzel, Dragan Mihailovic

Complex Matter Department, Jozef Stefan Institute, Ljubljana, Slovenia

Email: **ivan.madan@ijs.si*

Keywords: phase slips, ultrafast control, hidden states

Photon control of collective states is of great interest due to possible practical applications. Of particular interest are photo-induced transitions which occur on the picosecond time-scale. Up to now the discussion was limited to the transitions between steady-states. We expand the field by presenting the transitions between dynamical states, reporting switching between periodic states in 1D current-carrying superconductors.

Upon exceeding critical current the superconducting nanowire enters the dynamical resistive state characterised by periodically appearing normal regions in which phase of the order parameter slips by 2π - phase slip centers (PSCs). For a given current multiple dynamical configurations are possible, characterized by different spatial and temporal behavior of the order parameter. [1,2] Experimentally they can be easily distinguished by the time-averaged voltage drop on the nanowire. [3]

Switching between different PSCs can occur spontaneously giving rise to a “telegraph noise” behavior of resistance. This however occurs in a narrow region of currents and hard to investigate. Recently electrical noise assisted switching has been demonstrated allowing better understanding of the stability of phase slip centers. [4]

In this talk we present ultrafast optical experiments on the PSCs in δ -MoN nanowires with $T_c=11$ K. We report switching between different PSCs after application of the single 50-fs laser pulse of variable wavelength, including switching into PSC configurations apparently unachievable in quasi-equilibrium conditions

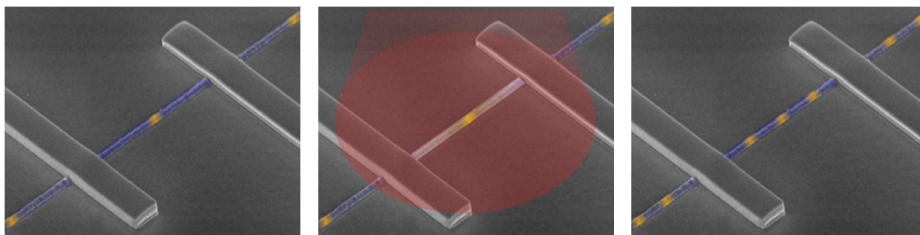
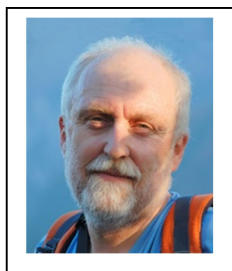


Figure 1: Schematic representation of the reported experiment. Order parameter drops to zero at phase slip centers (yellow). Laser pulse reduces order parameter and system evolves into different stable phase slip configuration.

References

1. V. V. Baranov, a. G. Balanov, and V. V. Kabanov, Phys. Rev. B 87, 174516 (2013).
2. A. G. Sivakov, A. M. Glukhov, A. N. Omelyanchouk, Y. Koval, P. Müller, and A. V. Ustinov, Phys. Rev. Lett. 91, 267001 (2003).
3. W. J. Skocpol, M. R. Beasley, and M. Tinkham, J. Low Temp. Phys. 16, 145 (1974).
4. J. Buh, V. Kabanov, V. Baranov, A. Mrzel, A. Kovič, and D. Mihailovic, Nat. Commun. 6, 10250 (2015).

All-optical femtosecond relaxation dynamics in iron based pnictides



T. Mertelj^{1,2,*}, L. Stojchevska¹, A. Pogrebna¹, D. Mihailovic^{1,2},
 N.D. Zhigadlo³, J. Karpinski³, G. Cao⁴, Z. A. Xu⁴, Z. Bukowski⁵
¹*Complex Matter Dept., Jozef Stefan Institute, 1000 Ljubljana, Slovenia*
²*CENN Nanocenter, Jamova 39, 1000 Ljubljana, Slovenia*
³*Laboratory for Solid State Physics, ETH Zürich, 8093 Zürich, Switzerland*
⁴*Department of Physics, Zhejiang University, Hangzhou 310027, People's Republic of China*

⁵*Institute of Low Temperature and Structure Research, Polish Academy of Sciences, 50-950 Wrocław 2, Poland*

Email: *tomaz.mertelj@ijs.si

Keywords: iron-based pnictides, spin density wave, time resolved dynamics

The richness of the iron-based-pnictides phase diagram is reflected also in the transient optical response. Systematic investigations[1-10] of the photo excited quasi-particle relaxation in electron doped 1111 and 122 iron-based pnictides by all-optical methods revealed information regarding the electron phonon coupling,[3, 5] charge gap in the spin-density wave (SDW) state,[3, 5, 6, 8, 9]gaps in the superconducting state[1, 2, 3, 4] and nematic fluctuations in the normal state.[5, 7] Another interesting aspect of the iron-based-pnictides is the presence of rare earth ions in the crystal structure enabling study of a coexistence of the ferromagnetic order of the rare-earth f -orbital spins in $\text{EuFe}_2(\text{As,P})_2$ and $\text{Eu}(\text{Fe,Co})_2\text{As}_2$ with the superconducting order of the Fe- d -bands carriers. [10]

I will briefly review the all-optical relaxation dynamics results in various parts of the phase diagram with emphasis on our recent results concerning the antiferromagnetic(SDW) state[9] and the rare-earth f -orbital spin dynamics in Eu based 122 compounds.[10]

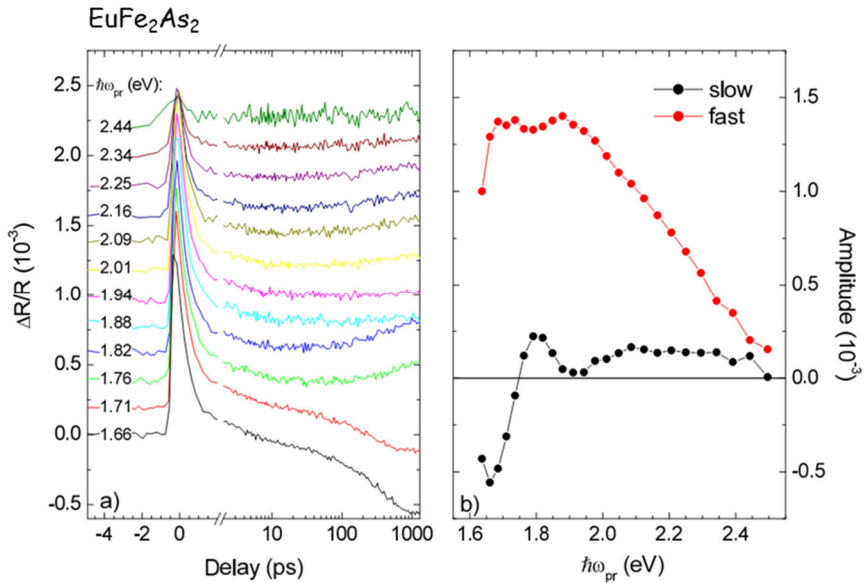


Figure 1: The resonant ultrafast transients in EuFe_2As_2 . The fast component corresponds to the relaxation of the FeAs-planes spin density wave while the slow one is related to the suppression of the antiferromagnetic order parameter of Eu^{+2} ions.

References

1. T. Mertelj *et al.*, *Phys. Rev. Lett.* **102**, 117002 (2009).
2. E. E. M. Chia *et al.*, *Phys. Rev. Lett.* **104**, 27003 (2010).
3. L. Stojchevska *et al.*, *Phys.Rev.* **B 82**, 012505 (2010).
4. D. H. Torchinsky *et al.*, *Phys.Rev.* **B 84**, 104518 (2011).
5. L. Stojchevska *et al.*, *Phys.Rev.* **B 86**, 024519 (2012).
6. K. W. Kim *et al.*, *Nature Mat.* **11**, 497 (2012).
7. A. Patz *et al.*, *Nat. Comm.* **5**, 3229 (2013).
8. T. Mertelj *et al.*, *Phys.Rev.* **B 87**, 174525 (2013).
9. A. Pogrebna *et al.*, *Phys.Rev.* **B 89**, 165131 (2014).
10. A. Pogrebna *et al.*, *Sci. Rep.* **5**, 7754 (2015).

Ultrafast relaxation dynamics study in iron-based pnictides, cuprates and charge-density waves



L. Stojchevska^{1,2*}, T. Mertelj¹, P. Sutar¹, D. Mihailovic¹ and U. Bovensiepen²

¹*Complex Matter Department, Jozef Stefan Institute, Jamova cesta 39 1000 Ljubljana, Slovenia*

²*University of Duisburg-Essen Faculty of Physics Lotharstr. 1 47048 Duisburg, Germany*

Email: ljupka.stojcevska@ijs.si

Keywords: high T_c, cuprates, iron-based pnictides, pseudogap, charge-density waves, hidden states

We have performed systematic study of the quasiparticle relaxation dynamics in various complex systems such as cuprates, iron-based pnictides superconductors and charge-density wave systems.

In undoped iron-based pnictides, exhibiting a spin-density wave (SDW) ordering, we observe a bottleneck associated with a partial charge-gap opening [1,2,3]. Similarly as in the previous reported studies, a single relaxation process is observed, showing a remarkable critical slowing down of the quasiparticle (QP) relaxation dynamics at the SDW transition temperature. On the other hand, in the optimally doped crystals, a multiple relaxation processes are present with distinct SC-state quasiparticle recombination dynamics exhibiting a BCS-like T -dependent superconducting gap, and a pseudogap (PG)-like feature at higher temperatures. In all optimally doped cuprates and iron-based pnictides, we observe a saturation of the superconducting relaxation component. By taking into account the optical constants such as penetration depth and reflectivity we can accurately calculate energy needed for destruction of the superconducting state. If we compare the magnitudes of the destruction and condensation energies we notice a significant discrepancy in cuprates and iron-based pnictides, which can be explained with a phonon-mediated QP bottleneck mechanism [4]. In contrast, in the charge-density wave systems, the destruction is faster and electronic; therefore it can not be explained in the frame of the proposed QP bottleneck mechanism.

The second moment of the Eliashberg function, obtained from the relaxation rate in the metallic state at higher temperatures, has similar values in different iron-based pnictides, which indicates a moderate electron phonon coupling.

More recently we have observed a switching between an equilibrium state to a metastable in 1T-TaS₂ charge-density wave system by means of ultrafast laser quench through a symmetry breaking transition [5].

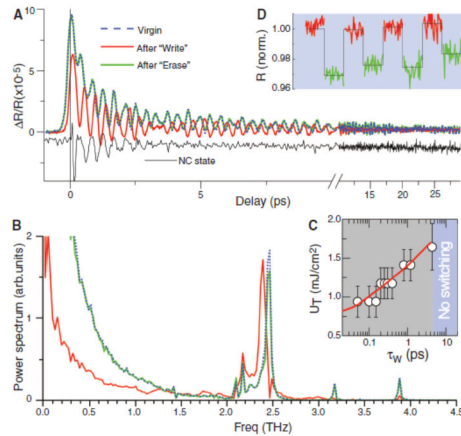


Figure 1: Spectral signatures of the HST process. (A) Transient reflectivity $DR(t)/R$ of 1T-TaS2 in the virgin state (blue dashed line), after exposure to a 50-fs W pulse (red line), and after an E pulse (green line). Black line: data in the NC state at 220 K recorded upon cooling (offset for clarity). (B) The corresponding Fourier-transformed power spectra $S(w)$ using the same color notation. (C) Switching threshold fluence U_T as a function of pulse length t_W measured optically with pump-probe experiments. The red line is predicted by the model calculation. (D) Reflectivity at 800 nm recorded with the photodiode during a sequence of alternating W and E pulses. (The noise is from the laser.)

References

1. T. Mertelj et al. Phys. Rev B 81, 224504 (2010)
2. L. Stojchevska et al. Phys. Rev 82, 012505 (2010).
3. L. Stojchevska et al. Phys. Rev B 86, 024512 (2012).
4. L. Stojchevska et al. Phys. Rev B 84, 180507 (2011).
5. L. Stojchevska et al. Science 344, 177 (2014).

High temperature superconductors far from equilibrium conditions



Luca Perfetti

¹Laboratoire des Solides Irradiés, Ecole Polytechnique-
CEA/DSM-CNRS UMR 7642, F-91128 Palaiseau, France

Email : luca.perfetti@polytechnique.edu

Keywords : cuprates – non-equilibrium

The dynamics of high temperature superconductors strongly driven by laser pulses will be investigated by Time Resolved THz spectroscopy and time resolved photoelectron spectroscopy. We will compare the critical fluence leading to the loss of phase coherence with the one necessary to destroy the pairing amplitude of Cooper pairs. Our data will also show that inelastic scattering of nodal quasiparticles decreases when the temperature is lowered below the critical value of the superconducting phase transition. This drop of electronic dissipation is astonishingly robust and survives to photoexcitation densities much larger than the value sustained by long-range superconductivity. The combination of these experimental results reveal that driven condensates experience complex non-equilibrium phenomena so that phase coherence, pairing amplitude and electronic dissipation are not proceeding on equal footing.

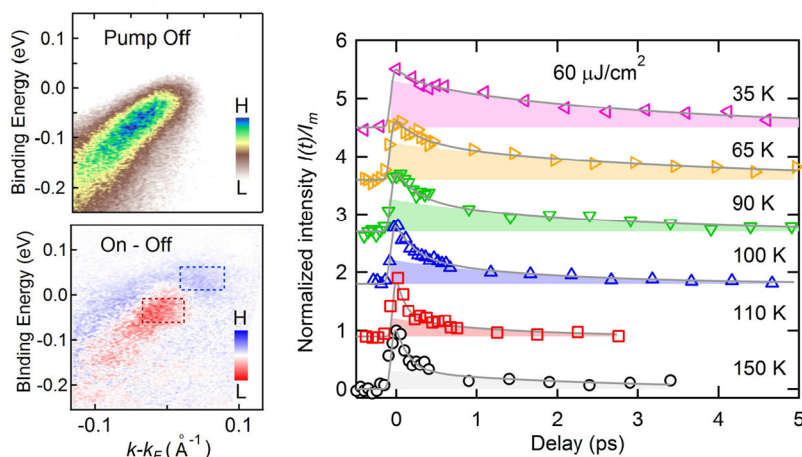


Figure 1: The typical timescale of quasi-particle dissipation monitored at different temperatures across the phase transition of optimally doped Bi2212.

References

1. L. Perfetti, B. Sciolla, G. Biroli, C. J. van der Beek, C. Piovera, M. Wolf, and T. Kampfrath, *Physical Review Letters* **114**, 067003 (2015).
2. M. C. Piovera, Z. Zhang, M. d'Astuto, A. Taleb-Ibrahimi, E. Papalazarou, M. Marsi, Z. Z. Li, H. Raffy, and L. Perfetti, *Phys. Rev. B* **91**, 224509 (2015).

Quasiparticle dynamics in the organic superconductors investigated with polarized femtosecond spectroscopy



Satoshi Tsuchiya^{1*}, Koichi Nakagawa¹, Jun-ichi Yamada², Yasunori Toda¹

¹*Department of Applied Physics, Hokkaido University*

²*Graduate School of Material Science, University of Hyogo*

Email: * satoshi.tsuchiya@eng.hokudai.ac.jp

Keywords: organic superconductors, time-resolved dynamics, pseudogap

Toward full understanding of high-temperature superconductivity (SC), unusual electronic properties in the normal state have been extensively studied in cuprate and organic superconductors. In the cuprates, various spectroscopic measurements have revealed that a pseudogap was appeared in the electronic energy spectrum above the SC transition temperature (T_c) and the temperature where the pseudogap was formed, has a unique carrier doping dependence [1]. On the other hand, in organic superconductors κ -(BEDT-TTF)₂X (X: inorganic anions) whose electronic phase diagram is quite similar to the cuprates if doping is replaced with effective electron correlation (or pressure), it remains unclear whether such the pseudogap exists or not because only a few spectroscopic studies have been performed so far.

In this study, to investigate the electronic properties above T_c , we have carried out time-resolved pump-probe spectroscopy with different probe polarizations in the organic superconductors κ -(BEDT-TTF)₂Cu(NCS)₂ (κ -NCS, $T_c \sim 10$ K) and κ -(BEDT-TTF)₂Cu[N(CN)₂]Br (κ -Br, $T_c \sim 12$ K), which has effectively stronger electron correlation than κ -NCS. The optical measurements were performed using 120 fs pulses centered at 400 nm for a pump (63-134 $\mu\text{J}/\text{cm}^2$) and 800 nm for a probe from a cavity-dumped Ti:sapphire oscillator with a repetition rate 54 kHz. The pump and probe beams were coaxially overlapped and irradiated perpendicular to the conducting plane. The probe pulse polarization was rotated by a half-wave plate.

Figures 1 (a) and (b) show probe-polarization-angle dependences of the amplitude of transient reflectivity changes $\Delta R/R$ in κ -NCS for 45 and 78 K, respectively. We found that the anisotropic response appeared below 70 K, indicating a spontaneous spatial symmetry breaking [2,3]. Moreover as shown in Fig. 1(d), the amplitude of anisotropic component steeply developed with decreasing temperature. Since $\Delta R/R$ is proportional to photo-excited quasi-particle density, the steep increase of the amplitude can correspond to formation of energy gap. On the other hand, in κ -Br, although similar polarization angular dependences of $\Delta R/R$ were observed, the temperature dependence of the amplitude of $\Delta R/R$ showed gradual increase with decreasing temperature (Fig. 1(c)), which was qualitatively different from that in κ -NCS. The difference between them may be associated with spatial inhomogeneity due to strong electron correlation. The data will be discussed in detail at the conference.

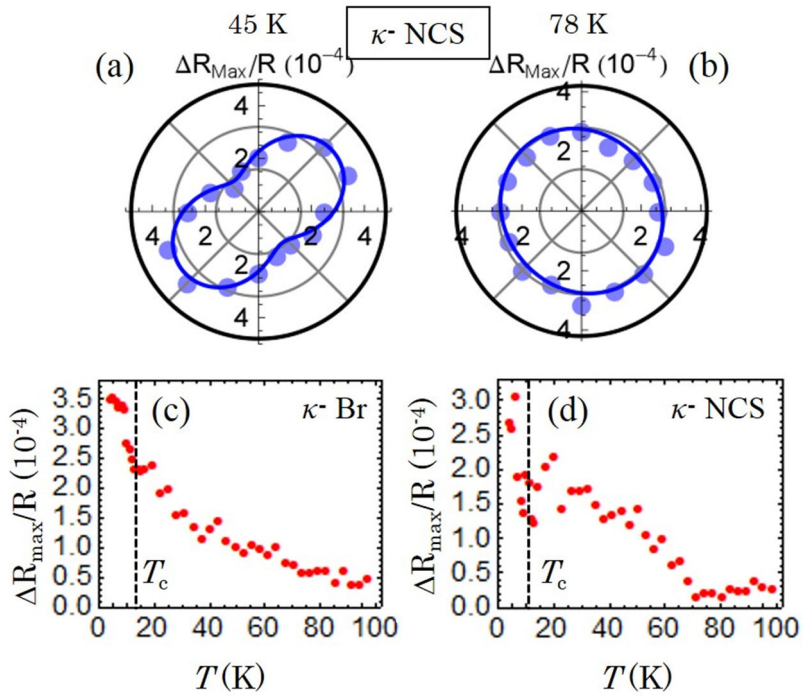


Figure 1: (a),(b) Probe polarization angular dependences of amplitude of $\Delta R/R$ transients for 45 K and 78 K. (c),(d) Temperature dependences of amplitude of $\Delta R/R$ transients of the anisotropic components in κ -Br and κ -NCS.

References

1. T. Timusk et al., Rep. Prog. Phys. **62**, 61 (1999).
2. Y. Toda et al., Phys. Rev. B **90**, 094513 (2014).
3. S. Tsuchiya et al., J. Opt. **17**, 085501 (2015).

Observation of multiferroicity in transition metal compounds with complex anionic lattice or complex magnetic structure



A. C. Komarek^{1**}, L. Zhao¹, L. H. Tjeng¹
¹Max-Planck-Institute for Chemical Physics of Solids

Email: * Komarek@cpfs.mpg.de

Keywords: multiferroic

Magnetolectric multiferroics have attracted enormous attention in the past years due to their possible application in future devices. Especially certain spiral magnetic structures are often responsible for the cross-coupling between magnetism and ferroelectricity in these materials. So far multiferroicity has been found especially in many oxide materials. Here, we report the observation of multiferroicity in two rather interesting transition metal compounds: the first one is a compound with a complex anionic lattice, i.e. with twice the number of anion types than cation types and the second one is a compound that possibly simultaneously hosts a helical and a cycloidal magnetic structure – Mn_3TeO_6 [1].

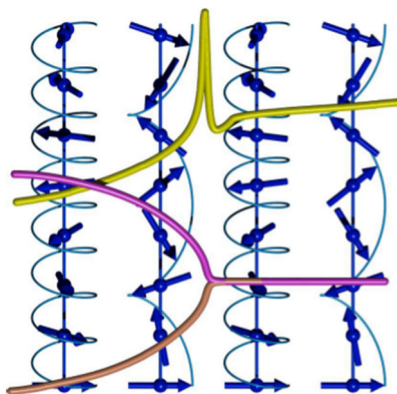


Figure 1: Possible coexistence of helical and cycloidal magnetic structures in Mn_3TeO_6 [2].

References

1. L. Zhao *et al.*, Phys.Status Solidii RRL 9, 730 (2015).
2. DOI: 10.1002/pssr.201570664

Complex magnetic incommensurability and electronic charge transfer in type-II multiferroic Co_3TeO_6



Wen-Hsien Li^{1*}, Chi-Hung Lee¹, Jeffrey W. Lynn², Helmuth Berger³

¹*University of Rome [Times 11 italic]* Department of Physics, National Central University, Jhongli 32001, Taiwan

²*NIST Center for Neutron Research, NIST, Gaithersburg, Maryland 20899, USA*

³*Department of Materials Sciences Institute of Physics of Complex Matter, EPFL, Lausanne, Switzerland*

Email: *whli@phy.ncu.edu.tw

Keywords: multiferroic, magnetic incommensurability, electronic charge transfer

Multiferroics, where both ferroelectric and magnetic order coexist, are quite uncommon, but are of particular interest both in understanding the fundamental interactions between the two types of order and in the developing devices for practical applications. For conventional (type-I, or proper) multiferroics the two types of order must be associated with different atoms, with generally a weak interaction between the two order parameters. For type-II (improper) multiferroics, on the other hand, the ferroelectric displacements originate from some other type of ordering, and of particular interest here, are when this is magnetic order. The novel metal tellurates $M_3\text{TeO}_6$, where M is a first-row transition metal, have been shown to be rich in crystalline chemistry. Ferroelectricity, ferromagnetic and antiferromagnetic spin orders, complex incommensurate (ICM) spin structures, and magnetic-field-driven polarization have all been observed. Here, we report on the observations of a strong interplay between the order parameters of ferroelectricity and both commensurate and incommensurate magnetic order in single crystal cobalt tellurate Co_3TeO_6 . We find Co_3TeO_6 to be a type-II multiferroic [1,2]. Long range ICM magnetic order develops below $T_{M1}=26$ K, which is followed by two additional zero-field phase transitions at $T_{M2}=19.5$ K and $T_{M3}=18$ K, where commensurate order and ferroelectricity develop, respectively [2,3]. We demonstrate directly that the intensity map of the k - l scattering plane excludes having commensurate (CM) order at the $(0 \ 1/2 \ 1/4)$ wave vector, suggested in a report based on the results from a powder sample. Polarized neutrons have also been used to confirm that the observed high order ICM reflections are magnetic in nature and the magnetic structure contributes no intensity to the (600) reflection even at base temperature. Two separated sets of magnetic modulation vectors were found between 19.5 and 18 K, revealing the appearance of magnetic incommensurability when the Co spins in the honeycomb web order below $T_{M2} = 19.5$ K, but the magnetic incommensurability disappears once ferroelectricity developed below $T_{M3} = 18$ K. Contributions from the Te ions at the crystallographic $8f$ sites to ferroelectric transition are also found, where a significant amount of electric charges shifts from the Te ions to their neighboring Co and O ions upon cooling through the

ferroelectric transition (Figure 1). The ferroelectric transition links closely to the increases of electronic charges in specific regions, where local crystallographic distortion is severe.

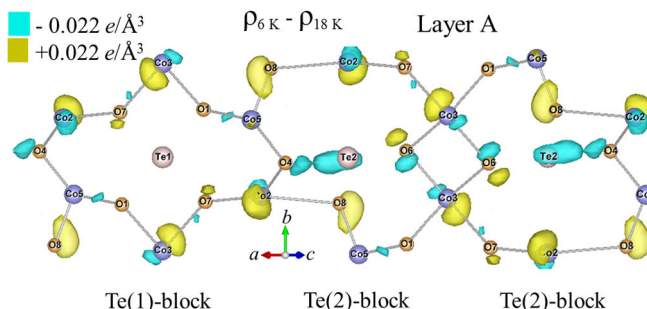


Figure 1: Contour map of the electronic charge densities in Layer A that developed upon cooling from 6 to 18 K, as inferred from the x-ray diffraction data. The regions mark in yellow indicates the contours having a difference density of $+0.022 e/\text{\AA}^3$; whereas those mark in green represents the contours having a difference density of $-0.022 e/\text{\AA}^3$.

References

1. S. A. Ivanov, R. Tellgren, C. Ritter, P. Nordblad, R. Mathieu, G. André, N. V. Golubko, E. D. Politova, and M. Weil, *Mater. Res. Bull.* **47**, 63-72 (2012).
2. Chin-Wei Wang, Chi-Hung Lee, Chi-Yen Li, Chun-Ming Wu, Wen-Hsien Li, Chih-Chieh Chou, Hung-Duen Yang, Jeffrey W. Lynn, Qingzhen Huang, A. Brooks Harris, and Helmuth Berger, *Phys. Rev. B* **88**, 184427(2013).
3. W.-H. Li, C.-W. Wang, D. Hsu, C.-H. Lee, C.-M. Wu, C.-C. Chou, H.-D. Yang, Y. Zhao, S. Chang, J. W. Lynn, and H. Berger, *Phys. Rev. B.* **85** 094431(2012).

High Field Dependence of the Magnetocaloric Effect in Laves Phase Compounds



J. Ćwik^{1*}, Y. Koshkidko¹, K. Nenkov², A. Hackemer³,
M. Miller¹

¹*International Laboratory of High Magnetic Fields and Low Temperatures, PAS, 53-421 Wrocław, Poland*

²*IFW Dresden, Institute of Metallic Materials, D-01171 Dresden, Germany*

³*Institute of Low Temperature and Structure Research, PAS, 50-422 Wrocław, Poland*

Email: * jacek.cwik@ml.pan.wroc.pl

Keywords: Rare earth intermetallic – Magnetic properties – Magnetic application – Magnetocaloric effect

The investigation of magnetocaloric materials has been focused on obtaining a compound appropriate for the magnetic refrigeration at both near-room and cryogenic temperatures. According to the literature data, RNi₂ is a potential magnetic refrigerant for low temperature applications such as hydrogen liquefaction. The magnetic properties of the RNi₂ compounds have been studied intensively in [1]. The distinctive feature of this series of compounds consists in the absence of a magnetic moment at nickel atoms; in this case, the magnetic interaction involves only the R sublattice. The high magnetocaloric effect (MCE) values of the compounds are strongly influenced by crystalline electric fields. Theoretical data show that some of RNi₂ compounds exhibit high MCE [2-4]. It can be expected that $\Delta T_{ad} = 8.1$ K for TbNi₂, $\Delta T_{ad} = 13.8$ K for HoNi₂ and $\Delta T_{ad} = 10.4$ K for ErNi₂ induced by $\Delta H = 5$ T. Most of experiments performed for this material system were focused on the intermediate magnetic field range ($\Delta H \leq 2$ T) that the more relevant for applications [5-6]. However, extending the field range of the MCE derivation is of importance from both fundamental and applied points of view. High-field magnetocaloric data are advantageous for the optimization of the MCE at intermediate field. The majority of reports on this subject focus on the experimental investigations that are usually performed by heat capacity measurements with and without an applied magnetic field or by magnetic methods, with the help of Maxwell thermodynamic relations. The aim of the present work is to exhibit the correlations between the external magnetic field value and the magnetocaloric effect in ferromagnetic Laves-phase compounds at temperatures close to the their magnetic phase transition temperatures. The MCE measurements have been performed by direct measurements in high magnetic fields ($\Delta H = 11$ T) (Fig. 1) and the results are compared with theoretical considerations.

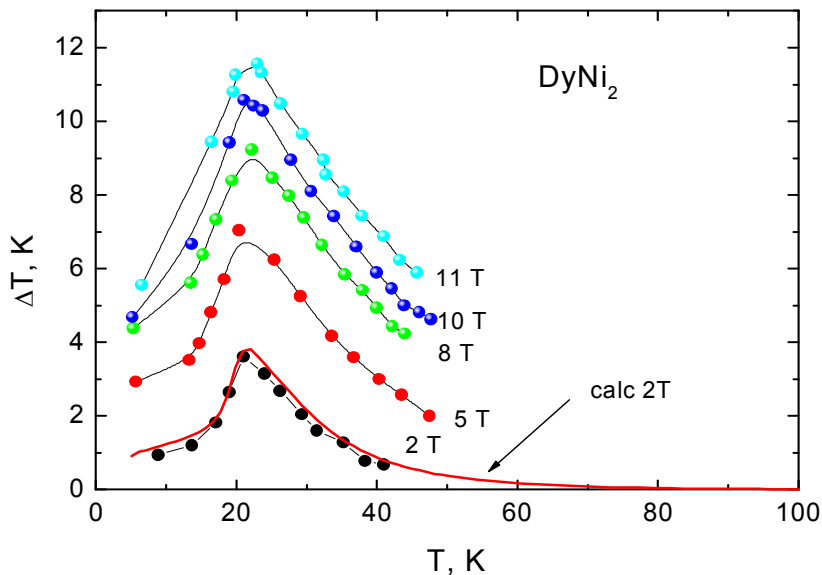


Figure 1: Temperature dependence of ΔT_{ad} for DyNi_2 compound near its ordering temperature.

References

1. K.H.J. Buschow, in: E.P. Wohlfarth (Ed.), *Ferromagnetic Materials*, vol.1, North Holland, Amsterdam, 1980.
2. von Ranke et al. *J. Appl. Phys.* 93, No. 7 (2003).
3. Plaza et al. *J. Appl. Phys.* 105, 013903 (2009).
4. V.S.R. de Sousa et al. *Journal of Magnetism and Magnetic Materials* 321, 3462 (2009).
5. O. Tegus, E. Brück, K. H. J. Buschow, F. R. de Boer, *Nature* 415, 150 (2002).
6. N. H. Dung, Z. Q. Ou, L. Caron, L. Zhang, D. T. Cam Thanh, G. A. de Wijs, R. A. de Groot, K. H. J. Buschow, E. Brück, *Adv. Energy Mater.* 1, 1215 (2011).

Designing Quantum Matter with Superconducting Nanowires



Nina Marković^{1,2*}, Tyler Morgan-Wall¹, Hannah Hughes^{1,3},
Atikur Rahman^{1,4}, Nikolaus Hartman^{1,5}, Jerome T. Mlack^{1,3}

¹*Department of Physics and Astronomy, Johns Hopkins University*

²*Department of Physics and Astronomy, Goucher College*

³*Department of Physics and Astronomy, University of Pennsylvania*

⁴*Brookhaven National Laboratory*

⁵*Department of Physics and Astronomy, University of British*

Columbia

Email: * nina.markovic@goucher.edu

Keywords: superconductivity in nanowires, vortices, proximity

Superconducting nanowires are an experimental realization of a model quantum system that features collective degrees of freedom and exhibits a host of non-equilibrium and non-local phenomena. The nature of the quantum states in nanowires is particularly sensitive to size and shape quantization, coupling with the environment and proximity effects. I will demonstrate how we can utilize these features to tailor the quantum states in nanowires in desirable ways [1]. Specifically for this purpose, we have developed a unique nanoprinting method for fabrication of ultranarrow nanowires with unprecedented control over their physical texture and their transport properties [2,3]. I will show how short nanowires exhibit a tunable vortex-in-a-box blockade phenomenon [1], and how tunable interfaces with graphene and topological insulators lead to unusual properties [4,5]. Finally, I will discuss the bigger picture for how the texture of the superconducting wavefunction can be precisely controlled by the size, shape, magnetic field and tunable interfaces with materials that exhibit unconventional order, spin texture or topological properties.

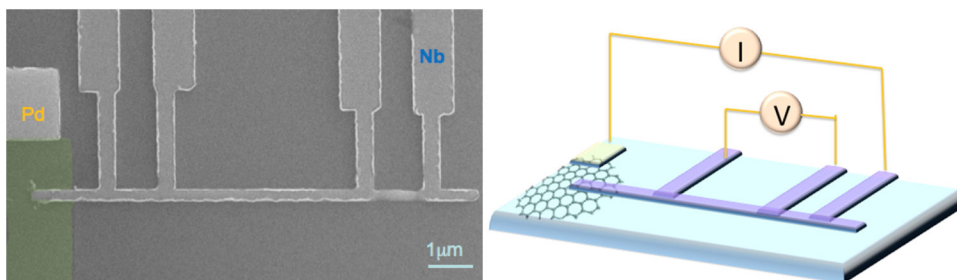


Figure 1: A superconducting niobium nanowire with a graphene lead (left) and a measurement schematic (right).

References

1. T. Morgan-Wall, B. Leith, N. Hartman, A. Rahman and N. Markovic, *Phys. Rev. Lett.* **114**, 077002 (2015).
2. T. Morgan-Wall, H. J. Hughes, N. Hartman, T. M. McQueen and N. Markovic, *Appl. Phys. Lett.* **104**, 173101 (2014).
3. J. L. Wasserman, K. Lucas, S. H. Lee, A. Ashton, C. T. Crawl and N. Markovic, *Rev. Sci. Inst.* **79**, 073909 (2008).
4. J. T. Mlack, A. Rahman, G. L. Johns, K. J. T. Livi, and N. Markovic, *Appl. Phys. Lett.* **102**, 193108 (2013).
5. A. Rahman, J. W. Guikema and N. Markovic, *Nano Lett.* **14**, 6621 (2014).

Shot Noise in Quantum Phase Slip Wires vibrations



Andrei D. Zaikin^{1,2*}, Andrew G. Semenov²

¹*Institute of Nanotechnology, Karlsruhe Institute of Technology, 76021 Karlsruhe, Germany*

²*P.N. Lebedev Physics Institute, 119991 Moscow, Russia*

Email: * andrei.zaikin@kit.edu

Keywords: superconducting nanowires, quantum fluctuations

Can a superconductor generate voltage fluctuations? More specifically, if an external bias is applied to a superconductor could the latter produce shot noise? At the first sight, negative answers to both these questions should be given purely on fundamental grounds. In this talk we will demonstrate that these answers are actually positive in superconducting nanowires with proliferating Quantum Phase Slips (QPS). Employing Keldysh technique and making use of the phase-charge duality arguments we develop a theory of QPS-induced voltage noise in such nanowires. We demonstrate that quantum tunneling of the magnetic flux quanta across the wire yields shotnoise which obeys Poisson statistics and is characterized by a power law dependence of its spectrum on the external bias.

STM studies of the superconductor-insulator transition in MoC ultrathin films



P. Szabó,¹V. Hašková,¹ T. Samuely,¹ J. Kačmarčík,¹ M. Žemlička,²M. Grajcar,² J. G. Rodrigo,³ and P. Samuely¹

¹*CLTP @ Inst. Exp. Phys. SAS, SK-04001 Košice, Slovakia*

²*DEP, Comenius University, SK-84248 Bratislava, Slovakia*

³*LBT, Facultad de Ciencias UAM, E-28049 Madrid, Spain*

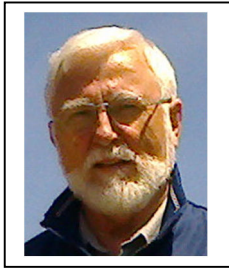
Email: *pszabo@saske.sk

Keywords: superconductor-insulator transition, low temperature

STM, disorder

STM and STS studies on ultrathin MoC films provide evidence that, in contrast to TiN, InO_x and NbN, where the bosonic scenario of SIT is found, in the ultrathin MoC films the superconducting state is very homogeneous for all the thicknesses down to 3 nm where the superconducting transition is suppressed from bulk $T_c = 8.5$ K to 1.3 K and the strong disorder is characterized by $k_F l$ close to unity. The global superconducting coherence in MoC films is supported by detection of the superconducting vortices. Finally, the superconducting energy gap or order parameter terminates, $\Delta \rightarrow 0$ as the bulk superconductivity ceases with $T_c \rightarrow 0$. All this points to the fermionic route of the SIT. Then, two principally different scenarios of SIT can be realized depending on the physical parameters of the systems.

Charge order-to-superfluid transition for 2D hard-core bosons and emergent domain structures



A.S. Moskvina^{1*}, Yu.D. Panov¹, F.N. Rybakov^{1,2}, and
A.B. Borisov^{1,2}

¹*Ural Federal University, 620083, Ekaterinburg, Russia*

²*Institute of Metal Physics UD RAS, 620990, Ekaterinburg, Russia*

*alexander.moskvina@urfu.ru

Keywords: hard-core bosons, CO-SF transition, supersolids, filamentary superfluidity

A phase transition between a correlation-induced insulating phase, with localized charge carriers, and an itinerant phase is a typical feature of strongly correlated systems such as high-temperature superconductors, manganites *etc.* The simplest example of such a transition from a charge order (CO) to a superfluid (SF) with an intervening supersolid (SS) phase is provided by the hard-core (*hc*) boson Hubbard model described by a Hamiltonian as follows:

$$\hat{H}_{hc} = -\sum_{i>j} t_{ij} (\hat{B}_i^\dagger \hat{B}_j + \hat{B}_j^\dagger \hat{B}_i) + \sum_{i>j} V_{ij} N_i N_j - \mu \sum_i N_i ,$$

where $B^\dagger(B)$ are the Pauli creation (annihilation) operators, μ the chemical potential, t_{ij} is an effective transfer integral, V_{ij} is an intersite interaction. The model of *hc*-bosons is equivalent to a system of $s=1/2$ spins exposed to an external magnetic field in the z -direction. We made use of a special algorithm for CUDA architecture for NVIDIA graphics cards, a nonlinear conjugate-gradient method to minimize energy functional, and Monte-Carlo technique to directly observe the forming of the ground state configuration for the 2D *hc*-bosons with lowering the temperature and under deviation $\Delta N=N-1/2$ from half-filling. The technique allowed us to uncover novel features of the phase transitions, in particular, look upon the nucleation of odd domains and the emergence of topological structures. We start with the *hc*-bosons on a 256×256 square lattice at half-filling given “easy-axis” Ising anisotropy $V>t$. For moderate anisotropy $V=3t$ the annealing is accompanied by formation a fragile unstable CO domain structure with a filamentary superfluidity (FLSF) nucleated inside the antiphase 180° domain walls (DW). Typically the annealing is finished by formation a system of domains with closed-loop DWs which quickly collapse setting a uniform single-domain CO ground state (Fig.1a). In rare cases there occur stable stripe-like disconnected DWs (Fig.1b). These 1D DWs can reveal unconventional multi-domain structure of the phase for the SF order parameter with a high density of 2π DWs separating the 1D phase domains with opposite chirality. For stronger anisotropy $V=9t$ the annealing results in formation of a well developed robust CO domain structure with a FLSF nucleated at the antiphase DWs (Fig.1c). Evolution of all the three *hc*-boson configurations a), b), c) under doping away from half-filling is illustrated in Fig.1

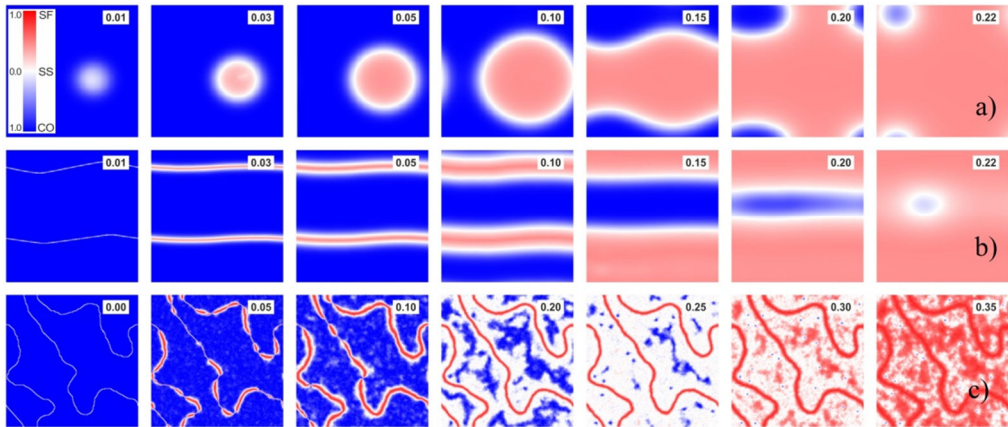


Figure 1: a) At $\Delta N = 0.01$ one observes a sudden nucleation of a rather large "blob" composed of a SF core and a ring shaped SS boundary that does accommodate all the "injected" bosons. Under further deviation from half-filling the blob grows up to a full CO-SF phase transformation close to a critical value of $\Delta N = 0.225$; b) Doped bosons do localize in narrow FLSF DWs of the striped CO phase leading to their broadening. In a well developed phase separation regime we arrive at a system of nearly parallel CO and SF domains separated by the SS DWs; c) At $\Delta N < 0.01$ the doped bosons do localize in the center of the narrow DWs breaking the FLSF without any visible transformation of the domains. The regular DW shape breaks under further doping, these are nonuniformly "swelled" with the emergence and rise of widenings. Step by step these widenings and "blobs" nucleated inside domains spread until these cover all lattice. The CO domain topology survives up to very high doping. Different color in a), b), c) does highlight the value of the order parameters.

*The work was supported by the Government of the Russian Federation, Program 02.A03.21.0006 and by the Ministry of Education and Science, projects 1437 and 2725.

Optical Study of the AFM state in electron doped CaNdFeAs



Xianggang Qiu^{1*}, Run Yang¹
¹*Institute of Physics, Chinese Academy of Sciences*

Email: * xgqiu@iphy.ac.cn

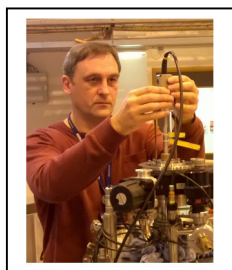
Keywords: Iron-based superconductor, Far-infrared spectroscopy

In $\text{Ca}_{1-x}\text{RE}_x\text{FeAs}_2$ (RE= rare earth), an antiferromagnetic (AFM) phase as well as a structural transition is uncovered, even in electron-overdoped area. Here we investigated the temperature-dependent in-plane optical spectroscopy of overdoped $\text{Ca}_{0.77}\text{RE}_{0.23}\text{FeAs}_2$. Across the transition, we found a sudden reduction of low frequency ($500\text{-}2000\text{ cm}^{-1}$) spectral weight in the optical conductivity. Unlike most undoped iron pnictides, which also form AFM ordered state at low temperature, we did not observe any signature of spin-density-wave (SDW) transition near Fermi surface. This may come from the terrible nesting condition between hole and electron pockets. On the other hand, spectral weight analysis shows that the reduced spectral weight at low frequency has been transferred to the high frequency area ($>4000\text{ cm}^{-1}$), indicating a localizing effect. These unique features combined with the strong magnetism in electron-overdoped system could be understood in terms the hybridization between Fe 3d and As 4p orbitals which can be affected by the pnictogen height to the Fe layer and reflects the multiband nature of Iron-based superconductors.

References

1. P.A. Lee et al., Rev. Of Modern Phys., 78, 17 (2006).
2. P. Richard et al. Phys. Rev. Lett. 104, 137001(2010).

Symmetry of C4 magnetic phase in hole-doped 122 iron based superconductors



D. D. Khalyavin^{1*}, S. W. Lovesey^{1,2}, P. Manuel¹, F. Krüger^{1,3}, S. Rosenkranz⁴, J. M. Allred⁴, O. Chmaissem^{4,5}, and R. Osborn⁴

¹ISIS Facility, Rutherford Appleton Laboratory, UK

²Diamond Light Source Ltd., UK

³University College London, UK

⁴Argonne National Laboratory, USA

⁵Northern Illinois University, USA

Email: * dmitry.khalyavin@stfc.ac.uk

Keywords: high T_c, C4-phase, orbital ordering, spin nematicity

Magneto-structural phase transitions in hole-doped Ba_{1-x}A_xFe₂As₂ (A = K, Na) superconductors are widely interpreted using two competitive theories one of which is based on magnetically and another on orbitally driven mechanisms. Both mechanisms predict identical orthorhombic space group symmetries for the nematic and magnetic phases observed over much of the phase diagram, but they predict different tetragonal space-group symmetries for the newly discovered re-entrant C4 tetragonal phase in the hole-doped systems with x ~ 0.25. In the magnetic scenario, the primary magnetic order parameter does not allow any type of orbital order, and the symmetry of the system is described by the *Pc4₂/ncm* magnetic space group. This symmetry does not involve any atomic displacements, in comparison with the parent *I4/mmm1'* space group. In the orbital scenario, we have determined two possible orbital patterns, specified by *P4/mnc1'* and *I4221'* space groups, which also do not require atomic displacements relative to the parent symmetry and, in consequence, are indistinguishable in conventional diffraction experiments. We demonstrated [1] that the three possible space groups are however, distinct in resonant X-ray Bragg diffraction patterns created by Templeton & Templeton scattering. This provides an experimental method for distinguishing between magnetic and orbital models. In addition a single-*k* versus two-*k* magnetic structures are expected in the orbital and magnetic scenarios providing an additional experimental way to determine the right model. We will present results of a resonant X-ray Bragg diffraction study of the C4-phase in Ba_{0.75}Na_{0.25}Fe₂As₂ single crystal as well as neutron diffraction measurements in applied magnetic field.

References

1. D. D. Khalyavin, S. W. Lovesey, P. Manuel, F. Krüger, S. Rosenkranz, J. M. Allred, O. Chmaissem, and R. Osborn, Phys. Rev. B 90, 174511 7(2014)

Antisymmetric exchange interactions tuning of the magnetic properties of La-substituted $\text{BiFe}_{0.5}\text{Sc}_{0.5}\text{O}_3$



P. Manuel^{1*}, D.D. Khalyavin¹, A.N. Salak², N.M. Olekhnovich³, A.B. Lopes², E.L. Fertman⁴

¹*ISIS Neutron Facility, STFC Rutherford Appleton Laboratory, Chilton, OX11 0QX, United Kingdom*

²*Department of Materials and Ceramic Engineering/CICECO, University of Aveiro, 3810-193, Aveiro, Portugal*

³*Scientific-Practical Materials Research Centre of National Academy of Science of Belarus, Minsk, 220072, Belarus*

⁴*B. Verkin institute for Low temperature Physics and Engineering of National Academy of Science of Ukraine, Kharkov, 61103, Ukraine*

Email: pascal.manuel@stfc.ac.uk

Keywords: multiferroics

BiFeO_3 is the most studied compound among multiferroic and magnetoelectric materials because its large polarization at room temperature makes it ideal for devices [1]. Subsequently, there is abundant literature on various attempts in controlling its properties (especially the coupling between magnetic and electric properties) through substitution or growth on different substrates. Within this context, we present a careful study on La-substituted $\text{Bi}_{1-x}\text{La}_x\text{Fe}_{0.5}\text{Sc}_{0.5}\text{O}_3$ ($x=0.2, 0.35$). These samples are obtained by high pressure-high temperature synthesis and investigated using electron, X-ray and neutron diffraction and magnetometry. Interestingly, the two samples have different structures with the 20% sample exhibiting an incommensurately modulated phase (Fig.1) whilst the 35% displays a more conventional orthorhombic structure [2-3]. Both samples display a magnetic transition below $\sim 220\text{K}$. A rigorous symmetry analysis allows us rationalize these experimental findings and highlights the key role played by the antisymmetric exchange interaction in controlling the magnetic structure, in particular, the weak ferromagnetism especially relevant for multiferroics.

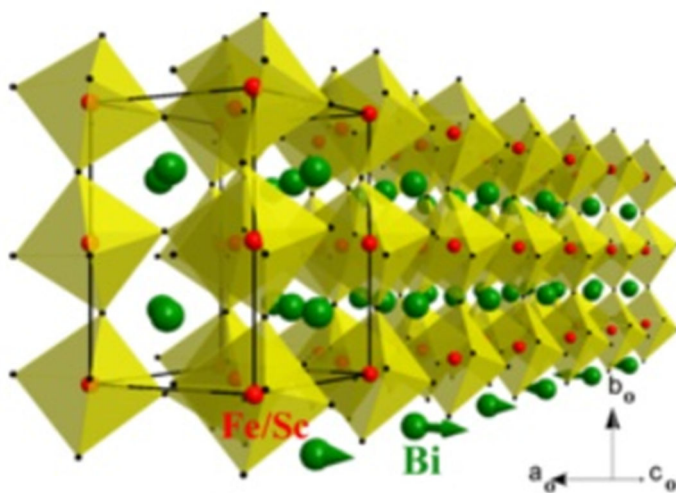


Figure 1: Incommensurate crystal structure of $\text{Bi}_{0.8}\text{La}_{0.2}\text{Fe}_{0.5}\text{Sc}_{0.5}\text{O}_3$. The incommensurate atomic displacements of Bi are represented by the arrows (only one chain shown for clarity).

References

1. eg G. Catalan and J.F. Scott, *Advanced Materials* 21, 2463 (2009)
2. D.D. Khalyavin et al, *Phys. Rev. B* 92, 224428 (2015)
3. D.D. Khalyavin et al, *Zeitschrift für Kristallographie* 230, 767 (2014).

Modulated spin helicity stabilized by incommensurate orbital density waves in a quadruple perovskite manganite



R. D. Johnson^{1,2*}, D. D. Khalyavin², P. Manuel², A. Bombardi³,
C. Martin⁴, L. C. Chapon⁵, and P. G. Radaelli¹

¹Clarendon Laboratory, Department of Physics, University of Oxford, Oxford, OX1 3PU, United Kingdom

²ISIS facility, Rutherford Appleton Laboratory-STFC, Chilton, Didcot, OX11 0QX, United Kingdom

³Diamond Light Source, Harwell Science and Innovation Campus, Didcot, OX11 0DE, United Kingdom

⁴Laboratoire CRISMAT, ENSICAEN, UMR F-6508 CNRS, 6 Boulevard du Marechal Juin, F-14050 Caen Cedex, France

⁵Institut Laue-Langevin, BP 156X, 38042 Grenoble, France

Email: * roger.johnson@physics.ox.ac.uk

Keywords: multiferroics, manganites, orbital density waves, magnetic structure

Through single crystal and powder neutron diffraction experiments combined with symmetry analysis and Landau theory, we report on the spin ordering in the magnetic ground state of the quadruple perovskite manganite $\text{CaMn}_7\text{O}_{12}$ - a material that supports an unusual incommensurate orbital density wave that onsets above the magnetic ordering temperature. The magnetic structure was found to be an unprecedentedly complex multi- \mathbf{k} helix with modulated spin helicity, which implies a novel mechanism for the coupling between the spin and orbital degrees of freedom. This magnetic structure can be expanded into a set of helical components with wavevectors $\mathbf{k}_{n\pm} = \mathbf{k}_0 \pm n\mathbf{k}_s$, where the fundamental term, $n = 0$, is combined with the higher-order members $n=1,2,\dots$ to couple to the orbital density wave of wavevector \mathbf{k}_s . At a microscopic level, the coupling can be understood by taking into account the continuous variation of the orbital occupancies on Mn^{3+} -sites, resulting in a modulation of the frustrated exchange topology of the system.

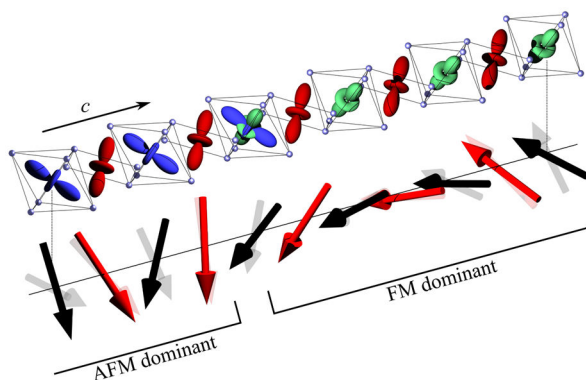


Figure 1: The ground state magnetic structure of $\text{CaMn}_7\text{O}_{12}$ projected along the c -axis. The manganese sites at $(0.5, 0, z)$, $z = n$, and $n+1/2$ are shown parallel to a cartoon of the orbital density waves projected onto the same sites.

Pseudogap phase diagram in cuprates studied by high field interlayer magnetotransport of overdoped Bi-2212



T. Watanabe^{1*}, T. Usui¹, S. Adachi¹, Y. Teramoto¹,
I. Kakeya², A. Kondo³, K. Kindo³, S. Kimura⁴

¹Graduate School of Science and Technology, Hirosaki University, Hirosaki 036-8561, Japan

²Department of Electronic Science and Engineering, Kyoto University, Kyoto 615-8510, Japan

³Institute for Solid State Physics, University of Tokyo, 5-1-5 Kashiwanoha, Kashiwa, Chiba 277-8581, Japan

⁴Institute for Materials Research, Tohoku University, Sendai

980-8577, Japan

Email: * twatana@hirosaki-u.ac.jp

Keywords: high- T_c cuprates, Bi-2212, pseudogap, out-of-plane resistivity, magnetoresistance, density-of-states (DOS) fluctuation

To determine the mechanism of high transition temperature (high- T_c) superconductivity in cuprates, we must understand the relationship between the pseudogap and superconductivity[1]. In this respect, it is important to determine an accurate pseudogap phase diagram experimentally. The main problem we encounter for this purpose is that it is difficult to determine, in the overdoped region, whether the observed effect is related to the pseudogap or the superconductivity[2]. For example, although a negative slope in the out-of-plane resistivity $\rho_c(H)$ for higher fields has been previously reported[3], the origin of this phenomenon is still being debated.

In general, the pseudogap is insensitive to magnetic fields compared with superconductivity[4]. Therefore, if we can obtain a high enough field near the upper critical field H_{c2} , we can expect to observe the pseudogap and superconductive contributions separately for the magnetic field dependence of ρ_c . For this purpose, we measure the out-of-plane resistivity $\rho_c(H)$ of an overdoped $\text{Bi}_{1.6}\text{Pb}_{0.4}\text{Sr}_2\text{CaCu}_{1.96}\text{Fe}_{0.04}\text{O}_{8+\delta}$ (Bi-2212) single crystal under pulsed magnetic fields up to 60 T.

Above T_c , magnetoconductivity (MC) is due to two positive components: one component gradually increases as H^2 , and the other component adds to it for lower fields (Fig.1 (a)-(e)). The latter decreases with increasing temperature and vanishes around the onset temperature of superconductive fluctuation T_{scf} . Thus, it is attributed to the superconductive density-of-states (DOS) depletion effect. The former is present both below and above T_{scf} . Thus, it is attributed to the pseudogap effect. Subsequent analysis below T_c shows that the negative slope for $\rho_c(H)$ is primarily due to the superconductive DOS depletion effect. Comparison with a single-layer compound (Bi-2201) shows that the pseudogap contribution in Bi-2212 is unexpectedly small in the superconducting state, suggesting that some portion of the pseudogap changes into a

superconducting gap in this compound. This result implies that the pseudogap merges with superconductivity in more overdoped states, supporting the scenario that the pseudogap results in high- T_c superconductivity.

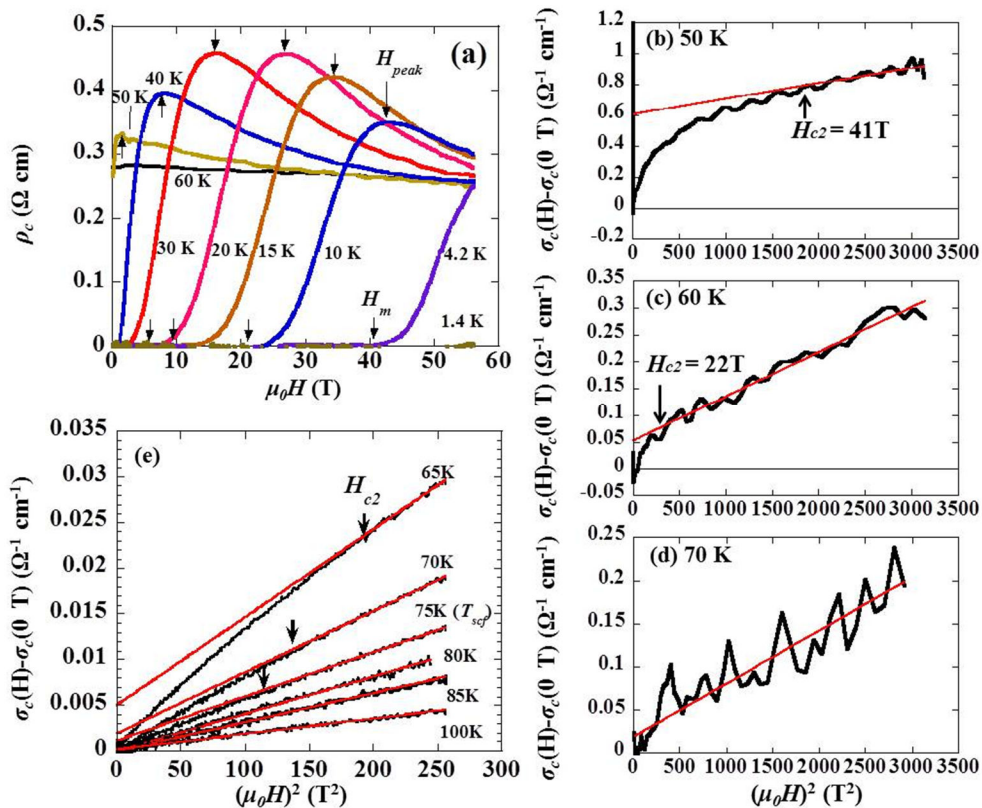


Figure 1: (a) Magnetic field dependence of ρ_c for $\text{Bi}_{1.6}\text{Pb}_{0.4}\text{Sr}_2\text{CaCu}_{1.96}\text{Fe}_{0.04}\text{O}_{8+\delta}$ below and above T_c . (b)-(d) Out-of-plane magnetoconductivity (MC), $\sigma(H) - \sigma(0\text{T})$, at 50, 60, and 70 K, respectively. (e) $\sigma(H) - \sigma(0\text{T})$, using a steady magnet up to 16 T.

References

1. B. Keimer, S. A. Kivelson, M. R. Norman, S. Uchida, and J. Zaanen, *Nature* 518, 179 (2015).
2. T. Usui, D. Fujiwara, S. Adachi, H. Kudo, K. Murata, H. Kushibiki, T. Watanabe, K. Kudo, T. Nishizaki, N. Kobayashi, S. Kimura, K. Yamada, T. Naito, T. Noji, and Y. Koike, *J. Phys. Soc. Jpn.* 83, 064713 (2014).
3. T. Shibauchi, L. Krusin-Elbaum, G. Blatter, and C. H. Mielke, *Phys. Rev. B* 67, 064514 (2003).
4. V. M. Krasnov, A. E. Kovalev, A. Yurgens, and D. Winkler, *Phys. Rev. Lett.* 86, 2657 (2001).

Competing orders/fluctuations in high-temperature superconductors revealed by ARPES



Atsushi Fujimori
¹*University of Tokyo*

Email: fujimori@phys.s.u-tokyo.ac.jp

Keywords: high T_c, nano-clusters, shell structure

Competition between magnetism, charge order, and superconductivity observed in various high-temperature superconductors has been the subject of extensive research. Through the observation of band folding signature caused by such orders or fluctuations, ARPES yields deep insights into the nature of competing orders whose fluctuations might enhance the superconductivity. In this talk, two dramatic observations are presented and discussed: (i) In electron-doped cuprates after “protect annealing” [1], the band folding due to antiferromagnetic short-range order is suppressed while the signature of charge fluctuations remains as strong as the hole-doped cuprates [2]. The range of the superconducting phase is enlarged from under-doped to over-doped regions with a nearly constant T_c. (ii) In a parent compound BaFe₂As₂ of iron-based superconductors, the band folding signature of the antiferromagnetic order, i.e., the Dirac cone, persists well above the Neel temperature, within the so-called “nematic phase”. We attribute this observation to the existence of antiferro-orbital component in the latter phase [3].

This work has been done in collaboration with M. Horio, T. Adachi, Y. Koide, K. Koshiishi, L. Liu, K. Okazaki, T. Yoshida, T. Mizokawa, M. Hashimoto, Z.-X. Shen, H. Kumigashira, K. Ono, T. Terashima, S. Ishida, M. Nakajima, Y. Tomioka, T. Itoh, K. Kiho, C.-H. Lee, A. Iyo, H. Eisaki, S. Uchida, A. Ino, H. Anzai, M. Arita, H. Namatame, and M. Taniguchi.

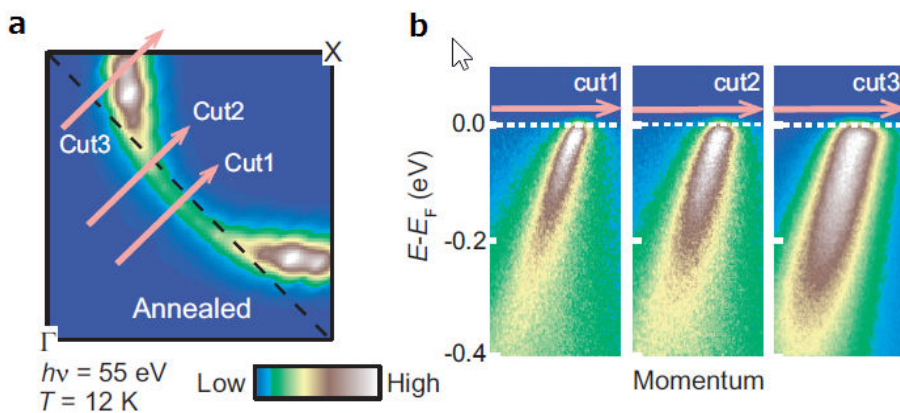


Figure 1: ARPES spectra of “protect annealed” $\text{Pr}_{1.3-x}\text{La}_{0.7}\text{Ce}_x\text{CuO}_4$ [2]. The absence of antiferromagnetic (AFM) pseudogap at the “hot spots” indicates suppression of the AFM short-range order commonly seen in the electron-doped cuprates.

References

1. T. Adachi et al., J. Phys. Soc. Jpn 82, 063713 (2013).
2. M. Hiroi et al., Nat. Commun., to appear; arXiv:1502.03395.
3. K. Koshishi et al., in preparation.

Variety of Fermi surface nesting and the pairing mechanism beyond it in iron-based superconductors



S. Tajima^{1*}, S. Miyasaka¹, M. Nakajima¹, A. Takemori¹, M. Uekubo¹, T. Kobayashi¹, K. T. Lai^{1,2}, H. Mukuda¹, K. Tanaka³

¹Osaka University, Osaka, Japan

²Max-Planck Institute, Dresden, Germany (Present Address)

³Institute of Molecular Science, Okazaki, Japan

Email: * tajima@phys.sci.osaka-u.ac.jp

Keywords: Iron based superconductors, Fermi surface nesting, Multiband system

The electronic band structure of iron-based superconductors is complicated and determined by a delicate valence of the contributions from the five Fe *d*-orbitals. This makes physical properties (including a superconducting transition temperature T_c) very sensitive to local crystal structure and chemical composition. Conversely, we can tune the physical properties by changing chemical compositions, which enables us to find a key ingredient for electronic state and superconductivity mechanism.

In my talk, I report our systematic study on LaFeAsO (1111) system. We have controlled two factors. One is carrier doping level in a sense of rigid band model. It was achieved by Sr/La substitution and F/O or H/O substitution. The other is local chemical pressure achieved by P/As substitution. (Pnictogen height from Fe-layer is changed.) We have synthesized various series of LaFe(P_{1-x}As_x)O for various carrier doping levels. From transport and magnetic measurements, unusual electronic phase diagram has been revealed, indicating three different superconducting phases.

For the F-free system LaFe(P_{1-x}As_x)O and the hole doped system (La_{0.9}Sr_{0.1})Fe(P_{1-x}As_x)O, two superconducting phases (SC1 and SC2) were found [1]. These are separated by an antiferromagnetic phase. According to the band calculation [2], Fermi surface configurations are different in these two phases and thus the orbital characters contributing to the Fermi surface nesting are different. In the SC2 phase, with increasing As-content (*x*), *T*-dependence of resistivity changes from $\rho \sim T^2$ to $\rho \sim T$ and T_c increases accordingly. At the T_c maximum composition (*x*=0.6), resistivity shows *T*-linear behavior and the NMR measurement indicates a strong spin fluctuation [3]. All these results point to a spin fluctuation mechanism determined by the Fermi surface nesting. By contrast, the SC1 phase is too narrow to observe such a systematic change in the physical properties.

When electrons are doped by F- or H-substitution, both of the SC1 and SC2 phases expand and merge with each other. For further electron doping, the SC1 is suppressed probably because the d_{xy} hole Fermi surface crucial for the SC1 shrinks.

In the heavily electron doped regime (30% H-doping), as Hosono's group reported [4], another superconducting phase (SC3) appears. We found that this superconductivity is rapidly suppressed by a small amount of P-substitution. Even after superconductivity disappears with P-substitution, the system remains a conventional good metal and no magnetic phase appears. This indicates that the low energy spin fluctuation is very weak because of the bad nesting condition. In order to explain high T_c superconductivity in this region, a more localized picture is required.

Summing up, we have revealed three different superconducting phases in 1111-system. The Fermi surface configurations are different in these phases, which gives different mechanisms of bosonic fluctuation that is crucial for superconductivity. The electronic properties near the SC3 phase cannot be described by the Fermi surface nesting scenario. Such a variety of electronic state suggests that the iron-based superconductors are near the crossover from weakly interacting electronic system to strongly correlated system.

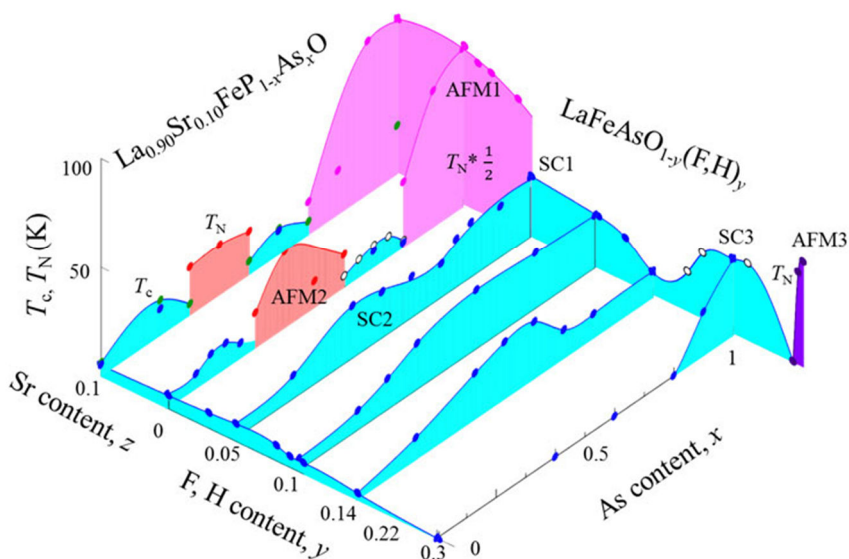


Figure 1: Electronic phase diagram of (La,Sr)Fe(P,As)(O,F/H)

References

1. K. T. Lai *et al.*, Phys. Rev. B **90**, 064504 (2014).
2. K. Kuroki *et al.* Phys. Rev. B. **79**, 224511 (2009)
3. H. Mukuda *et al.*, J. Phys. Soc. Jpn. **83**, 083702 (2014).
4. M. Hiraishi *et al.*, Nat. Phys. **10**, 300 (2014).

Infrared measurements of the superfluid and normal-fluid densities in the cuprate superconductors



D.B. Tanner
University of Florida

Email: tanner@phys.ufl.edu

Keywords: high T_c, infrared, cuprate

Measurements for a number of cuprate families of optical reflectance over a wide spectral range (far-infrared to ultraviolet) have been analyzed using Kramers-Kronig analysis to obtain the optical conductivity, $\sigma(\omega)$, and (by integration of the real part of the conductivity) the spectral weight of low- and mid-energy excitations. For the Kramers-Kronig analysis to give reliable results, accurate high-frequency extrapolations, based on x-ray atomic scattering functions, were used. When the optical conductivities of the normal and superconducting states are compared, a transfer of spectral weight from finite frequencies to the zero-frequency delta-function conductivity of the superconductor is seen. The strength of this delta function gives the superfluid density, ρ_s . There are two ways to measure ρ_s , using either the partial sum rule for the conductivity or by examination of $\sigma_2(\omega)$; both estimates show that 98% of the *ab*-plane superfluid density comes from energies below 0.15 eV.

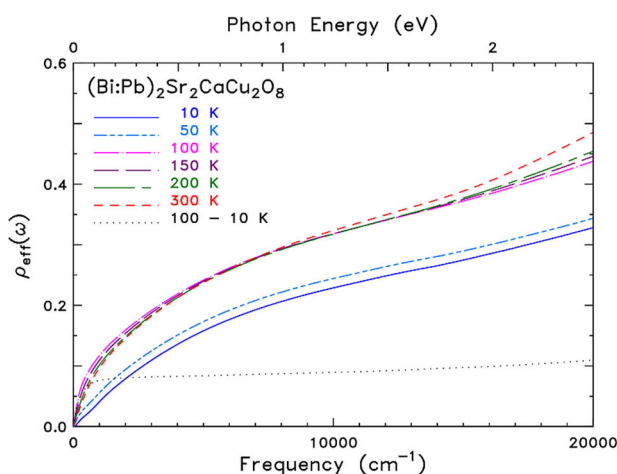


Figure 1: Integrated spectral weight in a $(\text{Bi:Pb})_2\text{Sr}_2\text{CaCu}_2\text{O}_8$ crystal as a function of the upper limit of integration. The low energy spectral weight is exhausted by about $12,000 \text{ cm}^{-1}$ (1.5 eV). Below T_c about 20% of the total, spectral weight is removed to the zero-frequency delta function. Note that the difference (dotted line) saturates at around 1000 cm^{-1} .

Moreover, there is a notable difference between a clean metallic superconductor and the cuprates. In the former, the superfluid density is essentially equal to the conduction electron density. The cuprates, in contrast, have only about 20% of the *ab*-plane low-energy spectral weight in the superfluid. The rest remains in finite-frequency, midinfrared absorption. In underdoped materials the superfluid fraction is even smaller.

Musr detection of free spins in granular Al films near the Metal to Insulator transition



Guy Deutscher¹, Nimrod Bachar^{1,2}, A. Levy¹, S.Lerer¹, H. Saadaoui³, Z. Zalman³ and E. Morenzoni³.

¹*Tel Aviv University, School of Physics and Astronomy*

²*University of Geneva, Department of Condensed Matter Physics*

³*laboratory for Muon Spin Spectroscopy, Paul Scherrer Institute*

Email: * guyde@tau.ac.il

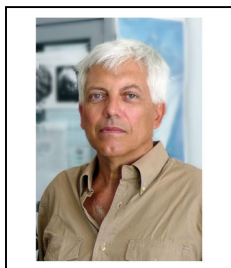
Keywords: high Tc, nano-clusters, shell structure,

We report on Muon Spin Rotation measurements (musr) performed on granular Al films of medium to high normal state resistivity, ranging from a few 100 $\mu\Omega\text{cm}$ to 100,000 $\mu\Omega\text{cm}$, approaching the Metal to Insulator transition (M/I). The data could be fitted to the Kubo-Toyabe theory, involving both static, temperature independent, Al nuclear fields and a temperature dependent contribution indicating the presence of free spins. These measurements confirm the presence of magnetic impurities first derived indirectly from the negative magneto-resistance observed up to high temperatures [1] and by preliminary musr data [2]. At high temperatures the free spin contribution to the musr signal is seen to increase strongly with the normal state resistivity as the metal to insulator transition is approached. This is in line with the behavior of the negative magneto-resistance that becomes vanishingly small at high temperatures in samples away from the M/I transition[1]. The dependence of the free spin contribution is less strong at low temperatures, possibly indicating a progressive freezing of the spins. Possible origins of the free spin contribution will be discussed. It has been predicted that the occurrence of free spins is a generic feature of a system approaching a Mott transition [3]. Such could be the case in granular Al films since it has been argued that they undergo a Mott M/I transition at high resistivity [2].

References

1. N. Bachar, S. Lerer, S. Hacoheh-Gourgy, B. Almog and G. Deutscher, Phys. Rev. B **87**, 214512 (2013).
2. N. Bacar, S. Lerer, A. Levy, S. Hacoheh-Gourgy, B. Almog, H. Saadaouyi, Z. Salman, E. Morenzoni and G. Deutscher.
3. A. Georges, G. Kotliar, W. Krauth and M.J. Rozenberg, Rev. Mod. Phys. **68**, 13 (1996).

Systematic investigation of the effects of disorder at the lowest order throughout the BCS-BEC crossover



Giancarlo Calvanese Strinati^{*1,2}, Fabrizio Palestini¹
¹*Division of Physics, School of Science and Technology,
Università di Camerino, 62032 Camerino (MC), Italy*
²*INFN, Sezione di Perugia, 06123 Perugia (PG), Italy*

Email: * giancarlo.strinati@unicam.it

Keywords: BCS-BEC crossover, disorder, pseudo-gap

A systematic investigation of the effects of disorder on the BCS-BEC crossover at the lowest order in the impurity potential is presented for the normal phase above the critical temperature T_c [1]. Starting with the t-matrix approach for the clean system, by which pairing correlations between opposite-spin fermions evolve from the weak-coupling (BCS) to the strong-coupling (BEC) limits by increasing the strength of the attractive inter-particle interaction, *all* possible diagrammatic processes are considered where the effects of a disordered potential are retained in the self-energy at the lowest order. An accurate numerical investigation is carried out for all these diagrammatic terms, to determine which of them are mostly important throughout the BCS-BEC crossover. Explicit calculations for the values of T_c and chemical potential are carried out. In addition, the effect of disorder on the single-particle spectral function is analyzed, and a correlation is found between an increase of T_c and a widening of the pseudo-gap at T_c on the BCS side of unitarity in the presence of disorder, while on the BEC side of unitarity the presence of disorder favors the collapse of the underlying Fermi surface. The present investigation is meant to orient future studies when the effects of disorder will be considered at higher orders, with the purpose of limiting the proliferation of diagrammatic terms in which interaction and disorder are considered simultaneously.

References

1. F. Palestini and G. C. Strinati, Phys. Rev. B **88**, 174504 (2013).

Ubiquitous stripe charge order in low dimensional superconductors observed by scanning tunneling microscopy



J. Bruér, A. Novello, I. Maggio-Aprile, A. Scarfato, M. Spera, Ch. Berthod and Ch. Renner*

Department of Quantum Matter Physics, University of Geneva, 1211 Geneva 4, Switzerland

Email: * christoph.renner@unige.ch

Keywords: STM, tunneling spectroscopy, CDW, stripes

The interplay between charge density waves (CDWs) and superconductivity is the focus of an intensive research effort in a range of low dimensional superconducting materials. The role of charge order and charge stripes in particular, and whether they are competing or not with superconductivity are subject to detailed experimental scrutiny. Charge stripes have been observed in several transition metal dichalcogenides and in intercalated graphite compounds. In Cu intercalated $1T$ -TiSe₂, a compound with the highest T_c reported for any $1T$ -polytype, we have found an instability towards the formation of charge stripes in the CDW phase. In YBa₂Cu₃O_{7- δ} , the proper analysis of vortex core tunneling spectra provides new insight into the charge-ordered phases in high- T_c cuprates. In both systems, scanning tunneling spectroscopy does not show any obvious competition between the charge-ordered phase and the superconducting order parameter.

Finite wavevector nematic fluctuations in Fe-based Superconductors



D. Reznik^{2*}, J-P. Castellan, D. Parshall, L. Pinschovius³ F. Weber.

¹University of Colorado-Boulder, Boulder, CO USA

²Karlsruhe Institute of Technology, Karlsruhe, Germany

³NIST Center for Neutron Research, Gaithersburg, MD, USA

⁴Laboratoire Leon Brillouin, Saclay, France

Email: * Dmitry.reznik@colorado.edu

Keywords: high T_c , iron pnictides, nematic fluctuations,

Nematic order and fluctuations in Fe-based superconductors break tetragonal symmetry due to anisotropic magnetic fluctuations, which couple to the atomic lattice via magnetostriction. As a result the shear mode of the bulk modulus, C_{66} , typically measured by resonant ultrasound (RUS), and long-wavelength acoustic phonons, measured by neutron or x-ray scattering, soften as these fluctuations build up. The talk will focus on our new published [1] and unpublished results of a systematic multiyear study of nematic fluctuations in iron pnictides where we probed nematic fluctuations at finite wavevectors by measuring long-wavelength transverse acoustic phonons.

Both C_{66} and acoustic phonons that connect to the shear mode in the long wavelength limit, soften on cooling from room temperature in the tetragonal nonsuperconducting phase of $\text{BaFe}_{2-x}\text{Co}_x\text{As}_2$. In the orthorhombic phase, C_{66} cannot be measured due to twinning. We found that the phonons show hardening indicating that orthorhombic distortion suppresses nematic fluctuations.

It is well-known that in the superconducting tetragonal phase C_{66} hardens on cooling [2] i.e. superconductivity competes with zone center nematic fluctuations. We found that transverse acoustic phonons at small wavevectors show the opposite behavior: They soften in the superconducting phase and have no sign of competition with superconductivity. (Fig. 1) In fact in the overdoped sample, which is far from the structural transition, the phonon softening at small q continues through T_c with no observable feature at T_c .

The main unexpected result of our investigation is that nematic fluctuations with nonzero wavevector do not compete with superconductivity. I will discuss its implication for our understanding of iron-based superconductors and also present new results on LiFeAs.

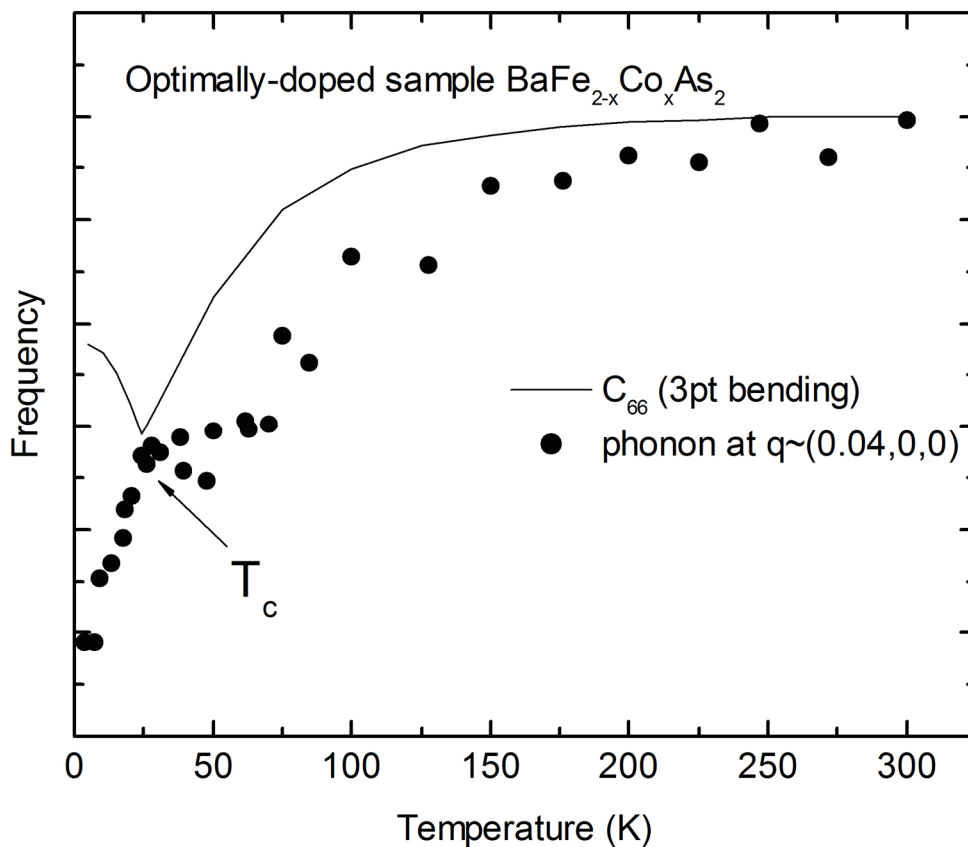


Figure 1: Temperature-dependence of the phonon frequency and C_{66} measured by 3-point-bending technique [2] showing opposite behavior below superconducting T_c . The plateau between 25K and 70K is caused by short-range ordered orthorhombic domains. The phonon result will be published in the near future.

References

1. D. Parshall et al. Phys. Rev. B **91**, 134426 (2015).
2. A. E. Böhmer et al. Phys. Rev. Lett. **112**, 047001 (2014).

Synchrotron Spectroscopic Experiments on Ruthenates



C. G. Fatuzzo^{1*}, M. Dantz², S. Fatale¹, O. Ivashko³, P. Olalde-Velasco², N. E. Shaik¹, B. Dalla Piazza¹, S. Toth⁴, J. Pellicciari², R. Fittipaldi^{5,6}, A. Vecchione^{5,6}, N. Kikugawa^{7,8}, J. S. Brooks⁸, H. M. Rønnow^{1,9}, M. Griioni¹, Ch. Rüegg^{4,10}, T. Schmitt², and J. Chang^{1,3}

¹*Institute for Condensed Matter Physics, EPFL, Switzerland*

²*Swiss Light Source, Paul Scherrer Institut, Switzerland*

³*Physics Institute, University of Zurich (UZH), Switzerland*

⁴*Laboratory for Neutron Scattering and Imaging, Paul Scherrer Institut, Switzerland*

⁵*CNR-SPIN, I-84084 Fisciano, Salerno, Italy*

⁶*Dipartimento di Fisica "E.R. Caianiello", Università di Salerno, Italy*

⁷*National Institute for Materials Science, 1-2-1 Sengen, Tsukuba, Japan*

⁸*National High Magnetic Field Laboratory, Tallahassee, USA*

⁹*Institute for Solid State Physics (ISSP), University of Tokyo, Japan*

¹⁰*Department of Quantum Matter Physics, University of Geneva, Switzerland*

Email of the presenting author* claudia.fatuzzo@epfl.ch

Keywords: Ruthenates – Spin-Orbit – d-Electrons – Synchrotron – Spectroscopy Experiments

Ruthenate-oxide materials attract much attention due to the interesting ground states they exhibit, such as unconventional superconductivity in Sr_2RuO_4 or Mott physics in Ca_2RuO_4 . The role of electron correlations, Hund's coupling and spin-orbit interactions is still being debated and explored [1,2].

In this talk, we present recent experimental study on the Ru 4d-orbital occupation and excitations in $(\text{Ca}/\text{Sr})_2\text{RuO}_4$, performed through a combination of synchrotron spectroscopic techniques.

References

1. T. Mizokawa et al., Phys. Rev. Lett. 87, 077202 (2001)
2. M. W. Haverkort et al., Phys. Rev. Lett. 101,026406 (2008)

High Magnetic Field Studies of Novel Superconductors



Fedor F. Balakirev¹

¹*National High Magnetic Field Laboratory, Los Alamos National Laboratory, MS-E536, Bikini Atoll Road, Los Alamos, New Mexico 87545, USA*

Email: *fedor@lanl.gov

Keywords: high T_c , Phase transitions, Cuprates, Iron based superconductors

High magnetic fields have proven to be an invaluable tool for exploring magnetic and electronic properties of novel materials. Exposing unconventional superconductors to the extreme conditions of high fields enables direct probes of the superconducting order and vortex matter, high-resolution studies of the size and shape of Fermi surfaces, and elucidates competing orders and underlying ground states.

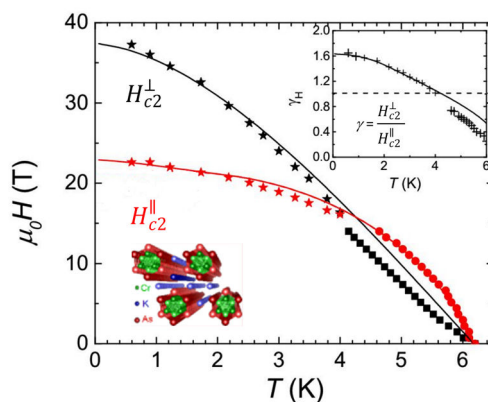


Figure 1: A recent example of high field probe of the upper critical field in novel non-organic one dimensional superconductor comprised of $[\text{Cr}_3\text{As}_3]_\infty$ double-walled subnanotubes. The critical field anisotropy reversal suggest unusual superconducting state in the vicinity of magnetic order[1,2].

References

1. Jin-Ke Bao et al., Phys. Rev. X 5, 011013 (2015)
2. F. F. Balakirev et al., Phys. Rev. B 91, 220505(R) (2015)

Intrinsic Spin-Hall Effect in Systems with Striped Spin-Orbit Coupling



G. Seibold^{1*}, S. Caprara², M. Grilli², R. Raimondi³

¹*BTU Cottbus-Senftenberg, Cottbus, Germany*

²*University of Rome 'La Sapienza', Rome, Italy*

³*University 'Roma Tre', Rome, Italy*

Email: goetz.seibold@b-tu.de

Keywords: spin Hall effect, Rashba spin-orbit coupling

The Rashba spin-orbit coupling arising from structure inversion asymmetry couples spin and momentum degrees of freedom providing a suitable (and very intensively investigated) environment for spintronic effects and devices. In this framework, the spin-Hall effect is a crucial ingredient since it allows for the manipulation of spin degrees of freedom without magnetic fields. Here we show that, in the presence of disorder, a striped modulation of a two-dimensional electron gas, affecting both density and Rashba spin-orbit coupling, gives rise to a finite spin Hall conductivity in contrast with the corresponding homogeneous system. We suggest that this mechanism can be exploited for a practical realization of a spin-Hall device. This could be implemented at oxide interfaces with periodic top gating (cf. Fig. 1), leading to a large ratio between the induced spin and charge currents.

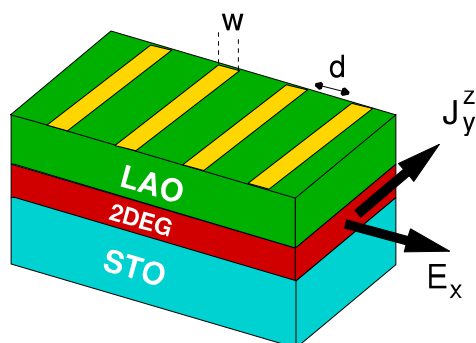


Figure 1: Schematic view of a possible device in which the spin-Hall effect is enforced in the 2DEG at the interface of a LAO/STO heterostructure. The yellow stripes represent top-gating electrodes of width w and interspacing d .

Fermi-surface in the presence of magnetic-vortex checkerboard



Pavel Dolgirev^{1,2}, Boris V. Fine^{1,3**},

¹*Skolkovo Institute of Science and Technology, Territory of Skolkovo Innovation Center, Nobel Str. 3, Moscow 143026 Russia*

²*Department of General and Applied Physics, Institutskiy per. 9, Moscow Institute of Physics and Technology, Dolgoprudny, Moscow Region, 141700, Russia*

³*Institute for Theoretical Physics, University of Heidelberg, Philosophenweg 12, 69120 Heidelberg, Germany*

Email: * b.fine@skoltech.ru

Keywords: high-Tc cuprate superconductors, stripes, checkerboards, Fermi-ark, pseudogap

One of the puzzles associated with 1/8-doped lanthanum cuprates is the observation of the nodes of the pseudogap at angle 45 degrees with respect to the principal lattice directions[1,2]. In the framework of the stripe scenario, the above directions are also at 45 degrees with respect to the supposed stripe orientation - the fact that is difficult to explain. We consider an alternative to stripes known as magnetic-vortex checkerboard[3,4] and perform the calculation of the Fermi-surface in the framework of a simplified model imitating the magnetic modulation. We find that, for a certain range of parameters, the Fermi surface has a character of a small Fermi-ark with the same orientation as the experimentally observed pseudogap nodes.

References

1. T. Valla et al., Science **314**, 1914 (2006)
2. R. He et al., Nat. Phys. **5**, 119 (2009)
3. B. V. Fine, Phys. Rev. B **75**, 060504R (2007)
4. B. V. Fine, J. Supercond. Nov. Magn. **24**, 1207 (2011).

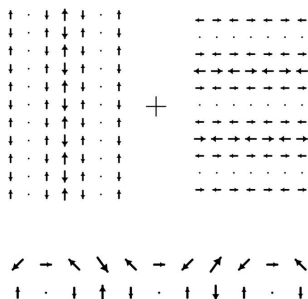


Figure 1: Checkerboard of magnetic vortices

Topological superconductivity: from materials to topotronics



A. Brinkman^{1*}

¹*MESA+ Institute for Nanotechnology, University of Twente, the Netherlands*

Email: * a.brinkman@utwente.nl

Keywords: topological insulator, Josephson junction, Majorana bound state

Josephson vortices in topological junctions have been predicted to host Majorana bound states. In order to create a platform for braiding these non-Abelian anyons, topological Josephson junctions are studied on the surface of a three-dimensional topological insulator.

The materials science of the Bi-based topological insulators has now advanced to the point where bulk conduction can be neglected. By in-situ scanning tunneling microscopy as well as in-situ angle resolved photoemission spectroscopy we show that the Fermi energy of our molecular beam epitaxy grown Bi_2Te_3 thin films only crosses the topological Dirac states [1]. Also exfoliated single crystal flakes of $\text{Bi}_{2-x}\text{Sb}_x\text{Te}_{3-y}\text{Se}_y$ reveal negligible bulk conduction [2]. Hall bar devices are made of this material with functional top and back gates. We show at high magnetic fields that the Fermi energy can be tuned throughout the Landau levels of the half integer quantum Hall effect of the topological bottom and top surfaces.

The pairing symmetry associated with the proximity induced topological superconductivity has a p-wave component. Theory suggests zero-bias conductance peaks as soon as time reversal symmetry is broken [3]. We have made superconductor – topological insulator – normal metal junctions in which we study the differential conductance, revealing the topological proximity effect.

Gate tunable Josephson junctions on the surface of Bi-based topological insulator have been realized. We study the relative contribution of the Majorana bound state to the Josephson supercurrent by measuring and analyzing the magnetic field dependence as well as the junction behavior under microwave irradiation.

References

1. P. Ngabonziza, R. Heimbuch, R.A. Klaassen, M.P. Stehno, M. Snelder, A. Solmaz, S.V. Ramankutty, E. Frantzeskakis, E. van Heumen, G. Koster, M.S. Golden, H.J.W. Zandvliet, and A. Brinkman, *Phys. Rev. B* **92**, 035405 (2015).
2. Y. Pan, D.Wu, J.R. Angevaere, H. Luigjes, E. Frantzeskakis, N. de Jong, E. van Heumen, T.V. Bay, B. Zwartsenberg, Y.K. Huang, M. Snelder, A. Brinkman, M.S. Golden, and A. de Visser, *New Journ. Phys.* **16**, 123035 (2014).
3. M. Snelder, Y. Asano, A.A. Golubov, A. Brinkman, *J. Phys.: Condens. Matter* **27**, 315701 (2015).

Lattice dynamical properties of superconducting SrPt₃P studied via inelastic x-ray scattering and density functional perturbation theory



Diego A. Zocco^{1*}, Sven Krannich¹, Rolf Heid¹, Klaus-Peter Bohnen¹, Thomas Wolf¹, Thomas Forrest², Alexei Bosak², and Frank Weber¹

¹*Institute of Solid State Physics, Karlsruhe Institute of Technology, D-76021 Karlsruhe, Germany*

²*European Synchrotron Radiation Facility (ESRF), F-38043 Grenoble, France*

Email: *diego.zocco@kit.edu

Keywords: superconductivity, spin-orbit coupling, electron-phonon coupling, inelastic x-ray scattering

We present a study of the lattice dynamical properties of superconducting SrPt₃P ($T_c = 8.4$ K) via high-resolution inelastic x-ray scattering (IXS) and *ab initio* calculations. Density functional perturbation theory including spin-orbit coupling results in enhanced electron-phonon coupling (EPC) for the optic phonon modes originating from the Pt(I) atoms, with energies ~ 5 meV, resulting in a large EPC constant $\lambda \sim 2$. An overall softening of the IXS powder spectra occurs from room to low temperatures, consistent with the predicted strong EPC and with recent specific-heat experiments ($2\Delta_0/k_B T_c \sim 5$) [1,2]. The low-lying phonon modes observed in the experiments are approximately 1.5 meV harder than the corresponding calculated phonon branch. Moreover, we do not find any changes in the spectra upon entering the superconducting phase. We conclude that current theoretical calculations underestimate the energy of the lowest band of phonon modes indicating that the coupling of these modes to the electronic subsystem is overestimated.

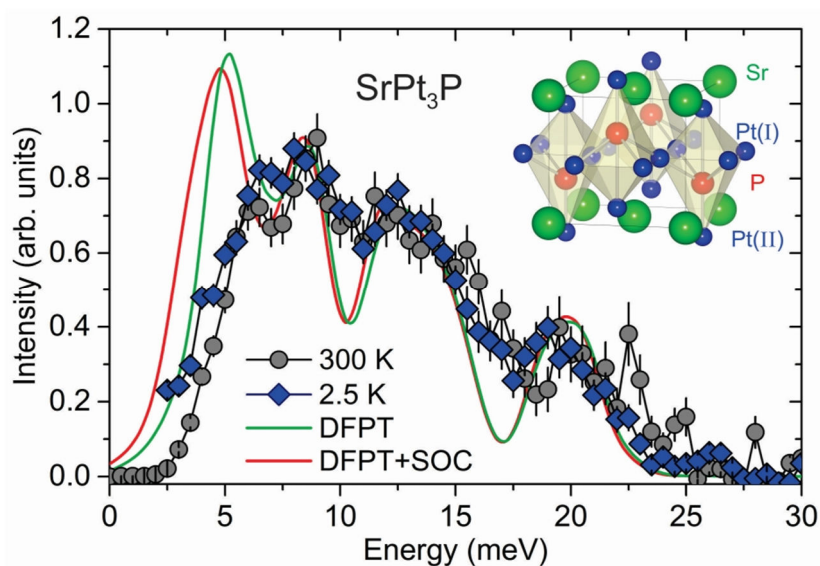
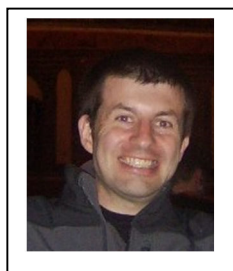


Figure 1: Inelastic data of powder SrPt₃P from combined energy scans at $Q = 5.7 \text{ \AA}^{-1}$ obtained at 300 K (circles) and 2.5 K (diamonds). An overall softening of the IXS powder spectra occurs from room to low temperatures, consistent with the predicted strong EPC. Powder-average calculations of the dynamical structure factors are shown as green (no SOC) and red (with SOC) lines. The low-lying phonon modes observed in the experiments are approximately 1.5 meV harder than the corresponding calculated phonon branch. Inset: crystal structure of SrPt₃P. Platinum atoms occupy two distinct positions, Pt(I) and (II).

References

1. T. Takayama et al., Phys. Rev. Lett. 108, 237001 (2012)
2. D. A. Zocco et al., Phys. Rev. B 92, 220504(R) (2015)

Charge Ordered Structure of $\text{La}_{2-x}\text{Sr}_x\text{CoO}_4$



P. G. Freeman^{1,2}, P. Babkevich², D. Prabhakaran³, and A. T. Boothroyd³.

¹*Jermiah Horrocks Institute, University of Central Lancashire, Preston, U.K.*

²*Laboratory for Quantum Magnetism, Institute of Condensed Matter Physics (ICMP), EPFL, Lausanne, Switzerland.*

³*Department of Physics, University of Oxford, Clarendon Laboratory, Oxford, OX1 3PU, UK*

Email: * pgfreeman@uclan.ac.uk

Keywords: high Tc, copper oxide, charge order

The discovery of an hourglass shaped magnetic excitation spectrum in $\text{La}_{5/3}\text{Sr}_{1/3}\text{CoO}_4$ was thought to pose a solution to the origin of the universal magnetic excitation spectrum of hole doped cuprate superconductors, as due to charge-stripes [1]. The unexpected discovery of partial two dimensional checkerboard charge order in $\text{La}_{2-x}\text{Sr}_x\text{CoO}_4$ $x < 0.5$, has brought into question the charge-stripe model of magnetic interactions in $\text{La}_{2-x}\text{Sr}_x\text{CoO}_4$ below half doping[2]. Here we present a new diffraction study of $\text{La}_{5/3}\text{Sr}_{1/3}\text{CoO}_4$, which reveals the complexity of the charge ordering in $\text{La}_{2-x}\text{Sr}_x\text{CoO}_4$, further building on the present understanding of this material. Our new findings provides insight into the complex ordering processes observed by muon spectroscopy on $\text{La}_{5/3}\text{Sr}_{1/3}\text{CoO}_4$ [3]. We will discuss a charge ordering scenario for $\text{La}_{2-x}\text{Sr}_x\text{CoO}_4$ that is consistent with present experimental findings, and the implications for understanding the hourglass shaped magnetic excitation spectrum of $\text{La}_{2-x}\text{Sr}_x\text{CoO}_4$.

References

1. A. T. Boothroyd, P. Babkevich, D. Prabhakaran and P. G. Freeman, *Nature* 471, 341 (2011).
2. Y. Drees et al., *Nature Commun.* 4, 2449 (2013) ; Y. Drees et al., *Nature Commun.* 5, 5731 (2014).
3. T. Lancaster et. al., *Phys. Rev B* 89, 020405R (2014).

Optical spectroscopy and pump-probe studies on charge density wave orders in LaAgSb₂



R. Y. Chen¹, S. J. Zhang¹, M. Y. Zhang¹ and N. L. Wang^{1,2*}

¹*International Center for Quantum Materials, School of Physics, Peking University, Beijing 100871, China*

²*Collaborative Innovation Center of Quantum Matter, Beijing 100871, China*

Email: *nlwang@pku.edu.cn

Keywords: charge density wave (CDW), amplitude modes, pump-probe, optical spectroscopy

The layered lanthanum silver antimonide LaAgSb₂ exhibits many interesting physical properties. The compound was known to experience two charge density wave (CDW) phase transitions at 207 and 186 K, respectively. Recent transport measurement revealed a large linear magnetoresistance, suggesting possible contribution from Dirac fermions. Presence of linear Sb 5p_{x,y} band dispersion and the Dirac-cone-like structure was indeed observed by ARPES experiment. We present optical spectroscopy and pump-probe measurement on the compound. We observe clearly energy gap formation below the CDW phase transition temperatures in optical conductivity, which removes most part of the free carrier spectral weight. The time resolved pump-probe measurement indicates that the photoinduced reflectivity can be well described by a single exponential decay for the whole measurement temperature range, except for the emergence of strong oscillations upon entering the CDW states. The oscillations come from the amplitude mode of CDW collective excitations. We find that the frequencies of the two amplitude modes are surprisingly low: only 0.12 THz for the CDW order with higher transition temperature and 0.34 THz for the lower one. The low energy scale of the CDW amplitude mode implies that the acoustic phonon mode, which experiences a softening to zero frequency and triggers the CDW transition, also has very low energy scale. The observations further suggest that the nesting wave vectors for the two CDW orders are extremely small, close to the center of Brillouin zone.

Delafossite metals: ultra high conductivity on two-dimensional triangular lattices



Andy Mackenzie^{1,2}

¹*Max Planck Institute for Chemical Physics of Solids, Dresden, Germany and*

²*University of St Andrews, Scotland*

Email: * mackenzie@cpfs.mpg.de

Keywords: electron-phonon coupling, angle resolved photoemission, electronic structure

The delafossites are a series of layered compounds with triangular lattices similar to that of NaCoO_2 but with a different stacking sequence along the c axis. They are host to intriguing magnetic insulators and semimetals, as well as metals such as PdCoO_2 , PtCoO_2 , PdCrO_2 and PdRhO_2 . The properties of these metals are remarkable. Although they are strongly two-dimensional, their room temperature conductivity is higher per carrier than that of any element, and PdCoO_2 crystals can have a low temperature resistivity of only a few $\text{n}\Omega\text{cm}$, corresponding to mean free paths of tens of microns. Our group is attempting on the one hand to accept this huge conductivity and profit from it, and on the other hand to investigate it, concentrating on spectroscopic properties and electronic structure calculations.

Main collaborators: Pallavi Kushwaha¹, Veronika Sunko^{1,2}, Nabhanilia Nandi¹, Philip Moll¹, Clifford Hicks¹, Phil King², Burkhard Schmidt¹, Helge Rosner¹ and Maurits Haverkort¹

Camelback-shaped band reconciles heavy-electron behavior with weak electronic Coulomb correlations in superconducting TINi_2Se_2



Ming Shi^{1*}

¹*Swiss Light Source, Paul Scherrer Institut, CH-5232 Villigen PSI, Switzerland*

Email: * ming.shi@psi.ch

Keywords: high-T_c, iron pnictides, correlation, ARPES, band filling

Combining photoemission spectroscopy, Raman spectroscopy, and first-principles calculations, we characterize superconducting TINi_2Se_2 as a material with weak electronic Coulomb correlations leading to a bandwidth renormalization of 1.4^[1]. We identify a camelback-shaped band, whose energetic position strongly depends on the selenium height. While this feature is universal in transition metal pnictides, in TINi_2Se_2 it lies in the immediate vicinity of the Fermi level, giving rise to a pronounced van Hove singularity (VHS). The resulting heavy band mass resolves the apparent puzzle of a large normal-state Sommerfeld coefficient in this weakly correlated compound. The correlation effect evolution in pnictides upon *d*-shell filling in the presence of significant Hund's exchange coupling will also be discussed [2 – 5]

References

1. N. Xu *et al.*, Phys. Rev. B 92, 081116(R) (2015)
2. N. Xu *et al.*, Phys. Rev. B 88, 220508(R) (2013).
3. N. Xu *et al.*, Phys. Rev. X 3, 011006 (2013).
4. N. Xu *et al.*, Phys. Rev. B 88, 220508(R) (2013)
5. S. Wu *et al.*, Phys. Rev. B 91, 235109 (2015)

Pressure-induced superconductivity in iron-based spin-ladder compound BaFe_2S_3



Hiroki Takahashi^{1*}, Chizuru Kawashima¹, Hideto Soeda¹, Yasuyuki Hirata², Takafumi Hawai³, Yusuke Nambu⁴, Taku J. Sato³, Kenya Ohgushi⁵

¹*College of Humanities & Sciences, Nihon University, Japan*

²*ISSP, University of Tokyo, Japan*

³*Institute of Multidisciplinary Research for Advanced Materials University, Tohoku, Sendai, Japan*

⁴*Institute for Materials Research, Tohoku University, Japan*

⁵*Department of Physics, Tohoku University, Japan*

Email: * hiroki@chs.nihon-u.ac.jp

Keywords: iron-based spin-ladder, insulator-metal transition, high pressure, pressure-induced superconductivity

Iron-based superconductor has a two-dimensional iron lattice as a common feature and exhibits characteristic magnetic phases next to the superconducting phase. A stripe-type magnetic order is observed in the 1111, 122, 111 and 11 type, and a block-type magnetic order is observed in 245 type iron-based superconductors.

Recently, quasi-one-dimensional iron-based spin-ladder compounds have attracted much attention. These compounds exhibit various kinds of magnetic ordering phase, which are one-dimensional analog of both stripe and block magnetism related to the iron-based superconductors [1,2]. Due to such a similarity of magnetic property, superconductivity was expected in these compounds. However, these compounds show insulating behavior.

Here we report the pressure-induced superconductivity in the spin-ladder compound BaFe_2S_3 . In order to find the metallic phase, intensive high pressure studies have been carried out. The insulator-metal transition was observed at ~ 11 GPa, and just after appearance of metallic phase, superconductivity was observed, as shown in Fig.1. The dome-shaped superconducting phase was obtained in the P - T phase diagram, as shown in Fig.2, in which the maximum T_c was 17 K [3]. The results of high pressure studies for substituted compounds $\text{Cs}_{1-x}\text{Ba}_x\text{Fe}_2\text{S}_3$ and $\text{Ba}(\text{Fe}_{1-x}\text{Co}_x)_2\text{S}_3$, which correspond to the hole and electron doped compound, respectively, will be presented in the conference.

References

1. Y. Nambu *et al.*, Phys. Rev. **B85**, 064413 (2012).
2. F. Du *et al.*, Phys.Rev. **B85**, 214436 (2012).
3. H. Takahashi *et al.*, Nat.Mater. **14**, 1008 (2015).

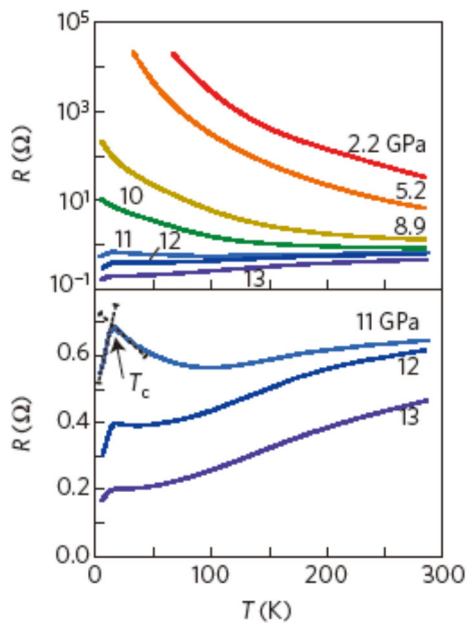


Figure 1: Electrical resistance of BaFe_2S_3 for each pressure. The insulator-metal transition is observed between 10 and 11 GPa. The resistance drop due to superconductivity can be seen above 11 GPa.

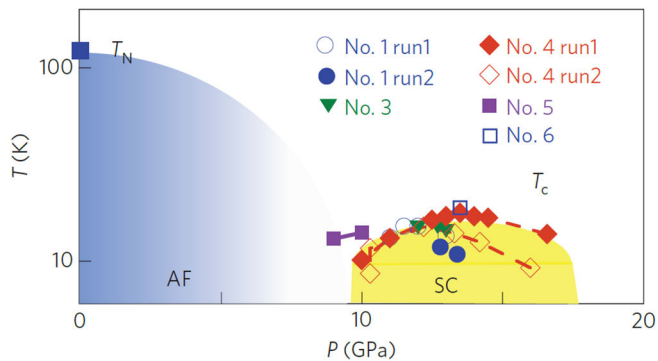


Figure 2: P-T phase diagram of BFS, which shows antiferromagnetic phase at ambient pressure. Superconducting transition appears above 10 GPa and disappears above 17 GPa. The maximum T_c is ~ 17 K.

Superconductivity in two-dimensional layered materials through electron-doping by metal-intercalation and electrostatic technique



Yoshihiro Kubozono^{1*}, Eri Uesugi¹, Lu Zheng¹, Saki Nishiyama¹, Xiao Miao¹, Takahiro Terao¹, Hidenori Goto¹, Ritsuko Eguchi¹, Tomoko Kagayama² and Katsuya Shimizu²
¹Okayama University, ²Osaka University

Email: *kubozono@cc.okayama-u.ac.jp

Keywords: 2D-layered materials, Iron based materials, LnOBiS₂, metal-doping, electrostatic electron doping

Superconductivity was observed in various two-dimensional (2D) layered materials such as FeSe_{1-z}Te_z, MoSe_{1-z}Te_z and LnOBiS₂ (Ln: La and Ce) through electron-doping by metal-intercalation and electrostatic technique. The metal-intercalation was achieved for the above 2D layered materials using liquid NH₃ technique. The highest superconducting transition temperature, T_c , in the (NH₃)_yM_xFeSe materials fabricated in this study reached 49 K at 21 GPa. We recently found various superconducting phases in (NH₃)_yM_xFeSe_{1-z}Te_z (0 ≤ z ≤ 1.0). For example, (NH₃)_yNa_xFeSe_{1-z}Te_z at z = 0 and z = 0.5 have multiple superconducting phases. Furthermore, we intercalated various metal atoms to MoSe_{1-z}Te_z crystals using liquid NH₃ technique, and (NH₃)_yNa_xMoSe₂ showed the T_c as high as 5 K. In this study, we discovered the superconductivity in metal-doped LaOBiS₂. For example, (NH₃)_yRb_xLaOBiS₂ showed the T_c as high as 4.3 K, indicating that electron-doping can produce superconductivity as in LaO_{0.5}F_{0.5}BiS₂ in which a substituent of O with F donates electrons to BiS₂ layer. Moreover, the electron-doping of LaOBiS₂ was also achieved by electrostatic technique. Figure 1(a) shows the temperature dependence of resistance (R), $R - T$ plot, measured by applying the gate voltage, V_g , of 6 V to ionic-liquid gate-dielectric in the LaOBiS₂ single-crystal field-effect transistor (FET); the R rapidly dropped below 4 K. The R -drop disappeared by applying magnetic field H of 0.5 T under $V_g = 6$ V (Figure 1(b)), guaranteeing the successful field-induced superconductivity.

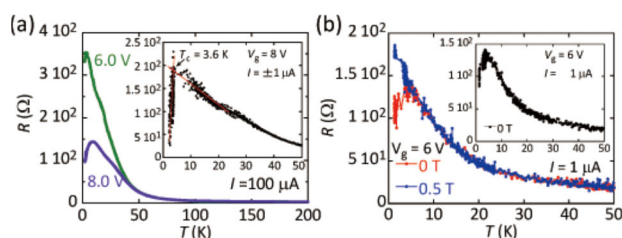


Figure 1: (a) $R - T$ plot at $V_g = 6$ and 8 V under H of 0 T, and (b) $R - T$ plot at $V_g = 6$ V under $H = 0$ and 0.5 T investigated using LaOBiS₂ single-crystal EDL FET.

Why some iron-based compounds are more correlated than others?



Massimo Capone¹

¹*International School for Advanced Studies (SISSA) and CNR-IOM, Trieste (Italy)*

²*European Synchrotron*

Email: * massimo.capone@sissa.it

Keywords: Electron correlation, orbital-selective Mott physics,

The link between high-temperature superconductivity and the physics of strong correlations has been forged by an immense number of studies of the copper-based superconductors (cuprates) in which a robust d-wave superconducting state emerges doping an antiferromagnetic Mott insulator.

The iron-based superconductors display strong similarities with the cuprates, but the parent compounds are not Mott insulators despite the magnetic ordering. I will not argue that the metallic parent compounds (LaFeOAs, BaFe₂As₂, ...), which have 6 electrons in the d orbitals, are close to a Mott transition, but rather than the whole phase diagram as a function of doping is dominated by the distance from the Mott insulating global half-filling (5 electrons in the d orbitals) which plays the same role of the parent compound of the cuprates. I will review the experimental evidence for this and the theoretical understanding, based on an important role of the Hund's coupling leading to a strong differentiation between the orbitals [1]. This leads to a surprising unification of the phase diagrams of cuprates and iron-based superconductors.

In the final part of the talk I will explore the landscape of materials in the family, discussing why KFe₂As₂, RbFe₂As₂ and CsFe₂As₂ are “heavy fermions” metals with large effective masses, while La₂O₃Fe₂Se₂ and K_{0.8}Fe_{1.6}Se₂ are insulators. At first glance the latter result seems to contradict the consensus that the parent compounds of iron-based superconductors are far from Mott insulators, since both La₂O₃Fe₂Se₂ and K_{0.8}Fe_{1.6}Se₂ have 6 electrons in the d orbitals. Yet a closer inspection shows that these two materials have a remarkably different electronic structure with respect to, e.g., FeSe. In La₂O₃Fe₂Se₂ a larger crystal-field splitting and a smaller kinetic energy per band [3] favor a full Mott localization, while in K_{0.8}Fe_{1.6}Se₂ the iron vacancies give rise to a reduction of interorbital kinetic energy terms which leads to an orbital-selective Mott state which turns into a magnetic insulator at low temperatures [4]

On the other hand KFe₂As₂, RbFe₂As₂ and CsFe₂As₂ turn out to be more correlated than the parent compounds because of their filling of 5.5 nominal electrons per iron. The experimental trend of the effective masses in the different materials is well reproduced by calculations combining density-functional theory and many-body methods [5].

We finally briefly discuss how the degree of correlation is related to superconductivity and nematicity [6].

References:

1. A. Georges, L. de' Medici, and J. Mravlje, *Ann. Rev. Cond. Matt. Phys.* 4, 137 (2013)
2. L. de' Medici, G. Giovannetti and M. Capone, *Phys. Rev. Lett.* 112, 177001 (2014)
3. G. Giovannetti, L. de' Medici, M. Aichhorn and M. Capone, *Phys. Rev. B* 91, 085124 (2015)
4. G. Giovannetti, L' de Medici, M. Aichhorn and M. Capone, preprint (2016).
5. F. Hardy et al., preprint (2016); S. La Fuerza et al., preprint (2016).
6. L. Fanfarillo, G. Giovannetti, M. Capone and E. Bascones, preprint (2016).

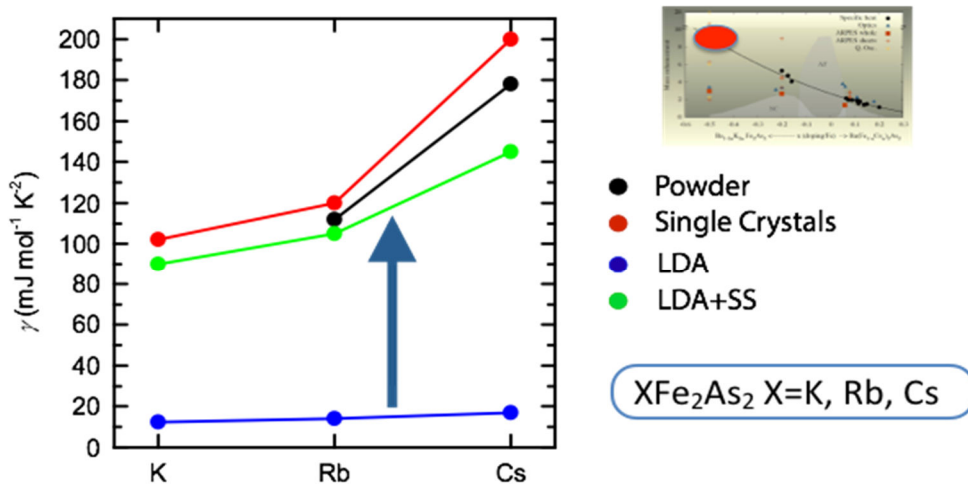


Figure 1: Sommerfeld coefficient of XFe_2As_2 ($X=K, Rb, Cs$). The large experimental values are reproduced introducing correlations without fitting parameters, while band theory completely fails.

Origin of the resistive anisotropy in the electronic nematic phase of BaFe₂As₂ revealed by optical spectroscopy



L. Degiorgi*, C. Mirri, A. Dusza and M. Chinotti
Laboratorium für Festkörperphysik, ETH - Zürich, CH-8093
Zürich, Switzerland

Email: * *degorgi@solid.phys.ethz.ch

Keyword : iron-pnictides, nematic phase, optical properties

The ferropnictides harbor a structural tetragonal-to-orthorhombic transition at T_s that may either coincides or precedes a transition into a long-range antiferromagnetic order at T_N , usually ascribed to a spin-density-wave state. There is an ongoing debate as to whether the dc anisotropy (both in the nematic phase ($T_N < T < T_s$) or in the tetragonal phase above T_s in the presence of an external symmetry breaking field) is primarily determined by the Fermi surface or scattering rate anisotropy. We measure the in-plane optical reflectivity of BaFe₂As₂ over a broad spectral range, covering the energy interval from the far infrared to the ultraviolet, at several combinations of uniaxial pressure, used to detwin the specimen, and temperature. Our goal is to probe the anisotropic response in the real part $\sigma_1(\omega)$ of the optical conductivity, extracted from the reflectivity data via Kramers-Kronig transformations. We thus elucidate how the anisotropic optical metallic response evolves as a function of stress, considered as an external symmetry breaking field, and across the ferro-elastic structural transition at $T_s = T_N = 135$ K. The infrared response reveals that the dc transport anisotropy in the orthorhombic antiferromagnetic state is determined by the interplay between the Drude spectral weight and scattering rate, but that the dominant effect is clearly associated with the metallic spectral weight. In the paramagnetic tetragonal phase, though, the dc resistivity anisotropy of strained samples is almost exclusively due to stress-induced changes in the Drude weight rather than anisotropy in the scattering rate. This result definitively establishes that the primary effect driving the resistivity anisotropy in the paramagnetic orthorhombic phase (i.e., the electronic nematic state) is the anisotropy of the Fermi surface [1].

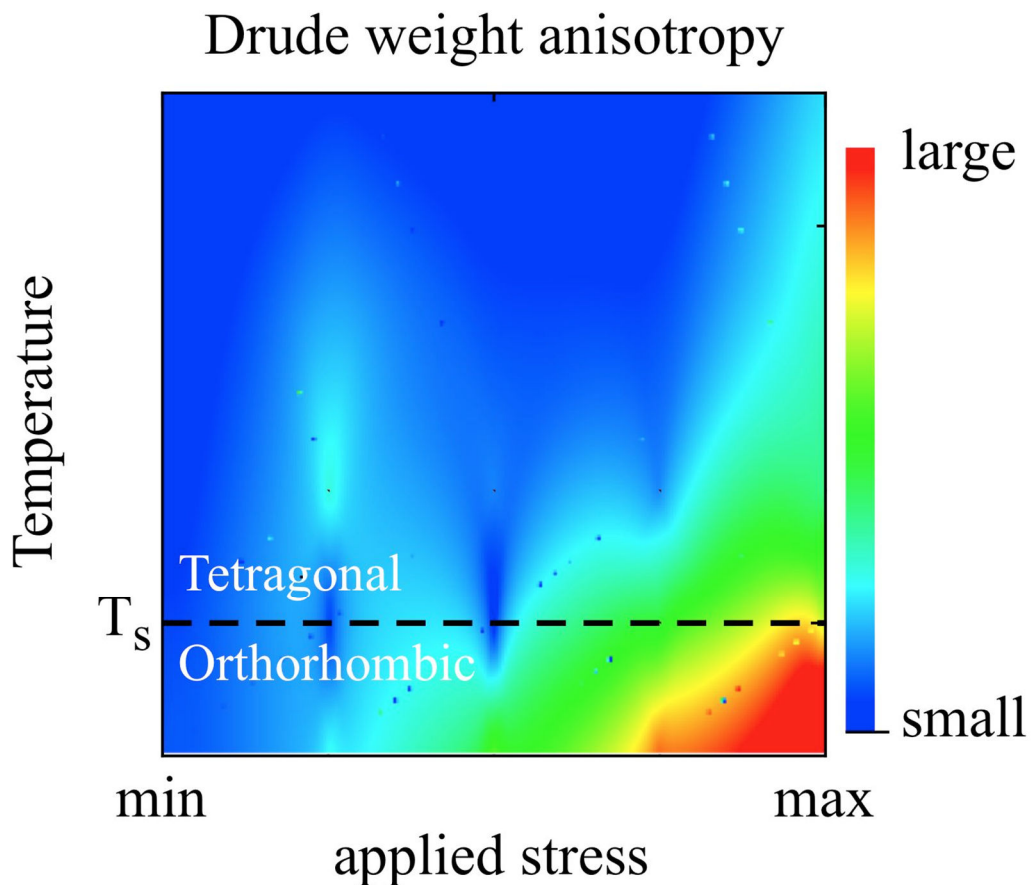


Figure 1: Temperature and stress dependence of the Drude weight anisotropy.

References

1. C. Mirri et al., Phys. Rev. Lett. **115**, 107001 (2015).

Renormalization group study of nematic order in iron superconductors



Carsten Honerkamp *,
RWTH Aachen University

Email: *Honerkamp@physik.rwth-aachen.de*

Keywords: iron superconductors, nematic order, orbital order

We present new results on a simple three-orbital model for iron superconductors, obtained in a renormalization group approach with orbitally resolved interactions. We show that nematic orbital ordering occurs very naturally in different forms as competitor but also concomitant ordering tendency to the more conventional antiferromagnetic ordering and spin-fluctuation-induced pairing at low energies. We discuss physical conditions under which nematicity is favored.

Single Crystals of Superconducting $\text{SmFeAsO}_{1-x}\text{H}_x$: Structure and Properties



S. Katrych^{1*}, A. Pisoni¹, A. Arakcheeva¹, M. Bokor², P. Matus¹, J. Karpinski¹, L. Forró¹

¹*I-PHYS, EPFL, CH-1015 Lausanne, Switzerland*

²*Institute for Solid State Physics and Optics, Wigner RCP of the HAS, Budapest, Hungary*

Email: [*sergiy.katrych@epfl.ch](mailto:sergiy.katrych@epfl.ch)

Keywords: superconductivity – iron based superconductors – hydrogen doping – upper critical field – electrical anisotropy.

The main motivation of this research is the recently reported superconductivity in hydrogen doped $\text{LnFeAsO}_{1-x}\text{H}_x$ ($\text{Ln} = \text{La}, \text{Ce}, \text{Sm}$) polycrystalline samples [1, 2, 3]. In comparison to other possible dopants (like Th, F) [4, 5], the uniqueness of hydrogen consists in its considerably larger solubility which allows to study the phase diagram in broad (up to $x=0.53$) concentration range [6].

The novelty of our study involves growth of $\text{SmFeAsO}_{1-x}\text{H}_x$ single crystals, detailed structure analysis and magnetotransport measurements in two orthogonal crystallographic directions.

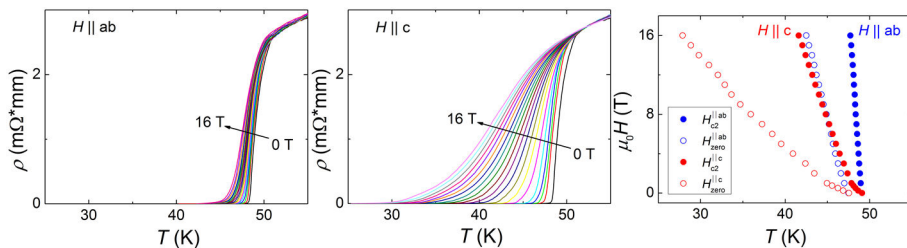


Figure 1: Temperature and magnetic field dependence of resistivity of $\text{SmFeAsO}_{0.84}\text{H}_{0.16}$ single crystals measured with fields applied parallel to the Fe_2As_2 layers ($H \parallel ab$) and perpendicular to them ($H \parallel c$). The values of magnetic field are 0, 0.25, 0.5, 1, 2, 3, 4, 5, 6, 7, 8, 9, 10, 11, 12, 13, 14, 15 and 16 T following the arrow in the panels. Right panel shows the magnetic field-temperature phase diagram from resistivity measurement with $H \parallel ab$ (blue points) and $H \parallel c$ (red points). Filled dots correspond to values of upper critical field (H_{c2}) estimated from the midpoint of resistive transitions while empty dots represent the fields evaluated at the zero-resistivity point.

The crystals were grown at high pressure using a cubic anvil technique. The presence of hydrogen in the crystals was confirmed by NMR characterization. The residual

electron density map analysis reveals a remarkable disorder for $\text{SmFeAsO}_{1-x}\text{H}_x$ induced by hydrogen incorporation into Sm_2O_2 layer.

We measured the temperature dependence of electrical resistivity of $\text{SmFeAsO}_{1-x}\text{H}_x$ crystals ($x=0.07, 0.1, 0.16$) in magnetic field up to 16 T, oriented along the two main crystallographic directions (Fig. 1). The results show an increase of critical temperature with hydrogen content in good agreement with what was reported for polycrystalline samples. From magnetotransport analysis we estimated the zero-temperature upper critical fields and the magnetic anisotropy as a function of hydrogen content. Significantly higher values of upper critical field and magnetic anisotropy are observed in $\text{SmFeAsO}_{1-x}\text{H}_x$ compared to $\text{SmFeAsO}_{1-x}\text{F}_x$ single crystals.

References

1. Miyazawa, K. et al., Appl. Phys. Lett. 96,072514 (2010).
2. Hanna, T. Et al., Phys. Rev. B 84, 024521 (2011).
3. Matsuishi, S. et al., Phys. Rev. B 85, 014514 (2012).
4. N. D. Zhigadlo, et al., Phys. Rev. B 82, 064517 (2010)
5. Y. Kamihara, et al., Journal of the American Chemical Society 130, 3296 (2008).
6. Iimura, S. et.al., Nat Commun 3, 943 (2012).

Quantitative description of disorder effects in iron-based superconductors: Correlated RKKY-exchange, impurity clusters and more.



Brian M. Andersen¹ and Maria Navarro Gastiasoro¹
¹*Niels Bohr Institute, University of Copenhagen, Denmark*

Email: * *bma@nbi.ku.dk*

Keywords: iron-based superconductors, disorder, electron correlations, Tc suppression, cooperative RKKY effects, emergent impurity clusters.

The nature and origin of superconductivity and the importance of electronic correlations in the iron-based superconducting materials remain a topic of great interest. In this talk I will focus on some recent developments in our understanding of disorder in these materials. Overall the effects of various kinds of impurities is highly complicated in these multiband systems, and their effects on e.g. superconducting order exhibits a remarkable variation between the compounds and strong dependence on the particular impurity ions. For example, only 0.3% of Mn is enough to completely kill superconductivity in some (but not all) 1111 materials, whereas Ru has only minor effects on superconductivity. Ru, however, induces a magnetic phase and the onset of magnetic order seems to be roughly universal with around 25% Ru substitution.[1,2] Fig.1 shows an example of the role of Coulomb repulsions on the Tc suppression rate versus magnetic impurity concentration.

I will explain the physics governing this behavior, and show the crucial importance of electronic correlations in both renormalizing the local impurity potential and inducing cooperative quasi-long-range magnetic order with important consequences for the superconducting condensate.[3,4]

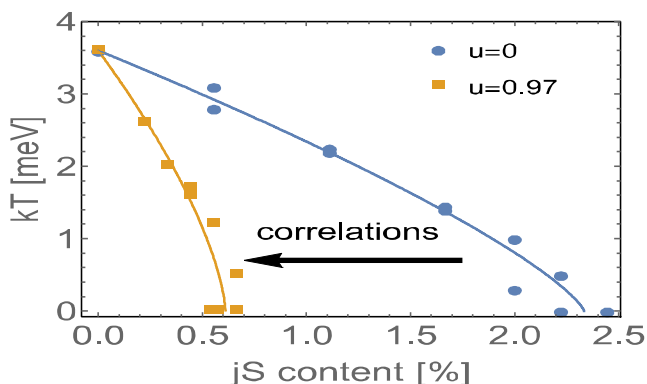


Figure 1: Model calculation of the effect of Coulomb correlations on the Tc suppression rate versus magnetic impurity concentration for iron pnictides.

References

1. F. Hammerath et al., Phys. Rev. B **89**, 134503 (2014).
2. S. Sanna, et al., Phys. Rev. B **87**, 134518 (2013).
3. M. N. Gastiasoro and B. M. Andersen, Phys. Rev. Lett. **113**, 067002 (2014).
4. M. N. Gastiasoro and B. M. Andersen, *preprint*.

Nature, origin and detection of double-Q phases in Fe-pnictides



M. N. Gastiasoro^{1*}, I. Eremin², R. M. Fernandes³ and B. M. Andersen¹

¹Niels Bohr Institute, University of Copenhagen ²Institute for Theoretical Physics, Ruhr-Universität Bochum ³School of Physics and Astronomy, University of Minnesota

Email: *fbp809@nbi.ku.dk

Keywords: itinerant magnetism, spectroscopy, Fe-pnictides

In the first part of the presentation, I will review our recent efforts to understand the nature and origin of the recently experimentally discovered double-Q (C_4 symmetric) magnetic phases in the iron-based superconductors within a fully self-consistent microscopic approach that includes a realistic band structure and Hubbard-Hund correlations. The general phase diagram displays prominent regions of stability of these unusual magnetic structures as shown in Fig. 1. I will discuss their properties, and the implications the double-Q phases have for our general understanding of the electronic correlations of the iron-based materials.

In the second part of the presentation, I turn to new proposed experiments to test for tetragonal double-Q magnetism by local scanning spectroscopy. Specifically, it will be shown how measurements of the total (non-spin-resolved) local density of states near magnetic impurity moments allow for a unique determination of the preferred magnetic ground state of the system.

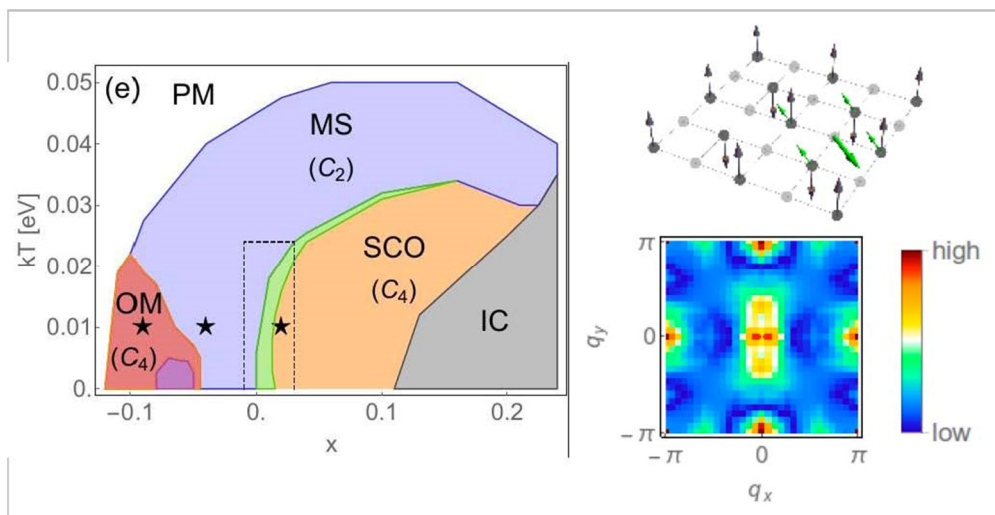


Figure 1: Phase diagram of the single-Q and double-Q magnetic phases. Single magnetic impurity in a double-Q state and its spectral signature.

References

1. M N Gastiasoro and B M Andersen, Phys. Rev. B 92, 140506(R) (2015)

Interplay of charge and spin degrees of freedom in pnictides and dichalcogenides



Philip Turner^{*}, Laurent Nottale^{2*}, Dmitri Efremov¹
¹*IFW Dresden*

Email: *d.efremov@ifw-dresden.de*

Keywords: Iron-based superconductors, transition metal dichalcogenides, renormalization group

We consider the interplay of the magnetic, charge and superconducting instabilities in multiband systems like Fe-based superconductors having tetragonal crystal structure and transition metal dichalcogenides having hexagonal crystal structure. The magnetism in Fe-based superconductors is explained by nesting of the hole pockets at Γ -point and electron pockets at M-points. Similar nesting conditions exist between hole pockets at Γ -point and electron pockets at M-points in TiSe₂. But spin density wave (SDW) state and superconductivity are realized in Fe-based superconductors, while charge density wave (CDW) state and superconductivity in dichalcogenides. The problem can be resolved by considering the interplay spin, charge degrees of freedom. The effective interactions in spin, charge and cooper channels logarithmically flow at low energies, i.e., all these channels must be treated on equal footings. Additional umklapp process which is allowed in hexagonal systems like TiSe₂, push the system to CDW instability. It is expected that in TiSe₂ the chiral superconductivity is realized. Finally, we consider the dynamical coupling between the magnetic and the superconducting instabilities. For this purpose a dynamical mode-mode coupling theory is developed based on the coupled Bethe-Salpeter equations. We focus on the region in the vicinity to the tetracritical point where spin fluctuations are strongly coupled to superconductivity.

References

1. A.V. Chubukov, D. Efremov, I. Eremin, Phys. Rev. B 78, 134512 (2008)
2. R. Ganesh, G. Baskaran, Jeroen van den Brink, Dmitry V. Efremov, Phys. Rev. Lett. 113, 177001 (2014)
3. M. N. Kiselev, D.V. Efremov, S. L. Drechsler, Jeroen van den Brink, K. Kikoin, . arXiv:1601.03552.

Cluster perturbation approach to iron-based superconductors



M.M.Korshunov^{1*}, S.V. Nikolaev^{1,2}, Yu.N. Togushova^{1,2}

¹*Kirensky Institute of Physics, Krasnoyarsk, Russia*

²*Siberian Federal University, Krasnoyarsk, Russia*

Email: * mkor@iph.krasn.ru

Keywords: iron-based superconductors, spin fluctuation pairing, cluster perturbation theory

Fe-based superconductors represent a non-cuprate class of high- T_c systems with the unconventional superconducting state [1]. The origin of the latter is still intensively debated [2]. Iron-based systems can be broadly divided into the two subclasses, pnictides and chalcogenides, with the square lattice of iron as the basic element. In spite of the variety of materials, the multiorbital spin-fluctuation theory of pairing can explain many observed features of iron-based superconductors, in particular, the different variants of the experimentally examined behaviors of the superconducting gap [2]. In particular, the RPA (random-phase approximation) spin fluctuation approach gives the extended s-wave gap that changes sign between hole and electron Fermi surface sheets (s_{\pm} state) as the main instability for the wide range of doping concentrations [3-7]. Such anisotropic s_{\pm} state and its nodal structure on Fermi surfaces are quite sensitive to some details of the electronic structure, such as the orbital character of the bands, spin-orbit interaction, and changes in the band structure due to the doping, see Fig. 1 [7]. However, RPA treats local Coulomb interactions selectively and has a narrow range of proved applicability. To go beyond this limitation, we use a norm-conserving cluster perturbation technique that allows to consider local interactions within the cluster exactly [8]. We show how the band structure and the Fermi surface evolves with increasing Hubbard U and discuss the metal-insulator transition absent in RPA.

This work was partially supported by the RFBR (grant 16-02-00098).

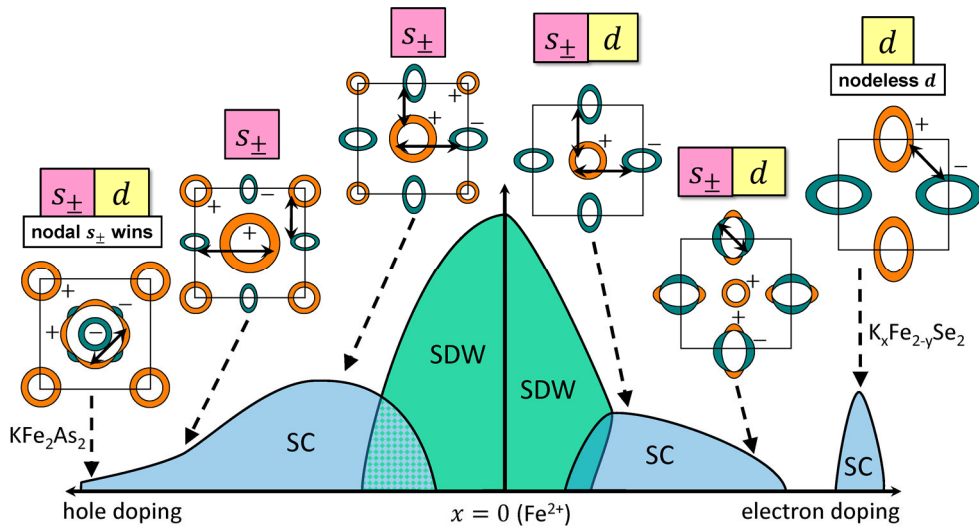


Figure 1: Schematic phase diagram of iron compounds for both hole and electron dopings. The qualitative picture of the symmetries of the superconducting parameter that follows from the RPA spin fluctuation theory [2-5] and from LAHA (leading angular harmonics approximation) [6] for the two-dimensional system is shown on schematic Fermi surfaces in the insets above the phase diagram. Captions (s_{\pm} , d) mark the dominant and subdominant symmetries of pairing. Solid lines with an arrow at both ends (\leftrightarrow) indicate the dominant interaction at the Fermi surface.

References

1. See, e.g. M.V. Sadovskii, *Physics-Uspekhi* 51, 1201 (2008);D.C. Johnston,*Advances in Physics* 59, 803 (2010); G.R.Stewart, *Rev. Mod. Phys.* 83, 1589(2011).
2. P.J. Hirschfeld, M.M. Korshunov, and I.I. Mazin, *Rep. Prog. Phys.* 74, 124508 (2011).
3. I.I. Mazin, D.J. Singh, M.D. Johannes, and M.-H. Du,*Phys. Rev. Lett.* 101, 057003 (2008).
4. S. Graser, T.A. Maier, P.J. Hirschfeld, and D.J. Scalapino,*New. J. Phys.* 11, 025016 (2009).
5. K. Kuroki, S. Onari, R. Arita, H. Usui, Y. Tanaka, H. Kontani, and H. Aoki, *Phys. Rev. Lett.* 101, 087004 (2008).
6. S. Maiti, M.M. Korshunov, T.A. Maier, P.J. Hirschfeld, and A.V. Chubukov, *Phys. Rev. B* 84, 224505 (2011).
7. M.M. Korshunov, *Physics-Uspekhi* 57, 813 (2014).
8. S.V. Nikolaev and S.G. Ovchinnikov, *JETP* 111, 635 (2010).

Holography without translational invariance

Shang-Yu Wu

¹Department of Electrophysics, National Chiao Tung University, Taiwan

Email: loganwu@gmail.com

Keywords: quenched disorder, impurity, AdS/CMT

In this talk, I will briefly review the works of holographic models with momentum dissipations like lattice or linear axion and massive gravity. Then we calculate the fermion spectral function in holographic massive gravity which can be interpreted as quenched disorders on the boundary theory. We show as the disorder strength increases, the quasiparticle peak becomes broader and broader and the sharp Fermi surface disappear which leads to a disorder-induced remnant Fermi surface.

References

1. Gary T. Horowitz, Jorge E. Santos, David Tong, “Optical conductivity with holographic lattices”, JHEP 1207 (2012) 168, arXiv:1204.0519 [hep-th].
2. Tomas Andrade, Benjamin Withers, “A simple holographic model of momentum relaxation”, JHEP 1405 (2014) 101, arXiv:1311.5157 [hep-th].
3. David Vegh, “Holography without translational symmetry”, arXiv:1301.0537 [hep-th].
4. Jackson Wu, Shang-Yu Wu, in preparation.

Electronic ferroelectricity in carbon based materials



Natasha Kirova^{1,3*}, Serguei Brazovskii^{2,3}

¹*LPS, CNRS, Univ. Paris Sud, Université Paris–Saclay
91405, Orsay, France*

²*LPTMS, CNRS, Univ. Paris Sud, Université Paris–Saclay
91405, Orsay, France*

³*Moscow Institute for Steel and Alloys, Moscow, Russia.*

Email: * kirova@lps.u-psud.fr.

Keywords: ferroelectricity, organic conductor, conjugated polymers, polyacetylene, graphene, soliton, non-integer charge, domain wall

We review existing manifestations and prospects for ferroelectricity in electronically and optically active carbon-based materials. The focus point is the proposal for the electronic ferroelectricity in conjugated polymers from the family of substituted polyacetylenes. The attractive feature of synthetic organic ferroelectrics is a very high polarizability coming from redistribution of the electronic density, rather than from conventional displacements of ions. Next fortunate peculiarity is the symmetry determined predictable design of perspective materials. The macroscopic electric polarization follows ultimately from combination of two types of a microscopic symmetry breaking which are ubiquitous to quasi-1D electronic systems. The state supports anomalous quasi-particles - microscopic solitons, carrying non-integer electric charges, which here play the role of nano-scale nucleus of ferroelectric domain walls. Their spectroscopic features in optics can interfere with low-frequency ferroelectric repolarization providing new accesses and applications. In addition to already existing electronic ferroelectricity in organic crystals and donor-acceptor chains, we point to a class of conducting polymers and may be also to nano-ribbons of the graphene where such a state can be found. These proposals may lead to potential applications in modern intensive searches of carbon ferroelectrics.

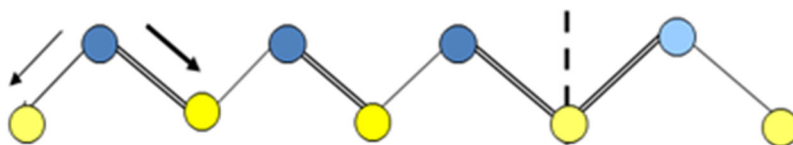
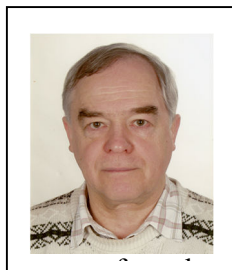


Figure 1: : Instruction for the ferroelectric design - combined symmetry breaking. The zig-zag structure is typical but not important

References

1. N. Kirova, S. Brazovskii, *Synth. Met.*, [doi:10.1016/j.synthmet.2015.10.015](https://doi.org/10.1016/j.synthmet.2015.10.015)

Nanoscale phase separation in ferroelectric materials



Vyacheslav I. Yukalov^{1*}, Elizaveta P. Yukalova²

¹*Bogolubov Laboratory of Theoretical Physics*

Joint Institute for Nuclear Research, Dubna 141980, Russia

²*Laboratory of Information Technologies*

Joint Institute for Nuclear Research, Dubna 141980, Russia

Email: *yukalov@theor.jinr.ru

Keywords: nanoscale phase separation, ferroelectric materials

Many materials exhibit nanoscale phase separation, when inside the host thermodynamic phase there arise nanosize embryos of another thermodynamic phase. A prominent example of this phenomenon is provided by ferroelectric materials. The theoretical description of such phase heterogeneous materials is quite challenging, since they are essentially nonuniform, the nonuniformity is random, and often they are quasiequilibrium, but not absolutely equilibrium. An approach is suggested for the theoretical description of phase separated ferroelectrics, consisting of a ferroelectric matrix with nanoscale paraelectric inclusions. The properties of the heterophase ferroelectrics are studied.

References

1. V.I.Yukalov and E.P. Yukalova, *Laser Phys.* 21, 1448 (2011).
2. V.I. Yukalov and E.P. Yukalova, *Laser Phys.* 22, 1070 (2012).
3. V.I. Yukalov and K. Ziegler, *Phys. Rev. A* 91, 023628 (2015).

The influence of 1 GPa isostatic pressure on J_c , B_{irr} , B_{c2} and T_c in MgB_2 wires and iron-based superconducting materials



D. Gajda¹, A. Morawski², A. Zaleski³, T. Cetner², M. Rindfleisch⁴, M. Tomsic⁴, W. Häbler⁵, K. Nenkov⁵, A. Yamamoto⁶, M. Akdoğan⁷, Y. Hakana⁷, M. Małecka³, B. İbrahim⁷, K. Buchkov⁸, E. Nazarova⁸, N. Balchev⁸, Ł Fajfrowski¹

¹ International Laboratory of High Magnetic Fields and Low Temperatures, Wrocław, Poland

² Institute of High Pressure Physics Polish Academy of Sciences, Warsaw, Poland

³ Institute of Low Temperature and Structure Research Polish Academy of Sciences, Wrocław, Poland

⁴ Hyper Tech Research Inc., Columbus, USA.

⁵ Institute for Solid State and Materials Research Dresden, Dresden, Germany

⁶ Department of Applied Physics, Tokyo University of Agriculture and Technology, , Tokyo, Japan

⁷ Abant İzzet Baysal University, Department of Physics, Bolu, Turkey

⁸ Institute of Solid State Physics, Bulgarian Academy of Sciences, Sofia, Bulgaria

Email: dangajda@op.pl

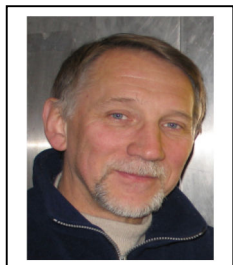
Keywords: MgB_2 wires, iron-based superconducting materials, HIP process,

We show results of the critical current density (J_c), pinning force density (F_p) measurements and analysis of pinning force density scaling, critical temperature (T_c), irreversible magnetic field (B_{irr}) and upper magnetic field (B_{c2}) that have been made for multicore Monel-sheathed type MgB_2 wires. One batch of MgB_2 wires were manufactured by Hyper Tech Research Inc., in USA with their standard technology (continuous in tube forming and filling e.g. (CTFF) of Cu-based monocore wire with the precursor 1.1Mg+2B powder. The *in-situ* method with Nb barrier was used. These wires were doped nano-SiC and C and have fill factors of 15%. A second batch of MgB_2 wires were manufactured Abant İzzet Baysal University in Turkey with their standard technology (powder in tube – PIT). These MgB_2 wires have one filament, iron shield, without barriers, 50 % fill factor, and were filled with amorphous boron (both nano- and large size Pavezyum). The $FeSe_{0.94} + Ag$ bulks were made in Institute of Solid State Physics, Bulgarian Academy of Sciences. The initial Se, Fe and Ag powders have purity 99.9%, 99.5% and 99.9%. The bulks were first annealed at 700 °C for 8 hours in vacuum then at 400 °C for 10 hours. The sample of $Ba(Fe,Co)_2As_2$ was made in Department of Applied Physics, Tokyo University of Agriculture and Technology. This sample was placed inside Nb barrier and inserted into iron container (length of 2.2 cm and a diameter of 4 mm). The Hot Isostatic Pressing (HIP) process was performed at IHPP PAS Unipress using high Ar gas pressure. The 0.1 MPa to 1.4 GPa argon gas pressure was used in the HIP annealing, and at different temperatures

from 570 °C to 800 °C and annealing durations. The critical current was measured at 4.2 K in ILHMFLT PAS and at 10K, 20 K and 25 K at the Institute for Solid State and Materials Research, Dresden. A perpendicular field configuration (to the 25 mm length of the samples) was used for measuring of critical temperature and critical magnetic fields. Microstructure investigations were performed with SEM and EDX.

The results show that the HIP (1 GPa) process increased the uniformity of MgB₂ material and the critical current density (J_c) in MgB₂ wires (Hyper Tech Research). In these wires, we obtained 100 A/mm² at 20 K in 5 T and 100 A/mm² at 4.2 K in 14 T. Results for MgB₂ wires from Turkey show that the HIP process can increase J_c at 4.2 K and T_c , B_{irr} and B_{c2} . We obtained 100 A/mm² in 6.5 T. The results for iron-based superconducting materials show that the HIP process can increase T_c , B_{irr} , B_{c2} , eliminate voids and significantly improve the homogeneity of the material. The results for bulk FeSe_{0.94} show that a pressure of 1 GPa increased T_c of about 3 K and B_{irr} of about 80%. Results for Ba(Fe, Co)₂As₂ bulk show that T_c of 27 K was achieved with a pressure of 1 GPa .

Anharmonicity and EXAFS Studies Beyond the Quasiharmonic Approximation



Juris Purans

Institute of solid State Physics, University of Latvia

Email: *purans@cfi.lu.lv*

Keywords: Anharmonicity, EXAFS, perovskites, NTE, HTSC

Anharmonicity of lattice dynamics is very important in relation to many effects in crystals as thermal expansion, structural phase transitions, soft modes in ferroelectrics and related HTSC phenomena. In strongly anharmonic systems the so-called explicit anharmonicity effect links the phonon frequencies and interatomic forces to the amplitude of the atomic vibrations that is realised in the ab-initio calculations beyond quasiharmonic approximation (BQHA).

Femtometer accuracy in the determination of interatomic distances is now attainable [1,2], therefore additional information on the lattice dynamics can be obtained from EXAFS spectra. We propose an approach beyond the quasiharmonic approximation for the interpretation of original EXAFS, neutron PDOS, Raman and infrared data. Ab initio BQHA calculations of electronic and vibration properties are performed not at the equilibrium positions atoms but at the most probable positions for a given temperature, one can obtain from EXAFS data that describes the system at elevated temperatures

References

1. J. Purans, N. D. Afify, G. Dalba, R. Grisenti, S. De Panfilis, A. Kuzmin, V.I. Ozhogin, F. Rocca, A. Sanson, S. I. Tiutiunnikov, P. Fornasini, *Phys.Rev.Lett.*, 100, 00055901 (2008).
2. J. Purans, P. Fornasini, S. E. Ali, G. Dalba, A. Kuzmin, and F. Rocca, *Phys. Rev. B* 92, 014302 (2015).

Magnetic pair distribution function (mPDF) analysis of short-range magnetism in strongly correlated materials



Ben Frandsen¹, Julie B. Staunton², Simon J. L. Billinge^{1,3*},
¹*Columbia University, Department of Physics*
²*Department of Physics, University of Warwick*
³*Brookhaven National Laboratory, Condensed Matter Physics
and Materials Science Department*

Email: *sb2896@columbia.edu

Keywords: magnetism, short-range order, local structure, PDF analysis, neutron diffraction

Short-range magnetic correlations are known to exist in a variety of strongly correlated electron systems, but our understanding of the role they play is challenged by the difficulty of experimentally probing such correlations. Magnetic pair distribution function (mPDF) analysis is a newly developed neutron total scattering method that can reveal short-range magnetic correlations directly in real space, and may therefore help ameliorate this difficulty [1,2].

After a brief introduction to the mPDF method, we present temperature-dependent mPDF measurements of the short-range magnetic correlations in the paramagnetic phase of antiferromagnetic MnO, an archetypal strongly correlated transition-metal oxide. In addition to recovering the expected long-range magnetic structure at low temperature, we observe significant correlations on a ~ 1 -nm length scale persisting into the high-temperature paramagnetic phase. With no free parameters, *ab initio* calculations using the self-interaction-corrected local spin density approximation of density functional theory quantitatively reproduce the high-temperature magnetic correlations to a high degree of accuracy. These results yield valuable insight into the magnetic exchange in MnO and showcase the utility of the mPDF technique for studying magnetic properties of strongly correlated electron systems. This work will appear in PRL (available on arXiv) [3].

We will also discuss mPDF results from other strongly correlated electron systems.

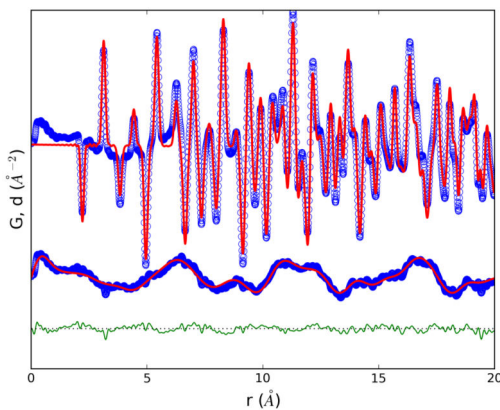


Figure: Atomic and magnetic PDF of MnO at 15 K. The combined atomic and magnetic PDF is shown as the top blue curve, with the refined atomic PDF overlaid in red; the residual from the atomic PDF fit is shown as the lower blue curve, with the refined mPDF overlaid in red; and the green curve gives the overall fit residual.

References

1. B. A. Frandsen, X. Yang, and S. J. L. Billinge, *Acta Crystallogr. A* **70**, 3 (2014). doi: 10.1107/S2053273313033081
2. B. A. Frandsen and S. J. L. Billinge, *Acta Crystallogr. A* **71**, 325 (2015). doi: 10.1107/S205327331500306X
3. B. A. Frandsen, M. Brunelli, K. Page, Y. Uemura, J. B. Staunton and S. J. L. Billinge, *Phys. Rev. Lett.*, to be published. (2016). Available on arXiv (<http://arxiv.org/abs/1512.06270>)

Orbital Polarization Driven by Anisotropic Hybridization in a Nickelate Heterostructure determined by Resonant Inelastic X-Ray Scattering



M. P. M. Dean^{1,*} and G. Fabbris¹
¹Brookhaven National Laboratory

Email: * mdean@bnl.gov

Keywords: Nickelates, heterostructures, electronic structure, orbital engineering

Heterostructures built from one-unit-cell thick layers of transition metal oxides (TMOs) represent an exciting opportunity to design new electronic states with improved properties. LaNiO₃-based systems are a prototype for such efforts ever since it was predicted that it might be possible to reconstruct its electronic structure into a state that is analogous to the cuprate high temperature superconductors [1]. This involves breaking the symmetry of the initially degenerate e_g states to generate a half-filled $3d\ x^2-y^2$ ground state and an unoccupied $3z^2-r^2$ orbital – generating what is called “orbital polarization”. To date, these effects have been interpreted in terms of changing the energies of the orbitals, which naturally causes preferential occupation of the lower energy orbital. We use Ni L -edge resonant inelastic x-ray scattering to determine the Ni electronic configuration in LaTiO₃/LaNiO₃/(LaAlO₃)₃ heterostructures, a model system with exceptionally large orbital polarization [2] shown in Fig. 1. We find that charge transfer from Ti to Ni drives LaNiO₃ out of its initial itinerant state into a localized Ni d^8 -ligand hole state that we model in detail using multiplet calculations plotted in Fig. 1. Surprisingly, octahedral elongation generates only minor changes in the Ni $3d$ crystal fields that were previously thought to be the driving force behind the observed large orbital polarization. Instead, orbital polarization is caused by an anisotropic reconstruction of the Ni $3d - O\ 2p$ states, in which the $3d\ x^2-y^2$ orbital is significantly more hybridized with O $2p$ than the $3d\ 3z^2-r^2$ [3]. We therefore suggest that efforts to target new electronic properties that require large orbital polarization focus on anisotropic hybridization, rather than orbital energy levels, in order to generate the largest effects.

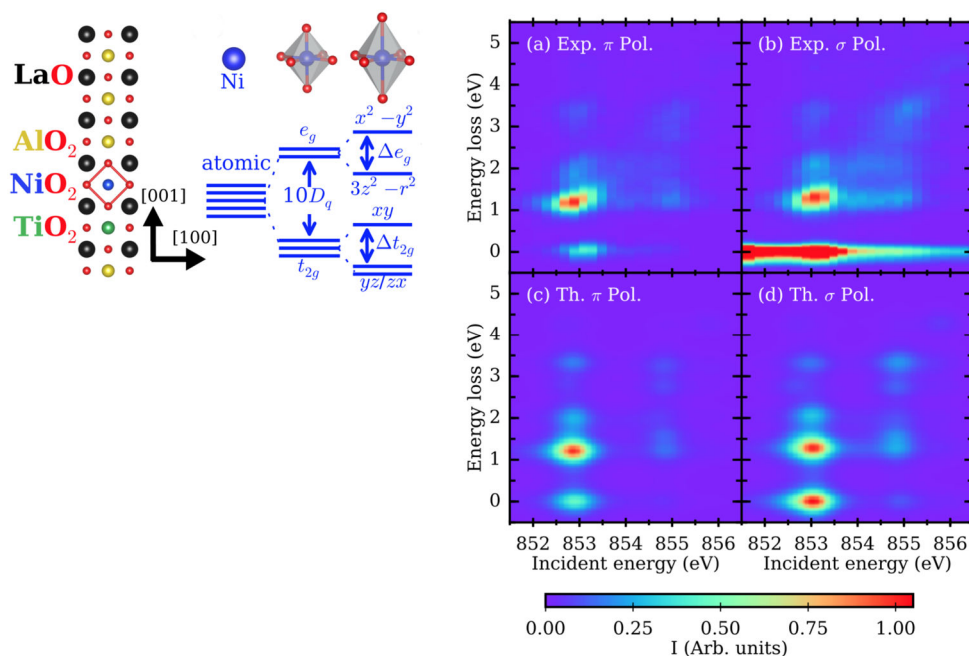


Figure 1: Left: the basic structural unit studied here composed of LaTiO₃, LaNiO₃ and LaAlO₃ layers in a 1:1:3 ratio with a related Ni orbital energy level diagram. Right: RIXS measurements of the heterostructure (a)&(b) plot the measured intensity with π and σ polarized incident x-rays. (c)&(d) plot our corresponding multiplet calculations for the two different polarizations.

References

1. J. Chaloupka and G. Khaliullin, Phys. Rev. Lett. 100, 016404 (2008)
2. Ankit S. Disa, Divine P. Kumah, Andrei Malashevich, Hanghui Chen, Dario A. Arena, Eliot D. Specht, Sohrab Ismail-Beigi, F. J. Walker, and Charles H. Ahn, Phys. Rev. Lett. 114, 026801 (2015).
3. G. Fabbris, D. Meyers, J. Okamoto, J. Pellicciari, A. S. Disa, Z.-Y. Chen, W. B. Wu, C. T. Chen, S. Ismail-Beigi, C. H. Ahn, F. J. Walker, D. J. Huang, T. Schmitt and M. P. M. Dean (In preparation)

Local structural aspects of metal-metal transition in IrTe₂



Emil S. Bozin^{1*}, Runze Yu¹, Haidong Zhou², J.F. Mitchell³,
Simon J. L. Billinge^{1,4}

¹Brookhaven National Laboratory, Upton, NY, USA

²University of Tennessee, Knoxville, TN, USA

³Argonne National Laboratory, Argonne, IL, USA

⁴Columbia University, New York, NY, USA

Email: * bozin@bnl.gov

Keywords: iridates, dimerization, local atomic structure

Exploring the details of competition and cooperation in electronic, orbital, spin, and lattice sectors of complex electronic systems is a challenging task in condensed matter. Materials with structures containing corner sharing triangular and tetrahedral motifs often exhibit complexity and compelling ground states, providing fruitful playground for studying the interplay of these entangled degrees of freedom. Iridates featuring such topological motifs on iridium sublattice are no exception. IrTe₂ has been in focus over the past several years not only because it displays an unusual first-order metal-metal (M-M) transition [1] origin of which has been heavily debated, but also due to the emergence of superconductivity upon chemical substitution and intercalation [2]. In trigonal (P-3m1) phase at room temperature Ir populates flat network of equilateral triangles, sandwiched into slabs between two triangular Te sheets forming edge sharing octahedra. Upon cooling resistivity exhibits an abrupt jump, magnetic susceptibility is suppressed, and the average structure becomes triclinic (P-1) [3]. Although Ir sheets become puckered in a zig-zag fashion with fraction of Ir presumably dimerizing in a stripe-like morphology (Fig. 1(a)) with Ir-Ir distance on a dimer shortened by amazing ~ 0.7 Å, the system remains metallic. Diverse set of scenarios has been considered to explain the transition [4], such as charge density wave (CDW), Ir dimerization associated with instabilities of the t_{2g} orbital sector, crystal-field effect splitting p_{xy} and p_z of Te, interlayer and intralayer hybridization, and reversible depolymerization below the transition temperature of polymeric networks of interlayer covalent Te-Te bonds. Due to similarities in observed properties, IrTe₂ has often been compared to CuIr₂S₄thiospinel (Ir on a pyrochlore sublattice, Fig. 1(b)), a system exhibiting metal-insulator (M-I) transition and structural transformation from cubic to triclinic [5], with 50% of Ir dimerizing and ~ 0.5 Å large dimer bond contraction, proposed to have orbitally driven Peierls character [6]. In both IrTe₂ [4] and CuIr₂S₄ [7] a possibility of persistence, on a nanometer lengthscale, of disordered Ir-dimers in the high-T metallic regime has been explored. This presentation will focus, in a comparative manner, on evolution of local structural features across the M-M and M-I transitions in the two systems as seen by the x-ray scattering based atomic pair distribution function (PDF) approach, providing further insights to the debate on the character of the transitions. Results of the PDF analysis reveal that nanoscale and average structures of IrTe₂ are in accord in both low-T and high-T regimes, conforming to P-1 and P-3m1 models

respectively. Local distortions at low T are consistent with CDW-like or charge disproportionation state. No evidence is found of nanoscale survival of Ir dimers in the high-T metallic regimes of IrTe_2 and CuIr_2S_4 . In CuIr_2S_4 however, although dimers are *not* present in the cubic phase [8], PDF data suggest that the t_{2g} degeneracy may already be lifted at high T by weak *local* tetragonal distortion of I41/amd type. This purely local effect is quickly stabilized by small Cr substitution. This provides further insights relevant for deeper understanding of the M-I transition and poor metallic behavior at high temperature [7].

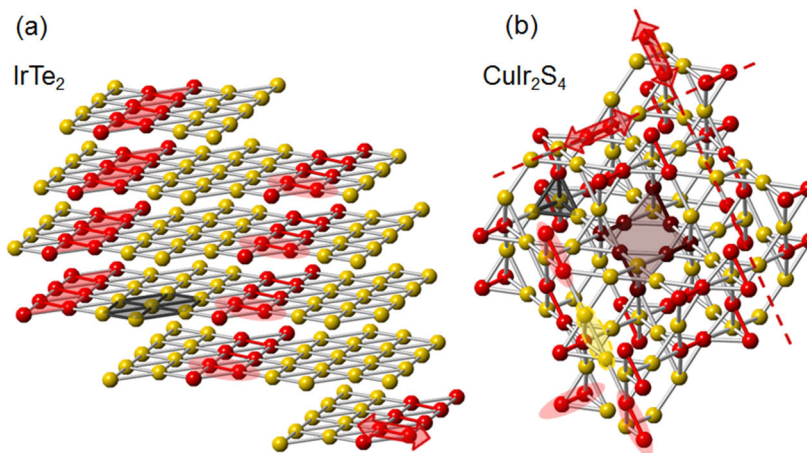
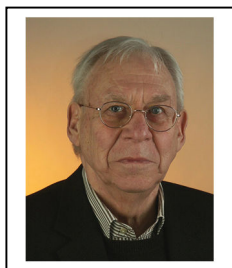


Figure 1: Iridium sublattice in the low temperature regimes of IrTe_2 and CuIr_2S_4 . (a) In IrTe_2 partial Ir dimerization occurs along one of the trigonal directions within triangular Ir sheets with $5\times$ periodicity. Within the sheets they form stripe-like arrangement (shaded red), exhibiting staircase staggering perpendicular to the sheets with the same periodicity. (b) In CuIr_2S_4 partial Ir dimerization occurs along nonintersecting $[1,1,0]$ and $[1,-1,0]$ 1D chains (dashed red lines) of pyrochlore sublattice of corner-sharing Ir_4 tetrahedra. These chains also feature $-\text{Ir}^{4+}-\text{Ir}^{4+}-\text{Ir}^{3+}-\text{Ir}^{3+}$ tetramer order. Dimers, shown in red, further arrange themselves in isovalent octamers (shaded dark red). At high-T dimers disappear on all lengthscales.

References

1. N. Matsumoto et al., J. Low. Temp. Phys. **117**, 1129 (1999).
2. S. Pyon et al., J. Phys. Soc. Jpn. **81**, 053701 (2012); J. J. Yang, et al., Phys. Rev. Lett. **108**, 116402 (2012); M. Kamitani et al., Phys. Rev. B **87**, 180501 (2013).
3. T. Toriyama et al., J. Phys. Soc. Jpn. **83**, 033701 (2014); G. L. Pascut et al., Phys. Rev. Lett. **112**, 086402 (2014).
4. B. Joseph et al., Phys. Rev. B **88**, 224109 (2013) and references therein.
5. P. G. Radaelli et al., Nature **416**, 155 (2002).
6. D. I. Khomskii and T. Mizokawa Phys. Rev. Lett. **94**, 156402 (2005).
7. K. Yagasaki *et al.*, J. Phys. Soc. Jpn. **75**, 074706 (2006); K. Takubo *et al.*, Phys. Rev. B **78**, 245117 (2008).
8. E. S. Bozin et al., Phys. Rev. Lett. **106**, 045501 (2011)

Influence of Lifshitz transitions and correlation effects on the scattering rates and the effective mass of the charge carriers in ferropnictides and ferrochalcogenides.



Jörg Fink^{1,2}

¹*IFW Dresden, Germany*

²*Technische Universität Dresden, Germany*

Email: J.Fink@ifw-dresden.de

Keywords: high T_c , ferropnictides, ferrochalcogenides, Lifshitz transitions, correlation effects.

Unconventional/high temperature superconductivity (SC) is observed in heavy fermion systems, cuprates, molecular crystals, and ferropnictides close to a point in the phase diagram where, as a function of a control parameter such as pressure, chemical pressure, or doping, the antiferromagnetic order is suppressed. A widespread view is that at this point, which is called a quantum critical point, strong antiferromagnetic fluctuations are a candidate for the glue mediating superconductivity and that these fluctuations would also account for the strange normal state non-Fermi-liquid behavior as is visible in transport and thermal properties. Using angle-resolved photoemission spectroscopy (ARPES) we have studied the scattering rates and band dispersion of various chemically pressurized, electron doped, and hole doped iron-based superconductors [$\text{BaFe}_2(\text{As}_{1-x}\text{P}_x)_2$, $\text{Ba}(\text{Fe}_{1-x}\text{Co}_x)_2\text{As}_2$, $\text{Ba}(\text{Fe}_{1-x}\text{Mn}_x)_2\text{As}_2$, $\text{Na}(\text{Fe}_{1-x}\text{Co}_x)\text{As}$, $\text{Ba}_{1-x}\text{K}_x\text{Fe}_2\text{As}_2$] and iron chalcogenides ($\text{FeTe}_{1-x}\text{Se}_x$) as a function of the control parameter. In addition we have studied non-superconducting similar compounds with lower and higher 3d count [BaFe_2Cr_2 , $(\text{K,Rb,Cs})\text{Fe}_2\text{As}_2$, BaCo_2As_2] to obtain information on the character of the interaction of the charge carriers with electronic excitations. The detected scattering rates of all electron and hole pockets do not diverge at optimal doping, i.e., at the expected quantum critical point. This result is at variance with the above described scenario for quantum critical behavior. The scattering rates strongly differ for pockets having different orbital character, and are linear in energy, indicating marginal Fermi liquid behavior. The scattering rates for hole doped compounds are considerably larger than those of the electron doped systems, indicating a dependence on the Fe 3d count related to strong local interactions and leading for a $3d^5$ configuration to a strongly correlated Hund's metals. Near optimal doping the measurements also indicate a crossing of the top of hole or electron pockets, through the Fermi level which is related to pocket vanishing Lifshitz transitions. Based on these experimental results together with minimum model calculations, we establish the following scenario which is different from the traditional view related to a strong coupling of the charge carriers to fluctuations at the quantum critical point: a co-action between a highly correlated electron liquid *and* a Lifshitz transition. In the normal state, the present work can explain the strange transport and

thermal properties, e.g. the huge mass enhancement near optimal doping. In the superconducting state the small effective Fermi energy favors a Bardeen-Cooper-Schrieffer-Bose-Einstein crossover state. The results can be generalized to other unconventional superconductors.

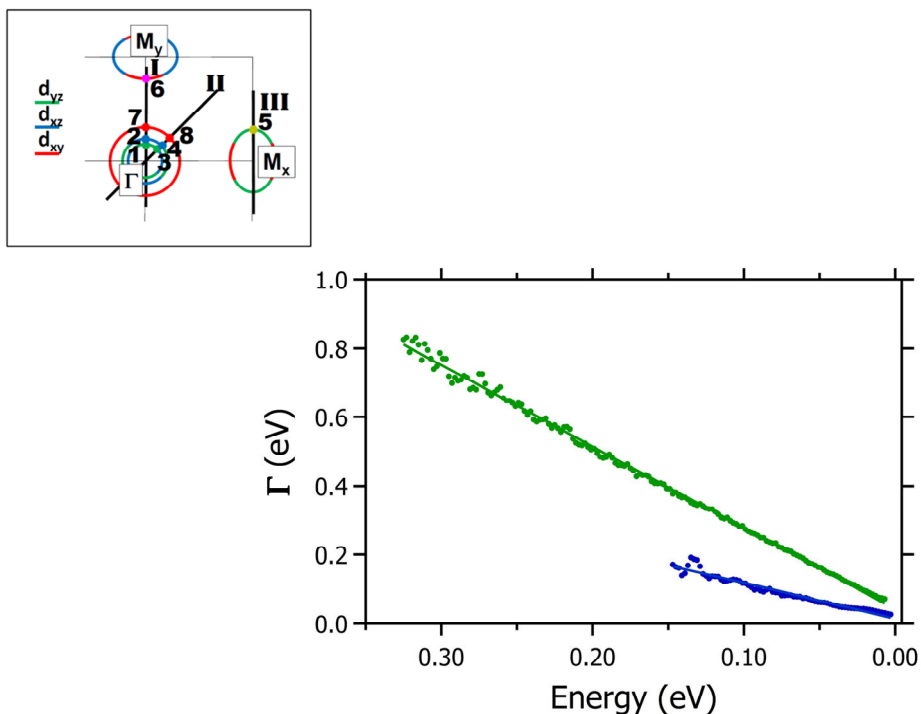


Figure 1: Left upper corner: sketch of Fermi surfaces in ferropnictides. Linear in energy scattering rates Γ in the hole doped superconductor $\text{Ba}_{0.6}\text{K}_{0.4}\text{Fe}_2\text{As}_2$ near points 1 and 2.

This work has been done in collaboration with I. Avigo, B. Borisenko, U. Bovensiepen, B. Büchner, A. Chernukha, H. Dürr, I. Eremin, C. Felser, K. Filsinger, P. Gegenwart, M.S. Golden, Y. Huang, H.S. Jeevan, Z.-H. Liu, K. Lochner, C. Meingast, I. Morozov, N. Nayak, R. Ovsyannikov, E.D.L. Rienks, M. Roslova, F. Roth, E. Slooten, S. Thirupathaiah, M. Vojta, and Th. Wolf.

References

1. J. Fink et al., Phs. Rev. B 92, 201106 (R) (2016)
2. J. Fink, EPL in print, arXiv:1601.06516

Solitonic lattice and Yukawa forces in the rare earth orthoferrite TbFeO_3



Dimitri N. Argyriou^{1,2*}, Maxim Mostovoy^{3*}

¹*European Spallation Source ERIC, Lund, Sweden.*

²*University of Lund, Division of Synchrotron Radiation, Lund, Sweden*

³*Institute for Advanced Materials, University of Groningen, Nijenborgh 4, 9747 AG, Groningen, The Netherlands*

Email: dimitri.argyriou@ess.se, M.Mostovoy@rug.nl

Keywords: Solitons, multiferroics, Yukawa forces,

incommensurate, orthoferrites

Spin fluctuations give rise to many interesting physical phenomena, such as the "order-from-disorder" in frustrated magnets and unconventional Cooper pairing in magnetic superconductors. Here we show that the exchange of spin waves between extended topological defects, such as domain walls, can result in novel magnetic states. We report the discovery of an unusual incommensurate phase in the orthoferrite TbFeO_3 using neutron diffraction under an applied magnetic field.

Materials with magnetic transition metal and rare earth ions show a variety of spectacular effects originating from the coupling between the two spin subsystems. The transition metal spins interact stronger and order at higher temperatures than the spins of rare earth ions, but they are also much less anisotropic. That is why their orientation can be controlled by the rare earth magnetism. Such re-orientation transitions observed in many rare earth ferrites, chromites and manganites have profound effects on their magnetic, optical and elastic properties. [1]

Recently it was realized that interactions between transition metal and rare earth spins also play an important role in multiferroic and magnetoelectric materials [2]. Thus the coupling between the Mn spins forming a spiral state in the multiferroic TbMnO_3 and the Ising-like Tb spins leads to a significant enhancement of the electric polarisation induced by the spiral [3]. In GdFeO_3 orthoferrite the polarisation only appears when the independent magnetic orders of Fe and Gd sublattices are present simultaneously, while in DyFeO_3 the interplay between the spins of Fe and Dy ions gives rise to one of the strongest linear magnetoelectric responses observed in single-phase materials.

Using single crystal neutron diffraction we have probed the A,C,G and F-type orders in TbFeO_3 by tracking the intensity of the corresponding magnetic Bragg reflections in zero field and in an applied field along the c -axis. We have discovered an unusual magnetic stripe-like modulation to occur just above 2.8K with a magnetic field applied along the c -axis (see Fig. 1).

The magnetic modulation has a very long period of 340 Å at 3 K and exhibits an anomalously large number of higher-order harmonics, allowing us to identify it with the periodic array of sharp domain walls separated by many lattice constants. These domain walls are formed by Ising-like Tb spins. They interact by exchanging magnons

propagating through the Fe magnetic sublattice. The resulting force between the domain walls has a rather long range that determines the period of the incommensurate state and is analogous to the pion-mediated Yukawa interaction between protons and neutrons in nuclei.

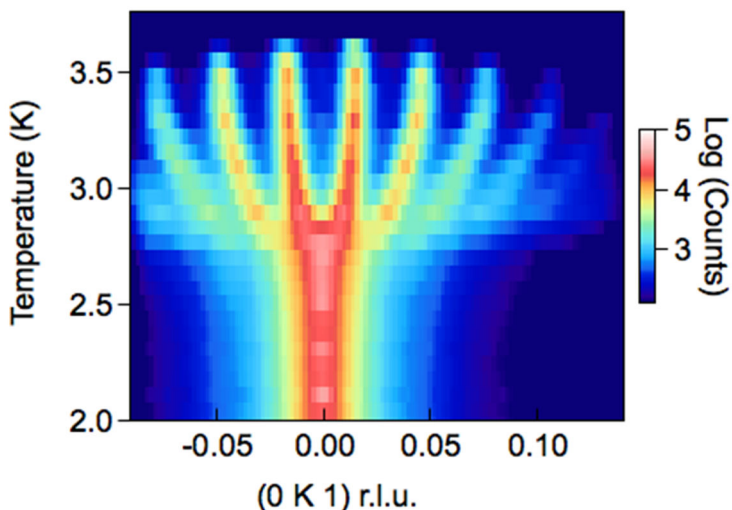


Figure 1: Temperature dependent single crystal neutron diffraction data from TbFeO_3 . The measurements were taken on cooling and in a magnetic field parallel to the c -axis of $H=2\text{ T}$. All scans are measured in reciprocal space along $(0,k,1)$. Here the data are represented in a two-dimensional plot with intensity depicted as colour on a log scale shown on the right of the panel. In this specific scan harmonics up to 9th order can be seen on the right hand side above 2.8K and up to 5th order on the left hand side. In separate scans, the 11th harmonic has also been observed.

References

1. K.P. Belov, et al. Sov. Phys. Usp. 19, 574-596 (1976); V.D. Buchel'nikov, et al. . Phys. Usp. 39, 547-572 (1996); A.V. Kimel, et al. Nature 435, 655-657 (2005).
2. T. Kimura, et al. Nature 426, 55-58 (2003); Hur, N. et al. Nature 429, 392-395 (2004); A.K. Zvezdin & A. A. Mukhin, JETP Letters 88, 505-510 (2008); Y. Tokunaga, et al, Nature Mater. 8, 558-562 (2009).
3. O. Prokhnenko, et al. Phys. Rev. Lett. 99, 177206 (2007); N. Aliouane, et al. J. Phys.: Condens. Matter 20, 434215 (2008).
4. Y. Tokunaga, et al. Phys. Rev. Lett. 101, 097205 (2008).

Reentrance of superconductivity in parallel fields



Andreas Glatz^{1,2*}, Gregory J. Kimmel^{1,3}, Igor Aronson¹,
Yong-Lei Wang¹, and Zhili Xiao^{1,2}

¹Argonne National Laboratory, Materials Science Division,
9700 S.Cass Avenue, Argonne, Illinois 60637, USA

²Northern Illinois University, Department of Physics, DeKalb,
Illinois 60115, USA

³Department of Engineering Sciences and Applied
Mathematics, Northwestern University, Evanston, Illinois
60208, USA

Email: * glatz@anl.gov

Keywords: Vortex dynamics, Large-scale TDGL simulations, reentrance, magnetoresistance

I will present new results on the re-entrance of the superconducting state in systems placed into a parallel magnetic field.

In recent experiments [1] on Molybdenum-Germanium it was observed that the magneto-resistance first increases with magnetic field, but at higher field drops again such that superconductivity is recovered. This effect is strongly temperature dependent and can lead to a suppression of resistance below the measurable threshold over a range of a few kG.

We study the vortex dynamics and magneto-resistance in this situation in the framework of a large-scale time-dependent Ginzburg Landau simulation [2]. A small external current as well as the magnetic field are applied in the x-direction, the latter is then ramped up.

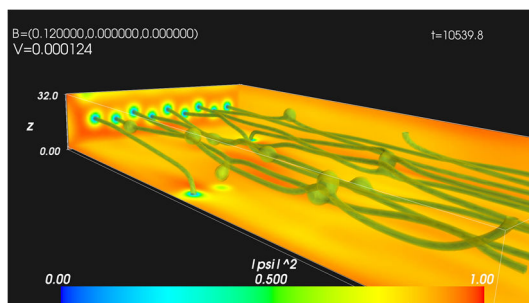


Figure 1: Vortex configuration at intermediate fields, exhibiting a periodic dynamic resistive state, where vortex ends “travel” around the surface.

Our simulations reveal the mechanism for the observed behavior: the intermediate resistive state is due to a vortex instability leading to an unwinding of twisted vortex configurations (see Fig. 1). This leads to a periodic dynamic resistive state.

When the field increases these instabilities get stabilized and the resistance drops upon increasing the magnetic field due to a higher vortex concentration, leading to a vortex lattice “straightening”.

An important factor in these consideration is the presence of a small amount of defects in the system: Without defects, vortices would just align with the current until thermal fluctuations bend them and the resulting Lorentz force leads to a resistive state.

This would happen at relatively high fields. On the other hand, with a high concentration of defects, vortices never get the chance to straighten up and we observe only a resistive state above the depinning field.

References

1. Glatz, et. al., to be published (2016).
2. A. Sadovskyy, A. E. Koshelev, C. L. Phillips, D. A. Karpeev, A. Glatz, *J. of Comp. Phys.* **294**, 639 (2015).

Towards a complete Fermi surface in underdoped high T_c superconductors



Neil Harrison^{1*},
¹*Los Alamos National Labs.*

Email: * nharrison@lanl.gov

Keywords: high T_c, Fermi surface, quantum criticality, charge order

The discovery of magnetic quantum oscillations in underdoped high T_c superconductors raised many questions, and initiated a quest to understand the origin of the Fermi surface the like of which had not been seen since the very first discovery of quantum oscillations in elemental bismuth. While studies of the Fermi surface of materials are today mostly assisted by computer codes for calculating the electronic band structure, this was not the case in the underdoped high T_c materials. The Fermi surface was shown to reconstructed into small pockets, yet there was no hint of a viable order parameter. Crucial clues to understanding the origin of the Fermi surface were provided by the small value of the observed Fermi surface cross-section, the negative Hall coefficient and the small electronic heat capacity at high magnetic fields. We also know that the magnetic fields were likely to be too weak to destroy the pseudogap and that vortex pinning effects could be seen to persist to high magnetic fields at low temperatures. I will show that the Fermi surface that appears to fit best with the experimental observations is a small electron pocket formed by connecting the nodal “Fermi arcs” seen in photoemission experiments, corresponding to a density-wave state with two different orthogonal ordering vectors. The existence of such order has subsequently been detected by x-ray scattering experiments, thereby strengthening the case for charge ordering being responsible for reconstructing the Fermi surface. I will discuss new efforts to understand the relationship between the charge ordering and the pseudogap state, discussing the fate of the quasiparticles in the antinodal region and the dimensionality of the Fermi surface. The author acknowledges contributions from Suchitra Sebastian, Brad Ramshaw, Mun Chan, Yu-Te Hsu, Mate Hartstein, Gil Lonzarich, Beng Tan, Arkady Shekhter, Fedor Balakirev, Ross McDonald, Jon Betts, Moaz Altarawneh, Zengwei Zhu, Chuck Mielke, James Day, Doug Bonn, Ruixing Liang, Walter Hardy.

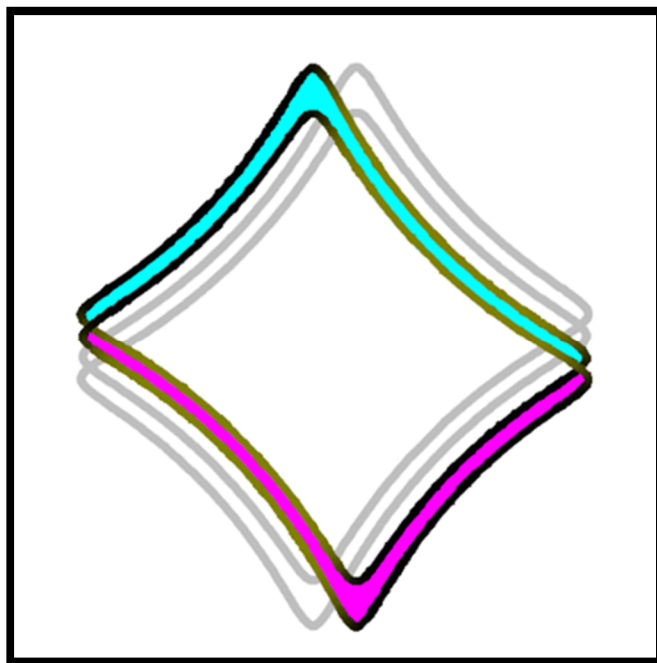


Figure 1: Fermi surface according to angle-dependent magnetoresistance measurements, indicating 4-fold in-plane Fermi surface shape and 2-fold anisotropy in the Fermi surface warping.

References

This work is supported by DOE BES “100 tesla science” program

Quantum effect on atomic dynamics in superfluid ^4He



Takeshi Egami^{1,2*}, Souleyman O. Diallo²

¹*University of Tennessee*

²*Oak Ridge National Laboratory*

Email: *egami@utk.edu

Keywords: Bose-Einstein condensation, superfluidity, neutron scattering

Superfluidity in ^4He has been studied for a long time since its discovery in 1938. Yet fundamental questions remain controversial. Initially Fritz London explained the phenomena in terms of Bose-Einstein condensation (BEC) [1]. However, BEC is well defined in ideal gas, whereas He is liquid, not gas. Liquid is a condensed matter with significant atomic interaction via the dispersion (Van der Waals) force. Indeed the successful explanation by Lev Landau [2] does not mention BEC. The conflict was theoretically resolved by Feynman [3] and others, but microscopic details, for instance atomic dynamics, remain poorly understood.

We carried out a study of atomic dynamics in ^4He by inelastic neutron scattering. We measured the dynamic structure factor, $S(Q, E)$, where Q and E are the momentum and energy exchange in scattering, at various temperatures above and below the condensation temperature, $T_\lambda = 2.17$ K [4]. It is well known that the roton-phonon dispersion becomes very narrow below T_λ , because of gap opening as shown in Fig. 1(a). In order to study the dynamic atomic correlations we Fourier-transformed $S(Q, E)$ into the dynamic pair-density correlation function (DPDF), $g(r, E)$. DPDF describes local dynamic atomic correlations, and was used for the first time in the study of relaxor ferroelectrics [5]. As shown in Fig. 1(b) the DPDF of ^4He at 1.83 K showed a strong peak at $r = 4$ Å and $E = 0.75$ meV. The temperature dependence of the intensity of this peak follows the temperature dependence of the BEC order parameter. The energy of this peak and the temperature dependence suggests that it is due to correlations between atoms involved in the roton excitation.

It is interesting to note that the average interatomic distance in ^4He is known to be 3.6 Å. Our total, or instantaneous, PDF, $g(r)$, obtained by integrating DPDF over energy, also gives this distance. Therefore the atomic distance for the roton is longer by 10% than the average distance. This difference is totally beyond statistical and experimental uncertainty. This observation was not expected by the current theories. The volume fraction of the BE condensate is only 7% even at $T = 0$ K. Atoms randomly go in and out of the BEC, and the atomic correlation is supposed to be the same for BEC and non-BEC. The present result is in disagreement with such expectation.

We believe this result represents a quantum effect on electrons. Currently theories presume the Born-Oppenheimer approximation and assume that BEC occurs only for the nuclear degrees of freedom. This is because the electronic energies (of the order of

10 eV) are much larger than kT_{λ} . However, the Van der Waals interaction, which occurs due to the s - p hybridization of He electrons, is weak. The energy-scale involved in the s - p hybridization is similar to the roton energy. Therefore electrons may be involved in BEC. In the normal state electrons from two neighboring He atoms hybridize and form a narrow band. But in the BEC state because of the Pauli principle electrons cannot overlap, and will not form a band. If that is the case, just like the case of electrons with spin parallel and anti-parallel, distances between non-overlapping atoms will be longer. In the case of two electrons this difference results in the exchange energy. Thus our result suggests that a novel quantum phenomena may be at work in superfluid ^4He .

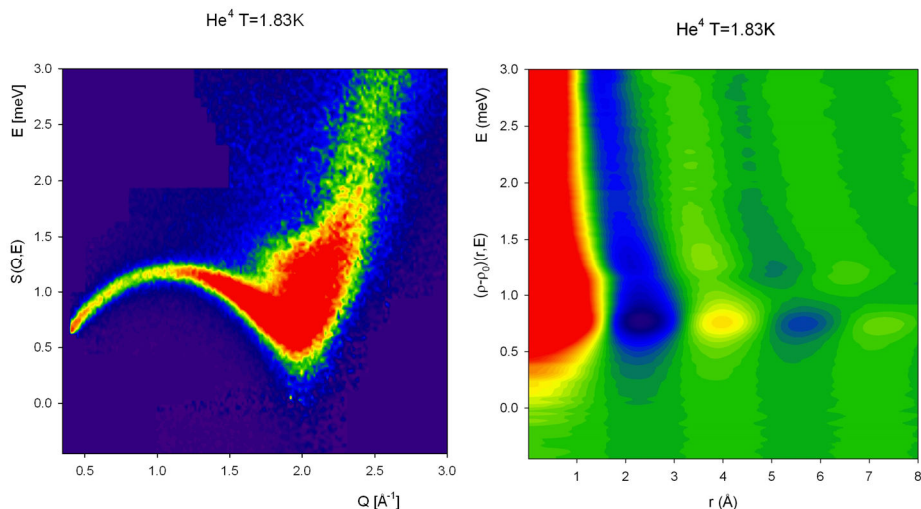


Figure 1: (a) Roton-phonon dispersion, and (b) DPDF of ^4He at $T = 1.83\text{K}$ determined by inelastic neutron scattering [4].

References

1. F. London, Nature (London), **141**, 643 (1938).
2. L. D. Landau, Phys. Rev. **60**, 356 (1941).
3. R. P. Feynman, Phys. Rev. **91**, 1291; 1308 (1953).
4. W. Dmowski, S. O. Diallo, K. Lokshin, G. Ehlers and T. Egami, unpublished.
5. W. Dmowski, S. B. Vakhrushev, I.-K. Jeong, M. P. Hehlen, F. Trouw and T. Egami, Phys. Rev. Lett., **100**, 137602 (2008).

Phase separation, first order transition and precursor states in unconventional superconductors, Mott insulators and Skyrmion systems --- analogy with 3-d and 2-d superfluid He --

Yasutomo J. Uemura,
Columbia University

Email: tomo@lorentz.phys.columbia.edu

Microscopic phase separation was observed by MuSR, STM, nano-optics and other probes in disappearance of magnetically ordered states in (a) high-T_c cuprates: 1/8 stripe and oxygen overdoped La₂CuO₄; (b) iron based systems: Ba(Fe,Ni)₂As₂, Na(Fe,Cu)As; (c) heavy-fermion system CeNiAsO; (d) Mott transition systems RENiO₃ and V₂O₃; and (e) itinerant magnets MnSi under pressure. Adjacent paramagnetic states of these systems exhibit exotic phases of high-T_c superconductivity with magnetic resonance modes in (a)(b); precursor "pseudo-gap" state in (d) as found by STM; and fluctuating chiral Skyrmion liquid in (e); associated with non-fermi-liquid transport in normal metallic states. Phase separation was also found between superconducting and normal phases in: (a) Zn-doped and overdoped Tl₂201 and LSCO cuprates; (b) overdoped Ba(Fe,Ni)₂As₂; (c) CeCo(In,Sn)₅.

Comparisons with 3-d superfluid He will provide wisdom about precursor states with "roton-like" soft-mode spin fluctuations for the former case of destruction of magnetic order. Comparisons with 2-d superfluid He films and 3He/4He fermion/boson mixture in porous media and/or powder adsorption provide insights into superconducting Bose-Einstein condensation of short coherence-length systems with phase separation in highly disordered media. All these considerations shed new lights on novel role of first-order transitions and generic importance of phase separation in strongly correlated systems.

Cooper Pairing and Phase Coherence in Iron-based Superconductor $\text{Fe}_{1+x}(\text{Te,Se})$

Shuheng H. Pan

Institute of Physics, Chinese Academy of Sciences

Dept. of Physics/Texas Center for Superconductivity, University of Houston

Cooper pairing and phase coherence are the two fundamental aspects of superconductivity¹. In research of cuprate high T_c superconductivity (HTS), pseudogap, preformed pair, and phase fluctuation were the concepts often mentioned. However, microscopic experimental demonstrations of these concepts have been difficult, likely due to Mottness and inhomogeneity. In this talk, I will present our comprehensive STM/S study on the iron-based superconductor $\text{Fe}_{1+x}(\text{Te,Se})$ over a wide range of interstitial Fe impurity (IFI) concentration. We have found that, in addition to generating robust zero-energy bound states locally (*Nature Physics* **11**, 543, (2015)), these IFIs also have significant global effects on the superconducting ground state. Our high resolution tunneling spectroscopy and quasi-particle interference data show that IFIs hardly affect the electron pairing strength, while they cause significant decoherence of the Cooper pairs, eventually drive the ground state of the system from strong-coupling-superconducting state to diffusive-metallic state with incoherent electron pairs. These experimental results demonstrate a clear coherent picture for those concepts long discussed in research of HTS.

Probing Energy Scale in the Interacting 2D Electron System by Transport and Thermodynamic Measurements



V.M. Pudalov, L.A. Morgun, A.Yu. Kuntsevich
P.N. Lebedev Physical Institute, Moscow

Email: * pudalov@lebedev.ru

Keywords: strongly correlated electrons, two-dimensional electron system, metal-insulator transition

Two-dimensional (2D) interacting low density carrier systems in the past two decades attracted considerable interest, demonstrating fascinating electron-electron interaction effects, such as metallic temperature dependence of resistivity [1,2], metal-insulator transition (MIT) [1,3], strong positive magnetoresistance (MR) in the in-plane field [4,5], strong renormalization of the effective mass and spin susceptibility [6-8], etc. Far off the critical MIT density n_c , in the well “metallic regime”, these effects are explained within framework of the Fermi liquid theory - in terms of interaction quantum corrections, or temperature dependent screening of the disorder potential. In the close vicinity of the critical density n_c , the renormalization group approach is used to describe interaction effects in the diffusive interaction regime [9,10]. On the other side, a number of theories predict breakdown of the uniform paramagnetic 2D Fermi liquid state as interaction strength increases [11-15]. Some recent thermodynamic experiments also reveal the two-phase inhomogeneous and non-Fermi liquid state in the 2D correlated electron system [16-18]. However, it remains almost unexplored how the instabilities in thermodynamics may reveal in transport properties.

We report results of the transport, magnetotransport and magnetization measurements with 2D correlated electron system, which demonstrate the existence of a novel characteristic energy scale T^* , that is smaller than the Fermi temperature T_F , but much bigger than $1/\tau$. Obviously, no such large energy scale may exist in the pure Fermi liquid. T^* reveals itself (i) in the weak in-plane field magnetotransport, (ii) in zero field transport, and (iii) in the spin magnetization M . In magnetoconductivity, we found a sharp onset of the novel regime $\delta\sigma(B,T) \propto (B/T)^2$ above a density dependent $T^{\text{kink}}(n)$, the high-energy behavior that “mimics” the low-temperature diffusive interaction regime [19]. $T^{\text{kink}}(n)$ correlates well with an inflection point $T_{\text{infl}}(n)$ in the zero field resistivity temperature dependence. Finally, the two remarkable temperatures correlate with the temperature $T_{\text{dM/dn}}$ for which the spin susceptibility per electron $\partial\chi/\partial n$ (and $\partial M/\partial n$) changes sign. All three notable temperatures, $T^{\text{kink}}(n)$, $T_{\text{infl}}(n)$, and $T_{\text{dM/dn}}$ behave critically $\propto (n-n_c)$, are close to each other, and are intrinsic to high mobility samples only; we therefore associate them with a novel energy scale T^* caused by interactions in the 2DE system. We shall discuss a potential microscopic origin of this characteristic energy scale T^* . We associate it with an energy structure of the collective

electron states that emerge in the Fermi liquid as a consequence of the disorder and interactions.

References

1. S.V. Kravchenko, G.V. Kravchenko, J. E. Furneaux, V. M. Pudalov, and M.~D'Iorio, Phys. Rev. B **50**, 8039 (1994).
2. Y. Hanein, U. Meirav, D. Shahaar, C. C. Li, D. C. Tsui, Hadas Shtrikman, Phys. Rev. Lett. **80**, 1288 (1998).
3. S.V.Kravchenko, W.E.Mason, G.E.Bowker, J.E.Furneaux, V.M.Pudalov, M.D'Iorio, Phys. Rev. B **51**, 7038 (1995).
4. D. Simonian, S.V. Kravchenko, M.P. Sarachik, V.M. Pudalov, Phys. Rev. Lett. **79**, 2304 (1997).
5. V.M. Pudalov, G. Brunthaler, A. Prinz, G. Bauer, JETP Lett. **65**, 932 (1997).
6. V.M. Pudalov, M.E. Gershenson, H. Kojima, in: *Fundamental problems of mesoscopic physics*, NATO science series **154**, 309, (Kluwer, 2004), Ed. by I. Lerner, B. Altshuler, and Y. Gefen. Arxiv: cond-mat/0401396.
7. A.A. Shashkin, S.V. Kravchenko, V.T. Dolgoplov, T.M. Klapwijk, Phys.Rev. B **66**, 073303 (2002).
8. V.M. Pudalov, M.E. Gershenson, H. Kojima, N. Butch, E.M. Dizhur, G. Brunthaler, A. Prinz, G. Bauer, Phys. Rev. Lett. **88**, 196404 (2002).
9. A.M. Finkel'stein, Z. Phys. B: Condens. Matter **56**, 189 (1984). Sov. Sci. Rev. Sect. A **14**, 1 (1990).
10. C. Castellani, C. Di Castro, P.A. Lee, Phys. Rev. B **57**, 9381 (1998).
11. M.W.C. Dharma-wardana, and F. Perrot, Phys. Rev. Lett. **90**, 136601 (2003).
12. B.N. Narozhny, I.L. Aleiner, and A. I. Larkin, Phys. Rev. B **62**, 14 898 (2000).
13. J. W. Clark, V.A. Khodel, M.V. Zverev, Phys. Rev. B **71**, 012401 (2005).
14. B. Spivak, Phys. Rev. B **67**, 125205 (2003). B. Spivak, and S. A. Kivelson, Phys. Rev. B **70**, 155114 (2004).
15. Y.V. Stadnik, O. P. Sushkov, Phys. Rev. B **88**, 125402 (2013).
16. N. Teneh, A.Yu. Kuntsevich, V.M. Pudalov, M. Reznikov, Phys. Rev. Lett. **109**, 226403 (2012).
17. A.Yu. Kuntsevich, Y.V. Tupikov, V.M. Pudalov, I.S. Burmistrov, Nature Commun. **6**, 7298 (2015).
18. V. M. Pudalov, A. Yu. Kuntsevich, I. S. Burmistrov, M. Reznikov, J. Low Temp. Phys. **181**(3,4), 99 (2015).
19. G. Zala, B.N. Narozhny, I.L. Aleiner, Phys. Rev. B **65**, 020201 (2001).

Lifshitz transitions and BCS-BEC crossover in multigap superconductors as a root for room temperature superconductivity

Andrea Perali^{1,2*}

¹*School of Pharmacy, Physics Unit, University of Camerino, Italy*

²*International MultiSuper Network*

***Email:** andrea.perali@unicam.it

Keywords: Lifshitz transition, high-T_c, shape resonance, multigap superconductivity, isotope effects.

The superconductivity in iron-based, magnesium diborides, and other novel high-T_c superconducting materials, possibly including the recently discovered superconducting hydrogen disulfide, has a strong multi-band and multi-gap character [1,2] and recent experiments support the possibility for a BCS-BEC crossover induced by strong-coupling and proximity of the chemical potential to the band edge of one of the bands, with evidences for Lifshitz transitions associated with changes in the Fermi surface topology [3, 4]. Here we study the simplest theoretical model which accounts for the BCS-BEC crossover in a two-band / two-gap superconductor, considering tunable interactions. When the gap is of the order of the local chemical potential, superconductivity is in the crossover regime of the BCS-BEC crossover and the Fermi surface of the small band is completely smeared by the gap opening. In this situation, small and large Cooper pairs coexist in the total condensate, which is the optimal condition for high-T_c or even for room temperature superconductivity [5]. Using available experimental data, our analysis shows that iron-based superconductors have the partial condensate of the small Fermi surface which is in the crossover regime of the BCS-BEC crossover [6], supporting in this way the recent ARPES findings [7, 8]. We also discuss different physical systems in which the multigap and multiband BCS-BEC crossover can be realized, pointing toward very high-T_c superconductivity. Two examples are considered here: (i) superconducting stripes in which shape resonances and multigap physics at the band edge play a cooperative role in enhancing superconductivity in the crossover regime of pairing [9], and (ii) our prediction of high-T_c superconductivity using nanoribbons of doped graphene [10]. Finally, we focus on a key prediction of the above discussed physics: the isotope effect of the superconducting critical temperature in the vicinity of a Lifshitz transition, which has a unique dependence on the energy distance between the chemical potential and the Lifshitz transition point. Comparisons with available experimental data for superconducting cuprates and hydrogen disulfide will be discussed [2,11].

References

1. S.V. Borisenko et al., *Symmetry* **4**, 251 (2012). See also the International Network MultiSuper: <http://www.multisuper.org>
2. A. Bianconi, T. Jarlborg, *Eur. Phys. Lett.* **112**, 37001 (2015).
3. D. Innocenti, N. Poccia, A. Ricci, A. Valletta, S. Caprara, A. Perali, and A. Bianconi, *Phys. Rev. B* **82**, 184528 (2010).
4. For an overview, see, A. Bianconi, *Nature Phys.* **9**, 536 (2013).
5. A. Perali, C. Castellani, C. Di Castro, M. Grilli, E. Piegari, and A. A. Varlamov, *Phys. Rev. B* **62**, R9295 (2000).
6. A. Guidini and A. Perali, *Supercond. Sci. Technol.* **27**, 124002 (2014).
7. Y. Lubashevsky, et al., *Nat. Phys.* **8**, 309 (2012).
8. K. Okazaki et al., *Sci. Rep.* **4**, 4109 (2014).
9. A. Perali, A. Bianconi, A. Lanzara, N.L. Saini, *Solid State Comm.* **100**, 181, (1996).
10. A. Perali, D. Neilson, M. Zarenia, M. Milosevic, and F. M. Peeters, in preparation.
11. A. Perali, D. Innocenti, A. Valletta, A. Bianconi, *Supercond. Sci. Technol.* **25**, 124002 (2012).

Pairing in a dry Fermi sea



T.A. Maier^{1*}, P. Staar², V. Mishra³, U. Chatterjee⁴, J.C. Campuzano⁵, and D.J. Scalapino⁶

¹*Computer Science and Mathematics Division and Center for Nanophase Materials Sciences, Oak Ridge National Laboratory*

²*IBM Research — Zürich*

³*Joint Institute of Computational Sciences, University of Tennessee, Knoxville*

⁴*Department of Physics, University of Virginia*

⁵*Department of Physics, University of Illinois at Chicago*

⁶*Department of Physics, University of California, Santa Barbara*

Email: * maiert@ornl.gov

Keywords: high- T_c cuprates, pseudogap, superconductivity, spin fluctuations

After 30 years, the search for the mechanism responsible for pairing in the high- T_c superconductors continues. In the traditional BCS theory of superconductivity, the presence of an electron Fermi sea gives rise to a logarithmic singularity of the amplitude for the propagation of a Cooper pair as the temperature decreases. This, together with an attractive interaction, no matter how weak, eventually leads to a pairing instability. There is evidence, however, that this log singularity is suppressed in the pseudogap regime of the cuprate superconductors, where parts of the Fermi surface are destroyed [1]. This raises the question of how pairing can arise in the absence of a Fermi sea. Here we report results from numerical quantum Monte Carlo calculations and an analysis of angular resolved photoemission experiments on a cuprate superconductor. In contrast to the BCS theory, we find that in the pseudogap regime the pairing instability arises through an increase in the strength of the spin-fluctuation pairing interaction as the temperature is lowered.

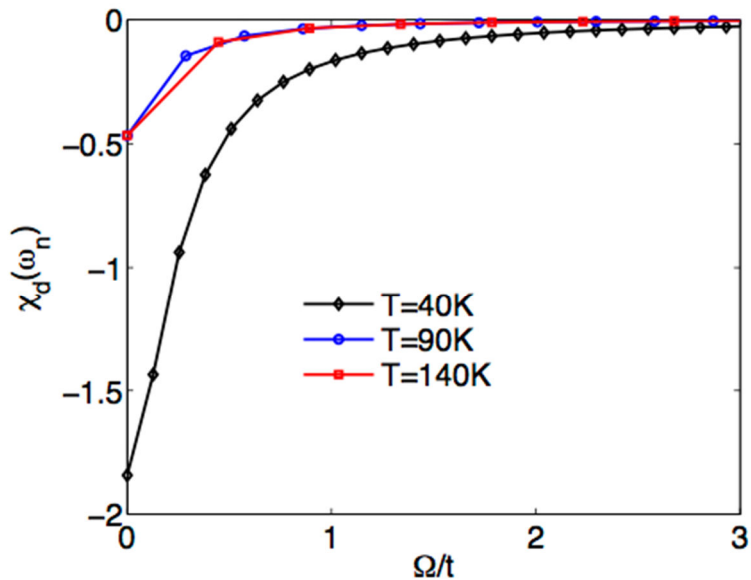


Figure 1: Temperature dependence of the spin-fluctuation interaction. d -wave projected spin susceptibility versus Matsubara frequency for $T = 40$ K calculated from 40 K ARPES spectral weight data $A(k, \omega, T = 40$ K), and for $T = 90$ K and 140 K calculated from 40 K ARPES data for $A(k, \omega, T = 140$ K). The strength of the spin-fluctuation interaction increases significantly as the temperature is lowered.

References

1. V. Mishra, U. Chatterjee, J. C. Campuzano, and M. R. Norman, Nat. Phys. **10**, 357 (2014).

Sign changing pairing via spin-fluctuations of incipient bands close to the Fermi level



A. Linscheid^{1*}, S. Maiti¹, Y. Wang², S. Johnston², P. J. Hirschfeld¹

¹*Department of Physics, University of Florida, Gainesville, FL 32611* ²*Department of Physics and Astronomy, University of Tennessee, Knoxville, Tennessee 37996*

Email: * linscheid@ufl.edu

Keywords: high T_c , FeSe monolayers, Lifshitz transition, doping

Several experiments in the context of the Fe based superconductors(SC) have investigated a scenario where the positions of electronic bands are modified by doping and one is eventually pushed through a Lifshitz transition and becomes “incipient”. Examples include but are not limited to Co-doped LiFeAs [1] where the gap on the incipient band remains fairly constant throughout the transition and FeSe derived intercalates [2] and monolayers [3]. We show that it is possible to understand the behavior of the gap in Co-doped LiFeAs within repulsive spin-fluctuation driven weak-coupling BCS theory and no strong coupling models are necessary [4]. One of the most studied phenomena in the field of Fe-based SC in recent years are FeSe derived materials that can reach critical temperatures of 35-45K while the FeSe monolayer on SrTiO₃ shows a gap closing in ARPES at above 65K (see [5] for a review). These materials share the feature that only the electron pocket crosses the Fermi level while the top of the hole-pocket is ~50meV below. Their apparent s-wave gap [6] directly challenges the usual Fermi-level based sign changing s⁺- explanation for the Fe-based SC. Noting that there are signs of strong interactions, here, we show that s⁺-pairing can be retained in a simple two band model that reflects this experimental situation [7]. We model doping by shifting the top of the hole band (E_h). Within our RPA approach, the paramagnon excitation softens as a square root when the system is doped to the point where it turns magnetic, while the electronic coupling between the bands behaves inversionally proportional to this distance. Based on the limiting behavior of the Eliashberg equations, we find that T_c remains finite even though the coupling diverges. We solve the incipient Eliashberg equations as shown in Fig. 1 and, interestingly, T_c initially rises and we find an optimal trade-off between pairing bandwidth and coupling strength before, upon a further doping, T_c is suppressed by the distance of the hole band to the Fermi level. Experiments have highlighted signs of replica bands in FeSe on SrTiO₃ [6] that corresponds to a strong electron phonon interaction at small momentum. An additional coupling in the spirit of this forward scattering (q=0) scenario is capable of further enhancing the critical temperature [8] and thus explains higher T_c in this system as compared to the intercalates with a similar band structure. Finally, we want to discuss an extension of this simple model to a more realistic band structure.

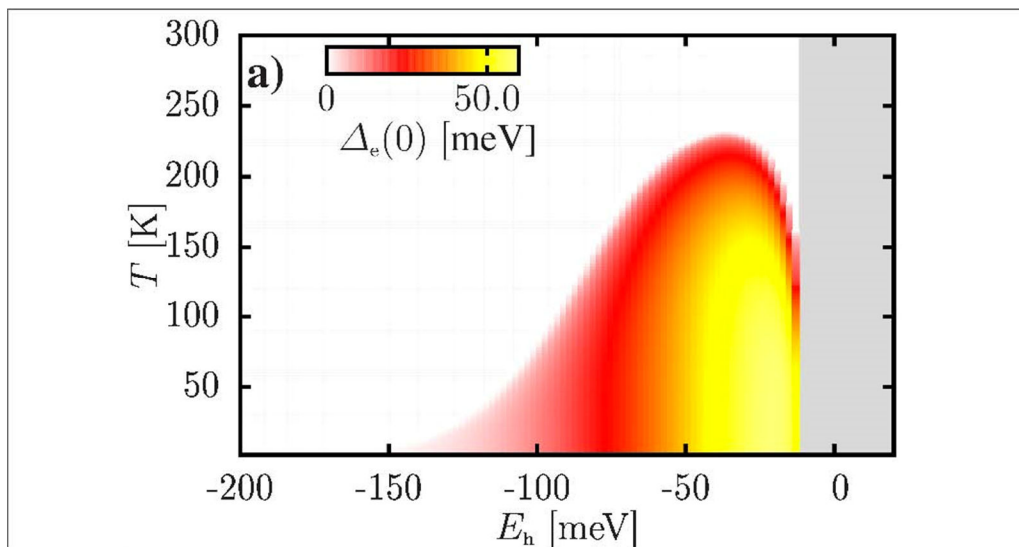


Figure 1: Eliashberg gap on the electron band as a function of T and position of the incipient hole band. The grey area is beyond the SDW transition.

References

1. H. Miao *et al.*, Nat. Com. **6**, 6056 (2015).
2. F. Wang *et al.*, Europhys. Lett. **93**, 57003 (2011).
3. Q.-Y. Wang *et al.*, Chinese Physics Letters **29**, 037402 (2012)
4. Xiao Chen *et al.*, Phys. Rev. B **92**, 224514 (2015)
5. P. J. Hirschfeld Comptes Rendus Physique **17**, 197 (2016).
6. D. Liu *et al.*, Nat. Com. **3**, 931 (2012).
7. S. He *et al.*, Nat. Mat. **12**, 605 (2013).
8. J.J. Lee *et al.*, Nature **515**, 245 (2014).
9. A. Linscheid *et al.*, arXiv:1603.03739.
10. L. Rademaker *et al.*, New J. Phys **18**, 022001 (2016).

Boson-Fermion resonant model for nonconventional superfluids



R. Micnas

*Faculty of Physics, Adam Mickiewicz University,
ul.Umultowska 85, 61-614 Poznań, Poland*

Email of the presenting author *rom@amu.edu.pl*

Keywords: boson-fermion model, pseudogap, BCS-BEC crossover, resonant superfluidity

We outline briefly the properties of a mixture of mutually interacting bosons (bound fermion pairs) and itinerant fermions on a lattice (the boson-fermion model). The boson-fermion (BF) model with resonant interaction is a basic model for superconductivity that has been adopted to explain high- T_c superconductivity and the BCS-BEC crossover in ultra-cold fermionic atomic gases. Several authors have considered the BF scenarios in the investigation of superconductivity mechanism, exploring heterogeneity of the electronic structure of cuprate HTS, especially in the pseudogap phase, either in the momentum space (the Fermi arcs model) or in the real space (charge and spin inhomogeneities) [1-5]. Here, firstly, we analyze the BF model with isotropic and anisotropic pairing of extended s and $d_{x^2-y^2}$ -wave symmetries for a 2D square lattice within the mean field theory and the Kosterlitz-Thouless scenario. The superconducting characteristics of this (hard-core) boson-fermion mixture are determined as a function of position of the local pair level and the total particle concentration. Secondly, the superfluid transition temperature from the pseudogap state and phase diagrams of a 3D and quasi-2D boson-fermion resonant model are computed within a self-consistent T-matrix approach, which includes pairing fluctuations effect [2,5]. The main features of BCS-BEC crossovers for various fillings and across the superfluid-insulator transition in the BF model are analyzed. The results are discussed in the context of a two-component scenario of preformed pairs and unpaired electrons for high- T_c superconductors. They are also connected to the resonant superfluidity in ultra-cold atomic Fermi gases with a Feshbach resonance.

References

1. R. Micnas, S. Robaszkiewicz and A. Bussmann-Holder, Structure and Bonding: "Superconductivity in Complex Systems" **114**, 13 (2005).
2. R. Micnas, Phys. Rev. **B 76**, 184507 (2007).
3. G. Pawłowski, R. Micnas and S. Robaszkiewicz, Phys. Rev. **B 81**, 064514 (2010).
4. J. Krzyszczak, T. Domański, K.I. Wysokiński, R. Micnas and S. Robaszkiewicz, J. Phys. Condens. Matter **22**, 255702 (2010).
5. R. Micnas, Phil. Mag. **95**, 622 (2015).

Kinetic origin of the Rashba interaction and of the Dirac cone from the Zero Helicity States



Mauro M. Doria^{1,2,5*}, Marco Cariglia^{1,3,5}, Alfredo Vargas Paredes^{1,4}, Andrea Perali^{1,5}

¹*Dipartimento di Fisica, Università degli Studi di Camerino, Italy*

²*Instituto de Física, Universidade Federal do Rio de Janeiro, Brazil*

³*Departamento de Física, Universidade Federal de Ouro Preto, Brazil*

⁴*Departamento de Física, Universidade Federal Rural de*

Pernambuco, Brazil

⁵*International MultiSuper Network*

Email: * mauromdoria@gmail.com

web: <http://www.multisuper.org>

Keywords: Dirac cone, Rashba interaction, breaking of reflection symmetry, kinetic energy

There has been growing interest in the physics of two-dimensional electronic systems. Many experimental discoveries done in the past decades clearly point to the fact that reduced dimensionality offers new venues for the manifestation of novel electronic phenomena. We show here that the Rashba interaction and the Dirac cone single-particle dispersion are naturally present in the standard non-relativistic kinetic energy and are associated to the onset of zero helicity states. The zero helicity state entangles the two spin states into a single state in a quasi two-dimensional conducting layer yielding a "relativistic" equation describing "massless" carriers. Since helicity and chirality (Weyl) states coincide for massless spinors, this proposal provides a way to generate Weyl states [1] from the standard non-relativistic kinetic energy under the breaking of the spatial reflection symmetry in a layer. The zero helicity state carries current and produce a local magnetic field that brings topological stability to them through a skyrmionic number, thus protecting the decay into other states. This associated local magnetic field is an exact solution of the Ampère's law [2]. This results in topological equations which form a family of equations together with the Abrikosov-Bogomolny equations [3,4], which predict vortices, and the Seiberg-Witten equations [5], which describe four-dimensional massless magnetic monopoles. The natural onset of the Rashba term [6] and of the Dirac cone shows that in the present framework the breaking of the spatial reflection symmetry brought by the layer is of fundamental importance. In 1998, six years before the discovery of graphene, A.A. Abrikosov [7] explained the linear magneto-resistance of non-stoichiometric silver chalcogenides by assuming that carriers form a Dirac cone. The quantum magneto-resistance is found to be linear in many distinct layered materials suggesting of a

general mechanism to obtain the Dirac cone, such as the present one, solely based on the breaking of the spatial reflection symmetry in the layers. Indeed from the standard non-relativistic kinetic energy with parabolic dispersion relation gapless excitations with a linear dispersion relation is obtained (Dirac cone). The zero helicity states provide an explanation for the transverse magnetic moment observed in the LAO/STO system [8] in presence of a nearly perpendicular applied magnetic field to the interface [9]. We also suggest the presence of zero helicity states in the layered high-Tc superconductors at the intersection of the pseudogap line with the superconducting dome, as described in the doping versus temperature phase diagram [10]. Interestingly the present theory shows two states with distinct properties inside the two-dimensional layer, namely symmetrical and anti-symmetrical, respectively. Therefore the existence of continuum states outside, both propagating and evanescent ones, and of two discrete states inside the layer is suggestive of an intrinsic Fano resonance in the configuration interaction between open and closed scattering channels [11].

Mauro M. Doria and Marco Cariglia acknowledge CNPq support from fundings (014992/2015-39) and (205029/2014-0), respectively.

References

1. Editorial, *Nature Physics* 11, 697 (2015).
2. M. M. Doria, A. A. Vargas-Paredes, and M. Cariglia, *Superconductor Science and Technology* 27, 124008 (2014).
3. A. A. Abrikosov, *Soviet Physics JETP* 5, 1174 (1957).
4. E. B. Bogomolny, *Sov. J. Nucl. Phys.* 24, 449 (1976).
5. N. Seiberg and E. Witten, *Nuclear Physics B* 426, 19 (1994).
6. L.P. Gor'kov and E. I. Rashba, *Phys. Rev. Lett.* 87, 037004 (2001).
7. A. A. Abrikosov, *Phys. Rev. B* 58, 2788 (1998).
8. L. Li, C. Richter, J. Mannhart, and R. C. Ashoori, *Nat. Phys.* 7, 762 (2011).
9. Edinardo I. B. Rodrigues, Alfredo A. Vargas-Paredes, Mauro M. Doria and Marco Cariglia, submitted for publication, (2015).
10. Mauro M. Doria and Hugo Keller, *Journal of Magnetism and Magnetic Materials* 376, 1 (2015).
11. A. Bianconi, D. Innocenti, A. Valletta and A. Perali, *Journal of Physics: Conference Series* 529, 012007 (2014).

Vortex-Antivortex unbinding in the 2D BCS-BEC crossover



Luca Salasnich^{1*}, Giacomo Bighin¹

¹*Department of Physics and Astronomy “Galileo Galilei”
University of Padua, via Mazolo 8, 35131, Padua, Italy*

Email: * luca.salasnich@unipd.it

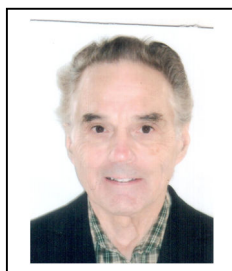
Keywords: Berezinskii-Kosterlitz-Thouless, ultracold atoms, BCS-BEC

Motivated by the recent experimental realization of trapped quasi-two-dimensional fermionic clouds of alkali-metal atoms [1], we include one-loop Gaussian fluctuations in the theoretical description of resonant Fermi superfluids in two dimensions [2]. We demonstrate that the equation of state is strongly renormalized, away from its mean-field value. In particular, we prove that in the intermediate and strong coupling regimes chemical potential and first sound are radically different when Gaussian fluctuations are taken into account [3]. Performing a Renormalization Group analysis of vortex-antivortex unbinding in the full 2D BCS-BEC crossover, we calculate the superfluid density and the Berezinskii-Kosterlitz-Thouless critical temperature, which shows a very good agreement with very recent experimental data [4] and, in the deep BEC regime, with previous diagrammatic Monte Carlo simulations [5].

References

1. V. Makhalov et al., Phys. Rev. Lett. 112, 045301 (2014).
2. L. Salasnich and F. Toigo, Phys. Rev. A 91, 011604(R) (2015).
3. G. Bighin and L. Salasnich, Phys. Rev. B 93, in press (2016).
4. P. A. Murthy et al., Phys. Rev. Lett. 115, 010401 (2015).
5. N. Prokofev et al., Phys. Rev. Lett. 87, 270 (2001).

A Generalized BEC Theory for Any Coupling



I. Chávez,¹ L.A. García,¹ M. Grether,² M. de Llano,¹a*, and V.V. Tolmachev³

¹*Instituto de Investigaciones en Materiales, Universidad Nacional Autónoma de México, 04510 Mexico City, MEXICO*

²*Facultad de Ciencia, Universidad Nacional Autónoma de México, 04510 Mexico City, MEXICO.*

³*N.E. Baumann State Technical University, 107005 Moscow, RUSSIA*

Email: *dellano@unam.mx

Keywords: high T_c ; BCS-Bose crossover; hole Cooper pairs

The generalized Bose-Einstein condensation (GBEC) theory[1-4] of superconductivity hinges on three distinct new ingredients: a) treatment of Cooper pairs (CPs) as actual bosons, in contrast to BCS pairs which do not obey Bose commutation relations; b) inclusion of two-hole (2h) pairs on an equal footing with two-electron (2e) ones (thus making this a complete boson-fermion, or BF, model); and c) inclusion in the resulting ternary ideal BF gas of particular BF vertex interactions that drive boson formation and disintegration processes. Besides subsuming as special cases both BCS (having its well-known 50-50 symmetry between 2e and 2hCPs) and ordinary BEC theories (having no 2hCPs) as well as the now familiar BCS-Bose crossover theory[5-7], the GBEC theory leads to several-orders-of-magnitude enhancements in the critical superconducting temperature T_c upon slight departures from this perfect 50-50 symmetry.

A critical discussion is presented of *four* possible dimensionless coupling constants:

- i) the usual BCS lambda $\lambda \geq 0$ (pairs huge compared to interelectron spacings) and limited to $\frac{1}{2}$ according to divers arguments by the Bogoliubov school[8-9], but still seemingly perceived controversial
- ii) the inverse of the Fermi wavenumber k_F times the S-wave scattering length a characterizing the two-body interaction, which varies from $-\infty$ (weak coupling)[10] to $+\infty$ (strong coupling)
- iii) the well-known Pippard coherence length ξ_0 times the Fermi wavenumber k_F [11], which can vary from 0 (tiny pairs compared to interelectron spacings) to ∞ (huge pairs compared to interelectron spacings), and
- iv) a new dimensionless quantity[4], the ratio of total electron number density n to the $T = 0$ number density n_f of unpaired electrons [which varies from 1 (when GBEC becomes the BCS theory) to ∞ (strong coupling or tiny, well-separated pairs)] usable in various BF gas models describing binary or ternary mixtures.

Acknowledgment. We thank G.C. Strinati for bringing Refs.[5] to our attention.

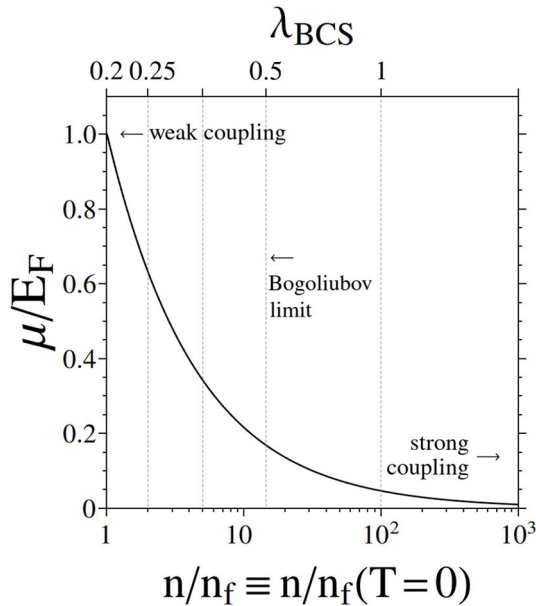
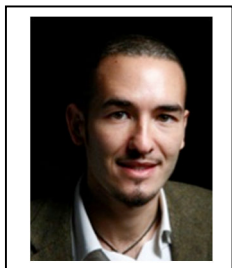


Figure 1: Dimensionless chemical potential μ/E_F vs dimensionless number density n/n_f of the BF gas for the GBEC theory [1-4]. Here $n/n_f = 1$ refers to a 50-50 mixture of 2e and 2hCPs, where n is the total number density of electrons in the system while $n_f \equiv n_f(T=0)$ is the number density of unpaired electrons at $T=0$. It illustrates the weak and strong limits where $\mu \rightarrow E_F$ and $\mu \rightarrow 0$, respectively. Also exhibited is an apparent correlation between n/n_f and the BCS dimensionless coupling constant λ . This correlation suggests that n/n_f can be considered another dimensionless coupling quantity that is *model-independent* as are also the quantities (ii) and (iii) mentioned before.

References

1. V.V. Tolmachev, Phys. Lett. A **266**, 400 (2000)
2. S.K. Adhikari, M. de Llano, F.J. Sevilla, M.A. Solís, and J.J. Valencia, Physica C **453**, 37 (2007)
3. M. de Llano and V.V. Tolmachev, Ukrainian J. Phys. **55**, 79 (2010) and refs therein.
4. M. Grether, M. de Llano, and V.V. Tolmachev, Int. J. Quant. Chem. **112**, 3018 (2012)
5. L.V. Keldysh and Yu. V. Kopaev, Sov. Phys. Sol. State **6**, 2219 (1965); V.N. Popov, Sov. Phys. JETP **50**, 1034 (1966)
6. J. Labbé, S. Barisic, and J. Friedel, Phys. Rev. Lett. **19**, 1039 (1967); D.M. Eagles, Phys. Rev. **186**, 456 (1969); A.J. Leggett, J. Phys. (Paris). Colloq. **41** C7-19 (1980)
7. R. Quick, C. Esebbag, and M. de Llano, Phys. Rev. B **47**, 11512 (1993)
8. N.N. Bogoliubov, N. Cim. **7**, 794 (1958)
9. V.V. Tolmachev and S.V. Tyablikov, Sov. Phys. JETP **34**, 46 (1958)
10. R. Haussmann, Phys. Rev. B **49**, 12975 (1994) esp. Fig. 1
11. M. Casas, J.M. Getino, M. de Llano, A. Puente, R.M. Carter, H. Rubio, and D.M. van der Walt, Phys. Rev. B **50**, 15945 (1994); R.M. Carter, M. Casas, J.M. Getino, M. de Llano, A. Puente, H. Rubio, and D. van der Walt, Phys. Rev. B **52**, 16149 (1995)

Cluster glass and superglass phases with cold atoms and 1.5 superconductors



Guido Pupillo¹
¹*University of Strasbourg*

Email: * pupillo@unistra.fr

Keywords: quantum glass, cold atoms, 1.5 superconductors

At low enough temperatures and high densities, the equilibrium configuration of an ensemble of ultrasoft particles is a self-assembled, ordered, cluster-crystal. In this talk, we present results for the non-equilibrium dynamics of two-dimensional realisations that are relevant to cold Rydberg atoms and superconducting materials with multi-scale intervortex forces. We demonstrate the existence of a superglass phase of Rydberg atoms where superfluidity coexists with structural disorder on a simple triangular optical lattice, and a novel mechanism for glass formation that can be realized with vortices in 1.5 superconductors in the absence of external disorder.

References

1. A. Angelone, F. Mezzacapo, and G. Pupillo, Phys. Rev. Lett. 116, 135303 (2016)
2. R. Diaz-Mendez, F. Mezzacapo, W. Lechner, F. Cinti, E. Babaev, and G. Pupillo, arXiv:1605.00553

Modification of spatial length-scales near the surface of a two-gap superconductor



Teet Örd^{*}, Artjom Vargunin, Küllike Rägo
*Institute of Physics, University of Tartu, Ravila 14c, 50411
 Tartu, Estonia*

Email: * teet.ord@ut.ee

Keywords: two-gap superconductivity, spatial inhomogeneity, length-scales, coherency, proximity effects

We study the spatial behaviour of superconducting ordering near the surface of a two-band system with intra-band attractions between electrons and inter-band pair-transfer interaction. It has been found that the restoration of two-gap superconductivity in the immediate vicinity of its interface is governed by two length-scales. The first one diverges at the critical temperature T_C , while the second one possesses a singularity at the temperature $T=T_{C+} < T_C$. At the same time the temperature T_{C+} associates with the appearance of metastable minima in the non-equilibrium free energy of a bulk two-band superconductor as well as with the autonomous phase transition temperature for the weaker intra-band superconductivity if inter-band coupling is absent. By moving away from the boundary, the coherency channels change substantially: in the bulk region the divergence at T_{C+} becomes removed by arbitrary weak inter-band coupling and the spatial scales under consideration transform into the critical and non-critical coherence lengths of two-gap superconductivity. Two divergent length-scales mentioned manifest themselves in proximity effects. As an example, we analyse the phase transition temperature of a normal-two-band-superconductor binary system and show that its critical temperature can be suppressed due to the coupling between superconducting components. The latter observation is opposite to the situation in a bulk superconductor, where inter-band pair-transfer interaction always enhances the critical temperature of the condensate.

The study was supported by the European Union through the European Regional Development Fund (Centre of Excellence "Mesosystems: Theory and Applications", TK114); the Estonian Science Foundation grant no. 8991; the Estonian Ministry of Education and Research through the Institutional Research Funding IUT2-27.

Anisotropic superconducting gaps in optimally doped $\text{Ba}_{1-x}\text{K}_x\text{Fe}_2\text{As}_2$ and $\text{BaFe}_{2-x}\text{Ni}_x\text{As}_2$ pnictides



T.E. Kuzmicheva^{1,2*}, S.A. Kuzmichev², V.M. Pudalov¹
¹*P.N. Lebedev Physical Institute RAS, 119991 Moscow, Russia*
²*M.V. Lomonosov Moscow State University, 119991 Moscow, Russia*

Email: kute@sci.lebedev.ru

Keywords: pnictides, multi-gap superconductivity, high T_c

We studied nearly optimal angle crystals $\text{Ba}_{0.65}\text{K}_{0.35}\text{Fe}_2\text{As}_2$ with $T_C \approx 34$ K [1] and $\text{BaFe}_{1.9}\text{Ni}_{0.1}\text{As}_2$ with $T_C \approx 19$ K by intrinsic multiple Andreev reflections effect (IMARE) spectroscopy (“break-junction” technique [2]). The current-voltage characteristics and the $dI(V)/dV$ spectra of SnS-Andreev contacts (S — superconductor, n — a ballistic layer of normal metal) showed a pronounced excess current at low bias, and two subharmonic gap structures (SGS) — series of dynamic conductance dips at positions $V_n = 2\Delta_{L,S}/en$ (n is a natural number) corresponding to the large and the small superconducting gaps [3,4]. The doublet-like shape of the SGS dips demonstrated the gap anisotropy in a k-space (extended s-wave symmetry) [5,6]. For nearly optimal potassium-doped $\text{Ba}_{0.65}\text{K}_{0.35}\text{Fe}_2\text{As}_2$ with $T_C \approx 34$ K we determined the large gap $\Delta_L = 5.5\text{--}8$ meV ($\sim 30\%$ anisotropy in k-space) and the small gap $\Delta_S = 1.7 \pm 0.3$ meV.

In nickel-doped single crystals $\text{BaFe}_{1.9}\text{Ni}_{0.1}\text{As}_2$ with $T_C \approx 19$ K, we observed two gaps with moderate anisotropy: $\Delta_L = 3.2\text{--}4.5$ meV ($\sim 30\%$ anisotropy in k-space, similarly to $\text{Ba}(\text{K})\text{Fe}_2\text{As}_2$), and $\Delta_S = 1.2\text{--}1.6$ meV ($\sim 25\%$ anisotropy).

The gap temperature dependences $\Delta_{L,S}(T)$ (Figure 1) agree well with two-band system of equations by Moskalenko and Suhl [7]. Both gaps turn to zero at common critical temperature. The two-band fit revealed a strong intraband coupling in a moderate interband one.

The data obtained by IMARE spectroscopy are in a good agreement with the data by measurements of the lower critical field [1], torque, heat capacity, infrared spectroscopy and studies of anisotropy of the second critical field [8].

We thank H.-H. Wen, M. Abdel-Hafiez, A.A. Kordyuk, Y. C. Chen for the providing samples and useful discussions.

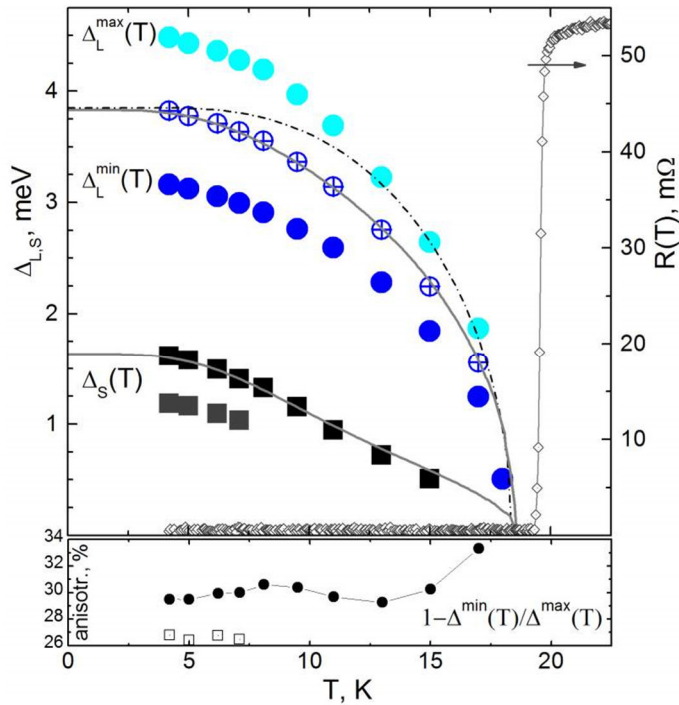


Figure 1: Temperature dependences of the anisotropic superconducting gaps in nearly optimal $\text{BaFe}_{1.9}\text{Ni}_{0.1}\text{As}_2$. Upper panel shows the dependence of the large gap extremes $\Delta_L^{\max}(T)$, $\Delta_L^{\min}(T)$ (solid circles) and the average value $\Delta_L^{\text{aver}}(T)$ (crossed circles), and the small gap extremes (solid squares). Dash-dot line show single-gap BCS-like curve solid lines — $\Delta_{L,s}(T)$ fit by two-band Moskalenko and Suhl system of equations, connected rhombs correspond to the resistive transition of the bulk single crystal. Lower panel shows temperature dependence of the large gap (circles) and the small gap (squares) anisotropy $1 - \Delta^{\min}(T)/\Delta^{\max}(T)$.

References

1. M. Abdel-Hafiez, et al., Phys. Rev. B 90, 054524 (2014).
2. J. Moreland and J. W. Ekin, J. Appl. Phys. 58, 3888 (1985).
3. M. Octavio, et al., Phys. Rev. B 27, 6739 (1983).
4. R. Kuemmel, et al., Phys. Rev. B 42, 3992 (1990).
5. T. P. Devereaux and P. Fulde, Phys. Rev. B 47, 14638 (1993).
6. A. Poenicke, et al., Phys. Rev. B 65, 220510(R) (2002).
7. V. A. Moskalenko, Fiz. Met. Metalloved. 8, 503 (1959); H. Suhl, et al., Phys. Rev. Lett. 3,552 (1959).
8. A.V. Muratov, et al., [in press].

Nanoscale Characterization of the Thermal Conductivity of Supported Graphite Nanoplates, Graphene and Few-layer Graphene by Scanning Thermal Microscopy



M. Tortello¹, S. Colonna², J. Gomez³, I. Pasternak⁴, W. Strupinski⁴, M. Pavese¹, F. Giorgis¹, G. Saracco¹, R.S. Gonnelli¹ and A. Fina²

¹*Dipartimento di Scienza Applicata e Tecnologia (DISAT), Politecnico di Torino, 10129 Torino, Italy,*

²*Dipartimento di Scienza Applicata e Tecnologia, Politecnico di Torino, 15121 Alessandria, Italy,*

³*AVANZARE Innovacion Tecnologica S.L., 26370 Navarrete (La Rioja), Spain*

⁴*Institute of Electronic Materials Technology, Wolczynska 133, 01-919 Warsaw, Poland*

Email: * mauro.tortello@polito.it

Keywords: Graphene, Scanning Thermal Microscopy, SThM, Thermal conductivity

The extraordinary properties of a single suspended layer of graphene change, sometimes dramatically, when the number of layers increases considerably or when it is supported or included as a filler in a polymer matrix. Thus, it is of utmost importance to know and control its properties in these conditions. In particular, it is highly desirable to investigate the thermal properties at the nanoscale because it is at this level that they are affected by the interfaces.

Here we show that [1] i) annealing in vacuum at 1700 °C for 1 h strongly reduces the amount of defects in graphite nanoplates (GNPs), as shown by Raman, XRD, XPS and TGA measurements. ii) As a consequence, their thermal conductivity considerably increases, as revealed by high resolution Scanning Thermal Microscopy (SThM) results on *individual* GNPs supported by SiO₂/Si. iii) This fact is more clearly observed when the GNPs are supported by a less conducting substrate (PET). iv) Lumped parameter models and finite element analysis are discussed in order to interpret the results and determine the thermal conductivity and the effect of the substrate. In particular, the models are tested in a case study of multilayer (1 to 4) CVD graphene [2], suspended or supported by different substrates like SiO₂/Si, PET, Al₂O₃, etc.

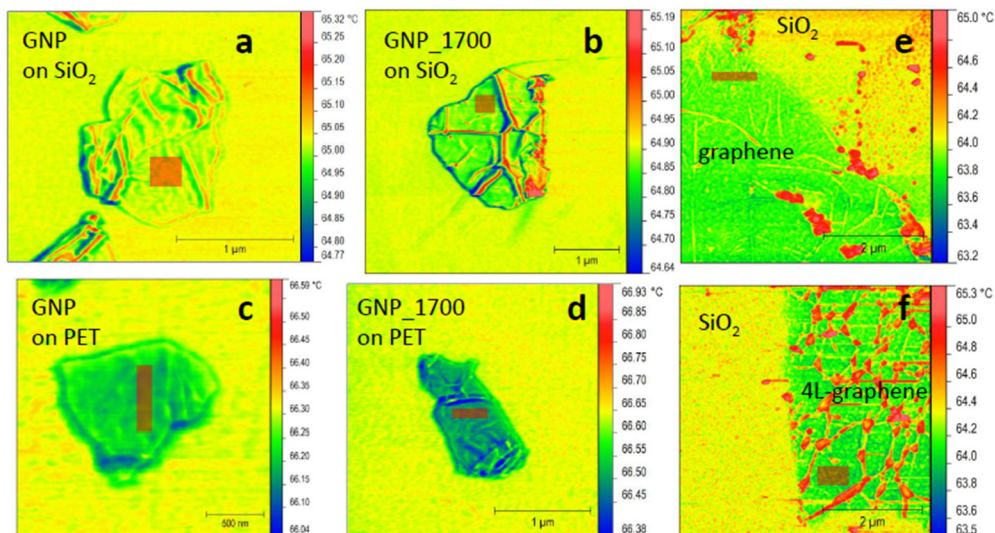


Figure 1: SThM maps of GNP (a) and GNP_1700 (b) supported by Si/SiO₂ and GNP (c) and GNP_1700 (d) supported by PET. (e) CVD graphene on SiO₂. (f) 4-layer CVD graphene on SiO₂. As the measurable parameter is the heater temperature, the more conducting nanoplates induce a larger temperature decrease (with respect to the substrate), than the less conducting ones. Red masked areas are used for calculating the average temperature on the samples.

References

1. M. Tortello, S. Colonna, J. Gomez, M. Pavese, F. Giorgis, G. Saracco, R.S. Gonnelli, A. Fina, submitted.
2. I. Pasternak, A. Krajewska, K. Grodecki, I. Jozwik-Biala, K. Sobczak, and W. Strupinski, AIP Advances **4**, 097133 (2014).

Electric-field delocalization in multiband superconductors



Artjom Vargunin^{1,2}, Mihail Silaev², and Egor Babaev²

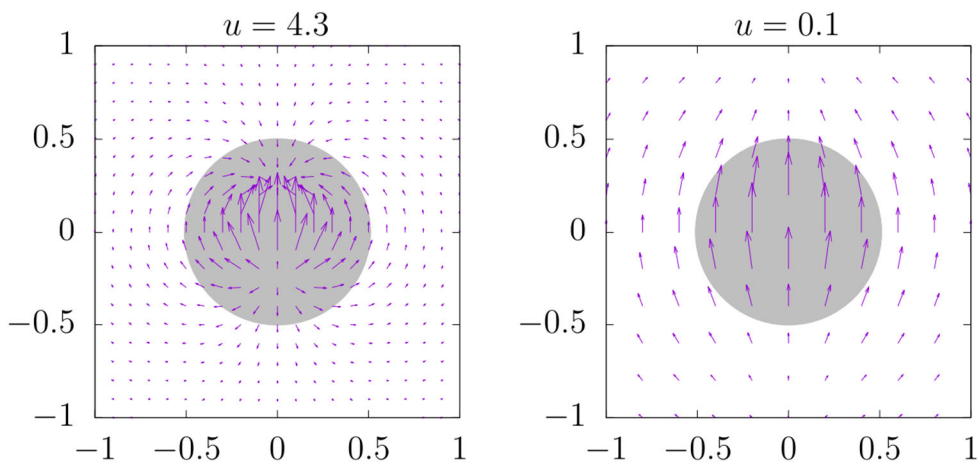
¹ *University of Tartu, Tartu, EE-50411, Estonia*

² *KTH Royal Institute of Technology, Stockholm, SE-10691, Sweden*

Email: *artjom.vargunin@gmail.com*

Keywords: multiband superconductivity, electric field, flux-flow resistivity

We show that extremely diverse flux-flow resistivity data for multiband superconductors can be explained by electric-field delocalized around moving composite vortices. Such a delocalization is due to multiband contribution to normal electrons trapped within vortex core. For a two-band case, qualitative description is proposed within effective single-component time-dependent Ginzburg-Landau approach with bands-specific parameter u . The latter measures correlation length in units of electric-field penetration depth.



Electric-field distribution around moving vortex (shaded area) in conventional (left) and multiband (right) superconductor.

New Perspective on the Cuprate Phase Diagram and the charge distribution in the copper-oxygen plane



Jürgen Haase^{1*}
¹University of Leipzig

Email: *j.haase@physik.uni-leipzig.de

Keywords: high T_c, cuprates, phase diagram, charge density

It will be shown that the charge content of the bonding Cu (n_d) and O (n_p) orbitals can be measured quantitatively with nuclear magnetic resonance (NMR) for all cuprates, doped (x), as well as parent materials ($x=0$). As a result the expected, simple stoichiometric expression, $1 + x = n_d + 2n_p$, emerges for the CuO_2 plane [1]. However, it is found that the parent materials share the nominal hole ($1 = n_d + 2n_p$) rather differently, i.e., the actual hole contents at Cu and O vary widely. While the optimal T_c occurs, as expected, near $x = 0.15$ for all cuprates, the maximum, possible T_c is set by the distribution of the nominal Cu hole: the higher the parent's oxygen hole content the higher the T_c. It is also shown that this dependence agrees with the famous Uemura scaling for the superconducting samples for which the superfluid density is related to a material chemistry parameter, the O (and Cu) hole content [2]. It appears that the maximum T_c could be raised substantially if the inter-layer chemistry leads to the transfer of more hole content from Cu to O for the parent system. Since it is not the total doped charge (x) that is of importance for the complex cuprate physics, one may want to resort to a 3D phase diagram that relates T_c to n_d and $2n_p$, cf. Fig. 1.

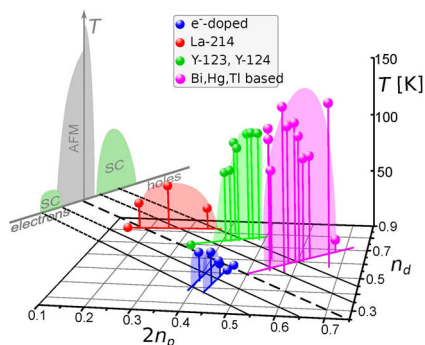


Figure 1: Cuprate phase diagram with temperature vs. Cu (n_d) and O (n_p) hole content (note, doping $x = n_d + 2n_p - 1$)

Based on the new findings, a number of interesting observations can be made. For example: (1) the parent's magnetism survives rather different Cu and O hole contents, up to at least $2n_p \sim 0.5$ ($1 = n_d + 2n_p$); (2) doping (x) appears necessary to destroy the magnetism, but it does not set the maximum T_c ; (3) given that the charge inhomogeneity in the CuO_2 plane is very different for different cuprates from NMR, either it is not important for T_c or a ubiquitous phenomenon that must be averaged on the NMR time scale. Further examples will be discussed.

References

1. M. Jurkutat et al., Phys. Rev. B **90**, 140504 (R) (2014).
2. D. Rybicki et al. Nature Comm. (under review).

Multiband superconductors with strong Pauli paramagnetic effect



K. Machida^{1*}, Y. Tsutsumi²

¹*Department of Physics, Ritsumeikan University, Kusatsu 525-8577, Japan*

²*Department of Basic Science, The University of Tokyo, Tokyo 153-8902, Japan*

Email: * *machidakazu@gmail.com*

Keywords: heavy Fermion superconductors, CeCu₂Si₂, UBe₁₃, UPt₃, Sr₂RuO₄

We theoretically study the interplay between the multiband effect and Pauli paramagnetic effect, focusing on strongly correlated superconductors; CeCu₂Si₂, UBe₁₃, UPt₃, and Sr₂RuO₄.

CeCu₂Si₂ is the first heavy Fermion superconductor discovered in 1979 and has been regarded as having the pairing with a d-wave symmetry because the strong onsite interaction may prohibit the s-wave pairing. However, recent angle resolved specific heat experiment [1] shows that the low-lying excitations under applied fields do not accord with the expected behaviors for nodal d-wave gap structure, pointing to a nodeless full gap.

Similarly, UBe₁₃ also exhibits the lack of low-lying nodal quasi-particles, consistent with a nodeless gap structure according to the low temperature specific heat experiment on high quality samples [2]. Those studies lead us to reconsider a conventional wisdom that the strong correlation implies unconventional pairing. We must carefully examine the pairing mechanism for stabilizing a full gap structure in those strongly correlated materials.

UPt₃ exhibits the Pauli paramagnetic effect for H//c because H_{c2} for this direction is suppressed compared with H//ab. This can be understood in terms of the d-vector locked to the c-axis in this triplet f-wave superconductor [3]. The angle-resolved thermal conductivity measurement detects a two-fold oscillation in high field and low temperature so-called C phase, which is associated with the order parameter symmetry of the E_{1u} f-wave.

In this context Sr₂RuO₄, which is regarded as a prime candidate for chiral p-wave pairing, is interesting to reexamine along this line [4, 5, 6, 7] because there exist several outstanding experiments which are apparently inconsistent with this identification, namely strong H_{c2} suppression and the first order phase transition [8, 9] at H_{c2}, some of those features are also common for CeCu₂Si₂ and UBe₁₃.

Here we will try to understand those prominent unexplained experimental facts by studying the low-lying quasi-particle structures in the vortex state under a field from the standpoint of the interplay between multiband effect and Pauli paramagnetic effect [10]. It turns out that this viewpoint is quite fruitful for describing those materials in a unified way.

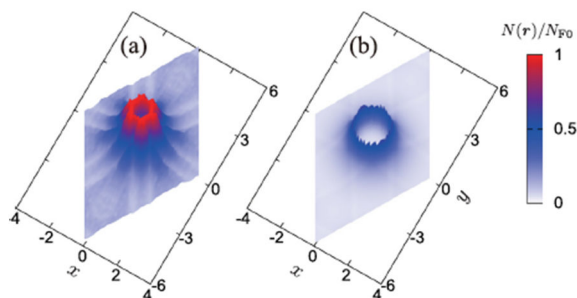
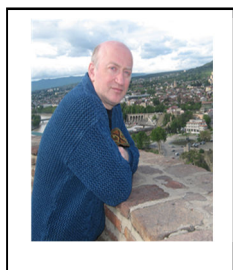


Figure 1: Local zero energy landscapes around a vortex core for two band model: major band with larger energy gap (a) and minor band with smaller gap (b), showing the empty vortex cores due to Pauli paramagnetic effect [10].

References

1. Kittaka, et al., Phys. Rev. Lett. 112, 067002 (2014).
2. Y. Shimizu, et al., Phys. Rev. Lett. 114, 147002 (2015).
3. Y. Machida, et al., Phys. Rev. Lett. 108, 157002 (2012).
4. Y. Amano, et al, Phys. Rev. B91, 144513 (2015).
5. Y. Amano, et al, Phys. Rev. B90, 144514 (2014).
6. M. Ishihara, et al, Phys. Rev. B87, 224509 (2013).
7. N. Nakai and K. Machida, Phys. Rev. B92, 054505 (2015).
8. S. Yonezawa, et al., Phys. Rev. Lett. 110, 077003 (2013).
9. S. Kittaka, et al., Phys. Rev. B90, 220402(R) (2014).
10. Y. Tsutsumi, et al., Phys. Rev. B92, 020502(R) (2015).

Suppression of stripe order by nonmagnetic impurities in cuprates



A. Shengelaya^{1,2*}, Z. Guguchia³, R. Khasanov³,
E. Pomjakushina³, K. Conder³, H. Keller⁴

¹*Department of Physics, Tbilisi State University,
GE-0128, Tbilisi, Georgia*

²*Tbilisi State University Andronikashvili Institute of Physics, 6
Tamarashvili Street, 0177 Tbilisi, Georgia*

³*Paul Scherrer Institute, CH-5232, Villigen PSI, Switzerland*

⁴*Physik-Institut der Universität Zürich, CH-8057, Zürich,
Switzerland*

Email: * alexander.shengelaya@tsu.ge

Keywords : superconductivity, stripes, impurity effects

Since the discovery of high temperature superconductivity (HTS) in cuprates much effort was invested in the investigation of the effect of the impurity substitution at the Cu site. It is now well established that in HTSs nonmagnetic Zn ions suppress T_c even stronger than magnetic ions. This behavior, which is in sharp contrast to that of conventional superconductors, led to the formulation of an unconventional pairing mechanism and a symmetry of the order parameter for cuprate HTSs. However, up to now surprisingly little is known concerning impurity effects on static stripe phase in cuprates.

We performed muon spin rotation (μ SR) and neutron scattering experiments in Zn-doped $\text{La}_{2-x}\text{Ba}_x\text{CuO}_4$ and $\text{La}_{1.48}\text{Nd}_{0.4}\text{Sr}_{0.12}\text{CuO}_4$ ($x=1/8$) samples to systematically study the effect of nonmagnetic impurities on static stripe order. The influence of Zn impurities on important parameters of the static spin-stripe phase: ordering temperature, wavevector and correlation length was investigated. It was found that the static spin-stripe ordering temperature T_{so} strongly decreases linearly with Zn doping. Intriguingly, the suppression of T_{so} is found to be similar to that of superconducting transition temperature T_c suppression by Zn impurities in $\text{La}_{2-x}\text{Sr}_x\text{CuO}_4$. Observed strong effect of in-plane nonmagnetic impurities on stripe order might provide important clue for better understanding of stripes formation and their relation with superconductivity in cuprates. More generally, since stripe order is also observed in other transition metal oxides, investigation of impurity effects and disorder on stripe formation can become an interesting research direction in correlated electron compounds.

Recent identifications of microscopic solitons in quasi 1d electronic systems and generalisations to higher dimensions.



Serguei Brazovskii^{1,2*}

¹*CNRS, University Paris-Sud, Orsay, France*

²*NUST MISiS, Moscow, Russia*

We update the STRIPES-2007 review [1] “Solitons and Their Arrays: From Quasi 1D Conductors to Stripes”, elucidating the role of microscopic solitons in quasi-1D electronic systems with a symmetry breaking. Solitons show up in conductivity, nano-scale tunnelling spectroscopy, optical absorption, they are seen directly at atomic scales and even manipulated by the STM. Instantons - the processes of dynamic conversion of normal electrons into solitons - are responsible for subgap transitions leading to a pseudogap formation. The solitons' aggregates – domain walls or vortices - show up in a time evolution under intense optical or current [2] and STM pulses [3]. The aggregation of solitons into walls (the stripes) can serve as a model for the confinement transition. The best playground for solitons is provided by the “electronic ferroelectricity” in organic Mott, Peierls and spin-Peierls insulators, and by Charge Density Wave materials. At more macroscopic scales, we recover the electronic vortices generated in mesa-junctions, and domain walls evolving in femtosecond pump-probe experiments.

On this basis we extrapolate to a picture of combined topological excitations in general strongly correlated systems: from doped antiferromagnets to spin-polarized superconductors.

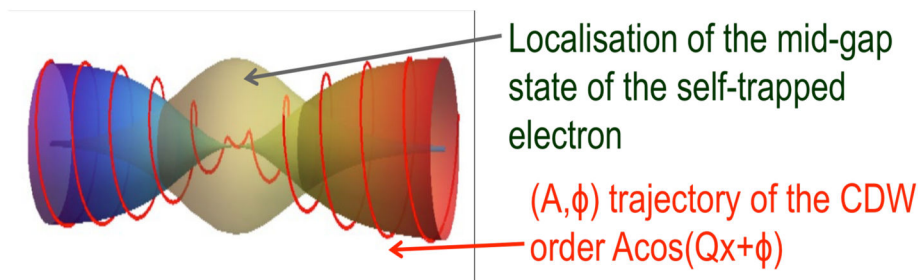
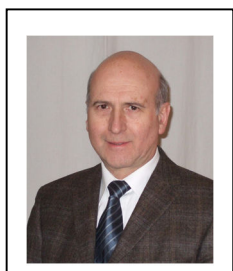


Figure 1: Schematic picture of the soliton – an incarnation of the spinon – as it was derived from exact solutions and observed by the STM upon the CDW state in NbSe₃ [4]. In a superconductor, it can be viewed as a nucleus of the FFLO stripe.

References

1. S. Brazovskii, *J. of Superconductivity and Novel Magnetism*, 20, 489 (2007)
2. D. Mihailovic et al., at this meeting and *Nature Communications*, to be publ.
3. D. Cho, et al., *Nature Communications*, 7, 10453 (2016)
4. S. Brazovskii, Ch. Brun, Zhao-Zhong Wang, and P. Monceau, *Phys. Rev. Lett.*, 108, 096801 (2012).

Fluctuations and Superconductivity in Fe-based Systems



Rudi Hackl,^{1,*} Thomas Böhm,^{1,2,3} F. Kretzschmar,^{1,2} B. Muschler,¹ U. Karahasanovic,⁴ J. Schmalian,⁴ S. Caprara,⁵ C. Di Castro,⁵ M. Grilli,⁵ B. Moritz,³ T. P. Devereaux,^{3,6} D. J. Scalapino,⁷ J.-H. Chu,^{3,6} I. R. Fisher,^{3,6} Hai-Hu Wen,⁸ P. Adelman⁹, T. Wolf⁹

¹Walther Meissner Institut, 85748 Garching, Germany

²Physik Department E23, Technische Universität München, 85748 Garching, Germany

³SIMES, SLAC National Accelerator Laboratory, Menlo Park,

CA 94025, USA

⁴TKM, KIT, 76128 Karlsruhe, Germany

⁵Department of Physics, University of Rome "Sapienza", 00185 Roma, Italy

⁶GLAM and Dept. Appl. Phys, Stanford Univ., CA 94305, USA

⁷Physics Department, University of California, Santa Barbara, CA 93106, USA

⁸National Laboratory of Solid State Microstructures and Department of Physics, Nanjing University, Nanjing 210093, China

⁹IFP, KIT, 76021 Karlsruhe, Germany

Email: * hackl@wmi.badw.de

Keywords: high T_c , nano-clusters, shell structure

Spin, charge or orbital fluctuations and order play an important role in material classes such as the cuprates, the iron-based compounds or the ruthenates and may be interrelated with superconductivity. In iron-based compounds signatures of nematicity have been observed in a variety of experiments. However, the fundamental question as to the relevance of the related spin, charge or orbital fluctuations remains open. To tackle this problem we study $\text{Ba}(\text{Fe}_{1-x}\text{Co}_x)_2\text{As}_2$ ($0 \leq x \leq 0.85$) and $\text{Ba}_{1-x}\text{K}_x\text{Fe}_2\text{As}_2$ ($x = 0.25$ and 0.4) by inelastic light (Raman) scattering for directly accessing nematicity and the underlying critical fluctuations with finite characteristic wavelengths. We show that the response from fluctuations appears only in $B_{1g}(x^2-y^2)$ symmetry and below a slightly doping dependent temperature T_f as shown in Fig. 1 for $\text{Ba}(\text{Fe}_{1-x}\text{Co}_x)_2\text{As}_2$. The colored field shows that the scattering amplitude increases towards the structural transition at T_s . A detailed analysis demonstrated the response from fluctuations vanishes only below the magnetic ordering transition at $T_{\text{SDW}} < T_s$, suggesting a magnetic origin of the fluctuations [1]. The theoretical analysis explains the selection rules and the temperature dependence of the fluctuation response. These results make magnetism the favorite candidate for driving the series of transitions. We analyze the superconducting spectra of $\text{Ba}_{0.6}\text{K}_{0.4}\text{Fe}_2\text{As}_2$ quantitatively and find indications for the relevance of spin fluctuations for Cooper pairing [3].

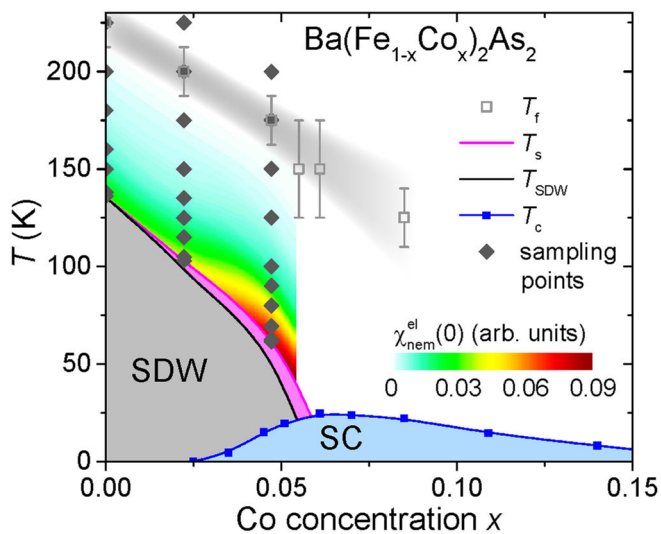


Figure 1: Phase diagram of $\text{Ba}(\text{Fe}_{1-x}\text{Co}_x)_2\text{As}_2$. The full lines limit the nematic phase (magenta) and the blue squares represent the transition temperature T_c of superconducting samples [2]. Grey diamonds represent doping and temperature positions of the Raman data. The colored field between T_s and T_f represents the initial slope of the spectra according to the included color scale.

References

1. F. Kretzschmar *et al.*, [Nature Phys. 10.1038/nphys3634 \(2016\)](#).
2. J.-H. Chu *et al.*, [Phys. Rev. B 79, 014506 \(2009\)](#).
3. T. Böhm *et al.*, [Phys. Rev. X 4, 041046 \(2014\)](#).

Competition between enhanced Cooper pairing and suppressed phase coherence in coupled aluminum nanograins



N. Bachar^{1,2,†}, U. S. Pracht³, L. Benfatto⁴, G. Deutscher², E. Farber¹, M. Dressel³, M. Scheffler³

¹ *Laboratory for Superconductivity and Optical Spectroscopy, Ariel University, Israel*

² *Raymond and Beverly Sackler School of Physics and Astronomy, Tel Aviv University, Israel*

³ *I. Physikalisches Institut, Universität Stuttgart, Germany*

⁴ *ISC-CNR and Department of Physics, Sapienza University of Rome, Italy*

[†] *Currently at Department of Quantum Matter Physics, University of Geneva, Switzerland*

Email: * nimrod.bachar@unige.ch

Keywords: Granular superconductors, shell effects, optical conductivity

Deterministic enhancement of the superconducting (SC) critical temperature T_c is a long-standing goal in solid-state physics. In a large variety of SC systems, the initial enhancement via tuning of a control parameter is followed by a suppression of T_c , shaping a superconducting dome in the phase diagram. This dome was postulated to be shaped by a competition between two energy scales: the superconducting energy gap Δ and the superfluid phase stiffness J [1]. One of the first evidence for such dome-like phase diagram was shown for granular Al, i.e. thin films composed of nano-scaled grains separated by thin insulating barriers, where grain-coupling acts as control parameter [2].

In this work, we used DC transport measurements and optical THz spectroscopy in order to study the development of T_c and the energy scales Δ and J as a function of the grain coupling and explain the phase diagram of granular Al [3]. Starting from well-coupled grains, Δ grows as the grains are progressively decoupled, causing the unconventional increase of T_c with sample resistivity. When the grain-coupling is suppressed further, Δ saturates while the critical temperature T_c decreases, concomitantly with a sharp decline of J , delimiting a SC dome in the phase diagram. The crossover to a phase driven SC transition is accompanied by a pseudogap observed in the normal state above T_c . Overall, we demonstrate that granular Al is an ideal testbed to understand the interplay between quantum confinement and global superconducting phase coherence due to nano-inhomogeneity.

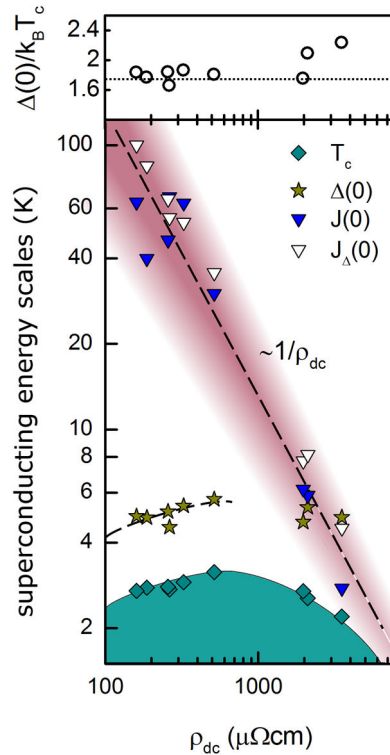


Figure 1: Superconducting energy scales as a function of the normal state resistivity of granular Al films [3]. T_c encloses a superconducting dome shaped by the energy gap Δ increase in the strong coupling (low resistivity) regime and the superfluid stiffness J decrease in the weak coupling (high resistivity) regime.

References

1. V. J. Emery and S. A. Kivelson, *Nature* **374**, 434 (1994).
2. B. Abeles, R. W. Cohen, and G. W. Cullen, *Phys. Rev. Lett.* **17**, 632 (1966); G. Deutscher, M. Gershenson, E. Grunbaum, and I. Y., *J. Vac. Sc. and Tech.* **10**, 6975 (1973).
3. U. S. Pracht, N. Bachar, L. Benfatto, G. Deutscher, E. Farber, M. Dressel, M. Scheffler, *arXiv:1508.04270*. (Submitted and under review).

Pair Correlations in Superconducting-Magnetic Hybrid Systems



Andreas Bill^{1*}

¹*Dept. of Physics & Astronomy, California State University
Long Beach, CA, USA*

Email: * abill@csulb.edu

Keywords: Proximity effect, Josephson effect, pair correlations, magnetic domain wall, hybrid systems, heterostructures.

Spin correlations of superconducting pairs leaking into a magnetic material are affected by magnetic inhomogeneities. Using the tunable domain wall of an exchange spring we investigate pair correlation mixing and current reversal ($0-\pi$ transitions) in wide Josephson junctions. The configurations span from a homogeneous ferromagnet to a full Bloch domain wall. Helical structures and multilayers of misaligned homogeneous ferromagnets are also considered. Analyzing the Gor'kov functions we show that these heterostructures display qualitatively different mixtures of pair correlations due to the cascade effect [1]. We find that so-called short-range singlet correlations are present deep in the magnetic material [2]. Further, the Josephson current can be tuned with the twisting of the domain wall, and the $0-\pi$ transition in the exchange spring is shown to result from the competition of singlet and triplet correlations. As a result, we divide hybrid systems into two classes that involve discrete and continuous domain walls, respectively [3,4]. We also propose a classification of $0-\pi$ transitions into three types, according to the symmetry of pair correlations responsible for the current reversal [4]. Support from the National Science Foundation (DMR-1309341) is greatly appreciated.

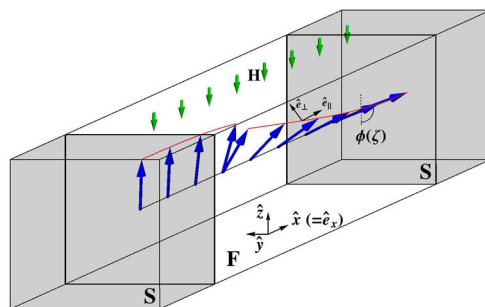


Figure 1: Magnetic Josephson junction with a partial domain wall. Continuous and discrete twists of the magnetization affect differently the spin correlations of superconducting pairs leaking into the magnetic material.

References

1. T.E. Baker, A. Richie-Halford, O.E. Icreverzi, and A. Bill, *Europhys. Lett.* **107**, 17001 (2014).
2. T.E. Baker, A. Richie-Halford, and A. Bill, *New J. Phys.* **16**, 093048 (2014). See also the video abstract!
3. T.E. Baker and A. Bill, *AIP Advances* (*in press*, 2016).
4. T.E. Baker, A. Richie-Halford, and A. Bill, *submitted*.

Complex Phase Diagram of $\text{Ba}_{1-x}\text{Na}_x\text{Fe}_2\text{As}_2$: A Multitude of Phases Striving for the Electronic Entropy



Frédéric Hardy^{1*}, Liran Wang¹, Thomas Wolf¹, Peter Schweiss¹, and Christoph Meingast¹

¹*Institute for Solid-State Physics, Karlsruhe Institute of Technology, Karlsruhe, Germany*

Email: * frederic.hardy@kit.edu

Keywords: $\text{Ba}_{1-x}\text{Na}_x\text{Fe}_2\text{As}_2$, iron pnictides, phase diagram, SDW, C_4 phase

We have re-examined in greater detail the underdoped region of $\text{Ba}_{1-x}\text{Na}_x\text{Fe}_2\text{As}_2$ using thermodynamic measurements (heat capacity and thermal expansion). Besides the magnetic C_2 phase, we found a small region of C_4 symmetry inside the SDW state similar to that of $\text{Ba}_{1-x}\text{K}_x\text{Fe}_2\text{As}_2$ [1,2]. However, no subsequent re-entrance to the C_2 phase was observed at lower temperature in $\text{Ba}_{1-x}\text{Na}_x\text{Fe}_2\text{As}_2$ and its phase diagram is shown to be considerably more complex than previously reported [3], containing 9 different phases [1]. Differences and similarities between the $\text{Ba}_{1-x}\text{Na}_x\text{Fe}_2\text{As}_2$ and $\text{Ba}_{1-x}\text{K}_x\text{Fe}_2\text{As}_2$ systems will be discussed and we will show how these new phases interact with superconductivity.

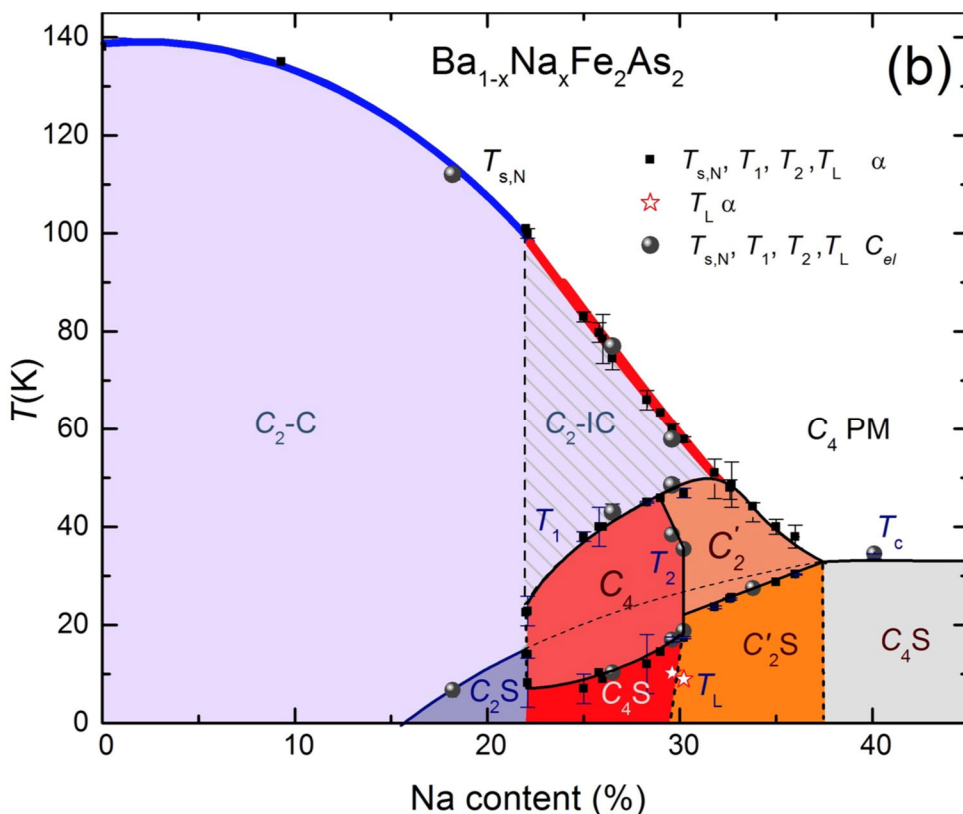


Figure 1: Phase diagram of $\text{Ba}_{1-x}\text{Na}_x\text{Fe}_2\text{As}_2$.

References

1. L. Wang, F. Hardy, A. E. Böhmer, T. Wolf, P. Schweiss, and C. Meingast, Phys. Rev. B 93, 014514 (2016).
2. A. E. Böhmer, F. Hardy, L. Wang, T. Wolf, P. Schweiss, and C. Meingast. Nature Communications 6, 7911 (2015)
3. S. Avci, O. Chmaissem, J. M. Allred, S. Rosenkranz, I. Eremin, A. V. Chubukov, D. E. Bugaris, D. Y. Chung, M. G. Kanatzidis, J. -P. Castellan, J. A. Schlueter, H. Claus, D. D. Khalyavin, P. Manuel, A. Daoud-Aladine, and R. Osborn, Nature Communications 5, 3845 (2014).

Higgs Spectroscopy of Superconductors in non-equilibrium



Dirk Manske^{1*}

¹*Max Planck Institute for Solid State Research*

Email: * d.manske@fkf.mpg.de

Keywords: Higgs oscillations, Leggett mode, Non-equilibrium

Time-resolved pump-probe experiments recently attracted great interest, since they allow to detecting hidden states and they provide new information on the underlying dynamics in solids in real time. With the observation of a Higgs mode in superconductors [6] it is now possible to investigate the superconducting order parameter directly. Recently, we have established a theory for superconductors in non-equilibrium, for example in a pump-probe experiment [1,2]. Using the Density-Matrix-Theory (DMT) we have developed an approach to calculate the response of conventional and unconventional superconductors in a time-resolved experiment. In particular, DMT method is not restricted to small timescales; in particular it provides a microscopic description of the quench, and also allows also the incorporation of phonons [2]. Furthermore, we employ DMT to time-resolved Raman scattering experiments [3] and make predictions for 2-band superconductors [4]. Very recently, we have focused on the theory for order parameter amplitude ('Higgs') oscillations which are the realization of the Higgs mode in superconductors [5,2]. New predictions are made for the Leggett mode in 2-band superconductors [8]. Finally, we address the question of induced superconductivity in non-equilibrium [9]. Our prediction has been recently confirmed experimentally [6,7].

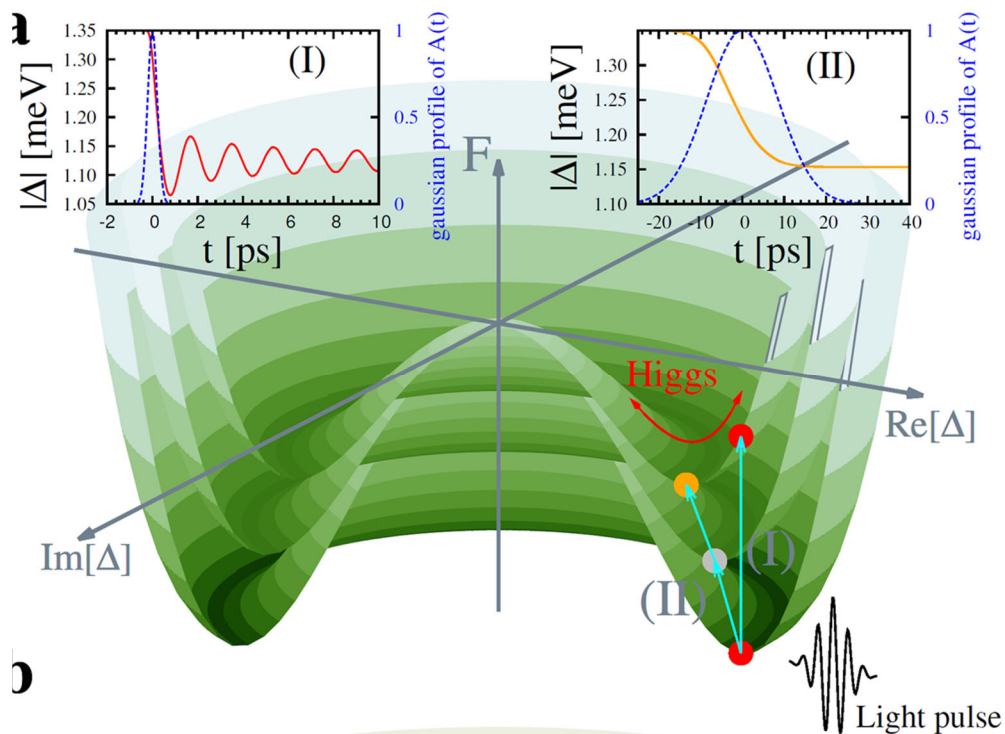


Figure 1: Mexican hat potential of the Free Energy in non-equilibrium as a function of time. Only in case (I), using a short pulse, Higgs oscillations can be generated.

References

1. J. Unterhinninghofen, D. Manske, and A. Knorr, Phys. Rev. B **77**, 180509(R) (2008).
2. A. Schnyder, D. Manske, and A. Avella, Phys. Rev. B **84**, 214513 (2011).
3. R.P. Saichu et al., Phys. Rev. Lett. **102**, 177004 (2009).
4. A. Akbari, A. Schnyder, I. Eremin, and D. Manske, Europhys. Lett. **101**, 17002 (2013).
5. H. Krull, D. Manske, A. Schnyder, G. Uhrig, Phys. Rev. B **90**, 014514 (2014).
6. R. Matsunaga *et al.*, PRL **111**, 057002 (2013).
7. A. Rusydi, D. Manske et al., submitted to PRL.
8. H. Krull *et al.*, arXiv:1512.08121, submitted to Nature Comm.
9. N. Bittner, T. Tohyama, and D. Manske, preprint

Fundamental building blocks of strongly correlated wave functions

Denis K. Sunko^{2*}



*Department of Physics, Faculty of Science, University of Zagreb,
HR-10000 Zagreb, Croatia*

Email: * *dks@phy.hr*

Keywords: strong correlations, nodal surfaces, fermion sign problem

The calculation of realistic N-body wave functions for identical fermions is still an open problem in physics, chemistry, and materials science, even for N as small as two. Here a recently discovered fundamental algebraic structure of many-body Hilbert space is described, which allows an arbitrary many-fermion wave function to be written in terms of a finite number of antisymmetric functions called shapes. Shapes naturally generalize the single-Slater-determinant form for the ground state to more than one dimension. Their number is exactly $N!^{d-1}$ in d dimensions. A general algorithm is given to list them all in terms of standard Slater determinants. Historically, shapes are the first fundamental antisymmetric invariants of many-fermion Hilbert space found since Heisenberg and Dirac introduced Slater determinants. Mathematically, Hilbert space can be naturally interpreted as a graded algebra over the ring of symmetric polynomials, and shapes are the generators of this (finite-dimensional!) algebra. Technically, these symmetric polynomials can be understood as a generalization of the c-numbers multiplying basis vectors in the standard formulation. Physically, the same symmetric polynomials can be understood as bosonic excitations of the shapes. These excitations are called Euler bosons. In brief, shapes are all the possible vacua for the Euler bosons. The algebraic structure of Hilbert space described here provides qualitative insights into long-standing issues of many-body physics, including the fermion sign problem and the microscopic origin of bands in the spectra of finite systems.

Covalent bonds against magnetism in transition metal compounds



Sergey Streltsov^{1*}, Daniel Khomskii²

¹*Institute of Metal Physics, Russia*

²*University of Cologne, Germany*

Email: * streltsov@imp.uran.ru

Keywords: orbital order, double exchange

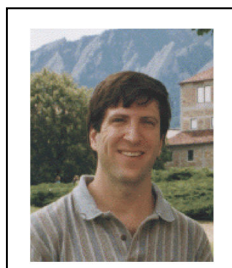
The 4d and 5d transition metal compounds attracts nowadays considerable attention due to their specific properties, such as large covalency, strong spin-orbit coupling, the possibility to observe topological effects, etc. Magnetic ordering in these systems often displays strong suppression of magnetic moments, becoming (much) less than the nominal ones. One usually explains this by single-site effects: possible role of spin-orbit interaction, with orbital contribution opposite to the spin one, or by strong hybridization with ligands, e.g. oxygens. We show that there exist in such system an intersite mechanism which, in particular, can lead to suppression or at least strong reduction of magnetism: the orbital-selective formation of covalent bonds (molecular orbitals) between metal ions, leading to "exclusion" of corresponding electrons from magnetic subsystem [1,2]. Especially spectacular are these effects in the situation with noninteger electron occupation, in which case this mechanism leads to suppression of the famous double exchange – the main mechanism of ferromagnetism in transition metals and compounds, including well-known colossal magnetoresistance manganites [3]. We demonstrate this novel mechanism by analytical and numerical model calculations, and show by ab-initio calculation that it explains magnetic behavior of several materials, including $\text{Nb}_2\text{O}_2\text{F}_3$ and $\text{Ba}_5\text{AlIr}_2\text{O}_{11}$ [4]. Interplay of covalent bond formation and spin-orbit coupling is also discussed. Our results thus demonstrate that the strong intersite interaction, typical for 4d and 5d compounds, may invalidate the standard single-site starting point for considering magnetism, and can lead to qualitatively different behavior. More specifically, they also show yet one more unexpected effect in the rich field of orbital physics.

We acknowledge financial support by RFBR grants 16-02-00451, 16-32-60070, and CRDF program FSCX-14-61025-0.

References

1. S.V. Streltsov and D.I. Khomskii *Phys. Rev. B* **89**, 161112(R) (2014)
2. S.V. Streltsov *Journal of Magnetism and Magnetic Materials* **383**, 27 (2015)
3. S.V. Streltsov and D.I. Khomskii arXiv:1602.06425
4. J. Terzic, J. C. Wang, Feng Ye, W. H. Song, S. J. Yuan, S. Aswartham, L. E. DeLong, S.V. Streltsov, D.I. Khomskii, G. Cao *Phys. Rev. B* **91**, 235147 (2015)

Electron Self-energies in Cuprate Superconductors: Their Role in Setting T_c and Other Properties.



Dan Dessau

Department of Physics, University of Colorado, Boulder

Email: *Dessau@Colorado.edu*

Keywords: high T_c , ARPES, Self-energies

We utilize high resolution ARPES and laser-ARPES to directly measure the electronic structure of the cuprate superconductors, paying special attention to the electron self-energies, extracted using new methods with enhanced accuracy and reliability. These self-energies are critical and dramatic, and by taking account of them we are able to make direct connections to optics, transport, and thermodynamics experiments. Understanding the origin of these self energies can thus unify and explain a great portion of cuprate phenomenology.

References

1. T. J. Reber, N. C. Plumb, Z. Sun, Y. Cao, Q. Wang, K. McElroy, H. Iwasawa, M. Arita, J. S. Wen, Z. J. Xu, G. Gu, Y. Yoshida, H. Eisaki, Y. Aiura, and D. S. Dessau “The Non-Quasiparticle Nature of Fermi Arcs in Cuprate High- T_c Superconductors” *Nature Physics* **8**, 606–610 (2012)
2. T. J. Reber, N. C. Plumb, Y. Cao, Z. Sun, Q. Wang, K.E. McElroy, H. Iwasawa, M. Arita, J.S. Wen, Z.J. Xu, G. Gu, Y. Yoshida, H. Eisaki, Y. Aiura, and D. S. Dessau “Prepairing and the “filling” gap in the cuprates from the tomographic density of states” *Phys. Rev. B* **87**, 060506 (2013).
3. T. J. Reber, S. Parham, N. C. Plumb, Y. Cao, H. Li, Z. Sun, Q. Wang, H. Iwasawa, M. Arita, J. S. Wen, Z. J. Xu, G.D. Gu, Y. Yoshida, H. Eisaki, G.B. Arnold, D. S. Dessau “Pairing, pair-breaking self energies, and their roles in setting the T_c of cuprate high temperature superconductors” arXiv:1508.06252
4. T.J. Reber, J.A. Waugh, N.C. Plumb, S. Parham, Y. Cao, Z. Sun, Q. Wang, J.S. Wen, Z.J. Xu, G. Gu, Y. Yoshida, H. Eisaki, Y. Aiura, G.B. Arnold, D. S. Dessau. “Power Law Liquid – A Unified Form of Low-Energy Nodal Electronic Interactions in Hole Doped Cuprate Superconductors” arXiv:1509.01611

Scanning Tunneling Microscopy and Spectroscopy of FeSe single crystals

S. A. Moore,¹ J. L. Curtis,² C. Di Giorgio,¹ E. Lechner,¹ M. Abdel-Hafiez,³
O.S. Volkova^{4,5} A. N. Vasiliev,^{14,5,6} D. A. Chareev,⁷ G. Karapetrov,² and M. Iavarone¹

¹*Department of Physics, Temple University, Philadelphia, Pennsylvania 19122, USA*

²*Department of Physics, Drexel University, Philadelphia, Pennsylvania 19104, USA*

³*Center for High Pressure Science and Technology Advanced Research, Shanghai, 201203, China*

⁴*Physics Faculty, M.V. Lomonosov Moscow State University, Moscow 119991, Russia*

⁵*Theoretical Physics and Applied Mathematics Department,
Ural Federal University, 620002 Ekaterinburg, Russia*

⁶*National University of Science and Technology "MISIS", Moscow 119049, Russia*

⁷*Institute of Experimental Mineralogy, Russian Academy of Sciences, 142432 Chernogolovka, Moscow District, Russia*

FeSe has the simplest structure among the Fe-based superconductors, and this very simplicity could provide the most appropriate venue of understanding the superconducting mechanism of Fe-based superconductors.

Low temperature scanning tunneling microscopy and spectroscopy measurements on FeSe_{1-x}S_x single crystals with $x = 0$, $x=0.04$ and 0.09 will be presented. The S substitution into the Se site is equivalent to a positive chemical pressure, since S and Se have the same valence and S has a smaller ionic radius than Se. The subsequent changes in the electronic structure of FeSe induce a decrease of the structural transition temperature and a small increase in the superconducting critical temperature. With increasing S concentration, we find signatures of an increase of the hole Fermi surface and reduced nematicity. In particular, the vortex core anisotropy, which has been associated with the orbital ordering in this material, is strongly suppressed by the S substitution.

Vortex matter in this system will be discussed as well.

Charge order driven by Fermi-arc instability and its connection with pseudogap in cuprate superconductors



Shiping Feng^{1*}, Deheng Gao¹, Huaisong Zhao²

¹*Department of Physics, Beijing Normal University, Beijing 100875, China*

²*College of Physics, Qingdao University, Qingdao 266071, China*

Email: * *spfeng@bnu.edu.cn*

Keywords: Charge order; Fermi arc; Pseudogap; Hot spot;

Electron Fermi surface

The recently discovered charge order is a generic feature of cuprate superconductors [1-4], however, its microscopic origin remains debated. Within the framework of the kinetic-energy-driven superconducting mechanism [5-7], the nature of charge order in the pseudogap phase and its evolution with doping are studied by taking into account the electron self-energy (then the pseudogap) effect [8]. It is shown that the antinodal region of the electron Fermi surface is suppressed by the electron self-energy, and then the low-energy electron excitations occupy the disconnected Fermi arcs located around the nodal region. In particular, the charge-order state is driven by the Fermi-arc instability, with a characteristic wave vector corresponding to the hot spots of the Fermi arcs rather than the antinodal nesting vector [8]. Moreover, although the Fermi arc increases its length as a function of doping, the charge-order wave vector reduces almost linearly with the increase of doping. The theory also indicates that the Fermi arc, charge order, and pseudogap in cuprate superconductors are intimately related each other, and all of them emanates from the electron self-energy due to the interaction between electrons by the exchange of spin excitations [8,9].

References

1. See, *e.g.*, the review, R. Comin and A. Damascelli, arXiv:1509.03313.
2. T. Wu *et al.*, Nature **477**, 191 (2011).
3. R. Comin *et al.*, Science **343**, 390 (2014).
4. R. Comin *et al.*, Nat. Mater. **14** (2015) 796
5. See, *e.g.*, the review, S. Feng *et al.*, Int. J. Mod. Phys. B **29**, 1530009 (2015).
6. S. Feng, Phys. Rev. B **68**, 184501 (2003); S. Feng *et al.*, Physica C **436**, 14 (2006).
7. S. Feng *et al.*, Phys. Rev. B. **85**, 054509 (2012).
8. S. Feng *et al.*, arXiv:1510.05384.
9. S. Feng *et al.*, Physica C **517**, 5 (2015).

Two-dimensional Quantum Liquid Crystals



Jaakko Nissinen^{1*}, Aron J. Beekman^{2,3,4}, Kai Wu⁵, Ke Liu¹, Robert-Jan Slager¹, Zohar Nussinov⁶, Vladimir Cvetkovic¹, Jan Zaanen¹

¹ *Instituut-Lorentz for Theoretical Physics, Leiden University, the Netherlands*

² *Department of Physics, and Research and Education Center for Natural Sciences, Keio University, Japan*

³ *Computational Materials Science Unit, National Institute for Materials Science, Tsukuba, Japan*

⁴ *RIKEN Center for Emergent Matter Science (CEMS), Japan*

⁵ *Stanford Institute for Materials and Energy Sciences, SLAC National Accelerator Laboratory and Stanford University, USA*

⁶ *Department of Physics, Washington University, USA*

Email: * nissinen@lorentz.leidenuniv.nl

Keywords: electronic nematics, high T_c, liquid crystals

We discuss the quantum liquid crystal phases of matter in two spatial dimensions at zero temperature: the quantum nematic and smectic [1,2,3]. Based on phenomenological symmetry arguments and Abelian-Higgs type duality, we describe the melting of a crystalline solid to a nematic and a smectic via dislocation condensates [4,5]. We identify the collective modes of the quantum nematics and smectics that arise at long distances from the spatial symmetry breaking. The quantum nematic has a rotational Goldstone mode [6], whose origin can be traced back to the crystal, and is a superfluid or a superconductor in the charged case. The smectic is a highly anisotropic phase and the collective modes interpolate between the nematic and the smectic in a non-trivial way. The electromagnetic response of the charged quantum nematic and smectic show collective modes that appear at finite momentum and are in principle observable via momentum-sensitive spectroscopy.

References

1. V. Oganesyan, S.A. Kivelson, and E. Fradkin, *Phys. Rev. B* **64**, 195109 (2001).
2. E. Fradkin, S.A. Kivelson, M.J. Lawler, J.P. Eisenstein, A.P. Mackenzie, *Annu. Rev. Condens. Matter Phys.* **1**, 153 (2010).
3. A.J. Beekman, J. Nissinen, K. Wu, K. Liu, R.-J. Slager, Z. Nussinov, V. Cvetkovic, J. Zaanen, arXiv:1603.04254 (2016).
4. J. Zaanen, Z. Nussinov, S.I. Mukhin, *Ann. Phys.* **310**, 181 (2004).
5. V. Cvetkovic and J. Zaanen, *Phys. Rev. Lett.* **97**, 045701 (2006).
6. A. J. Beekman, K. Wu, V. Cvetkovic, and J. Zaanen, *Phys. Rev. B* **88**, 024121 (2013).

Long range coherent magnetic bound states in superconductors



Gerbold C. Ménard ¹, Sébastien Guissart ², Christophe Brun ¹, Stéphane Pons ³, Vasily S. Stolyarov ¹, François Debontridder ¹, Matthieu V. Leclerc ¹, Etienne Janod ⁴, Laurent Cario ⁴, Dimitri Roditchev ³, Pascal Simon ², Tristan Cren ^{*1}

¹ *Institut des NanoSciences de Paris, CNRS & UPMC - Sorbonne University, Paris*

² *Laboratoire de Physique des Solides, CNRS & University Paris-Saclay, Orsay*

³ *Laboratoire de Physique et d'Étude des Matériaux, CNRS-*

Espci-UPMC, Paris

⁴ *Institut des Matériaux Jean Rouxel, CNRS & Université de Nantes, Nantes*

Email: * tristan.cren@upmc.fr

Keywords: Magnetic impurities, Shiba bound states, low dimensional superconductors

Individual local magnetic moments act destructively on Cooper pairs, leading to discrete spin-polarized states inside the superconducting energy gap as predicted by Yu, Shiba and Rusinov (YSR) [1,2,3]. Rusinov suggested that around magnetic atoms the decaying YSR wavefunction should have a spatially oscillating structure. We will show that in superconductors with a two-dimensional electronic band structure the YSR bound states indeed give rise to long range coherent magnetic quantum state [4]. We experimentally evidence coherent bound states with spatially oscillating particle-hole asymmetry extending tens of nanometers from individual iron atoms embedded in a 2H-NbSe₂ crystal and in Pb/Si(111) monolayers (see Figure 1). We theoretically elucidate how reduced dimensionality enhances the spatial extent of these bound states and describe their energy and spatial structure. These spatially extended magnetic states could be used as building blocks for coupling coherently distant magnetic atoms in new topological superconducting phases.

Recently a new type of electronic excitations being their own antiparticles were predicted to appear at the edges of a hybrid system constituted of a chain of magnetic atoms coupled to a superconductor [5]. These so-called Majorana end-states were claimed to have been observed in the case of chains of iron atoms on Pb (110) [6], however their spatial extent is restricted to a few atomic distances, making difficult to handle them for braiding. Enhancing the spatial extent of YSR bound states would facilitate the remote coupling of magnetic systems through a superconducting state, opening the route towards an easier manipulation of Majorana quasiparticles and the creation of new topological quantum devices.

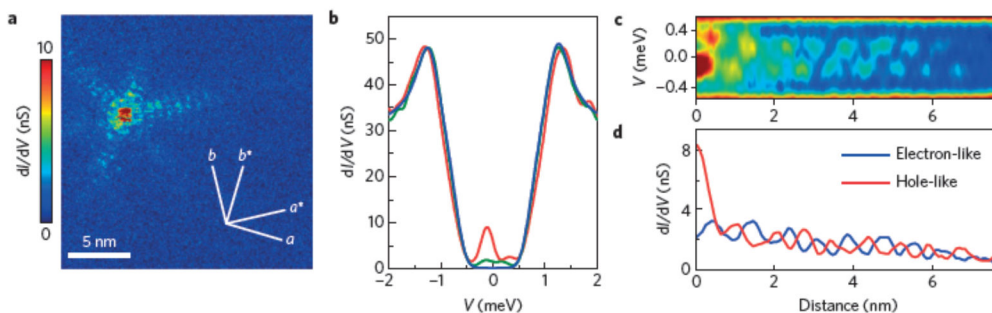


Figure 1: Spectral and spatial properties of an extended Yu–Shiba–Rusinov bound state in 2H–NbSe₂. **a**, Experimental conductance map taken at -0.13 meV. The a and b lines indicate the crystallographic axes of 2H–NbSe₂, whereas the a^* and b^* lines indicate the directions in the reciprocal space. **b**, Characteristic experimental spectra taken on top of the impurity (red), on the right branch, 4nm from the centre of the impurity (green), and far from the impurity (blue). **c**, Spatial and energy evolution of the experimental tunnelling conductance spectra, $dI/dV(x, V)$ along one branch of the star. The left side of the figure corresponds to the centre of the star and the right side to the top-right corner of the scanning area. The colour conductance scale is the same as that used in **a**. **d**, Conductance profiles of the electron- and hole-like YSR states as a function of the distance to the impurity along the same line as for **c**.

References

1. L. Yu, Bound state in superconductors with paramagnetic impurities, *Acta Phys. Sin.* **21**, 75 (1965).
2. H. Shiba, Classical Spins in Superconductors, *Prog. Theor. Phys.* **40**, 435 (1968).
3. A.I. Rusinov, On the theory of gapless superconductivity in alloys containing paramagnetic impurities, *JETP Lett.* **9**, 85 (1969).
4. G. Ménard et al., Coherent long-range magnetic bound states in a superconductor, *Nature Physics* **11**, 1013 (2015)
5. B. Braunecker and P. Simon, Interplay between Classical Magnetic Moments and Superconductivity in Quantum One-Dimensional Conductors: Toward a Self-Sustained Topological Majorana Phase, *Phys. Rev. Lett.* **111**, 147202 (2013).
6. S. Nadj-Perge, I.K. Drozdov, J. Li, H. Chen, S. Jeon, J. Seo, A.H. MacDonald, B.A. Bernevig, A. Yazdani, Observation of Majorana fermions in ferromagnetic atomic chains on a superconductor, *Science* **346**, 602 (2014).

NMR study on AF-SC-AF phase transition under a pressure of 3.0 GPa in LaFeAsO_{1-x}H_x : phase segregation around SC-AF phase boundary



N. Fujiwara^{1*}, N. Kawaguchi¹, S. Iimura², S. Matsuishi²,
and H. Hosono²

¹Kyoto University

²Tokyo Institute of Technology

Email: naoki@fujiwara.h.kyoto-u.ac.jp

Keywords: high T_c , iron-based pnictides, phase separation, NMR, high pressure

The phase diagram of the electron-doped high- T_c iron-based pnictide LaFeAsO_{1-x}H_x (H-doped La1111 series) is unique owing to the capability of electron doping: (i) it exhibits a superconducting (SC) phase with double domes covering a wide H-doping range from $x=0.05$ to $x=0.44$ [1], (ii) the SC phase is sandwiched by antiferromagnetic (AF) phases appearing in heavily and poorly electron-doped regimes [2-4], and (iii) the application of pressure transforms the double domes to a single dome. Intriguingly, upon applying pressure, the minimum T_c at ambient pressure becomes the maximum T_c of over 45 K [1]. The La1111 series under high pressure is the only material available for investigating the magnetic properties of pnictides with T_c in the range of 45 to 50 K. In fact, the Sm1111 series marks the highest T_c ($T_c = 55$ K) in all types of iron-based pnictides, however, it includes magnetic Sm ions, which hinders the investigation of the magnetic properties of iron-basal planes. In the F-doped La1111 series LaFeAsO_{1-x}F_x, T_c increases up to 40 K for $x=0.14$ upon applying pressure without the influence of low-energy spin fluctuations [5]. However, the phenomenon was observed only for $x=0.14$ because spin fluctuations remain in a lower doping range than $x=0.14$, and $x=0.14$ is the highest doping level. The H-doped La1111 series gives much information owing to the capability of electron doping.

We performed ⁷⁵As- and ¹H-NMR on LaFeAsO_{1-x}H_x ($0.2 \leq x \leq 0.6$) at 3.0 GPa to investigate whether AF fluctuations are involved in rising T_c , and investigated what happens at the phase boundary between the SC and second AF phases.

For $x=0.2$, T_c increased up to 48 K without the influence of low-energy spin fluctuations, which implies that other factors such as orbital fluctuations would be involved to achieve 45 to 50 K class of T_c . We observed from ¹H spectra that T_N of the second AF phase decreases upon applying pressure, and a mixed state of SC and AF domains manifests at the SC-AF phase boundary similar to the case of the AF-SC phase boundary [6]. These features are completely different from those of iron-based superconductors with T_c in the range of 20 to 35 K, in which SC and AF states coexist

homogeneously at the phase boundary. In the conference, we will present a full phase diagram of $\text{LaFeAsO}_{1-x}\text{H}_x$ obtained from the NMR measurements at 3.0 GPa.

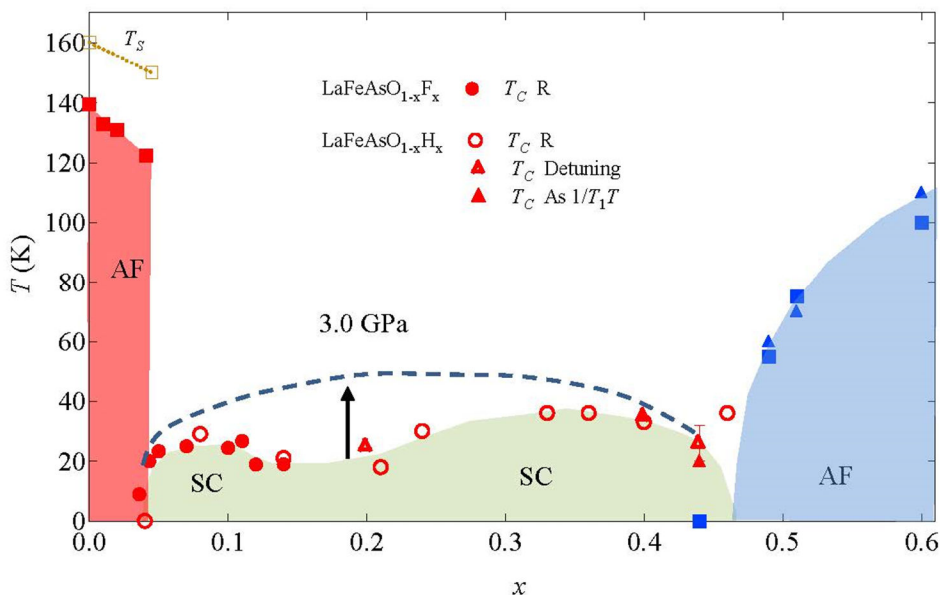


Figure 1: Phase diagram of $\text{LaFeAsO}_{1-x}\text{H}_x$. T_c was determined from the resistivity, the detuning of NMR resonance frequency, and $1/T_1T$ [2-4].

References

1. S. Iimura, et al., Nature communications, **3**,943 (2012).
2. N. Fujiwara, et al., Phys. Rev.Lett. **111**, 097002 (2013).
3. N. Fujiwara, et al., J. Supercond. Nov. Magn. **27**,933 (2014).
4. R. Sakurai, et al., Phys. Rev. B **91**, 064509 (2015).
5. T. Nakano, et al., Phys. Rev. B **81**, 100510(R) (2010)
6. N. Fujiwara, et al., Phys. Rev. B **85**,094501 (2012).

Negative charge-compressibility at the channel of SrTiO₃ field-effect transistor



Isao H. Inoue^{1*}, *, Alejandro R. Schulman¹, Neeraj Kumar¹, Ai Kitoh¹

¹National Institute of Advanced Industrial Science and Technology (AIST)

Email: *isaocaius@gmail.com

Keywords: negative charge compressibility, negative capacitance, Rashba effect, charge inhomogeneity, FET, SrTiO₃

Continuous electrostatic carrier-density control at the level of 10^{13}cm^{-2} on the surface of transition-metal oxides (TMO) is a major hurdle for the development of future oxide-based electronics as well as for the investigation of unknown electronic phenomena of two dimensional (2D) electronic system on the space symmetry broken surface. But the gate insulators employed for gating TMO to fabricate a field-effect transistor (FET) have so far resulted in ionic vacancies, randomness, (undesirable) electrochemical reactions, and low carrier mobility. They rendered the TMO FET devices unsuitable for integration to the present solid-state electronics, moreover the 2D electrons in the channel are too disturbed to show any critical electronic phenomena.

Our new approach using a bilayer of ultra-thin (6nm) Parylene-C and high- k HfO₂(20nm) thin films as a gate insulator has overcome those limitations. We have fabricated FET on a (100) surface of SrTiO₃ using the bilayer gate insulator, and have achieved the desired continuous electrostatic carrier doping from zero up to 10^{14}cm^{-2} while maintaining an extremely high quality channel (even at room temperature, the subthreshold swing is 170mV/decade and the carrier mobility is $11 \text{cm}^2/\text{Vs}$).

However, to our surprise, an unexpected phenomenon was observed: excess enhancement of the carrier density. That is, on the surface of SrTiO₃, the amount of the electrostatically accumulated charge measured by the Hall effect is about 10 times as much as what we have expected from the simple Gauss's law ($Q=CV$). The capacitance of our Parylene-C/HfO₂ bilayer gate insulator does not depend on the applied gate voltage, nor it changes with time during the long measurement of the Hall effect. Eliminating such possible artifacts driving the excess enhancement of the carrier density, finally remained is an interesting physics: *i.e.*, negative charge compressibility (negative capacitance) of the channel. Moreover, further intriguing twist is that the enhancement we observed is too large to be explained straightforwardly by the "common sense" of the negative charge compressibility. Thus, we proposed that the discrepancy is originated in some electronic inhomogeneity of the channel.

Because we succeeded to prepare the very clean channel on the (100) surface of SrTiO₃, it seems quite contradicting to assume the inhomogeneity. However, the appearance of the negative charge compressibility should drive some instability, which therefore induces an intrinsic charge disproportionation. A possible mechanism of the apparent carrier density enhancement by the inhomogeneity is discussed in the presentation.

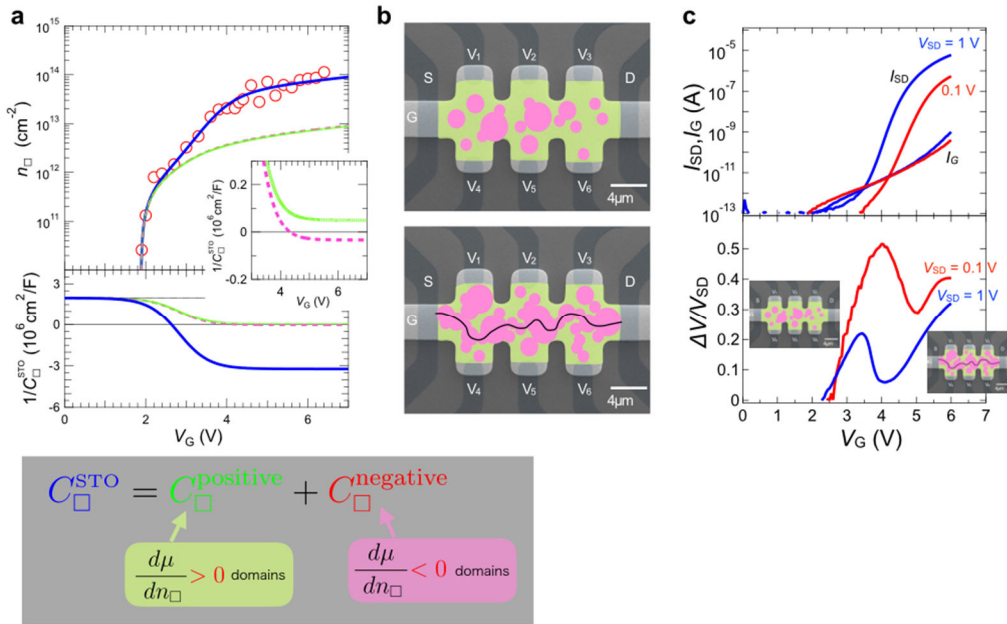


Figure 1: Interpretation of the excess n_{\square} enhancement by a negative charge compressibility (κ) + inhomogeneity model. **a**, Sheet carrier density n_{\square} (open circles) obtained by the Hall effect measurement. Solid line (blue) is a least-square fit of the data to $en = CV$, where $1/C = 1/C_{\text{ins}} + 1/C_{\text{sto}}$. C_{ins} is $0.28 \mu\text{F}/\text{cm}^2$, and the flat-band voltage is 1.88V . For C_{sto} , we used a model shown in the bottom panel, which are decomposed into C_{+} (dotted line in green) and C_{-} (dashed line in purple). $C_{+} \rightarrow 20 \mu\text{F}/\text{cm}^2$ while $C_{-} \rightarrow -30 \mu\text{F}/\text{cm}^2$. **b**, SEM picture of the FET device used for the Hall effect measurement ($L = 20 \mu\text{m}$, $W = 4 \mu\text{m}$ and the distance between V_1 and V_3 electrodes is $12 \mu\text{m}$). The domain-formation is schematically depicted. Top: each circle (pink) corresponds to a metallic island with $C_{\text{sto}} = C_{-}$ while the background (green) is less conductive with $C_{\text{sto}} = C_{+}$. Bottom: by increasing V_G , metallic domains become larger and finally the current path (solid line in black) is formed. **c**, I_{SD} and I_G as well as $\Delta V \equiv V_3 - V_1$ normalised by V_{SD} plotted against V_G . In general, ΔV is expected to increase monotonously as a function of V_G , but the sudden decrease of ΔV while increasing V_G suggests the formation of the metallic path in the channel.

Muon spin relaxation and transport studies in the electron-doped high- T_c T'-superconductors revealing the novel electronic state



T. Adachi^{1*}, A. Takahashi², T. Konno², T. Ohgi²,
M. A. Baqiya², K. Kurashima², K. M. Suzuki², T. Takamatsu²,
T. Kawamata², M. Kato², I. Watanabe³, A. Koda⁴,
M. Miyazaki⁴, R. Kadono⁴, H. Oguro⁵, S. Awaji⁵, Y. Koike²

¹*Department of Engineering and Applied Sciences, Sophia University, Japan*

²*Department of Applied Physics, Tohoku University, Japan*

³*Advanced Meson Science Laboratory, RIKEN Nishina Center, Japan*

⁴*Muon Science Laboratory, Institute of Materials Structure Science, KEK, Japan*

⁵*Institute for Materials Research, Tohoku University, Japan*

Email: *t-adachi@sophia.ac.jp

Keywords: electron-doped high- T_c T'-cuprate, transport properties, muon spin relaxation, Ce-free superconductivity

In order to investigate the electronic state relating to the Ce-free superconductivity in the parent compound of electron-doped high- T_c cuprates with the so-called T' structure [1,2], we have performed muon-spin-relaxation (muSR) and transport measurements of T'-Pr_{1.3-x}La_{0.7}Ce_xCuO_{4+δ} (PLCCO) single crystals and Ce-free T'-La_{1.8}Eu_{0.2}CuO_{4+δ} (LECO) polycrystals [3,4]. The muSR spectra of the reduced superconducting (SC) samples of PLCCO with $x = 0.10$ and LECO have revealed the formation of a short-range magnetic order coexisting with the superconductivity in the ground state. The formation of the short-range magnetic order due to a tiny amount of excess oxygen in the reduced SC samples suggests that the T'-cuprate exhibiting the Ce-free superconductivity is regarded as a strongly correlated electron system. As shown in Fig. 1, the Hall resistivity of the reduced SC PLCCO with $x = 0.10$ and 0.15 has revealed a nonlinear behavior in the magnetic field, suggesting the existence of both hole and electron carriers. These results can be explained in terms of a band picture based on the strong electron correlation [3]. That is, the collapse of the charge-transfer gap between the upper Hubbard band of the Cu $3d_{x^2-y^2}$ orbital and the O $2p$ band due to the square planer coordination of oxygen in the T'-cuprate results in the generation of a finite value of the density of states at the Fermi level due to O $2p$ holes and Cu $3d_{x^2-y^2}$ electrons without Ce substitution, leading to the appearance of superconductivity.

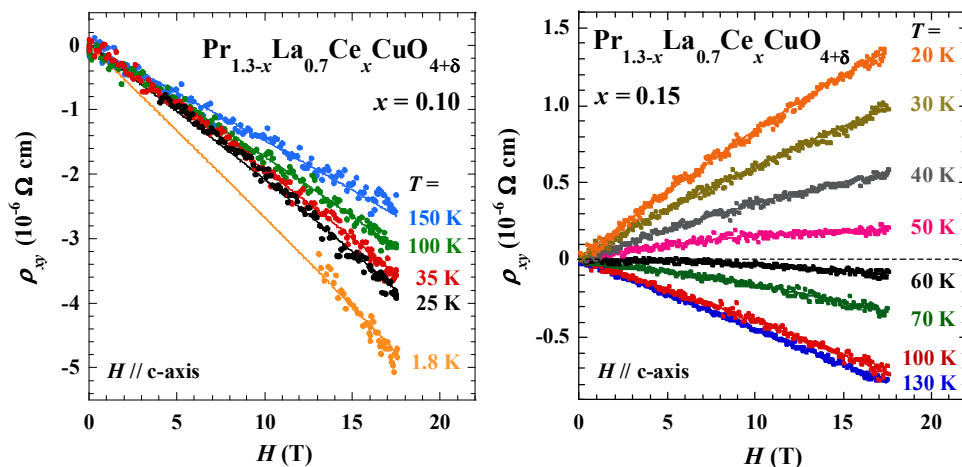


Figure 1: Temperature dependence of the Hall resistivity ρ_{xy} in magnetic fields parallel to the c -axis in $\text{Pr}_{1.3-x}\text{La}_{0.7}\text{Ce}_x\text{CuO}_{4+\delta}$ with $x = 0.10$ and 0.15 . Solid lines are the best-fit results using the two-carrier model.

References

1. A. Tsukada, Y. Krockenberger, M. Noda, H. Yamamoto, D. Manske, L. Alff and M. Naito, *Solid State Commun.* **133**, 427 (2005).
2. T. Takamatsu, M. Kato, T. Noji and Y. Koike, *Appl. Phys. Express* **5**, 073101 (2012).
3. T. Adachi, Y. Mori, A. Takahashi, M. Kato, T. Nishizaki, T. Sasaki, N. Kobayashi and Y. Koike, *J. Phys. Soc. Jpn.* **82**, 063713 (2013).
4. T. Adachi, A. Takahashi, K. M. Suzuki, M. A. Baqiya, T. Konno, T. Takamatsu, M. Kato, I. Watanabe, A. Koda, M. Miyazaki, R. Kadono and Y. Koike, arXiv: 1512.08095.

Fluctuations and Nambu-Goldstone-Higgs Modes in Multi-Condensate superconductors



Takashi Yanagisawa^{1*}

¹*Superconducting Research Group, Electronics and Photonics Research Institute, National Institute of Advanced Industrial Science and Technology, 1-1-1 Umezono, Central 2, Tsukuba, Ibaraki 305-8568, Japan*

Email: * t-yanagisawa@aist.go.jp

Keywords: multi-gap superconductors, Nambu-Goldstone modes, Leggett modes, Higgs modes, fluctuation, time-reversal symmetry breaking, fractional vortex, non-abelian generalization

1. Nambu-Goldstone-Leggett modes

Since the superconducting gap is complex number, it has two degrees of freedom, namely, amplitude and phase. In an N -gap superconductor, we have in general $U(1)^N$ phase invariance. This multiple-phase invariance is partially or totally broken in a superconductor. The Coulomb repulsive interaction turns one phase mode into a gapped plasma mode. There are at most $N-1$ modes and they can be low-energy excitation modes in superconductors. These modes are in general massive due to Josephson interactions. There is, however, a possibility that some of these modes become massless Nambu-Goldstone modes when Josephson couplings are frustrated. When the Josephson couplings are frustrated, there may appear many interesting phenomena in superconductors. They are, for example, time-reversal symmetry breaking, the existence of massless and low-energy excited states and fractionally quantized flux vortices [1-7].

2. Higgs modes in superconductors

The fluctuation of the amplitude of gap function is called the Higgs mode. Recently, there has been an increasing interest in a role of the Higgs mode in superconductors. The action of the Higgs part is given by the time-dependent Ginzburg-Landau functional when the temperature T is near T_c with vanishing gap at $T = T_c$. At low temperatures $T \ll T_c$, the action has instead the form of wave equation with second derivative with respect to time. The spectrum of Higgs mode has a gap that is proportional to the mean-field gap function. In a multi-gap superconductor, the gaps of Higgs modes are given by the eigenvalues of a Higgs matrix. The Higgs excitation spectra crucially depend on the strength of Josephson couplings (Fig.1) and there is a softening of the Higgs mode when Josephson couplings satisfy some conditions.

3. Josephson plasma and multi-gap superconductors

The Josephson plasma mode, observed in cuprate layered superconductors, is an oscillation mode of the phase of the superconducting gap. The Josephson plasma mode

comes from the Nambu-Goldstone or Leggett modes. The Josephson plasma phenomenon has been understood on the basis of the classical Maxwell equation and the Josephson equations such as $J = J_0 \sin \theta$ where θ is the phase difference of the gap between layered CuO_2 plane [9]. In this case, the Josephson plasma mode is the Leggett mode. The quantum theory of the Josephson plasma phenomenon based on a microscopic model should be developed [10, 11] considering the anisotropy of the gap function.

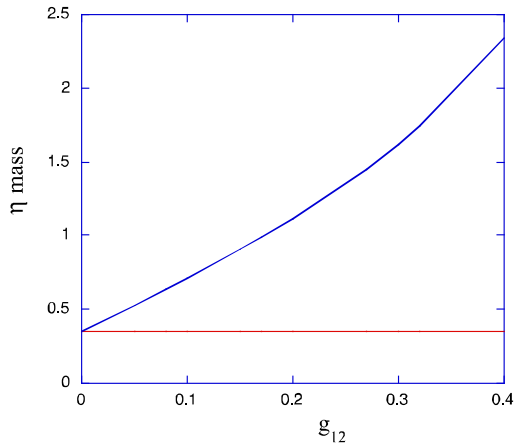


Fig.1. Higgs mass as a function of the inter-band BCS coupling g_{12} in a two-band superconductor.

The author expresses his sincere thanks to K. Yamaji, I. Hase and M. Kato for useful discussions.

References

1. Y. Tanaka and T. Yanagisawa, *J. Phys. Soc. Jpn.* **79**, 114706 (2010).
2. Y. Tanaka and T. Yanagisawa, *Solid State Commun.* **150**, 1980 (2010).
3. V. Stanev and Z. Tesanovic, *Phys. Rev. B* **81**, 134522 (2010).
4. R. G. Dias and A. M. Marques, *Supercond. Sci. Technol.*, **24**, 085009 (2011).
5. T. Yanagisawa, Y. Tanaka, I. Hase and K. Yamaji, *J. Phys. Soc. Jpn.* **81**, 024712 (2012).
6. B. J. Wilson and M. P. Das, *J. Phys. Condens. Matter*, **25**, 425702 (2013).
7. T. Yanagisawa and I. Hase, *J. Phys. Soc. Jpn.* **82**, 124704 (2013).
8. A. Bianconi, *Nature. Phys.* **9**, 536 (2013).
9. T. Koyama and M. Tachiki, *Phys. Rev. B* **54**, 16183 (1996).
10. T. Koyama, *J. Phys. Soc. Jpn.* **68**, 2010 (1999).
11. Y. Ohashi and S. Takada, *Phys. Rev. B* **59**, 4404 (1999).

Quantum and Thermal Fluctuations in Strongly Underdoped Cuprates near the Super-to-Insulator Critical Point



Thomas R. Lemberger*, Stanley F. Steers, John Draskovic,
¹*Ohio State University, Dept. of Physics*

Email: * trl@physics.osu.edu

Keywords: quantum critical fluctuations, cuprate superconductors, superfluid density

We draw attention to some unusual features of electron transport – primarily resistivity and superfluid density – of cuprate superconductors in the quantum critical regime near the super-to-insulator transition at low hole doping. In bulk samples of YBCO, either crystals[1] or films many tens of unit cells thick,[2] T_c scales as square-root of superfluid density, $n_s(0)$. In ultrathin YBCO films (two unit cells thick) T_c scales linearly with n_s , the required 2-d behavior if quantum fluctuations are responsible for the scaling.[3] Together, these results argue that quantum fluctuations are significant for T_c less than about 30 K. It is not such a surprise that the highly anisotropic Bi-2212 cuprate also exhibits 2-d scaling, $T_c \propto n_s^{1/2}$, in quantitative agreement with scaling in 2-d YBCO films, even in films many unit cells thick.[4]

The story of thermal fluctuations is mysterious. While ultrathin YBCO films and “thick” Bi-2212 films share the same 2-d quantum critical scaling, the former exhibit strong 2-d thermal critical fluctuations in the superfluid density, as expected theoretically, while the latter show no critical thermal behavior of 2-d or 3-d nature. YBCO crystals show no thermal critical behavior at strong underdoping, even though they exhibit strong 3-d fluctuations at optimal-to-moderate underdoping. Finally, “thick” YBCO films do not show thermal critical behavior at any doping.

Recently we have been able to determine the superconducting coherence length in underdoped cuprate films at small magnetic fields of tens of gauss, a field that has a negligible effect on the electronic structure of the material.[5] The technique involves a two-coil apparatus in which the driving ac magnetic field that is applied at the center of the film increases from very low to high enough that many vortices and antivortices penetrate the film, and field screening is negligible. The key result is that in strongly underdoped YBCO films, the critical momentum of Cooper pairs, which is inversely proportional to coherence length, is proportional to T_c . Since there are other energy scales, e.g., pseudogap, in the underdoped cuprates, this result is non-trivial.

Finally, we have observed an anomalously large offset between the T_c evidenced by resistivity and the T_c from superfluid density.[6] The offset grows with underdoping. It is too large to be explained by the usual Kosterlitz-Thouless-Berezinski theory. We have seen it in very thin YBCO films but it is absent from thick YBCO films. We have also seen it in a “thick” Bi-2212 film, Fig. 1. The origin of this phenomenon is likely to

involve inhomogeneity, but the question is whether the inhomogeneity is intrinsic to the material in the quantum critical regime or due to some chemical or structural inhomogeneity.

Acknowledgement. This research is supported by DOE-Basic Energy Sciences through Grant No. FG02-08ER46533.

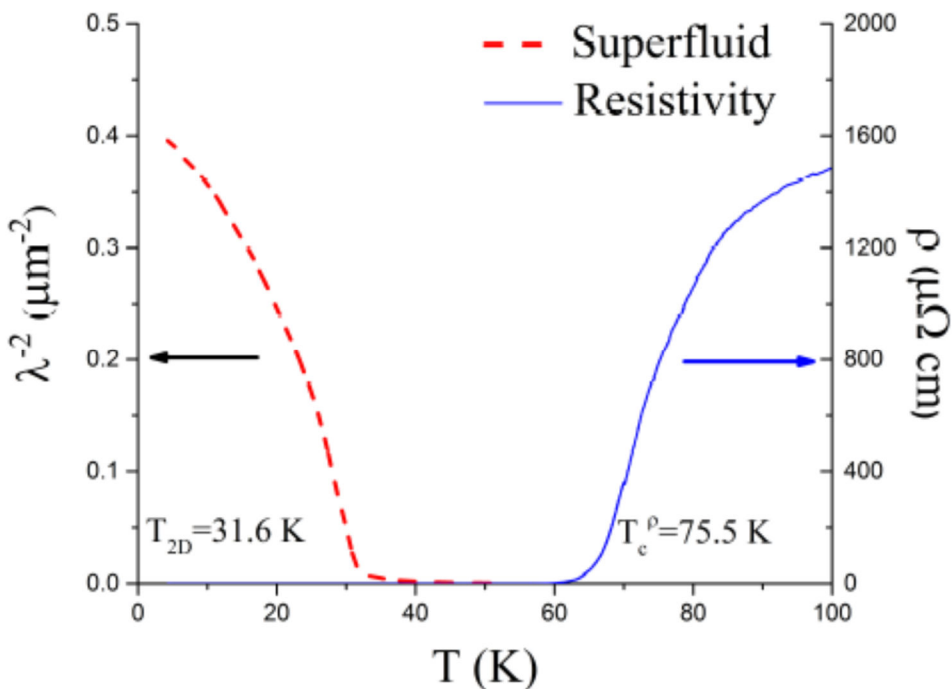
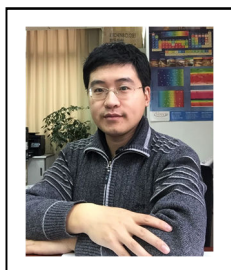


Figure 1: Superfluid density (red dashed) and resistivity (blue line) for an underdoped Bi-2212 film 65 unit cells thick showing the offset between resistive and superfluid T_c 's.

References

1. D. M. Broun et al., Phys. Rev. Lett. 99, 237003 (2007).
2. Y. Zuev, M. S. Kim, and T. R. Lemberger, Phys. Rev. Lett. 95, 137002 (2005).
3. I. Hetel, T. R. Lemberger, and M. Randeria, Nat. Phys. 3, 700 (2007).
4. M.J. Hinton et al., J Supercond Nov Magn 26, 2617 (2013).
5. J.D. Draskovic et al., Phys. Rev. B 91, 104524 (2015).
6. S.F Steers et al., subm. to Phys. Rev. B.

Manipulating the electronic structure and magnetism of spin-orbit Mott insulator by tailoring superlattices



Zhengtai Liu, Congcong Fan, Mao Ye and Dawei Shen*
State Key Laboratory of Functional Materials for Informatics, SIMIT, Chinese Academy of Sciences, Shanghai, 200050, China

Email o* dwshen@mail.sim.ac.cn

Keywords : In-situ ARPES – Oxide MBE – Iridates

In this talk, we will introduce how to fabricate and study the artificial 5d iridate superlattices by the combo of oxide molecular beam epitaxy (OMBE) and *in situ* angle-resolved photoemission spectroscopy (ARPES) techniques. We successfully fabricated a series of high-quality $[(\text{SrIrO}_3)_m/(\text{SrTiO}_3)]_n/\text{SrTiO}_3(100)$ superlattices using the layer-by-layer OMBE growth method, and consequently realized the magnetism and metal-insulator transition (MIT) by artificial dimensionality control of iridates. The mechanism of this MIT and the elemental specificity of magnetism were then investigated by our combined OMBE and ARPES system and the X-ray magnetic circular dichroism (XMCD), respectively. Our results could provide a comprehensive understanding of the phase transition in this spin-orbit Mott insulator

Magnetic Force Microscopy of spin reorientation of iron tin

Yeong-Ah Soh^{1,*}

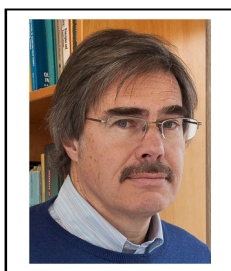
¹*Hanover, NH, USA*

Email: * yeongahsoh@gmail.com

Keywords: spin reorientation, first-order transition, magnetic force microscopy

In this talk I will show the application of temperature-dependent magnetic force microscopy to study magnetic phase transitions in magnets. We applied this probe to study iron in (Fe_3Sn_2) , which is a layered ferromagnet, whose building blocks are Kagome planes, with a Curie temperature of 640 K. It has a spin reorientation, where the magnetic moments rotate from the transverse direction towards the planes on cooling, displays thermal hysteresis, and previously it has been reported to exhibit glass-like phenomena. As the spin reorients, the domain structure evolves from a branched dendritic high temperature state to a completely different domain structure at low temperatures. Our studies show that the spin reorientation is of first order and the system displays phase coexistence of magnetic easy axis perpendicular and parallel to the Kagome plane.

Intertwined Superconductivity and Antiferromagnetism in Cuprates



John M. Tranquada
Brookhaven National Laboratory
Upton, NY 11973-5000, USA

Email: *jtran@bnl.gov*

Keywords: high T_c , cuprates, charge stripes, magnetic stripes

The concept of intertwined orders has been motivated in particular by stripe-related phenomena in $\text{La}_{2-x}\text{Ba}_x\text{CuO}_4$ [1]. The observation of 2D superconducting correlations in LBCO $x=1/8$ coexisting with charge and spin stripe order [2] is consistent with the concept of a pair-density-wave (PDW) state, in which a spatially-modulated superconducting wave function is interwoven with local antiferromagnetic order in the form of spin stripes. Experiments also demonstrate the presence of gapless spin-stripe fluctuations in good bulk superconductors such as LBCO $x=0.095$ [3] and LSCO $x=0.07$ [4], providing a circumstantial case for a PDW state, in agreement with recent calculations [5]. Now, because of the intertwining of the superconducting and antiferromagnetic modulations, ordering of the phase of each wave function must happen simultaneously. Hence, while the segregation of the holes into charge stripes can be good for pairing [6], the presence of the low-energy spin fluctuations can frustrate the development of phase order, thus depressing the superconducting transition temperature. A way around this is to gap the low-energy spin fluctuations, and establish spatially-uniform d-wave superconductivity, as is observed to occur near optimal doping. The fact that the spin gap tends to be smaller than the antinodal pairing gap may help to explain the fact that superconducting coherence tends to come from a finite arc of states in reciprocal space.

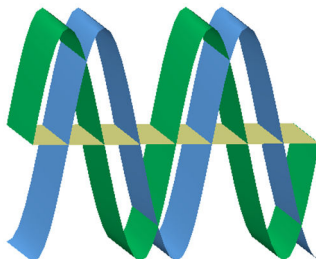


Figure 1: Sketch of intertwined PDW (blue) and amplitude envelope of the antiferromagnetic order (green) oscillating about zero amplitude (gold).

References

1. E. Fradkin, S. A. Kivelson, and J. M. Tranquada, *Rev. Mod. Phys.* **87**, 457 (2015).
2. Q. Li, M. Hücker, G. D. Gu, A. M. Tsvelik, and J. M. Tranquada, *Phys. Rev. Lett.* **99**, 067001 (2007)
3. Zhijun Xu, C. Stock, Songxue Chi, A. I. Kolesnikov, Guangyong Xu, Genda Gu, and J. M. Tranquada, *Phys. Rev. Lett.* **113**, 177002 (2014).
4. H. Jacobsen, I. A. Zaliznyak, A. T. Savici, B. L. Winn, S. Chang, M. Hücker, G. D. Gu, and J. M. Tranquada, *Phys. Rev. B* **92**, 174525 (2015).
5. M. H. Christensen, H. Jacobsen, T. M. Maier, and B. M. Andersen, [arXiv:1601.03251](https://arxiv.org/abs/1601.03251).
6. P. Corboz, T. M. Rice, and M. Troyer, *Phys. Rev. Lett.* **113**, 046402 (2014).

Topological surface states interacting with bulk spin excitons in the Kondo insulator SmB_6 as revealed by planar tunneling spectroscopy

Laura H. Greene

*National High Magnetic Field Laboratory, Florida State University and the Center for Emergent Superconductivity
Florida State University • University of Florida • Los Alamos National Laboratory
1800 E. Paul Dirac Drive, Florida State University, Tallahassee, FL 32310 USA*

Samarium hexaboride (SmB_6), a well-known Kondo insulator in which the insulating bulk arises from strong electron correlations, has recently attracted great attention owing to its possibly topological nature, thereby harboring protected surface states. Although there is strong evidence for this, corroborative spectroscopic evidence is still lacking; unlike in the weakly correlated counterpart, e.g., Bi_2Se_3 . We report planar tunneling spectroscopy results obtained on the (001) and (011) crystal faces that reveal the linear density of states (DOS) as expected for Dirac cones. Our spectroscopic results also reveal the bulk gap, whose signature arises from spin excitons in the bulk interacting with the surface states. Above ~ 4 K, the thermal population of the spin excitons keeps the surface state from being protected.

*This work is preformed by W.K. Park, with assistance from L. Sun, A. Noddings, D.-J. Kim, Z. Fisk, and L.H. Greene. We acknowledge support at UIUC by NSF DMR 12-06766, and at UCI by NSF DMR. 08-01253.

Statics and dynamics of crumpled graphene

Authors list –

G. Aeppli + authors of both papers cited below

Two-dimensional solids are intrinsically unstable, which leads to large amplitude lattice distortions. We describe scanning tunneling microscopy data, for the surfaces of calcium-intercalated graphite which image the random crumpling of graphene sheets, and correlate the visibility of this crumpling with electronic stripe formation. The implications of the motion of the ripples which define the static crumpling are then worked out, using molecular dynamics, for water droplets, which are found to diffuse at an unusually rapid rate. The underlying mechanism is similar to that of surfing, and could be exploited for efficient transport of materials, including perhaps even proteins, in aqueous solutions.

References

1. K.C. Rahnejat et al. , Nature Communications 2, Article number: 558 (2011) doi:10.1038/ncomms1574
2. M. Ma et al., Nature Materials 15, 66–71 (2016) doi:10.1038/nmat444

Induction & Dynamics of New States of Matter in 2D Materials

Tom Devereaux
Stanford University USA

Email: *tpd@stanford.edu*

Competition between ordered phases, and their associated phase transitions, are significant in the study of strongly correlated systems. Here, we examine one aspect, the nonequilibrium dynamics of a photoexcited Mott-Peierls system, using an effective Peierls-Hubbard model and exact diagonalization. Near a transition where spin and charge become strongly intertwined, we observe antiphase dynamics and a coupling-strength-dependent suppression or enhancement in the static structure factors. The renormalized bosonic excitations coupled to a particular photoexcited electron can be extracted, which provides an approach for characterizing the underlying bosonic modes. The results from this analysis for different electronic momenta show an uneven softening due to a stronger coupling near k_F . This behavior reflects the strong link between the fermionic momenta, the coupling vertices, and ultimately, the bosonic susceptibilities when multiple phases compete for the ground state of the system.

Time reversal symmetry breaking in multiband superconductors



James F. Annett¹

¹*University of Bristol, HH Wills Physics Laboratory, Bristol, BS8 1TL, UK*

Email: james.annett@bristol.ac.uk

Keywords: unconventional superconductivity, chiral superconductivity, multiband materials, complex fermiology of superconductors

The polar Kerr effect is an optical phenomenon which arises in states with broken time-reversal symmetry. This effect has recently been observed in a series of unconventional superconductors, including the layered perovskite compound Sr_2RuO_4 [1]. Confirmation of a Kerr signal below T_c supports the hypothesis of chiral p-wave superconductivity in this material. However, the nature of the unconventional superconducting state in this system remains a source of controversy. Even for a chiral superconductor the existence of a finite Kerr signal is not in general allowed by symmetry [2]. A mechanism for finding a finite Kerr signal in a chiral superconductor is the existence of inter-band optical matrix elements in a multiband material [3]. Here, we present a series of calculations for the chiral superconducting state including spin-orbit coupling (SOC). These extend the three dimensional, multiband model considered previously [4]. New classes of materials have recently also been found to display evidence of time reversal symmetry breaking (TRSB) in the superconducting state, including LaNiC_2 [5] LaNiGa_2 [6] and Re_6Zr [7] and La_7Ir_3 [8]. The evidence for TRSB in these systems is found from muon-spin resonance experiments. Most, but not all, of these systems are non-centrosymmetric. Here we discuss possible pairing states for these systems which are allowed by symmetry, including non-unitary triplet pairing [9] and multiband pairing scenarios.

References

1. J. Xia, Phys. Rev. Lett. 97, 167002 (2006).
2. V. P. Mineev, Phys. Rev. B 76, 212501 (2007)
3. E. Taylor and C. Kallin, Phys. Rev. Lett. 108, 157001 (2012)
4. M. Gradhand, et al. Phys. Rev. B 88, 094504 (2013).
5. A. D. Hillier, J. Quintanilla, and R. Cywinski, Phys. Rev. Lett. 102, 117007 (2009).
6. A. D. Hillier, J. Quintanilla, B. Mazidian, J. F. Annett, and R. Cywinski, Phys. Rev. Lett. 109, 097001 (2012).
7. R. P. Singh, A. D. Hillier, B. Mazidian, J. Quintanilla, J. F. Annett, D. McK. Paul, G. Balakrishnan, and M. R. Lees, Phys. Rev. Lett. 112, 107002 (2014).
8. J. A. T. Barker, D. Singh, A. Thamizhavel, A. D. Hillier, M. R. Lees, G. Balakrishnan, D. McK. Paul, and R. P. Singh, Phys. Rev. Lett. 115, 267001 (2015).
9. Jorge Quintanilla, Adrian D. Hillier, James F. Annett, and R. Cywinski, Phys. Rev. B 82, 174511 (2010).

Novel effects in orbital physics

D.I.Khomskii

II.Physikalisches Institut, Koeln University, Germany

After short introduction describing the basics of Jahn-Teller and orbital physics in transition metal compounds [1], I will address several novel effects in orbital physics, suggested or clarified recently. Among those are: spin and orbital ordering for different geometries (corner-, edge- and face-sharing MO6 octahedra) [2]; reduction of dimensionality due to orbital ordering [3]; orbital-driven Peierls transition [4]; orbital-selective dimerization and competition between molecular orbitals formation and double exchange [5, 6]; quantum effects in orbitals [7]. Some comments about the role of real relativistic spin-orbit coupling will be also made.

References

1. D.I. Khomskii, Transition Metal Compounds, Cambridge University Press, Cambridge 2014
2. K.I. Kugel, D.I. Khomskii, A.O. Sboychakov, S.V. Streltsov, arXiv:1411.3605 (2014)
3. D.I. Khomskii, Physica Scripta **72**, CC8--CC14 (2005)
4. D.I. Khomskii and T. Mizokawa, Phys. Rev. Lett. **94**, 156402 (2005)
5. Sergey V. Streltsov, Daniel I. Khomskii, Phys. Rev. **B 89**, 161112(R) (2014)
6. S. V. Streltsov and D. I. Khomskii, arXiv:1602.06425 (2016)
7. M. Skoulatos et al., Phys. Rev. B **91**, 161104(R) (2015)

Commensurate features of cuprate charge density modulations



Michael J. Lawler^{1,2**},

¹*Dept. of Physics, Applied Physics and Astronomy,
Binghamton University, Binghamton NY, 14850, USA*

²*Dept. of Physics, Cornell University, Ithaca, NY 14853, USA*

Email: * mlawler@binghamton.edu

Keywords: high T_c, charge density waves, STM

Theories of strong local Coulomb interactions have long predicted a state of unidirectional modulations of spin and charge, frequently with four-unit-cell periodicity, when holes are doped into a cuprate superconductor. Experimentally, even the lightest hole doping does produce nanoscale clusters of charge density modulations. Yet upon further doping, the reported wave vector Q of these modulations for some cuprates diminishes continuously as if driven by the weak coupling mechanism of nesting. To illuminate this debate between weak and strong coupling, I will present a novel data analysis scheme based on phase-resolved electronic structure visualization and our detailed study of the ordering wave vector in STM data on $\text{Bi}_2\text{Sr}_2\text{CaCu}_2\text{O}_{8+x}$. We find the dominant feature present in the charge density modulations is associated with period four modulations and that it is doping independent. This implies a strong coupling mechanism is at play in the formation of these modulations. I will conclude with a discussion of how this relates to other families of cuprate superconductors.

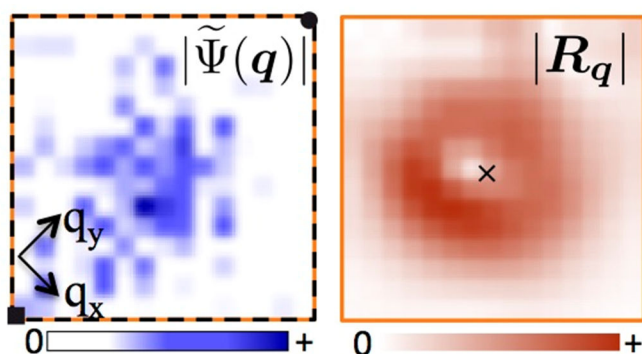


Figure 1: Analysis of the cuprate CDW as measured in STM data on $\text{Bi}_2\text{Sr}_2\text{CaCu}_2\text{O}_{8+x}$ at doping $p=0.06$. Left: the Fourier amplitudes of the wave near $Q=(0, 1/4)$. Right: a measure of phase winding across the real space image of the CDW after demodulating by wave vector q . A minimum is the optimal wave vector and is found near $q=Q$ marked by an “x”.

New twist on the vortex-core tunneling spectroscopy in $\text{YBa}_2\text{Cu}_3\text{O}_{7-\delta}$ 

Ivan Maggio-Aprile^{1*}, Jens Bruér¹, Nathan Jenkins¹, Zoran Ristic¹, Andreas Erb², Christophe Berthod¹, Øystein Fischer¹, Christoph Renner¹

¹*University of Geneva, DQMP, 24 quai E.-Ansermet, Geneva, Switzerland*

²*Walther-Meissner-Institut, Bayerische Akademie der Wissenschaften, Walther-Meissner-Strasse 8, D-85748 Garching, Germany*

Email: * ivan.maggio-aprile@unige.ch

Keywords: Scanning Tunneling Spectroscopy, High T_c superconductivity, Vortex cores

Scanning tunneling spectroscopy (STS) of vortex cores in the high-temperature cuprate superconductors has been challenging theory for years, since most of the observations made until now could not be easily explained. As a matter of fact, the detection of a robust pair of electron-hole symmetric states at finite subgap energy in $\text{YBa}_2\text{Cu}_3\text{O}_{7-\delta}$ (Y123) [1] was in total contradiction with the expected signature of a d-wave superconductor vortex core, characterised by a strong zero-bias conductance peak. We present here recent STS data on very homogeneous optimally doped Y123 at 0.4 K revealing that these subgap features are not exclusively linked to the vortex cores: they are actually observed everywhere along the surface with high spatial and energy reproducibility, and even in the absence of magnetic field. Detailed analysis and modelling show that these states remain unpaired in the superconducting phase and belong to an incoherent channel which contributes to the tunneling signal in parallel with the superconducting density of states. When subtracting this incoherent contribution from the total tunneling conductance, the remaining coherent channel exhibits the characteristic signature of a pure d-wave superconductor, for spectra acquired not only outside but even at the center of the vortex cores.

References

1. I. Maggio-Aprile et al., Phys. Rev. Lett. 75, 2754 (1995)

Fermiology of hole-doped PbTe: Insights to understand superconductivity in a valence disproportionated compound



Paula Giraldo-Gallo^{1,2*}, P. Walmsley², B. Sangiorgio³, M. Fechner³, L. Buchauer⁴, B. Fauque⁴, S. C. Riggs¹, R. D. McDonald⁵, T. H. Geballe², K. Behnia⁴, N. A. Spaldin³, and I. R. Fisher²

¹ National High Magnetic Field Laboratory, FL, USA.

² Stanford University, CA, USA

³ ETH Zurich, Switzerland

⁴ ESPCI, Paris, France

⁵ Los Alamos National Laboratory, NM, USA.

Email: * pgiraldo@magnet.fsu.edu

Keywords: Negative U, valence disproportionation, impurity band, superconducting semiconductor

Valence disproportionated materials are an intriguing class of compounds in which ions of the same chemical element can exist in two different states of oxidation. The phase diagrams of many of these compounds, as parameters such as chemical doping are varied, show unique characteristics, such as the presence of superconductivity with anomalous properties, potentially associated with the same mechanism leading to the valence disproportionation. Here I will present our study of the valence disproportionated semiconductor Tl-doped PbTe. The only impurity known to produce superconductivity in this host material is Tl, which has previously been tentatively associated with dynamic valence fluctuations of the Tl impurities. We performed a full Fermi surface characterization of $\text{Pb}_{1-x}\text{Tl}_x\text{Te}$, as well as its non-superconducting analog, $\text{Pb}_{1-x}\text{Na}_x\text{Te}$, via Shubnikov de Haas oscillations in magnetotransport, for magnetic fields up to 35T (DC) [1]. Our results show that beyond a critical impurity concentration close to the emergence of superconductivity, there are clear differences in the normal-state carriers. In non-superconducting $\text{Pb}_{1-x}\text{Na}_x\text{Te}$, all carriers reside at four ellipsoidal pockets of the Fermi surface, while in superconducting $\text{Pb}_{1-x}\text{Tl}_x\text{Te}$, there is an additional set of carriers, consistent with incoherent resonant impurity levels. The presence or absence of these states at or near the Fermi energy is intimately connected to the presence or absence of superconductivity in doped PbTe.

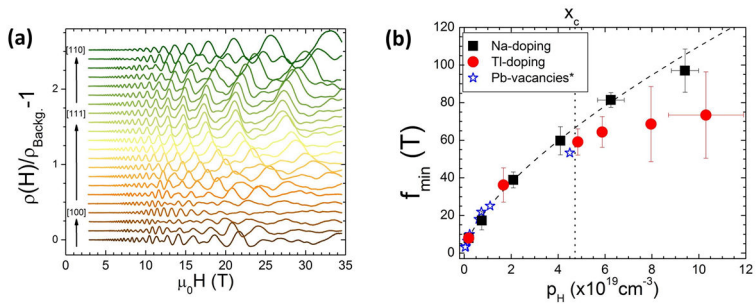


Figure 1: (a) Oscillating component of magnetoresistance for a $\text{Pb}_{1-x}\text{Na}_x\text{Te}$ sample with $x=0.62\%$, and different orientations of the magnetic field along the [110] plane. (b) Evolution of the L-pockets transverse cross-sectional areas for Na and Tl-doped PbTe samples, as a function of Hall number. The dashed curve indicates the expected dependence in a perfect ellipsoidal model, and one hole per dopant. The mismatch between Na and Tl-doped PbTe cross-sectional areas for a given p_H , above the x_c line for with the Tl-doped samples superconduct, indicates the presence of an extra set of carriers in Tl-doped PbTe, additional to the ones residing in the L-pockets.

References

1. P. Giraldo-Gallo, B. Sangiorgio, P. Walmsley, M. Fechner, S. C. Riggs, T. H. Geballe, N. Spaldin, and I. R. Fisher. *ArXiv:1603.04414v1* (2016).

Critical dynamics and inhomogeneity in complex materials



A. Ricci^{1,2}

¹*Deutsches Elektronen-Synchrotron DESY, Notkestraße 85, D-22607 Hamburg, Germany*

²*Rome International Center for Materials Science, Superstripes, RICMASS, via dei Sabelli 119A, I-00185 Roma, Italy*

Email: **alessandro.ricci@desy.de*

Keywords : inhomogeneous superconductors, stripes, nanoscale phase separation

Functional materials like high temperature superconductors (HTS) and complex oxides are characterized by an *intrinsic complexity*. Indeed, they show the coexistence of multiple striped-orders like Charge-Density-Wave (CDW), Spin-Density-Wave (SDW) and defects that get organized in different striped nano-domains and exhibit a strong dynamic competition. The study of the interplay among these multiple orders is challenging. The first step to understand the competition between these multiple striped orders is the investigation of their spatial-organization. On this purpose we developed a set of innovative techniques like scanning micro X-ray diffraction (μ XRD) and resonant scanning micro X-ray diffraction ($R\mu$ XRD) to directly visualize the spatial-organization of the SDW, CDW and defects nano-domains. By the use of μ XRD on several High temperature superconductors (HTS) we evidenced a common nanoscale phase separation scenario, characterized by the coexistence of competing scale-free networks of self-organized nano-domains promoting superconductivity [1-8]. Recently we discovered that the CDW stripes get self-organized in nano-domains defining a complex space available for the superconducting order [9], see Figure 1. In this process, the way how the nano-domains interact and evolve in time is still fundamental missing information. To study this process we used new experimental approaches that combine temporal and spatial resolution with bulk sensitivity like time-resolved X-ray Photon Correlation Spectroscopy (XPCS) [10]. Preliminary results show charge reorganization crossing the superconducting critical temperature [11].

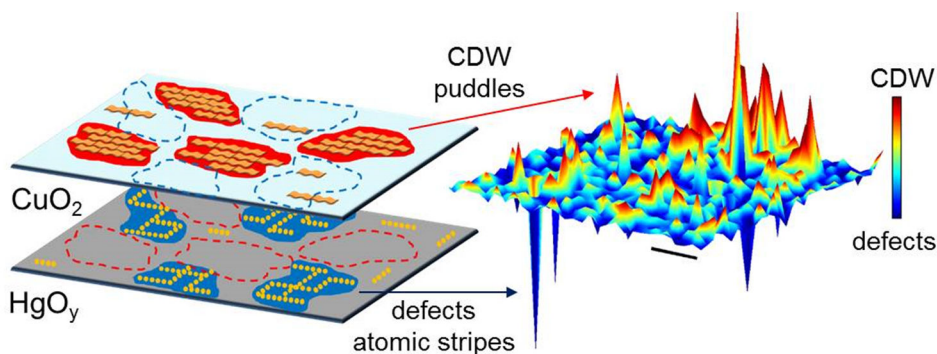


Figure 1. Anti-correlation between stripes and defects domains. (Left) The charge-stripes (CDW) rich areas (red) on the CuO_2 layers and defect-stripes rich areas (blue) on HgO_y layers. Spatial distribution of CDW and defects [9].

References

1. Y. Drees, et al., *Nature Communications* 5, 5731+ (2014)
2. A. Ricci, et al., *New Journal of Physics* 16, 053030+ (2014).
3. A. Ricci, et al., *Scientific Reports* 3, 2383+ (2013).
4. N. Poccia, et al., *Nature Materials*, 10, 733-736 (2011).
5. A. Ricci, et al., *Physical Review B* 84, 060511+ (2011).
6. A. Ricci, et al. *Physical Review B* 91.2 020503 (2015).
7. M. Fratini, et al., *Nature* 466, 841 (2010).
8. N. Poccia, et al., *Proceedings of the National Academy of Sciences* 109, 15685 (2012)
9. G. Campi, et al. *Nature* (in press the 17th of Sept 2015)
10. A. Ricci, *Journal of Superconductivity and Novel Magnetism* 1-4 (2014)
11. A. Ricci, et al. unpublished

Adjacent Fe – vacancy interactions s the Origin of room temperature Ferromagnetism in $(\text{In}_{1-x}\text{Fe}_x)_2\text{O}_3$



Alexander Moewes^{1*}, Robert Green^{1,2}

¹*University of Saskatchewan, Dept. of Physics, Saskatoon, SK S7N 5E2, Canada*

²*University of British Columbia, Quantum matter inst. Dept. of Physics & Astronomy, Vancouver, BC V6T 1Z1, Canada*

Email: * alex.moewes@usask.ca

Keywords: Spintronics, room temperature ferromagnetism and

vacancies

Dilute magnetic semiconductors (DMSs) show great promise for applications in spin-based electronics, but in most cases continue to elude explanations of their magnetic behavior. Here, we combine quantitative x-ray spectroscopy and Anderson impurity model calculations to study ferromagnetic Fe-substituted In_2O_3 films, and we identify a subset of Fe atoms adjacent to oxygen vacancies in the crystal lattice, which are responsible for the observed room temperature ferromagnetism. Using resonant inelastic x-ray scattering, we map out the near gap electronic structure and provide further support for this conclusion. Serving as a concrete verification of recent theoretical results and indirect experimental evidence, these results solidify the role of impurity-vacancy coupling in oxide-based DMSs [1].

References

1. R.J. Green, T.Z. Regier, B. Leedahl, J.A. McLeod, X.H. Xu, G.S. Chang, E.Z. Kurmaev, and A. Moewes, *Phys. Rev. Lett.* 115 , 167401 (2015).

Frustrated spin polarons and percolation in the electrostatically and chemically doped complex oxide LaCoO₃



Peter P. Orth^{1*}, Boris Shklovskii¹, Jeff Walter¹, Chris Leighton¹, Rafael M. Fernandes¹

¹*University of Minnesota, Minneapolis, MN, 55455, USA*

Email: * porth@umn.edu

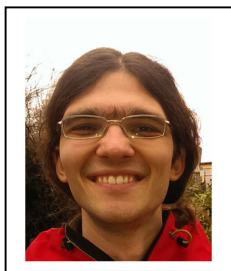
Keywords: complex oxides, percolation, frustrated magnetism

We investigate the role of spin polarons and magnetic frustration on the phase diagram of the chemically doped complex oxide La_{1-x}Sr_xCoO₃. Furthermore, stimulated by experimental advances in electrolyte gating methods, we examine theoretically percolation in thin films of inhomogeneous complex oxides, such as La_{1-x}Sr_xCoO₃(LSCO), induced by a combination of bulk chemical and surface electrostatic doping. Using numerical and analytical methods, we identify two mechanisms that describe how bulk dopants reduce the amount of electrostatic surface charge required to reach percolation: (i) bulk-assisted surface percolation, and (ii) surface-assisted bulk percolation. We show that the critical surface charge strongly depends on the film thickness when the film is close to the chemical percolation threshold. In particular, thin films can be driven across the percolation transition by modest surface charge densities *via* surface-assisted bulk percolation. If percolation is associated with the onset of ferromagnetism, as in LSCO, we further demonstrate that the presence of critical magnetic clusters extending from the film surface into the bulk results in considerable volume enhancement of the saturation magnetization, with pronounced experimental consequences. These results should significantly guide experimental work seeking to verify gate-induced percolation transitions in such materials.

Reference

1. P. P. Orth, R. M. Fernandes, J. Walter, C. Leighton, B. I. Shklovskii, arXiv :arXiv:1605.03463 (2016).

Superconducting percolation in the cuprates



Damjan Pelc*

¹*University of Zagreb, Faculty of Science, Department of Physics, Bijenička 32, HR-10000 Zagreb, Croatia*

Email: * dpelc@phy.hr

Keywords: superconductivity emergence, percolation, nonlinear conductivity, disorder

The superconducting emergence regime above the macroscopic T_c provides crucial information on both the normal and superconducting states and has long been the subject of controversy in the cuprate superconductors. We present a systematic investigation of the emergence of superconductivity in cuprates using nonlinear conductivity – a probe which eliminates background subtraction problems because the signal vanishes in the normal state. Through experiments on several cuprate families and throughout the phase diagram, we show that the regime above T_c is universally incompatible with the frequently evoked Ginzburg-Landau theory. Instead, it is dominated by disorder, irrespective of cuprate family or doping. A simple superconducting percolation model describes our results very well, allowing us to explain several conflicting results of previous investigations and create an overarching picture of charge carrier behavior in the cuprates, with disorder playing a crucial role.

Macroscopic character of composite high temperature superconducting wires

B.Spivak

¹*University of Washington*

spivak@uw.edu

“d-wave” symmetry of the superconducting order in the cuprate high temperature superconductors is a well established fact, and one which identifies them as “unconventional.” However, in macroscopic contexts – including many potential applications (i.e. superconducting “wires”) – the material is a composite of randomly oriented superconducting grains in a metallic matrix, in which Josephson coupling between grains mediates the onset of long-range phase coherence. Here, we analyze the physics at length scales large compared to the size of such grains, and in particular the macroscopic character of the long-range order that emerges. While XY-glass order and macroscopic d-wave superconductivity may be possible, we show that under many circumstances – especially when the d-wave superconducting grains are embedded in a metallic matrix – the most likely order has global s-wave symmetry. We also show that magnetic field may enhance superfluid density in the wires.

Exploring multi-component superconducting compounds by high pressure method and combinatorial solid state chemistry



Nikolai D. Zhigadlo^{1,2*}, S. Galeski¹, P.J.W. Moll^{1,3},
M. Iranmanesh², J. Hulliger², S. Katrych^{1,4}, R. Puzniak⁵, B.
Batlogg¹

¹Laboratory for Solid State Physics, ETH Zurich, Switzerland

²Department of Chemistry and Biochemistry, University of
Berne, Switzerland

³Max Planck Institute for Chemical Physics of Solids, Dresden,
Germany

⁴Institute of Condensed Matter Physics, Lausanne, Switzerland

⁵Institute of Physics, PAS, Warsaw, Poland

Email: * zhigadlo@phys.ethz.ch or nikolai.zhigadlo@dcb.unibe.ch

Keywords: high T_c , pnictides, cuprates, high pressure, combinatorial chemistry

In this talk we will provide some new insights into the materials synthesis and characterization of modern superconducting oxides. Two different approaches such as high-pressure, high-temperature method and combinatorial solid state chemistry will be presented with application to several typical examples. First, we highlight the key role of the extreme conditions in the growth of Fe-based superconductors, where a careful control of the composition-structure relation is vital for understanding the microscopic physics. The availability of high-quality $LnFeAsO$ ($Ln =$ lanthanide) single crystals with substitution of O by F, Sm by Th, Fe by Co, and As by P allowed us to measure intrinsic and direction-dependent superconducting properties, such as H_{c2} , J_c , and their anisotropies [1]. Moreover, we report for the first time on studies of anisotropic superconducting state properties of single crystals of $NdFeAsO_{1-x}OH_x$ with T_c as high as 45 K. We are going to show that the studied compound is characterized by very high in-plane upper critical field, caused most likely by formation of nonsuperconducting layers and shifting dimensionality of the studied material toward 2D (Fig. 1).

Then we demonstrate that combinatorial solid state chemistry is an efficient way to search for new superconducting compounds [2]. A single sample synthesis concept [3,4] based on multi-element ceramic mixtures can produce a variety of local products. Such a system needs local probe analyses and separation techniques to identify compounds of interest. We present the results obtained from random mixtures of Ca, Sr, Ba, La, Zr, Pb, Tl, Y, Bi and Cu oxides reacted at different conditions. By adding Zr but removing Tl, Y, and Bi the bulk state superconductivity got enhanced up to about 125 K. By magnetic separation superconducting grains in the size range of 50 to 300 μm were collected for further analyses (Fig. 2). Formation of several known and potentially new superconducting phases was observed. For the first time scanning

SQUID microscopy was applied to reveal micrometers large reaction centers showing superconductivity [2] within combinatorial ceramic samples.

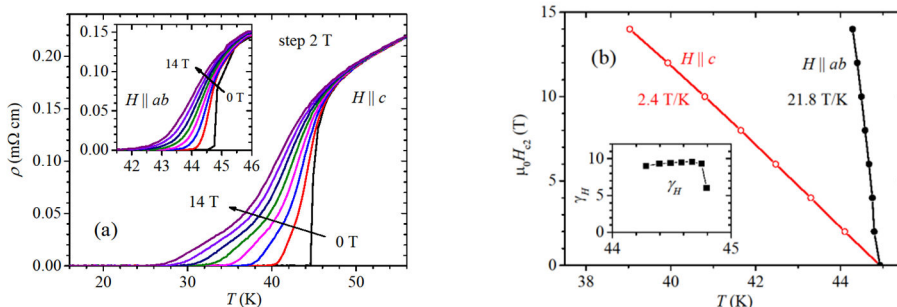


Figure 1: Temperature dependence of the resistivity and the upper critical field for $\text{NdFeAsO}_{1-x}\text{OH}_x$ single crystal with the field applied along the two principal directions. (a) Resistivity measured with the field applied perpendicular to the FeAs layers ($H||c$) are presented in the main panel and with the field parallel to them ($H||ab$) in the inset. (b) Temperature dependence of the upper critical field with $H||ab$ and $H||c$. To determine H_{c2} , the 50% ρ_n criterion was used. The inset shows temperature dependence of the upper critical field anisotropy defined as $\gamma_H = H_{c2}^{||ab}/H_{c2}^{||c}$.

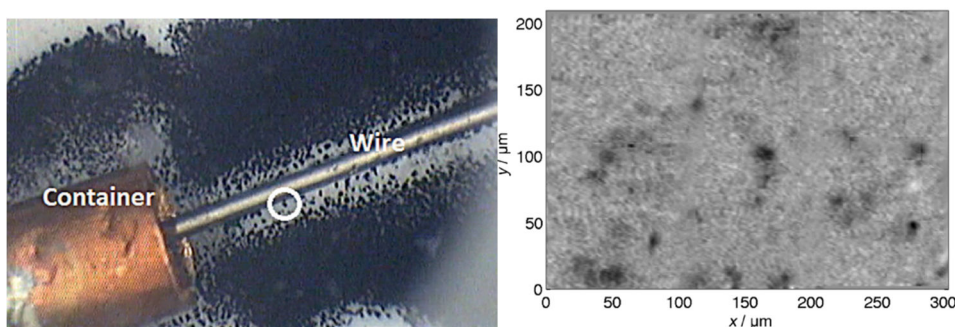


Figure 2: (Left panel) Demonstration of the capturing of superconducting particles by magnetic separation, perpendicular to a magnetized iron wire (AC field of 50 Hz and ZFC), moved into a container. (Right panel) Mosaic of scanning SQUID susceptometry images of a nine-element combinatorial sample at 100 K. Black regions feature the largest diamagnetic shielding, i.e. local formation of superconducting phases [2].

References

1. N.D. Zhigadlo, et al., Phys. Rev. B 82, 064517 (2010); 84, 134526 (2011); 86, 214509 (2012).
2. M. Iranmanesh, M. Stir, J.R. Kirtley, J. Hulliger, Chem. Eur. J. 20, 15816 (2014).
3. J. Hulliger, M.A. Awan, J. Comb. Chem. 7, 73 (2005).
4. J.B. Willems, et al., Solid State Sci. 11, 162 (2009).

Nonlocal Polarization Feedback in a Fractional Quantum Hall Ferromagnet



S. Hennel,^{1*} B. A. Bräm,¹ S. Baer,¹ L. Tiemann,¹ P. Sohi,¹ D. Wehrli,¹ A. Hofmann,¹ C. Reichl,¹ W. Wegscheider,¹ C. Rössler,¹ T. Ihn,¹ K. Ensslin,¹ M. S. Rudner,² and B. Rosenow³
¹*Solid State Physics Laboratory, ETH Zürich*
²*Center for Quantum Devices, Niels Bohr Institute, University of Copenhagen*
³*Institut für Theoretische Physik, Universität Leipzig*

Email: * hennels@phys.ethz.ch

Keywords: quantum Hall effect, spin phase transition, dynamic nuclear polarization

In a quantum Hall ferromagnet, the spin polarization of the two-dimensional electron system can be dynamically transferred to nuclear spins in its vicinity through the hyperfine interaction. The resulting nuclear field typically acts back locally, modifying the local electronic Zeeman energy. Here we report a nonlocal effect arising from the interplay between nuclear polarization and the spatial structure of electronic domains in a $\nu=2/3$ fractional quantum Hall ferromagnet with competing spin-polarized and spin-unpolarized ground states. In our experiments, we use a quantum point contact to locally control and probe the domain structure of different spin configurations emerging at the spin phase transition. Feedback between nuclear and electronic degrees of freedom gives rise to memristive behavior, where electronic transport through the quantum point contact depends on the history of current flow. We use NMR methods to investigate the time evolution of the electronic spin state within the QPC. We propose a model for this effect which suggests a novel route to studying edge states in fractional quantum Hall systems and may account for so-far unexplained oscillatory electronic-transport features observed in previous studies.

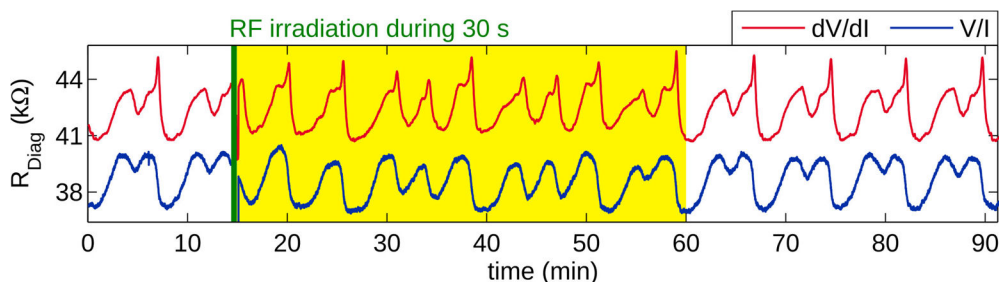


Figure 1: Time-periodic oscillations of the resistance measured across a QPC in the $\nu = 2/3$ state are observed in presence of a DC bias. The response to timed NMR pulses unveils the underlying evolution of electronic spin domains nucleating within the QPC.

References

1. S. Hennel, B. A. Bräm, S. Baer, L. Tiemann, P. Sohi, D. Wehrli, A. Hofmann, C. Reichl, W. Wegscheider, C. Rössler, T. Ihn, K. Ensslin, M. S. Rudner, and B. Rosenow, Phys. Rev. Lett. **116**, 136804 (2016)

On the theory of surface superconductivity in high magnetic fields for s- and d-wave pairing superconductor films.

Nils Schopohl

Institut für Theoretische Physik, Eberhard Karls-Universität Tübingen,
Auf der Morgenstelle 14, D-72076 Tübingen, Germany.

A theoretical study of the nucleation critical field B_{c3} of clean superconducting films in a parallel magnetic field is presented. Assuming specular reflection of quasiparticles at the back and at the top side of the film an exact integral equation for the nucleation pairing potential $\Delta(\mathbf{r})$ is derived on the basis of the Eilenberger equations of superconductivity. The solvability condition for the existence of a non trivial seed $\Delta(\mathbf{r})$ leads to an eigenvalue problem that determines the dependence of the nucleation critical field B_{c3} on temperature T and thickness L of the film. For d-wave pairing symmetry we determine first the nucleation critical field $B_{c3}(T)$ of a $[1\ 1\ 0]$ - orientated film as a function of L and show that the nodal orientation angle α of the d-wave pairing condensate relativ to the surface normal \mathbf{n} is a relevant parameter.

For $\alpha = \pi/4$ it is found that the nucleation field is approximately half the value it has for $\alpha = 0$.

Avalanches and hysteresis at the structural transition in stripe-ordered $\text{La}_{1.48}\text{Nd}_{0.4}\text{Sr}_{0.12}\text{CuO}_4$



Dragana Popović*

National High Magnetic Field Laboratory, Florida State University, Tallahassee, FL 32310, USA

Email: * dragana@magnet.fsu.edu

Keywords: structural transition, dynamics, cuprates, stripes

The coupling or intertwining of lattice, spin and charge orders and their effects on superconductivity are of great current interest in the physics of cuprates.[1] In particular, the low-temperature tetragonal (LTT) structure seems to stabilize static charge and spin stripes. The rare-earth-doped cuprate $\text{La}_{1.48}\text{Nd}_{0.4}\text{Sr}_{0.12}\text{CuO}_4$ (LNSCO), for example, exhibits a first-order structural phase transition (SPT) from the low-temperature orthorhombic (LTO) to the LTT phase, with the onset of the charge stripe order roughly coinciding with the SPT. In general, the dynamics of first-order phase transitions in the presence of disorder have been well studied, although some questions remain open. In the critical region, physical observables may exhibit hysteresis, return point memory, and a sequence of avalanches that link metastable states as the relevant field is tuned.[2,3] A previous study of the LTO-LTT transition in LNSCO by magnetoresistance (MR) measurements revealed hysteresis, which was attributed to a shift of the SPT temperature with an applied field.[4] However, the origin of the observed behavior was not well understood.

We carried out both in-plane and out-of-plane MR measurements around the LTO-LTT transition in LNSCO single crystals with magnetic fields H oriented both perpendicular and parallel to CuO_2 (ab) planes.[5] Hysteresis is observed for both field orientations, but for $H \parallel c$ we also find evidence for the existence of metastable states and collective dynamics in the form of avalanches and return point memory. Such behavior indicates that, in LNSCO, the LTO-LTT structural transition can be driven with H , and points to the existence of magnetostructural domains. A detailed analysis of the avalanche statistics is used to determine their size and field dependence, and to extract information about the domain structure and dynamics of domain walls. Our results shed light on the interplay of lattice, spin and charge degrees of freedom in stripe-ordered La-based cuprates.

This work was partially supported by NSF grant No. DMR-1307075 and NHMFL via NSF Cooperative Agreement DMR-1157490 and the State of Florida.

References

1. E. Fradkin et al., *Rev. Mod. Phys.* **87**, 457 (2015).
2. Eduard Vives and Antoni Planes, *Phys. Rev. B* **50**, 3839 (1994).
3. James P. Sethna et al., *Phys. Rev. Lett.* **70**, 3347 (1993).
4. Z. A. Xu et al., *Europhys. Lett.* **50**, 796 (2000).
5. P. G. Baity, G. Saraswat, T. Sasagawa, and D. Popović (unpublished).

First order quantum phase transitions



Mucio A. Continentino
Centro Brasileiro de Pesquisas Físicas

Email: *mucio@cbpf.br*

Keywords: quantum phase transitions, discontinuous transitions, critical exponents

We present a generalization of the scaling theory of quantum critical phenomena for discontinuous or first order quantum phase transitions [1]. As a test for our predictions, we consider fluctuation induced first order transitions, specifically the case of a superconductor coupled to the electromagnetic field [2]. While the neutral superfluid has a quantum critical point (QCP) associated with a superfluid-insulator transition, the charged one has a discontinuous zero temperature transition due to the coupling to the gauge field. At finite temperatures, above this transition, the superconductor obeys scaling laws governed by critical exponents associated with the QCP of the neutral superfluid. In particular the correlation length exponent is given by $\nu = 1/(d+z)$, where d is the dimensionality of the system and z the dynamic critical exponent associated with the QCP of the neutral superfluid. As temperature further decreases approaching zero, bubbles of superconducting regions start to form with a well-defined characteristic length. In this region the specific heat is thermally activated due to gapped excitations in bubbles of finite size [3]. We study other phase transitions where fluctuations arise from the proximity to another type of instability, for example the effect of superconducting fluctuations in an antiferromagnetic QCP [4]. Finally, we compare some exact results obtained for discontinuous zero temperature transitions with those of the scaling theory.

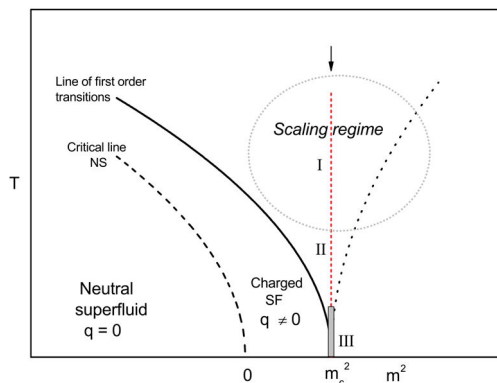


Figure 1: Phase diagram of a superconductor coupled to the electromagnetic field.

References

1. M.A. Continentino, A.S. Ferreira, *Physica A* 339, 461 (2004).
2. Mucio A. Continentino, *Quantum Scaling in Many-body Systems* , World Scientific, 2001.
3. M.A. Continentino, A.S. Ferreira, *Journal of Magnetism and Magnetic Materials* 310,828 (2007)
4. M. A. Continentino, to be published.

Bad-metal behavior and Mott quantum criticality



V. Dobrosavljevic

*Department of Physics and National High Magnetic Field
Laboratory, Florida State University, Tallahassee, Florida
32306, USA*

Email: *vlad@magnet.fsu.edu*

Keywords: Bad metal behavior, quantum criticality

Bad-metal (BM) behavior [1] featuring linear temperature dependence of the resistivity extending to well above the Mott-Ioffe-Regel (MIR) limit [2] is often viewed as one of the key unresolved signatures of strong correlation. Here we associate [3] the BM behavior with the Mott quantum criticality by examining a fully frustrated Hubbard model where all long-range magnetic orders are suppressed, and the Mott problem can be rigorously solved through dynamical mean-field theory. We show that for the doped Mott insulator regime, the coexistence dome and the associated first-order Mott metal-insulator transition are confined to extremely low temperatures, while clear signatures of Mott quantum criticality emerge across much of the phase diagram. Remarkable scaling behavior is identified for the entire family of resistivity curves, with a quantum critical region covering the entire BM regime, providing not only insight, but also quantitative understanding around the MIR limit, in agreement with the available experiments.

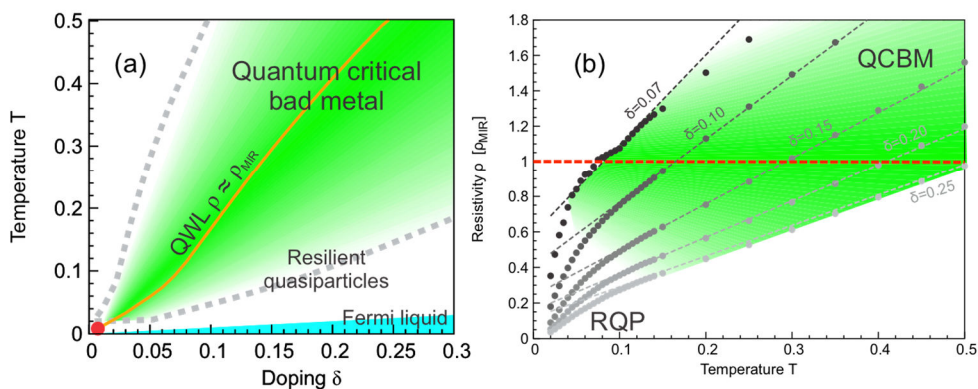


Figure 1: (a) DMFT phase diagram of the doped Mott insulator on a frustrated lattice. The bad metal (green) region matches perfectly the region of quantum critical scaling. (b) The bad metal regime features linear temperature dependence of resistivity with the slope roughly proportional to an inverse power law of doping, which we find to be a consequence of underlying quantum criticality.

References:

1. V. J. Emery and S. A. Kivelson, Phys. Rev. Lett. **74**,3253 (1995).
2. N. E. Hussey, K. Takenaka, and H. Takagi, Philos. Mag. **84**, 2847 (2004).
3. H. Terletska, J. Vucicevic, D. Tanaskovic, and V. Dobrosavljevic, Phys. Rev. Lett. **114**, 246402 (2015).

Plaquette Valence Bond Theory of Cuprate HTSC



A. Lichtenstein^{1*}, M. Harland¹, M. Katsnelson²

¹*University of Hamburg*

²*University of Nijmegen*

Email: * alichten@physnet.uni-hamburg.de

Keywords: high T_c , plaquette-clusters, shell structure

We present a strong-coupling approach [1] to theory of High-Temperature Superconductivity based on an observation of quantum critical point in the plaquette within t, t' Hubbard model with the crossing of ground state energies in $N=2,3,4$ sectors for parameters closed to the optimal doping. The theory predict the maximum of $d_{x^2-y^2}$ wave order parameter at the border between localized and itinerant electron behavior [2] and gives a natural explanation of the pseudo-gap formation via soft-fermion mode related to local singlet states of the plaquette in the environment.

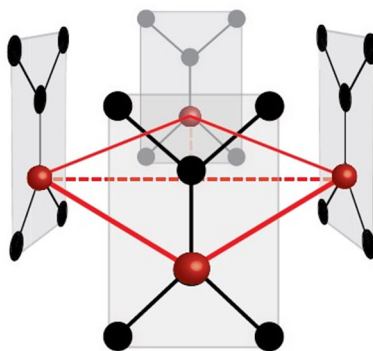


Figure 1: Sketch of a plaquette-Bethe lattice with connectivity $q=2$

References

1. A. I. Lichtenstein and M. I. Katsnelson, Phys. Rev. B 62, R9283 (2000)
2. M. Harland, M. I. Katsnelson, and A. I. Lichtenstein, arXiv:1604.01808

Scattering rate and carrier density throughout the phase diagram of the cuprates



N. Barišić*

Institute of Solid State Physics, Vienna University of Technology, 1040 Vienna, Austria

Email: * neven.barisic@tuwien.ac.at

Keywords: cuprates, scattering rate, carrier density

The enigmatic “strange-metal” phase of the cuprates remains one of the major puzzles in condensed matter physics. Numerous unconventional electronic scattering mechanisms have been proposed, and it has been suggested by many that Landau’s remarkably successful quasiparticle paradigm should be abandoned. In a series of papers, we demonstrated that, deep in the pseudogap (PG) regime, the nature of charge carriers is in fact best described as a Fermi liquid (FL): the scattering rate is quadratic in both temperature [1] and frequency [2], and Kohler’s rule for the magnetoresistance is obeyed [3]. Starting from this well-documented PG/FL state, we subsequently demonstrated that the transport scattering rate remains quadratic in temperature even in the strange-metal phase and, importantly, that this quantity is doping and compound independent, and hence universal [4]. We have thus been able to quantitatively connect the well-accepted FL properties at high doping with those recently established deep in the PG phase, and to demonstrate that the strange-metal phase hosts hidden FL behaviour and is not so strange after all. When interpreted in a simple, logical manner, our findings have several significant implications [4]: (i) the well-known temperature dependence of the Hall effect in the strange-metal phase mandates a conventional interpretation, namely a temperature-dependent carrier density; (ii) the PG phenomenon signifies the gradual localization of one hole per unit cell upon cooling; (iii) the mysterious T -linear resistive behaviour in the strange-metal phase is the result of a FL T^2 scattering rate combined with a T -linear increase in carrier density.

References

1. N. Barišić et al., Proc. Natl. Acad. Sci. U.S.A. 110, 12235 (2013)
2. S. I. Mirzaei et al., Proc. Natl. Acad. Sci. U.S.A. 110, 5774 (2013)
3. M. K. Chan et al., Phys. Rev. Lett. 113, 177005 (2014)
4. N. Barišić et al., arXiv: 1507.07885 (2015)

Fluctuation-driven helical magnetic order near criticality



G. Abdul-Jabbar¹, D.A. Sokolov¹, C. O'Neill¹, C. Stock¹, D. Wermeille², F. Demmel³, F. Krüger^{3,4*}, A. G. Green⁴, F. Levy-Bertrand⁵, B. Grenier⁶, and A. Huxley¹

¹*University of Edinburgh*

²*ESRF Grenoble*

³*ISIS, U.K.*

⁴*University College London*

⁵*CNRS Grenoble*

⁶*Universite Grenoble Alpes & CEA*

Email: *f.kruger@ucl.ac.uk

Keywords: strongly correlated electrons, quantum criticality, magnetism, complex ordering

Fluctuations around quantum critical points are known to be responsible for many unexpected phenomena, e.g. the discontinuous phase transitions seen in itinerant ferromagnets at low temperatures. Such fluctuation-induced first-order behaviour is a consequence of the interplay between magnetic order parameter and soft electronic particle-hole fluctuations.

Using a fermionic version of the quantum order-by-disorder mechanism, we demonstrate that the ferromagnetic quantum critical point is unstable towards the formation of incommensurate spiral order [1,2]. The key idea is that certain deformations of the Fermi surface associated with the onset of competing order enlarge the phase space available for low-energy particle-hole fluctuations and self-consistently lower the free energy. This reveals a new way to achieve complex, spatially modulated order, not requiring Fermi-surface nesting, breaking of inversion symmetry, or frustration. We apply this theory to PrPtAl where spiral order on the border of ferromagnetism is observed in neutron and x-ray scattering experiments. In this system, the coupling of the itinerant electrons to the local Pr(3+) moments leads to magnetic anisotropies which have characteristic experimental consequences [3].

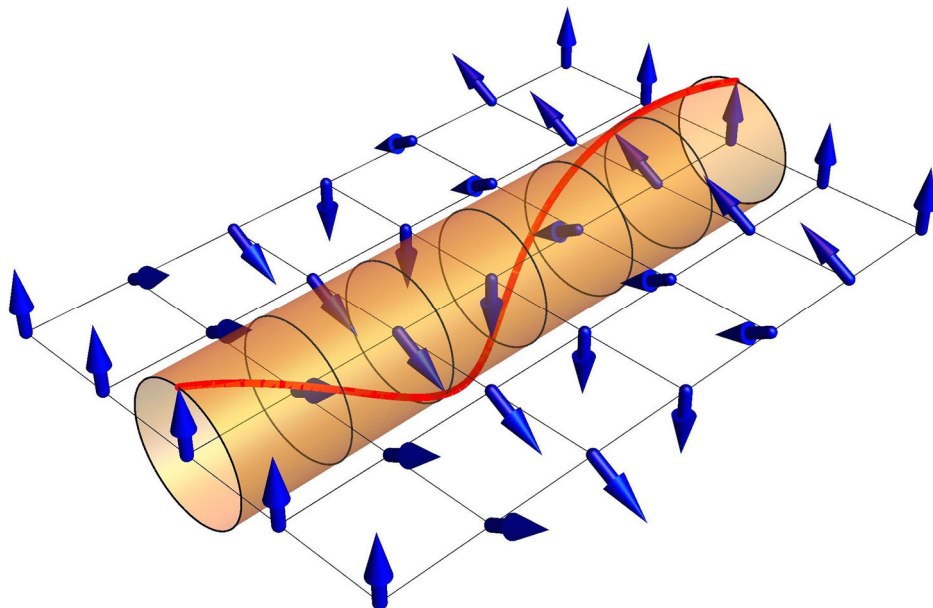


Figure 1: Illustration of spatially modulated, helical magnetic order. Such states have been predicted to form as a consequence of electronic quantum fluctuations if ferromagnetic phase transitions are tuned to very low temperatures. The complex spiral magnetic states observed in PrPtAl provide the first example of such a fluctuation-driven phase.

References

1. U. Karahasanovic, F. Kruger, and A.G. Green, *Phys. Rev. B* **85**, 165111 (2012);
2. C.J. Pedder, F. Kruger, and A.G. Green, *Phys. Rev. B* **88**, 165109 (2013);
3. G. Abdul-Jabbar, D. Sokolov, D. Wermeille, C. Stock, F. Demmel, F. Kruger, A.G. Green, and A. Huxley, *Nature Physics* **11**, 321 (2015).

Above-room-temperature formation of the magnetic skyrmion in β -Mn-type chiral magnets



Y. Tokunaga^{1,2*}, X.Z. Yu², J. S. White³, H. M. Rønnow^{4,2}, D. Morikawa², Y. Taguchi² & Y. Tokura^{2,5,1} *Department of Advanced Materials Science, University of Tokyo, Kashiwa, Chiba 277-8561, Japan*

²*RIKEN Center for Emergent Matter Science (CEMS), Wako, Saitama 351-0198, Japan*

³*Laboratory for Neutron Scattering and Imaging, Paul Scherrer Institut, CH-5232 Villigen, Switzerland*

⁴*Laboratory for Quantum Magnetism (LQM), École*

Polytechnique Fédérale de Lausanne (EPFL), CH-1015 Lausanne, Switzerland

⁵*Department of Applied Physics, University of Tokyo, Bunkyo-ku, Tokyo 113-8656, Japan*

Email: * y-tokunaga@k.u-tokyo.ac.jp

Keywords: skyrmion, helimagnet, magnetic nanostructures

Magnetic skyrmions are nanometric particle-like objects in magnets whose stability is topologically protected due to their vortex-like spin structures, and therefore have recently attracted increasing attention from the viewpoints of possible technological applications for spintronics, as well as their interesting emergent electro-magnetic responses[1]. Indeed, those in metallic systems had been shown to be controllable by low electrical current excitation, both experimentally[2,3] and theoretically[4], and thus proved to be very promising for the application to ultra-low power consumption high-density memory that can use one skyrmion as one information unit. For that purpose, skyrmions in the magnets with crystal chirality as mediated by Dzyaloshinskii-Moriya interaction are preferable due to their smallness in size (typically $< \sim 150$ nm) and unique helicity (spin-swirling direction in the vortex). However, skyrmions in chiral magnets have so far been observed only below room temperature and limited to a single class of materials, namely, B20-type (MnSi-type) alloys[5,6]. Toward technological applications, it has been crucial to overcome these limitations.

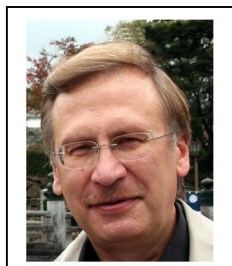
In this presentation, I will demonstrate the formation of skyrmions with unique spin helicity at and above room temperature in a new class of cubic chiral magnets, namely β -Mn-type Co-Zn-Mn alloys with a different chiral space group from that of B20 compounds. Combined investigations in terms of Lorentz transmission electron microscopy, magnetization, and small angle neutron scattering measurements unambiguously reveal the formation of the skyrmion crystal under the application of magnetic field in both thin-plate (thickness $< \sim 150$ nm) and bulk forms[7]. Our findings demonstrate the possibility that new skyrmion-hosting systems can be found in a variety of non-centrosymmetric crystal symmetries, which will stimulate further

experimental exploration of other realization. Likewise, our discovery of stable skyrmion beyond room temperature overcomes a key difficulty in integrating the skyrmions into technological spintronics devices and applications.

References

1. N. Nagaosa. & Y. Tokura, Nat. Nanotech. 8, 899 (2013).
2. F. Jonietz et al., Science 330, 1648 (2010).
3. X. Z. Yu, et al., Nat. Commun. 3, 988 (2012).
4. J. Iwasaki et al., Nat. Commun. 4, 1463 (2013).
5. S. Mühlbaue. et al., Science 323, 915 (2009).
6. X. Z. Yu et al., Nature 465, 901 (2010).
7. Y. Tokunaga et al., Nat. Commun., 6, 7635 (2015).

Possible magnetic field induced hidden order in the low-dimensional quantum magnet LiCuSbO_4



V. Kataev^{1,*}, H.-J. Grafé¹, M. Iakovleva^{1,2}, E. Vavilova², A. Alfonsov¹, H. Nojiri³, M.-I. Sturza¹, S. Wurmehl¹, S. Nishimoto¹, S.-L. Drechsler¹, U. Rößler¹, H. Rosner⁴, B. Büchner¹

¹ Leibniz Institute for Solid State and Materials Research IFW, Dresden, D-01069, Dresden, Germany

² Zavoisky Physical Technical Institute, RAS, 420029, Kazan, Russia

³ Institute of Materials Research, Tohoku University, 980-8577, Sendai, Japan

⁴ Max Planck Institute for Chemical Physics of Solids, D-01187 Dresden, Germany

Email: * v.kataev@ifw-dresden.de

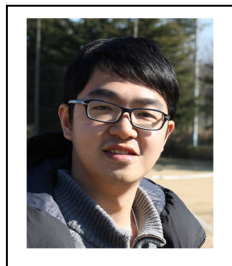
Keywords: high T_c, nano-clusters, shell structure, [Times 11]

Quantum spin-1/2 networks in reduced spatial dimensions are predicted to exhibit a plethora of novel ground states beyond classical ferro- or antiferromagnetic phases. The quest for experimental realizations of such theoretical models is majorly focused on complex transition metal (TM) oxides where magnetic coupling between the spins of the TM ions can be confined to one or two spatial directions. In this talk, I will review our recent results of high-field NMR and sub-THz ESR studies of the quantum magnet LiCuSbO_4 (LCSO). In this material Cu^{2+} ions ($S = 1/2$) are exchange coupled along the crystallographic a-axis and form well-isolated frustrated one-dimensional Heisenberg spin chains. Absence of a long-range magnetic order down to sub-Kelvin temperatures is suggestive of the realization of a quantum spin liquid state [1]. Our NMR and ESR measurements in strong magnetic fields up to 16 Tesla reveal clear indications for the occurrence of a new field-induced hidden phase which is likely to be of the multipolar character. A relationship of our experimental findings with recent theories of low-dimensional quantum spin magnets will be discussed.

References

1. S. E. Dutton, M. Kumar, M. Mourigal, Z. G. Soos, J.-J. Wen, C. L. Broholm, N. H. Andersen, Q. Huang, M. Zbiri, R. Toft-Petersen, and R. J. Cava, Phys. Rev. Lett. **108**, 187206 (2012)

Fractional Flux Plateau in Magnetization Curve of Multiband Superconductor Loop



Zhao Huang^{1*}, Xiao Hu^{2*}

¹*Research and Education Center for Natural Sciences, Keio University, Yokohama, Japan*

²*International Center for Materials Nanoarchitectonics (WPI-MANA), National Institute for Materials Science, Tsukuba, Japan*

Email: * huangzhaophysics@gmail.com, hu.xiao@nims.go.jp

Keywords: multiband superconductivity, vortex, fractional flux, time-reversal symmetry

Multiband superconductivity has become a prominent issue since the discovery of superconductivity in MgB₂ and iron pnictides. One interesting aspect is the interband couplings which results in nontrivial phase differences between gap functions. When there are three or more bands, repulsive couplings can induce a frustrated state where phase differences among order parameters are neither 0 nor π , leading to broken time-reversal symmetry [1, 2].

In this talk, we present our study on the magnetic response of this time-reversal-symmetry-broken (TRSB) state. We consider a superconductor loop where two halves are occupied by degenerate time-reversal-symmetry-broken (TRSB) states with opposite chiralities as shown in Fig. 1, where two domain walls with phase kinks appear at joint region-I and II. When the phase kinks are different, meaning that, for example, in region-I ψ_1 and ψ_2 form a phase kink while in region-II ψ_2 and ψ_3 form a phase kink (see Fig. 1), there is a 2π winding only in ψ_2 around the whole loop [3]. This yields a fractional flux $\eta\Phi_0$ ($0 < \eta < 1$) in the loop. The state with a fractional flux trapped in this loop is stable in a certain range of external magnetic field, leading to a fractional flux plateau in magnetization curve, which can be used as a unique phase sensitive probe for the TRSB state.

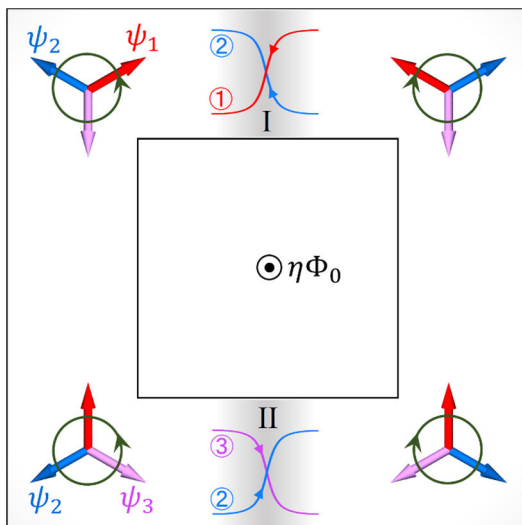


Figure 1: Schematic setup with a loop of TRSB superconductor, where the two halves are occupied by the two degenerate states with opposite chiralities. The three arrows denote the phases of order parameters and the circle indicates the chirality. Between the two halves of the loop there are two domain wall I and II accommodating interband phase kinks. Phase kinks between two different pairs of order parameters can trap a fractional flux.

References

1. X. Hu and Z. Wang, Phys. Rev. B 85, 064516 (2012). DOI: 10.1103/PhysRevB.85.064516
2. Z. Huang and X. Hu, Appl. Phys. Lett. 104, 162602 (2014). DOI: 10.1063/1.4872261
3. Z. Huang and X. Hu, Phys. Rev. B 92, 214516 (2015). DOI: 10.1103/PhysRevB.92.214516

BETS-based organic conductors as archetypical antiferromagnetic/superconducting nanostructures



M. V. Kartsovnik^{1,*}, M. Kunz^{1,2}, L. Schaidhammer^{1,2},
F. Kollmannsberger^{1,2}, W. Biberacher¹, N. D. Kushch³,
A. Miyazaki⁴, H. Fujiwara⁵

¹*Walther-Meißner-Institut, Garching, Germany*

²*Technische Universität München, Garching, Germany*

³*Institute of Problems of Chemical Physics, Chernogolovka, Russian Federation*

⁴*University of Toyama, Toyama, Japan*

⁵*Osaka Prefecture University, Osaka, Japan*

Email: * mark.kartsovnik@wmi.badw.de

Keywords: organic conductors; superconductivity and magnetism; correlated electrons; magnetic quantum oscillations

Thanks to high crystal quality, relatively simple conduction band structures, and very good tunability between various electronic states, organic charge transfer salts can often serve as model systems for studying correlated electron physics. In particular, the family of bis(ethylenedithio)tetraselenafulvalene (BETS) salts containing transition-metal ions like Fe^{3+} , Mn^{2+} , Cu^{2+} , etc. represents perfect natural nanostructures with alternating single-molecular conducting and magnetic layers, see, e.g., Fig. 1(a). The charge transport in such compounds is provided by delocalized π -electrons of fractionally charged BETS donors, whereas magnetic properties are dominated by localized d -electron spins in the insulating anionic layers. While the latter usually undergo antiferromagnetic (AF) ordering at low temperatures, the ground state of the π -electron system is determined by a subtle balance between different instabilities of the normal metallic state and is particularly sensitive to the interlayer π - d exchange interaction.

In the best-studied member of this family, λ -(BETS)₂FeCl₄, the low- T metal-insulator transition is triggered by the AF ordering in the anionic layers [1]. Moreover, at high magnetic fields where the AF insulating state is suppressed, the π - d interaction leads to a fascinating field-induced superconducting (SC) state. In the κ -(BETS)₂FeCl₄ salts, differing from the former by the structure of the BETS layers, the π - d interaction is weaker. As a result, they preserve metallic properties and even become SC below the Néel temperature [1]. However, the magnetic ordering has a strong impact on the conduction system: the consequences are readily reflected in a peculiar behavior of magnetoresistance and especially the magnetic quantum oscillations [Fig. 1(b)]. Interestingly, the AF order in the anion layers seems to even support superconductivity in a magnetic field. For a certain field direction the SC state is extended till the AF

phase boundary on the phase diagram, see Fig. 1(c), disappearing exactly at the boundary.

A further example of a hybrid conducting/magnetic system is κ -(BETS)₂Mn[N(CN)₂]₃ [2]. We argue that, by contrast to the previous compounds, here the ground state is primarily dictated by electron correlations within the BETS layers. The system undergoes a Mott transition resulting in localization and AF ordering of the itinerant π -electrons. The Mn²⁺ spin system forms a frustrated triangular lattice and therefore shows no long-range antiferromagnetism. However, a short-range order does appear below the Mott transition and is obviously induced by the coupling with the ordered π -electron spins [3]. At a rather low pressure of ~ 0.5 kbar the compound undergoes a first-order transition into a metallic/SC state, in which the π - d interaction is reflected in the interlayer magnetotransport.

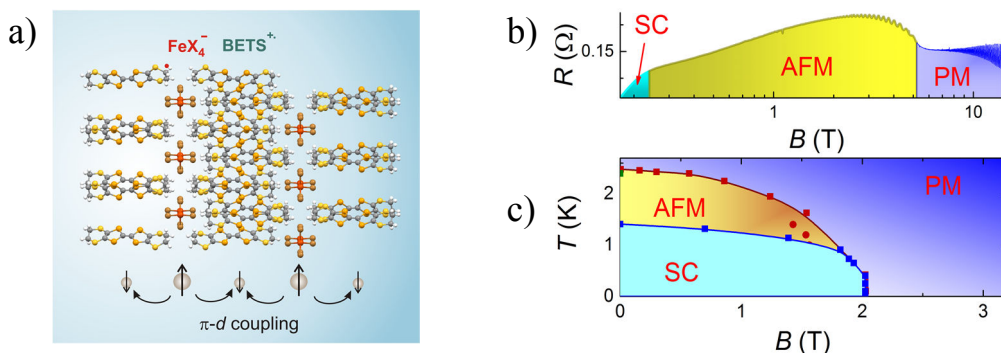
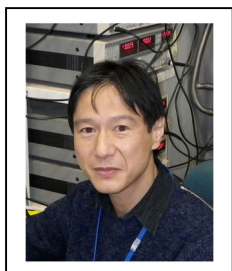


Figure 1: a) Crystal structure of κ -(BETS)₂FeX₄ (where X = Cl or Br) and cartoon of the AF π - d exchange interaction; b) low- T magnetoresistance of the X=Br salt at $B \perp$ layers, including quantum oscillations, throughout different electronic states; c) phase diagram of the X=Br salt for $B \parallel$ layers; note that the border of the AF and SC states coincide at low temperatures.

References

1. H. Kobayashi, H. B. Cui, and A. Kobayashi, Chem. Rev. **104**, 5265 (2004). doi: 10.1021/cr030657d.
2. N. D. Kushch, E. B. Yagubskii, M. V. Kartsovnik, et al., J. Am. Chem. Soc. **130**, 7238 (2008). doi: 10.1021/ja801841q.
3. O. M. Vyaselev, M. V. Kartsovnik, N. D. Kushch, and E. B. Yagubskii, JETP Lett. **95** 565 (2012) 565. doi: 10.1134/S0021364012110100.

FeSe under high pressure: phase diagram and electronic structure



Taichi Terashima

National Institute for Materials Science, Tsukuba, Japan

Email: *TERASHIMA.Taichi@nims.go.jp

Keywords: iron-based superconductors, high pressure, phase diagram, Fermi surface

FeSe is unique among iron-based superconductors. At ambient pressure, it exhibits a tetragonal-to-orthorhombic structural phase transition like iron-arsenide parent compounds LaFeAsO and BaFe_2As_2 , but, unlike them, FeSe does not order magnetically. This is rather puzzling if the structural transition is due to spin nematicity. This has therefore caused considerable debate [1].

We have recently found an anomaly in the temperature dependence of electrical resistivity in FeSe under high pressure, which is most likely associated with a pressure-induced antiferromagnetic transition previously suggested by μSR measurements [2]. The determined phase diagram (Fig. 1 [3]) is at odds with spin-nematic scenarios predicting that the magnetic phase is enclosed by the nematic one.

Our previous Shubnikov-de Haas (SdH) measurements on FeSe at ambient pressure indicated that the Fermi surface is strikingly different from that predicted by band-structure calculations, the carrier density being one order-of-magnitude smaller than predicted [4]. We have recently extended SdH measurements to high pressure [5]. We have found that the SdH oscillations change abruptly at the onset of the pressure-induced antiferromagnetism, suggesting that the Fermi surface is reconstructed by the antiferromagnetic order. In order to support this conclusion, analyses of magnetotransport data under high pressure will also be presented in the talk.

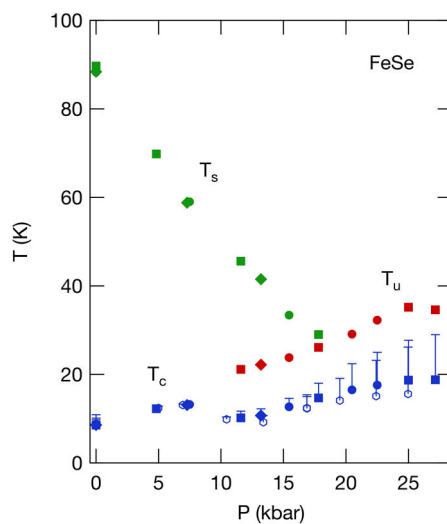


Figure 1: High-pressure phase diagram of FeSe [3]. Structural transition at T_s , unknown but most likely antiferromagnetic transition at T_u , and superconducting transition at T_c .

References

1. See for example, R. M. Fernandes *et al.*, Nature. Phys. **9**, 536 (2013).
2. M. Bendele *et al.*, Phys. Rev. Lett. **104**, 087003 (2010); Phys. Rev. B **85**, 064517(2012).
3. T. Terashima *et al.*, J. Phys. Soc. Jpn. **84**, 063701 (2015).
4. T. Terashima *et al.*, Phys. Rev. B **90**, 144517 (2014).
5. T. Terashima *et al.*, arXiv:1510.01840.

Change of carrier density at the pseudogap critical point of a cuprate superconductor

Wojciech Tabis^{1,2*}

¹*Laboratoire National des Champs Magnétiques Intenses, Toulouse, France*

²*AGH University of Science and Technology, Faculty of Physics and Applied Computer Science, 30-059 Krakow, Poland*

Email: * wojciech.tabis@lncmi.cnrs.fr

Keywords: high T_c , Hall effect, pseudogap, CDW

The pseudogap is a partial gap that opens in the normal state of cuprate superconductors whose origin is a long-standing puzzle. Its connection to the Mott insulator at low doping p remains ambiguous and its relation to the charge order that reconstructs the Fermi surface at intermediate p is still unclear. I will report measurements of the Hall coefficient in magnetic fields up to 88 T, which revealed that Fermi-surface reconstruction by charge order in YBCO ends sharply at a critical doping $p = 0.16$, distinctly lower than the pseudogap critical point at $p^* = 0.19$ [1]. This shows that pseudogap and charge order are separate phenomena. We find that the change of carrier density from $n = 1 + p$ at high p to $n = p$ at low p starts at p^* [1]. This sharp loss of 1.0 carrier per Cu atom is a new signature of the pseudogap. I will discuss some possible underlying mechanisms.

References

1. S. Badoux *et al.*, *Nature* **531**, 210 (2016).

Direct-space and real-time observation of quantum phenomena in plasmonic nanostructures



Fabrizio Carbone^{1*}

¹*EPFL, Lausanne Switzerland*

Email: * fabrizio.carbone@epfl.ch

Keywords: femtosecond, plasmons, nano-structures, Transmission Electron Microscopy

The collective motion of carriers at the surface of metals and its coupling with an electromagnetic field, enables the propagation of so called Surface Plasmon Polaritons (SPP) in confined spaces, which can be smaller than the wavelength of the field itself. Highly confined guided waves hold promise for applications and are an interesting tool for the investigation of fundamental aspects of quantum mechanics and condensed matter physics. In fact, their microscopic nature results from a subtle interplay between the material's electronic structure and the electro-magnetic field.

SPPs have been shown to share several of the quantum properties of light; entanglement between individual SPPs has been demonstrated, as well as two plasmons quantum interference and the wave-particle duality, to name a few. Recently, ultrafast transmission electron microscopy has been shown to be able to film the evolution SPPs in space and time with nm and femtosecond resolution.

In this seminar, we review some of these results and show that this technique can provide a unique observation angle on the quantum properties of SPPs. We also show that the spatial and temporal properties of a plasmonic near-field can be engineered using light excitation as a control parameter.

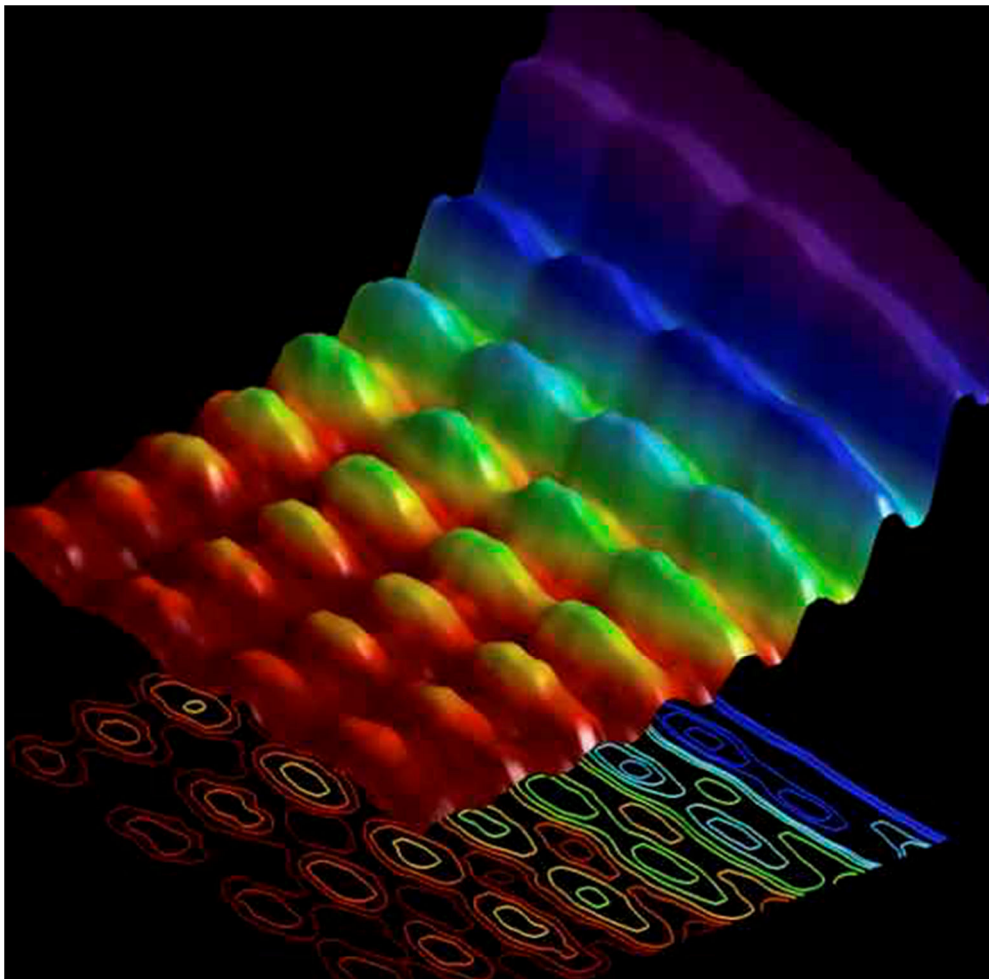


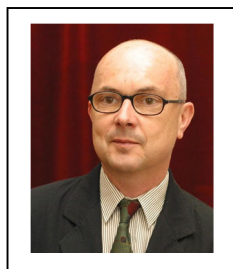
Figure 1: Energy-Space map of the interaction between one electron and a discrete number of surface plasmons confined on the surface of one Ag nanowire (1).

References

1. L. Piazza et al., Nat. Commun. 6, 6407 (2015).

G1

Interplay between superconductivity and charge density waves in Cu_xTiSe_2



Z. Medvecká¹, Z. Pribulová¹, P. Szabó¹, J. Kačmarčík¹, T. Klein², F. Levy², B. Michon², C. Marcenat², V. Cambel³, J. Šoltýs³, M. Iavarone⁴, G. Karapetrov⁵, P. Samuely^{1*}

¹*Centre of Ultra Low Temperature Physics @ Institute of Exp. Physics SAS and Šafárik University, Košice, Slovakia*

²*Université Grenoble Alpes, I. Néel CNRS, Grenoble, France*

³*Inst. Electrical Engineering SAS, Bratislava, Slovakia*

⁴*Temple University, Philadelphia, PA, USA*

⁵*Drexel University, Philadelphia, PA, USA*

Email: *samuely@saske.sk

Keywords: competing orders, superconductivity, CDW, quantum critical point

$1T - \text{TiSe}_2$ has been long known as the system with a CDW order below 200 K. Recently it was shown that CDW is gradually suppressed and superconductivity introduced by intercalation with Cu [1] or under pressure [2]. The questions on interplay between the superconductivity and chiral [3] CDW, the exact position of the quantum critical point, on the character of superconducting order parameter [4] and general superconducting properties [5] in Cu_xTiSe_2 single crystals in the whole doping range from the underdoped to overdoped regime will be addressed. The results of the subKelvin STM, the ac microkalorimetry, and the local Hall-probe magnetometry will be discussed.

References

1. E. Morosan, Nature Phys. 2, 544 (2006).
2. A. F. Kusmartseva, et al., Phys. Rev. Lett. 103, 236401 (2009)
3. M. Iavarone, et al., Phys. Rev. B 85, 155103 (2012).
4. J. Kačmarčík, et al., Phys. Rev. B 88, 020507(R) (2013).
5. P. Husaniková, et al. Phys. Rev. B 88, 174501 (2013).

Macroscopic quantum phenomena in spin filter ferromagnetic Josephson junctions



D. Massarotti^{1,2,3*}, R. Caruso^{1,2}, A. Pal⁴, D. Stornaiuolo^{1,2}, G. P. Pepe^{1,2}, G. Rotoli³, L. Longobardi^{3,5}, M. G. Blamire⁴, F. Tafuri^{2,3}

¹*Dipartimento di Fisica, Universita' Federico II di Napoli, Italy*

²*CNR-SPIN UOS Napoli, Italy*

³*Dipartimento di Ingegneria Industriale e dell'Informazione, Seconda Universita' di Napoli, Italy*

⁴*Department of Materials Science and Metallurgy, University of Cambridge, Cambridge, UK*

⁵*American Physical Society, 1 Research Road, Ridge, New York 11961, USA*

Email: * dmassarotti@na.infn.it

Keywords: Ferromagnetic Josephson junctions, phase dynamics, macroscopic quantum phenomena

A ferromagnetic Josephson junction (JJ) represents a special class of hybrid system where different ordered phases meet and generate novel physics. Spin filter NbN/GdN/NbN JJs represent the first junctions incorporating ferromagnetic-insulator tunnel barriers [1]. In these junctions the gadolinium nitride barrier generates spin-filtering properties and a dominant second harmonic component in the current-phase relation [2]. These features make spin filter junctions quite interesting also in terms of fundamental studies on phase dynamics and dissipation, since they are expected to provide further insights on transport processes through spin aligned triplet Cooper pairs. We will discuss the fingerprints of spin filter JJs through complementary transport measurements, and their implications on the phase dynamics, through measurements of switching current distributions. We demonstrate the first evidence for macroscopic quantum tunneling in ferromagnetic JJs [3], giving promise for the application of spin filter junctions in quantum hybrid circuits.

Finally, we compare the phase dynamics of spin filter JJs with the phase dynamics of both conventional low T_c NbN JJs and high T_c YBCO grain boundary junctions, in order to learn additional information on the relation between dissipation and different micro-structural configurations of the barrier.

References

1. K. Senapati, et al. *Nature Materials* 10, 849-852 (2011). doi:10.1038/nmat3116.
2. A. Pal, et al. *Nature Communications* 5, 3340 (2014). doi:10.1038/ncomms4340.
3. D. Massarotti, et al. *Nature Communications* 6, 7376 (2015). doi:10.1038/ncomms8376.

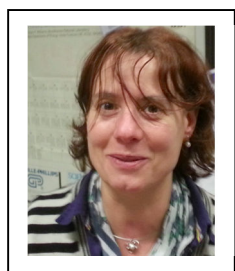
Non-volatile electrical and optical resistive switching in 2D electron gases at oxide heterostructures

Fabio Miletto Granozio
CNR-SPIN, Napoli, Italy

Email: fabio.miletto@spin.cnr.it

The combined effect of a back-gate voltage and of light was analyzed on a number of oxide heterostructures exhibiting interfacial 2DEGs, including $\text{LaAlO}_3/\text{SrTiO}_3$ and $\text{LaGaO}_3/\text{SrTiO}_3$. The strong hysteresis found in the plots of the 2DEG resistivity as a function of the gate voltage, suggestive of a ferroelectric-like behavior of the SrTiO_3 barrier, is analyzed.

We show that an appropriate procedure based on single gate-voltage pulses, applied below 100K, can drive our lowest-carrier-density samples to an insulating state, which is persistent in zero gate voltage and dark. This state can be destroyed by a relatively modest dose of visible-range photons, which cause a sudden collapse of the system back to the metallic ground state, with a resistivity decrease exceeding four orders of magnitude. The system is repeatedly switchable between the ON and OFF states by the alternate application of voltage and light pulses. Different intermediate resistance states can be stabilized by a proper tuning of the control parameters, hinting some potential for the design of multilevel devices. A model describing our findings in terms of a controlled electron transfer between mobile and localized interfacial states is proposed. We show that the actual device resistance depends on the history of the gate current and of the photon flux. The analogy with memristive devices is discussed.

$\sqrt{3}\times\sqrt{3}$ -Multilayer Silicene/Ag(111) or $\sqrt{3}\times\sqrt{3}$ -Ag/Si(111)7×7?

Paola De Padova*

^{*1} *Consiglio Nazionale delle Ricerche
Istituto di Struttura della Materia
Via Fosso del Cavaliere 100, 00133 Roma, Italy
Aix-Marseille Université, CNRS, PIIM UMR 7345, 13397
Marseille cedex, France*

Email: * Paola.DePadova@ism.cnr.it

Keywords: Multilayer silicene, LEED, AES, RAMAN, GIIXRD

After the synthesis of single layer silicene on different substrates [1], multilayer silicene was synthesized in situ under ultra high vacuum (UHV) on silver (111) surfaces [2]. These films show a honeycomb $\sqrt{3}\times\sqrt{3}R(30^\circ)$ surface structure, with respect to 1×1 silicene, as observed in Scanning Tunnelling Microscopy (STM) and reflected in Low Energy Electron Diffraction patterns (LEED) [2]. This $\sqrt{3}\times\sqrt{3}R(30^\circ)$ phase was first observed by Feng *et al.* [3] as arising from second, third and all upper silicene layers [2], although at present there is a debate on the possibility that the multilayer silicene is indeed thin film of bulk-like silicon [4].

Here we report the AES/LEED, Raman spectroscopy and grazing incidence in-plane x-ray diffraction (GIIXRD) measurements from $\sqrt{3}\times\sqrt{3}$ - $R30^\circ$ Multilayer silicene/Ag(111) and 1 monolayer (ML) Ag $\sqrt{3}\times\sqrt{3}$ - $R30^\circ$ /Si(111), which show that the in-plane, unit cell size is an *intrinsic* characteristic of silicene, with a 2.5% of contraction with respect that of 1 ML Ag $\sqrt{3}\times\sqrt{3}$ /Si(111). These results rule out that the $\sqrt{3}\times\sqrt{3}$ Multilayer silicene/Ag(111) is due to the $\sqrt{3}\times\sqrt{3}$ reconstruction from silver atoms that act as surfactant in the formation of diamond-like crystalline Si film [4].

References

1. Vogt P, De Padova *et al.*, Phys. Rev. Lett., 108, 155501 (2012); C. L. Lin *et al.*, *App. Phys. Exp.* **5**, 045802-1 (2012); L. Meng *et al.*, L., *Nano Lett.* **13**, 685 (2013); A. Fleurence *et al.*, Phys. Rev. Lett. 108, 245501 (2012).
2. P. De Padova *et al.*, Appl. Phys. Lett., 96, 26190, (2010); P. De Padova *et al.*, J. Phys.: Condens. Matter, Fast Track Comm. 25, 382202 (2013); P. De Padova *et al.*, 2D Materials 1, 021003 (2014). P. Vogt *et al.*, Appl. Phys. Lett. 104, 021602-1, (2014); E. Salomon *et al.*, J. Phys.: Condens. Matter, 7, 185003 (2014).
3. B. Feng *et al.*, Nano Lett. 11, 3507 (2012); L. Chen *et al.*, Phys. Rev. Lett. 109, 056804-1 (2012).
4. T. Shirai *et al.* Phys. Rev. B 89, 241403-1, 2414035 (R) (2014); J. Chen *et al.*, Sci. Rep., DOI: 10.1038/srep13590; J. Mannix *et al.*, ACS Nano, 8, 7538 (2014). Y. Borensztein, A. Curcella, S. Royer and G. Prévot, Phys. Rev. B **92**, 155407 (2015); S. K. Mahatha *et al.*, Phys. Rev. B, 92, 245127 (2015). 10.1073/pnas.1208492109.

Electronic Structure and Superconductivity of FeSe /SrTiO₃ Films and Related FeSe-Based Bulk Superconductors]

Shaolong He*

¹*National Lab for Superconductivity, Institute of Physics, Chinese Academy of Sciences, Beijing100190, China*

Email: * shaolonghe@iphy.ac.cn

Keywords: Iron-based Superconductors, Single-Layer FeSe films, Superconductivity, ARPES

The discovery of high temperature superconductivity with a transition temperature T_c above 65K in single-layer FeSe films epitaxially grown on SrTiO₃ substrates has attracted intense research interest[1-6]. A lot of efforts have been put to achieve even higher T_c and understand the mechanism of such a dramatic superconductivity enhancement.

In this talk, I will give a brief review of the investigations on the electronic structure and superconductivity of the single-layer FeSe/STO films by using high-resolution angle-resolved photoemission (ARPES) in our group [2-5]. I will also present the electronic structure of the newly discovered bulk (Li_{1-x}Fe_x)OHFeSe with a T_c at 41K. [7]. Latest results and implications on the superconductivity mechanism of the iron-based superconductors will be discussed.

* Work done in collaboration with Xingjiang Zhou, Junfeng He, Wenhao Zhang, Lin Zhao, Daixiang Mou, Defa Liu, Xu Liu, Lili Wang, Xuncun Ma, Qikun Xue, Xiaoli Dong, Zhongxian Zhao and others in the Institute of Physics, CAS, and Tsinghua University, Beijing

References

1. Q.Y. Wang et al., Chin. Phys. Lett. **29**, 037402 (2012).
2. D. F. Liu et al., Nature Communications **3**, 931 (2012).
3. S. L. He et al., Nature Materials **12**, 605(2013).
4. J. F. He et al., PNAS, **111**, 18501 (2014)
5. X. Liu, et al., Nature Communications **5**, 5047(2014).
6. X. Liu et al., Electronic structure and superconductivity of FeSe-related superconductors. Journal of Physics: Condensed Matter **27**, 183201 (2015).
7. L. Zhao et al., Nature Communications **7**, 10608 (2015)

Tunable magnetism and superconductivity in an oxide heterostructure



D. Stornaiuolo^{1,2*}, C. Cantoni³, G. M. De Luca^{1,2}, R. Di Capua^{1,2}, E. Di Gennaro^{1,2}, G. Ghiringhelli⁴, B. Jouault⁵, D. Marrè⁶, D. Massarotti^{1,2}, F. Miletto Granozio², I. Pallecchi⁶, C. Piamonteze⁷, S. Rusponi⁸, F. Tafuri^{2,9} and M. Salluzzo^{2*}

¹ *Dipartimento di Fisica, Università di Napoli "Federico II", Complesso Monte Sant' Angelo via Cinthia, I-80126 Napoli, Italy*

² *CNR-SPIN, Complesso Monte Sant' Angelo via Cinthia, I-80126 Napoli, Italy*

³ *Materials Science and Technology Division, Oak Ridge National Laboratory, 1 Bethel Valley Rd., Oak Ridge, TN 37831, USA*

⁴ *CNR-SPIN and Dipartimento di Fisica, Politecnico di Milano, Piazza Leonardo da Vinci 32, I-20133 Milano, Italy*

⁵ *Laboratoire Charles Coulomb, UMR 5221, CNRS, Université Montpellier 2, F-34095 Montpellier, France*

⁶ *CNR-SPIN and Dipartimento di Fisica, Università di Genova, Via Dodecaneso 33, I-14146 Genova, Italy*

⁷ *Swiss Light Source, Paul Scherrer Institut, CH-5232 Villigen PSI, Switzerland*

⁸ *Institute of Condensed Matter Physics, Ecole Polytechnique Fédérale de Lausanne, CH-1015 Lausanne, Switzerland*

⁹ *Dipartimento di Ingegneria dell'Informazione, Seconda Università degli Studi di Napoli (SUN), Aversa (CE), Italy*

Email: * Stornaiuolo@fisica.unina.it

Keywords: 2DEG, SrTiO₃, LaAlO₃, EuTiO₃, interface

Transition metal oxides possess a wide range of properties. The ability to fabricate oxide heterostructures paves the way to the realization of artificial systems where these properties can be combined, with the possibility to create also new functionalities.

A notable example is the LaAlO₃/SrTiO₃ interface, which hosts a 2 dimensional electron gas (2DEG) [1]. A superconducting transition and the presence of large Rashba spin-orbit coupling, both tunable using electric field effect, are two of the interesting properties coexisting in this system.

Here we show that, by depositing few unit cells of delta-doping EuTiO₃ between SrTiO₃ and LaAlO₃ (LAO/ETO/STO) robust ferromagnetism can be induced, giving rise to a 2DEG which is both superconducting and spin-polarized. The resulting phase diagram (Figure 1) shows how it is possible to span the different ground states of the 2DEG as function of the electric field effect-tuned carrier concentration [2].

The presence of a superconducting and of a ferromagnetic ground state in the same system, showing also spin orbit coupling, is of great interest for the emergence of novel quantum states in confined systems and in the view of the realization of topologically non-trivial edge states at the interface between transition metal oxides [3].

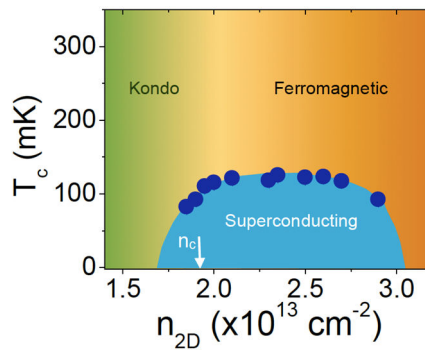


Figure 1: Temperature vs. carrier density phase diagram of the LAO/ETO/STO heterostructure. Blue closed circles are the zero resistance critical temperature. The shaded area indicates the different electronic states: Kondo-transport (green) below n_c ; Ferromagnetic state (orange) above n_c ; Superconducting state (blue).

References

1. A. Ohtomo et al., *Nature* 427, 423 (2004)
2. D. Stornaiuolo et al. *Nature Materials* 15, 278–283 (2016)
3. S. Nakosai, et al. *Phys. Rev. Lett.* **108**, 147003 (2012); K. Michaeli, et al. *Phys. Rev. Lett.* **108**, 117003 (2012).

Electron transport in thin oxide films: From phonon-polariton excitations to changes in the quantum structure of oxide-supported Gold nanoparticles



Wolf-Dieter Schneider^{1,2*}

¹*Fritz-Haber-Institute of the Max-Planck-Society, Berlin*

²*Ecole Polytechnique Fédérale de Lausanne (EPFL)*

Email: * wolf-dieter.schneider@epfl.ch

Keywords: electron transport, phonons, oxides, nano-clusters, quantum structure, physisorption, chemisorption

Scanning tunneling microscopy has developed into a powerful tool for the characterization of conductive surfaces, for which the overlap of tip and sample wavefunctions determines the image contrast. On insulating layers, as the CaO thin film grown on Mo(001) investigated here, direct overlap between initial and final states is not enabled anymore and electrons are transported via hopping through the conduction-band states of the oxide. In this case, the carrier transport is accompanied by strong phonon excitations, reflected by an oscillatory signature in the differential conductance spectra of the system. These excitations are tentatively assigned to surface-phonon-polariton excitations (Fuchs-Kliewer phonons). They show a characteristic spatial dependence and become softer around lattice irregularities in the oxide film, such as dislocation lines [1].

Moreover, STM conductance spectroscopy and mapping has been used to analyze the impact of molecular adsorption on the quantized electronic structure of individual metal nanoparticles supported on ultrathin oxide films. For this purpose, isophorone and CO₂, as prototype molecules for physisorptive and chemisorptive binding, were dosed onto two-dimensional monolayer Au islands grown on MgO thin films on Ag(001) single crystal surfaces. The molecules attach exclusively to the metal-oxide boundary, while the interior of the islands remains pristine. The Au quantum well states (see Fig. 1) are perturbed due to the adsorption process and increase their mutual energy spacing in the CO₂ case but move together for isophorone adsorption. The shifts disclose the nature of the molecule-Au interaction, which relies on electron exchange for the CO₂ ligands but on dispersive forces for the organic species. Our experiments reveal how molecular adsorption affects individual quantum systems, a topic of utmost relevance for heterogeneous catalysis. The present work demonstrates how the impact of molecular ligands on the properties of metal nanostructures can be investigated on a mechanistic level [2].

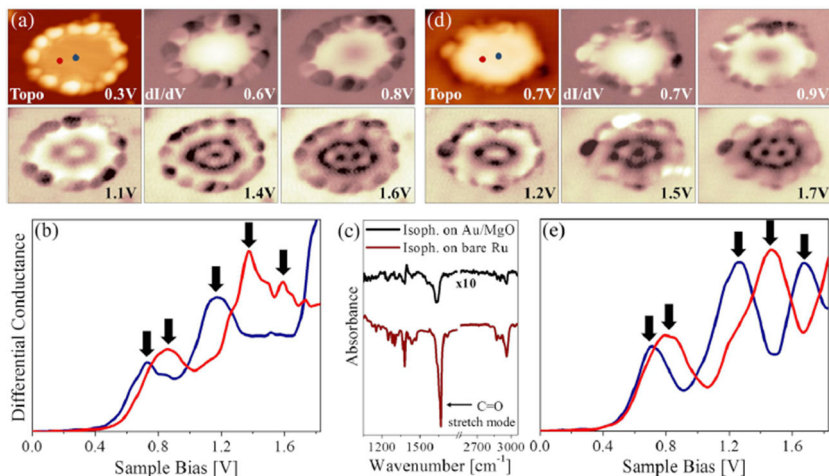


Figure 1: Topographic and dI/dV maps revealing characteristic standing wave patterns of a two-dimensional Au island (a) with and (d) without isophoronemolecules bound to its perimeter ($11 \times 8 \text{ nm}^2$). (b) and (c) associated differential conductance spectra taken in the center (blue) and the left part of the island (red) as indicated in (a) and (d). Gaussian fitting revealed five quantum well states (QWS)s which are marked by arrows. Their bias positions match the ones used for dI/dV imaging in (a) and (d). (c) Infrared absorption spectra of isophorone adsorbed on Au/MgO (black) and Ru(0001) (gray). Similar vibrational modes are resolved in both cases, indicating that the molecule adsorbs associatively on the two surfaces. (After Ref. [2]).

References

1. Y. Cui, S. Tosoni, W.-D. Schneider, G. Pacchioni, N. Nilius, and H.-J. Freund, Phys. Rev. Lett. 114, 016804 (2015).
2. C. Stiehler, F. Calaza, W.-D. Schneider, N. Nilius, and H.-J. Freund, Phys. Rev. Lett. 115, 036804 (2015).

New platforms for topological superconductivity: from Shiba to Majorana bound states



Pascal Simon¹

¹*Laboratoire de Physique des Solides, University Paris Sud, 91405 Orsay, France*

Email: pascal.simon@u-psud.fr

Keywords: Topological superconductivity, Shiba and Majorana bound states

The study of magnetic impurities in superconductors has a long history. Important effects include the renormalization reduction of the gap in the host superconductor by the impurities and the induced so-called Yu-Shiba-Rusinov bound states [1]. In recent years, a renewed interest in arrays of magnetic impurities in superconductors was furthermore driven by their potential to host exotic excitations called Majorana fermions, particles which are their own antiparticles.

I will first present new results for the single classical magnetic impurity case embedded in a two dimension (2D) superconductor and show that its spatial extent is actually long-ranged compared to what was observed in 3D superconductors [2]. I will also show that a spectroscopic analysis of the spin dependence of the Shiba bound state is able to bring relevant information on the nature of the order parameter of the host superconductor such as its degree of anomalous triplet pairing [3]. Analyzing two magnetic moments in a superconductor, I will show how the gap renormalizes for weakly and strongly coupled bound states. In the latter case, a transition from Shiba to Andreev states which is accompanied by two subsequent quantum phase transitions as the exchange coupling is varied is found [4]. I will then move on to the analysis of one-dimensional arrays of magnetic impurities on a superconducting substrate. In the limit where they form a dense conducting wire, I will show that the magnetic moments and the electrons become strongly entangled and that a magnetic spiral structure emerges without any adjustable parameters. For strong enough coupling between the impurities and the superconductor, this 1D system is driven into a topological superconducting phase supporting Majorana fermions without any fine-tuning of external parameters [5,6].

References

1. A. V. Balatsky, I. Vekhter, and J.-X. Zhu, *Rev. Mod. Phys.* 78, 373 (2006).
2. G. Ménard et al., *Nature Physics* 11, 1013 (2015).
3. V. Kaladzhyan, C. Bena, P. Simon, arXiv:1512.05575.
4. T. Meng, J. Klinovaja, S. Hoffman, P. Simon, D. Loss, *Phys. Rev. B* 92, 064503 (2015).
5. B. Braunecker, P. Simon, *Phys. Rev. Lett.* 111, 147202 (2013).
6. B. Braunecker, P. Simon, *Phys. Rev. B* 92, 241410 (2015).

Gorkov's equations in the instantonic "crystal" state



Sergei I. Mukhin*

*Department for Theoretical physics and quantum technologies,
Moscow Institute for Steel and Alloys, Moscow, Russia*

Email: * i.m.sergei.m@gmail.com

Keywords: Euclidean crystallization, "hidden order", Landau-Ginzburg-Wilson functional, double-periodic order parameter

An emergence of the instantonic "crystal" of entangled, antiferromagnetically organized electron-hole condensates below a temperature T^* is considered. The "crystal" manifests broken Matsubara time translational symmetry of the Fermi-system and plays the role of its "hidden order". Usually unstable [1], this "crystal" is shown to be stabilized by exchange of the electron-hole and Cooper pairs fluctuations. The latter process could be considered as an origin of the Cooper pairing "glue" in the initially repulsive Fermi-system. Below some T_c ($<T^*$) the Cooper pairs form superconducting condensate. This new scenario adds to the recent publications [2]-[4] that introduced Euclidean crystallization in correlated Fermi-system as an origin of a "hidden order" emerging as a self-consistent spin density wave (SDW) with Matsubara time-periodic amplitude. Such SDW breaks translational invariance of the system along the Matsubara axis. The SDW with an amplitude in the form of the snoidal Jacobi function of the Matsubara time has zero scattering cross section [2] for e.g. neutrons etc. external probes, thus revealing a peculiar case of the "hidden order" in the system. Fluctuations of this "hidden order" parameter are found self-consistently and their role in providing a Cooper pairing "glue" for the Fermi-system is investigated. The work advances the previous results [2-4]. In this work spectrum of the "hidden order" fluctuations is found. Before renormalization by the fermions, the spectrum possesses finite number of modes with the negative eigen-energies [3], [4], signifying well known instability of the bare instantonic "crystal" solution along the Matsubara axis [1]. The self-consistent impact of the Cooper pairing in the Fermi-system is shown to shift the bare negative modes into positive (stable) energies interval. The set of extended Gorkov's equations in the presence of instantonic "crystal" leads to emerging anomalous Green's functions above the superconducting T_c , but below the T^* . This new picture is considered in the present work and discussed in relation with the experiments in high- T_c superconductors.

References

1. A.M. Polyakov, "Gauge fields and strings", Harwood Academic Pub., 1987.

2. S. I. Mukhin, «Spontaneously broken Matsubara's time invariance in fermionic system: macroscopic quantum ordered state of matter», J. Supercond. Nov. Magn., vol. 24, 1165-1171 (2011).
3. S. I. Mukhin, «Euclidean action of fermi-system with "hidden order", Physica B:Physics of Condensed Matter, vol. 460, 264 (2015).
4. S. I. Mukhin, «Euclidian Crystals in Many-Body Systems: Breakdown of Goldstone's Theorem», J. Supercond. Nov. Magn., vol. 27, 945-950 (2014)

One-band vs. three-band models for weakly doped cuprates



Mona Berciu*

University of British Columbia, Vancouver, Canada

Email: **berciu@phas.ubc.ca*

Keywords: high T_c , quasiparticle dispersion

We use a variational method -- whose accuracy is validated by comparison with available exact diagonalization results for small clusters -- to study the dispersion of the quasiparticle that emerges when one hole is doped in an infinite CuO_2 layer described (a) by the three-band Emery model in the strongly correlated limit where a large onsite Hubbard repulsion prevents double occupancy of the $\text{Cu } 3d_{x^2-y^2}$ orbitals, and (b) by the one-band $t-t'-t''-J$ model. The variational method allows us to switch the spin fluctuations of the antiferromagnetic background on or off, to understand their effect on the dynamics of the quasiparticle. Although for suitable parameters the two models predict quantitatively similar quasiparticle dispersions, we find that spin fluctuations have essentially no effect on the shape of this dispersion for the three band model [1], whereas for the one-band model they are essential for obtaining the correct dispersion along $(0,0)-(\pi,\pi)$ [2]. This suggests that the two models describe qualitatively different quasiparticles in this insulating limit. This conclusion is further supported by a study of the same problem in a layer of tetragonal CuO , where the two models predict different quasiparticle dispersions [3].

References

1. H. Ebrahimnejad, G. A. Sawatzky, and M. Berciu, *Nature Phys.* 10, 951 (2014).
2. H. Ebrahimnejad, G. A. Sawatzky, and M. Berciu, arXiv:1505.04405
3. C. P. J. Adolphs, S. Moser, G. A. Sawatzky and M. Berciu, in preparation.

Upper critical fields near the spin density wave transition of $\text{BaFe}_2(\text{As}_{1-x}\text{P}_x)_2$



V. Grinenko^{1,2,3}, K. Iida^{1,2}, F. Kurth^{1,3}, D. V. Efremov¹, S.-L. Drechsler¹, I. Cherniavskii⁴, I. Morozov^{1,4}, J. Hänisch^{1,5}, T. Förster⁶, C. Tarantini⁷, J. Jaroszynski⁷, B. Maiorov⁸, M. Jaime⁸,

A. Yamamoto⁹, I. Nakamura², R. Fujimoto², T. Hatano², H. Ikuta², and R. Hühne¹

¹*IFW Dresden, Germany*

²*Department of Crystalline Materials Science, Graduate*

School of Engineering, Nagoya University, Japan

³*Dresden University of Technology, Germany*

⁴*Lomonosov Moscow State University, Russian Federation*

⁵*Karlsruhe Institute of Technology, Institute for Technical Physics, Germany*

⁶*Hochfeld-Magnetlabor Dresden (HLD-EMFL), Helmholtz-Zentrum Dresden-Rossendorf, Germany*

⁷*NHMFL, Florida State University, Tallahassee, USA*

⁸*MPA-CMMS, Los Alamos National Laboratory, USA*

⁹*Dept. of Applied Physics, Tokyo University of Agriculture and Technology, Tokyo, Japan*

Email: * v.grinenko@ifw-dresden.de

Keywords: coexistence of superconductivity and SDW, quantum criticality, multi-band superconductivity, upper critical field

In many unconventional superconductors a quantum critical point (QCP) related to the presence of a competing charge or spin density wave (CDW/SDW) phase lies beneath the superconducting dome.[1] In the normal state a QCP leads to non-Fermi liquid behavior and divergent quasiparticle mass due to low energy quantum fluctuations. However, whether there is a strong quasiparticle mass enhancement in a broad temperature range above the QCP of the SDW phase in iron pnictides is controversial. [2-4] Here, we investigate the effect of the SDW phase on the superconducting upper critical fields(H_{c2}) of high quality single crystalline $\text{BaFe}_2(\text{As}_{1-x}\text{P}_x)_2$ thin films. We used H_{c2} as a probe of the quasiparticle mass enhancement at T_c . Using high magnetic fields we probe the low temperature properties of the system close to the QCP. We have found that H_{c2} has a different doping dependence on the SDW and paramagnetic side of the phase diagram (Fig.1). However, we have not observed any effect of the expected quantum fluctuations on H_{c2} neither at high temperatures (in the slope of H_{c2} at T_c) nor at low temperatures down to 2K. The estimated $H_{c2}^{0.5}/T_c \propto (1 + \lambda)$ within the Eliashberg theory for clean superconductors [5] is shown in Fig1b, where $1 + \lambda \propto m_{\text{eff}}$ is obtained from the specific heat and de Haas van Alphen (dHvA) data [3]. The H_{c2} data at low temperatures are clearly inconsistent with the estimated ones using specific heat

data but are quite close to the estimated ones from dHvA data. The observed featureless behavior of H_{c2} across the QCP and the surprising agreement with the dHvA measurements are consistent with a lack of quasiparticle mass enhancement due to quantum fluctuations at T_c . We argue that the observed behavior of H_{c2} in $\text{BaFe}_2(\text{As}_{1-x}\text{P}_x)_2$ is triggered by the reconstruction of the Fermi surface due to the formation of the SDW phase.

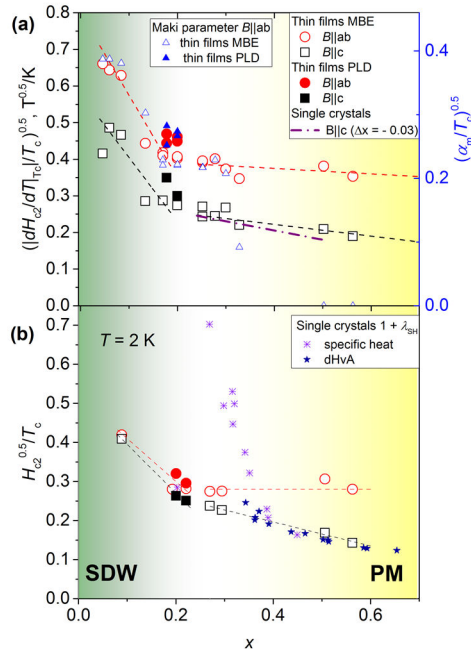


Figure 1: a) The normalized slope of H_{c2} at T_c (left axis) and the normalized value of the effective single-band Maki parameter α_m (right axis) for $\text{BaFe}_2(\text{As}_{1-x}\text{P}_x)_2$ thin films versus P doping. The dashed-dotted line is the single crystalline data set from Ref. [4] shifted by $\Delta x = -0.03$. b) The normalized H_{c2} at $T = 2$ K. The estimated doping dependencies of H_{c2} from the specific heat jump and dHvA data [3] are also shown

References

1. D. J. Scalapino, Rev. Mod. Phys. **84**, 1383, (2012); P.J. Hirschfeld et al., Rep. Prog. Phys. **74** 124508 (2011); P. Gegenwart et al., Nature Physics **4**, 186-197 (2008).
2. T. Shibauchi et al., Annu. Rev. Condens. Matter Phys. **5** 11335 (2014); K. Hashimoto et al., Science **336**, 1554 (2012); Y. Lamhot et al., Phys. Rev. B **91**, 060504(R) (2015); D. Chowdhury et al., Phys. Rev. Lett. **111**, 157004 (2013); D. Chowdhury et al., Phys. Rev. B **92**, 081113(R) (2015); J. Fink et al., Phys. Rev. B **92** 201106 (R) (2015).
3. P. Walmsley et al., Phys. Rev. Lett. **110**, 257002 (2013).
4. C. Putzke et al., Nature Communications **5**, 5679 (2014).
5. J. P. Carbotte, Rev. Mod. Phys., **62**, 102 (1990)

High temperature superconductivity in hydrogen-rich materials



Mikhail Erements*, Alexander Drozdov *Max Planck Institute of Chemistry, Mainz, Germany*

Email: * m.eremets@mpic.de

Keywords: high T_c , high pressure, hydrogen, hydrides

Recently superconductivity with $T_c > 200$ K has been found in hydrogen sulfide at high pressures [1]. The superconductivity has been proved by observation of zero resistance, Meissner effect, and isotope effect. X-ray diffraction studies [2] confirm predicted cubic structure of the superconductive phases. Fig. 1 summarizes the pressure dependence of superconducting temperature for hydrogen sulfide and its isotope deuterium sulfide. Apparently this pressure dependence reflects two phases with different pressure dependences. The determined cubic structure of these high T_c phases is in a good agreement with the $R3m$ and $Im3m$ structure predicted for H_3S [3]. We will present also recent results on further study of the superconductivity by different methods and compare the experimental results with available numerous theoretical calculations.

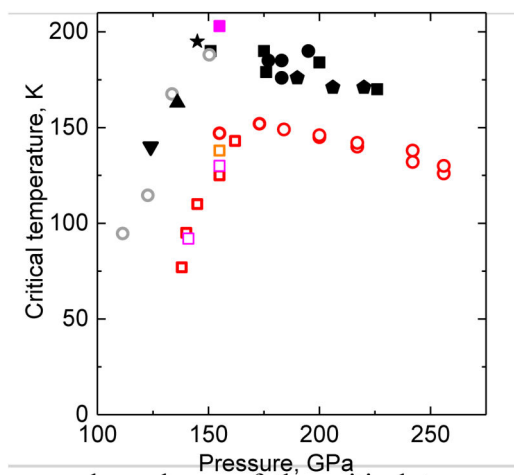
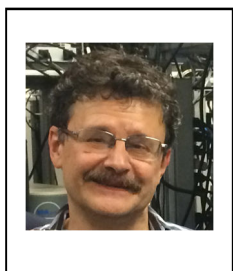


Figure 1: The pressure dependence of the critical temperature of superconductive transition for hydrogen sulfide (black points) and deuterium sulfide (red points) derived from electrical measurements. Magenta points are obtained from the magnetic susceptibility measurements in SQUID.

References:

- 1 Drozdov, A.P., et al., *Conventional superconductivity at 203 K at high pressures*. Nature 2015. **525**: p. 73-77.
- 2 Einaga, M., et al., *Crystal Structure of 200 K-Superconducting Phase of Sulfur Hydride System* arXiv:1509.03156, 2015.
- 3 Duan, D., et al., *Pressure-induced metallization of dense (H₂S)₂H₂ with high-T_c superconductivity*. Sci. Reports, 2014. **4**: p. 6968.

Hydrogen sulfide at high pressure: change in stoichiometry



Alexander F. Goncharov,^{1,2,3*} Sergey Lobanov,^{2,4} Ivan Kruglov,⁵
Xiao-Miao Zhao,^{2,7} Xiao-Jia Chen,^{1,2,6} Artem R. Oganov,^{5,8,9,10}
Zuzana Konôpková,¹¹ Vitali Prakapenka¹²

¹*Key Laboratory of Materials Physics, Institute of Solid State Physics, Chinese Academy of Sciences, Hefei, Anhui 230031, China*

²*Geophysical Laboratory, Carnegie Institution of Washington, Washington, D.C. 20015, USA*

³*University of Science and Technology of China, Hefei, 230026,*

China

⁴*V.S. Sobolev Institute of Geology and Mineralogy, SB RAS, 3 Pr. Ac. Koptyga, Novosibirsk 630090, Russia*

⁵*Moscow Institute of Physics and Technology, Dolgoprudny, Moscow Region 141700, Russian Federation*

⁶*Center for High Pressure Science and Technology Advanced Research, Shanghai 201203, China,*

⁷*Department of Physics, South China University of Technology, Guangzhou 510640, China*

⁸*Skolkovo Institute of Science and Technology, Skolkovo Innovation Center, Moscow 143026, Russia*

⁹*Department of Geosciences, Center for Materials by Design, and Institute for Advanced Computational Science, State University of New York, Stony Brook, NY 11794-2100.*

¹⁰*Northwestern Polytechnical University, Xi'an 710072, China.*

¹¹*DESY Photon Science, Notkestrasse 85, D-22607 Hamburg, Germany*

¹²*Center for Advanced Radiation Sources, University of Chicago, Chicago, Illinois 60637, USA*

Email: agoncharov@carnegiescience.edu

Keywords: high T_c , hydrides, high pressure, structure, stoichiometry

Hydrogen-sulfide (H_2S) was studied by x-ray synchrotron diffraction (XRD) and Raman spectroscopy up to 150 GPa at 180-295 K and by quantum-mechanical variable-composition evolutionary simulations. The experiments show that H_2S becomes unstable with respect to formation of new compounds with different structure and composition, including $Cccm$ and a body-centered-cubic (bcc) like ($R3m$ or $Im-3m$) H_3S , the latter one predicted previously to show a record-high superconducting transition temperature, T_c of 203 K [1]. These results are supported by theoretical structure searches that suggest the stability of new H_3S , H_4S_3 , H_5S_8 , H_3S_5 , and HS_2 compounds at elevated pressures.

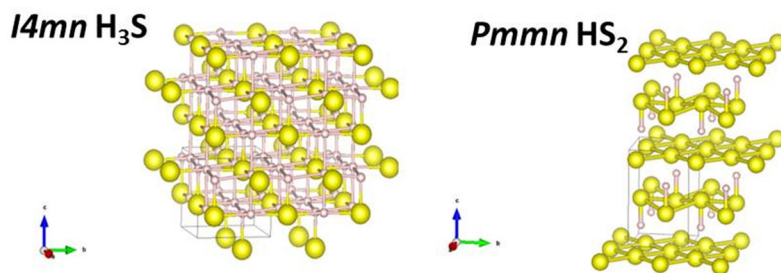


Figure 1: Crystal structures of H₃S and HS₂ compounds, which are predicted to become stable at high pressures.

References

1. A. P. Drozdov, M. I. Eremets, I. A. Troyan, V. Ksenofontov and S. I. Shylin, *Nature* **525**, 73 (2015).

200-K superconductivity in compressed hydrogen sulfide systems



K. Shimizu^{1*}, M. Einaga¹, M. Sakata¹, H. Nakao¹,
M. Eremets², A. Drozdov², I. Troyan², N. Hirao³, Y. Ohishi³
¹*KYOKUGEN, Grad. Sch. Eng. Sci., Osaka University*
²*Max Planck Institute for Chemistry*
⁴ *JASRI / SPring-8*

Email: *shimizu@stec.es.osaka-u.ac.jp

Keywords: high-T_c, H₂S, pressure

After finding superconductivity in 100 years ago, "room-temperature" superconductor has been long-fascinated target for physicists. Superconductivity above 200K was recently reported in the highly compressed hydrogen sulfide (H₂S) by Drozdov et al [1]. The crystal structure of the superconducting sulfur hydride systems was studied by using the synchrotron x-ray diffraction at room temperature and the superconducting temperature. H₂S and D₂S were compressed to 150 GPa in DAC with same process with Drozdov et al[1], and cooled down to 10 K in the cryostat in the x-ray diffractometer in SPring-8. The resistivity was monitored at all cooling process. The critical temperature and zero resistivity were observed around 180 K, and the collected x-ray diffraction data showed good agreement with the theoretically predicted structures of R3m and Im-3m[2]. No structural difference was observed between at 10 K and room temperature.

The creation of the high-temperature superconductor was experimentally also confirmed by our Osaka group. H₂S gas was cooled down to around 200 K and liquefied then compressed up to 150 GPa in a diamond-anvil cell (DAC). The resistance decreased with increasing pressure and showed metallic behavior in cooling process. The superconducting transition was observed at 60-70 K with zero resistance. At the second cooling after warmed up to room temperature, the resistance dropped to zero from 180 K.

This work was supported by JSPS KAKENHI Grant Number 26000006 and the European Research Council 2010-Advanced Grant 267777.

References

1. A. Drozdov et al., *Nature* **525** 73 (2015).
2. D. Duan et al., *Scientific Reports* **4**, 6968 (2014).

Fully non-empirical study on superconductivity in sulfur hydrides under high pressures



Ryotaro Arita*
RIKEN Center for Emergent Matter Science
JST ERATO Isobe Degenerate π -Integration Project,
Advanced Institute for Materials Research, Tohoku University

Email: * arita@riken.jp

Keywords: high T_c superconductivity, sulfur hydride

The recent discovery of superconductivity at 203K in sulfur hydrides at extremely high pressures [1] has stimulated a renewed interest in the phonon-mediated superconductivity in compounds comprising light elements. In Ref. [2], we performed a fully non-empirical calculation for sulfur hydrides based on the Migdal-Eliashberg (ME) theory, considering the effects which have been believed to be important but yet to be studied, and succeeded in reproducing the experimental T_c accurately.

The problems in the previous calculations based on the ME theory are: (1) empirical, adjustable parameter (μ^*) has been employed to represent the retardation effect, (2) the density of states (DOS) around the Fermi level has been assumed to be constant to simplify the Eliashberg gap equation (although it has been known that there are van Hove singularities around the Fermi level for H_3S), (3) the mass enhancement due to the electron-phonon coupling has not been calculated self-consistently, and (4) the impact of the vertex correction, i.e., the validity of the Migdal approximation has not been examined quantitatively.

In this study, we performed a calculation overcoming these problems. First, we go beyond the constant DOS approximation and explicitly consider the electronic structure over 40 eV around the Fermi level. In contrast with the previous calculations, this approach with a sufficiently large number of Matsubara frequencies enables us to calculate T_c without introducing μ^* (Fig.1). We show that while H_3S has much higher T_c than H_2S , the constant DOS approximation employed so far seriously overestimates (underestimates) T_c by $\sim 70K$ ($\sim 10K$) for H_3S (H_2S).

We then discuss the impact of the following effect due to the strong electron-phonon coupling on the superconductivity: (1) the feedback effect in the self-consistent calculation of the self-energy, (2) the effect of the energy shift due to the zero-point motion, and (3) the effect of the changes in the phonon frequencies due to strong anharmonicity. We show that the effects of (1)-(3) on T_c are about 10-30K for both H_3S and H_2S . Eventually, T_c is estimated to be 181K for H_3S at 250GPa and 34K for H_2S at 140GPa. Finally, we evaluate the lowest order vertex correction beyond the Migdal-Eliashberg theory and show that its impact on T_c is about 20-30K. Given the fact that the dynamical structure of the screened Coulomb interaction enhances T_c by $\sim 20K$ [3], we see that our calculated T_c remarkably agrees well with the experiment.

This work was done in collaboration with W. Sano, T. Koretsune, T. Tadano and R. Akashi.

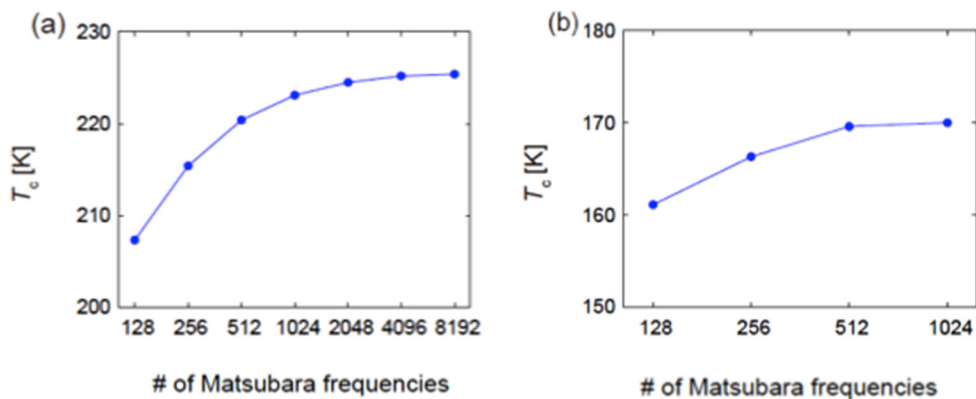


Figure 1: Number of Matsubara frequencies dependence of the calculated T_c for H_3S based on the ME theory (a) with the constant DOS approximation and (b) with energy dependent DOS.

References

1. A. P. Drozdov, M. I. Erements, I. A. Troyan, V. Ksenofontov, and S. I. Shylin, Nature (London) 525, 73 (2015).
2. R. Akashi, M. Kawamura, S. Tsuneyuki, Y. Nomura, and R. Arita, Phys. Rev.B 91, 224513 (2015).
3. W. Sano, T. Koretsune, T. Tadano, R. Akashi and R. Arita, arXiv: 1512.07365

Multi-condensates in BCS and BEC-BCS crossover regime near Lifshitz transitions in H_3S as in all high T_c superconductors



Antonio Bianconi^{1,2,3*}

¹*RICMASS, Rome Int. Center for Mat. Science Superstripes, Rome, Italy*

²*Natl. Research Nuclear University MEPhI Moscow Russia*

³*Institute of Crystallography, Consiglio Nazionale delle Ricerche, via Salaria, 00015 Monterotondo, Italy*

Email: * Antonio.bianconi@ricmass.eu

Keywords: Lifshitz transitions, Multi-condensates superconductors, Hydrates, room temperature superconductivity

Pressurized sulfur hydride shows the highest superconducting critical temperature 203 K. [1]. While the T_c predictions are based on standard BCS approximations and on the Migdal approximation we show that it fails for pairing of low velocity electrons near the van-Hove-singularities (vHs) and holes at the gamma point. We first focus on the neck disrupting Lifshitz transition, of type 2, where the vHs crosses the chemical potential at 210 GPa but these electrons are involved in the pairing since their energy remains around the chemical potential in the range of the pairing interaction $E_0=150 \pm 50$ meV [2,3]. Moreover the hydrogen zero-point-motion shifts the vHs through the chemical potential. In the pressure range 120-180 GPa the Im-3m structure is stabilized by the amplitude of the H zero-point-motion which is larger than the splitting of the S-H bonds in R3m structure. The Migdal approximation fails also at the Lifshitz transition of type 1, for the appearing of a new small-Fermi-surface spot at Gamma occurring at 130 GPa where T_c vanishes. The critical temperature reaches 203 K at 160 GPa where the shape resonance is predicted for $E_f = \pm E_0$. The small-Fermi-surfaces at Gamma are very sensitive to H-bond stretching fluctuations. The results indicate that in the holes in the small pockets at Gamma condensate in the BEC-BCS crossover regime and play in H_3S a similar role as the *states at anti-nodal points* in cuprates [4] the *sigma band* in magnesium diboride, [5] the and the $Fe(3d_{xy})$ band in iron based superconductors [6,7] and the upper subband in oxide-oxide 2D electron gas [8]. These BEC-BCS condensates in hot spots coexists with other BCS condensates in other points of the k-space, giving the scenario of multigaps superconductivity near a Lifshitz transition where shape resonance in the exchange interaction between condensates gives high T_c .

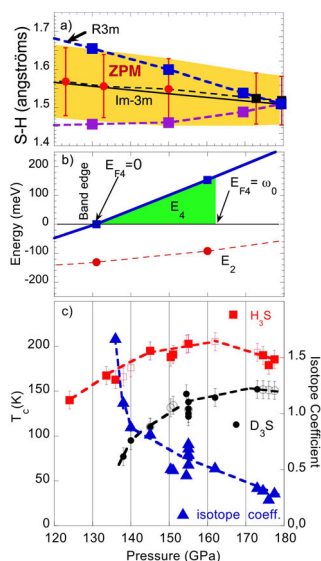


Figure 1: The upper panel shows the S-H bond length in the pressure range between 120 and 180 GPa where without the hydrogen ZPM, the R3m structure was expected to be stable with the S-H bond splitting into a long (blue squares) and short (violet squares) sulfur-hydrogen bond. The amplitude of the calculated ZPM of the S-H bond is indicated by the red error bars. The S-H amplitude of the zero point motion, ZPM, is larger than the S-H splitting in the range 130-180 GPa therefore in this pressure range the ZPM stabilizes the Im-3m structure in agreement with experiments. The panel (b) shows the Fermi energy in the small hole Fermi pocket at Gamma as a function of pressure. The top of this band crosses the chemical potential at 130 GPa giving the Lifshitz transition of type 1 for the appearing of a new Fermi surface. The position of the vHs E_2 remains below the chemical potential but it remains in the energy range of pairing interaction. Panel (c) shows the variation of the experimental isotope coefficient calculated from data which shows a divergence from 0.3 at 180 GPa to 1.5 at 135 GPa, which is not predicted by the BCS theory. The critical temperature decreases toward zero with a decrease of about 60 K in a range of 30 GPa, between 160 GPa and 130 GPa which is not predicted by the BCS theory. Both phenomena are predicted by the general theory of multigap superconductivity near a Lifshitz transition

References

1. A. Bianconi, T. Jarlborg, *EPL (Europhysics Letters)* **112**, 37001 (2015).
2. A. Bianconi, T. Jarlborg, *Novel Superconducting Materials* **1**, 37-49 (2015).
3. T. Jarlborg, A. Bianconi, *Scientific Reports* **6**, 24816 [doi:10.1038/srep24816](https://doi.org/10.1038/srep24816) (2016),
4. A. Bianconi, et al. *Physica C: Superconductivity* **296**, 269-280 (1998).
5. D. Innocenti, et al. *Physical Review B* **82**, 184528+ (2010).
6. R. Caivano et al. *Supercond. Sci. Technol.* **22**, 014004 (2009).
7. D. Innocenti, et al. *Supercond. Sci. Technol.* **24**, 015012 (2011).
8. A. Bianconi, et al. *Journal of Physics: Conference Series* **529**, 012007 (2014).

Structure and composition of the 200 K-superconducting phase of H₂S under ultrahigh pressure: the perovskite (SH⁻)(H₃S⁺).



Annette Bussmann-Holder¹, Elijah E. Gordon², Ke Xu, Hongjun Xiang³, Reinhard K. Kremer, Arndt Simon, Jürgen Köhler, Myung-Hwan Whangbo²

¹*Max-Planck-Institut für Festkörperforschung, Heisenbergstrasse 1, D-70569 Stuttgart, Germany*

²*Department of Chemistry, North Carolina State University, Raleigh, NC 27695-8204, USA*

³*Laboratory of Computational Physical Sciences (Ministry of Education), State Key Laboratory of Surface Physics,*

Collaborative Innovation Center of Advanced Microstructures, and Department of Physics, Fudan University, Shanghai 200433, P. R. China

Email: a.bussmann-holder@fkf.mpg.de*

Keywords: structure , computation, Pressurized H₂S

H₂S is converted under ultrahigh pressure (> 110 GPa) to a metallic phase that becomes superconducting with a record T_c of ~200 K [1]. It has been proposed that the superconducting phase is body-centered cubic H₃S (*In* $\bar{3}$ m, a = 3.089 Å) resulting from a decomposition reaction 3H₂S → 2H₃S + S [2-4]. The remarkably high T_c's in the 80–200 K range for the proposed H₃S under high pressure have been explained on the basis of the strong-coupling theory of superconductivity, with the electron-phonon coupling increasing strongly with increasing pressure where more than 90 % of the coupling arises from H vibrations [2-4]. This is supported by the observation of a substantial isotope effect upon deuteration. However, the T_c of the deuterated sample D₂S is reduced to ~90 K at the highest pressure corresponding to an isotope exponent $\alpha > 1$ that varies with pressure [4,5]. The deviations from the BCS value $\alpha = 0.5$ and the pressure dependence of α indicate that neither Eliashberg theory nor the Allen-Dynes formalism are adequate descriptions to achieve these high values of T_c, as discussed for cuprates [6,7]. In contrast, the analogy with MgB₂ [8-9] indicates that not single band BCS type approaches are the key ingredient, but that multiband effects have to be taken into account [4-6,10,11]. The analogy of H₂S and H₂O leads us to a very different conclusion. The well-known dissociation of water into H₃O⁺ and OH⁻ increases by orders of magnitude under pressure. An equivalent behavior of H₂S is anticipated under pressure with the dissociation, 2H₂S → H₃S⁺ + SH⁻ forming a perovskite structure (SH⁻)(H₃S⁺), which consists of corner-sharing SH₆ octahedra with SH⁻ at each A-site (i.e., the center of each S₈ cube). Our DFT calculations show that the perovskite (SH⁻)(H₃S⁺) is thermodynamically more stable than the *In* $\bar{3}$ m structure of H₃S, and suggest that the A-site H atoms are most likely fluxional even at T_c.

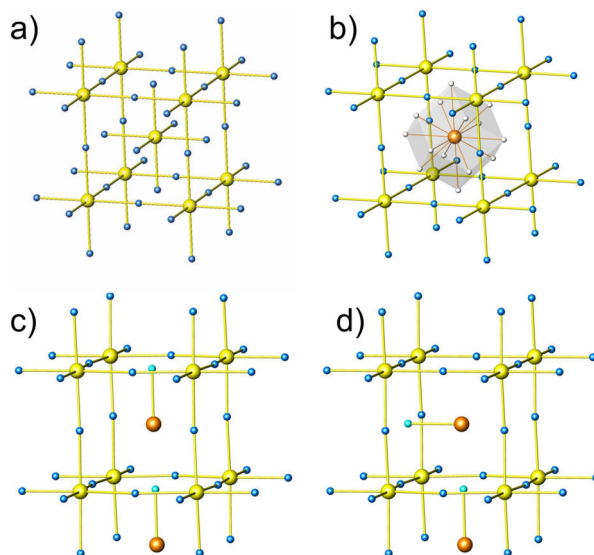
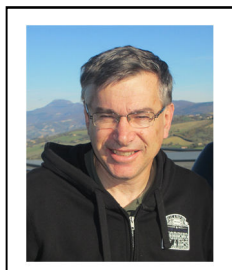


Figure 1: a) The proposed bcc structure of H_3S ($Im\bar{3}m$, $a = 3.089 \text{ \AA}$) emphasizing the presence of two interpenetrating SH_3 perovskite sublattices. b) Structure of the perovskite $(\text{SH})(\text{H}_3\text{S}^+)$ at ultrahigh pressure. The centering grey polyhedron represents the 14 orientations for the S–H bond (i.e., eight along the 3-fold rotational axes plus six along the 4-fold rotational axes). Only one of the 14 positions for the H atom of the SH unit is occupied. c) The structure of $(\text{SH})(\text{H}_3\text{S}^+)$ ($P4mm$, SG = 99) with A-site S–H bonds pointing to a face of the S_8 cube. d) The structure of $(\text{SH})(\text{H}_3\text{S}^+)$ in which every two adjacent S–H bonds are perpendicular to each other (see text). Large yellow and orange circles correspond to the S atoms, and small blue circles to the H atoms.

References

1. A.P. Drozdov, M.I. Erements, I.A. Troyan, V. Ksenofontov, S.I. Shylin, *Nature* **525**, 73 (2015)
2. D. Duan, X. Huang, F. Tian, D. Li, H. Yu, X. Liu, Y. Ma, B. Liu, W. Tian, T. Cui, *Phys. Rev. B* **91**, 180502. (2015)
3. T. Jarlborg and A. Bianconi, Preprint *arxiv:1509.07451*, URL <http://arxiv.org/abs/1509.07451>.
4. A. Bianconi and T. Jarlborg, *Nov. Supercond. Mater.* **1**, 37 (2015)
5. A. Bianconi, T. Jarlborg, *Europhys. Lett. J.* **112**, 37001 (2015)
6. A. Bussmann-Holder, H. Keller, R. Khasanov, A. Simon, A. Bianconi, and A. R. Bishop, *New Journal of Physics* **13**, 093009 (2011), URL <http://dx.doi.org/10.1088/1367-2630/13/9/093009>.
7. A. Bianconi, A. Valletta, A. Perali, N.L. Saini *Solid State Communications* **102**, 369-374 (1997)
8. A. Bussmann-Holder and A. Bianconi, *Physical Review B* **67**, 132509 (2003), URL <http://dx.doi.org/10.1103/physrevb.67.132509>.
9. A. Bianconi *Journal of Superconductivity* **18**, 625-636 (2005)
10. S. Deng, A. Simon, J. Köhler, *J. Supercond.* **17**, 227 (2004)
11. S. Deng, A. Simon, J. Köhler, *Int. J. Modern Physics B* **19**, 29 (2005)

Superconductivity in H₂S and in other superconductors; many band or band of many?



Frank Marsiglio^{1*}
¹University of Alberta
Department of Physics

Email: * fm3@ualberta.ca

Keywords: high T_c, superconductivity, microscopic mechanism

Strong correlations play an important part of all superconductors. In addition, ‘conventional’ markers, such as a relatively high characteristic pairing frequency and interaction, and a large density of states at the Fermi level can be important as well. We assess the relative importance of these properties, vs the correlations described through a competition between kinetic energy processes and potential energy considerations. In the Dynamic Hubbard model this competition becomes somewhat blurred; one immediate effect is a loss of electron-hole symmetry. We describe various effective models where the role played by hole-like quasiparticles becomes very distinct from that of their electron-like counterparts.

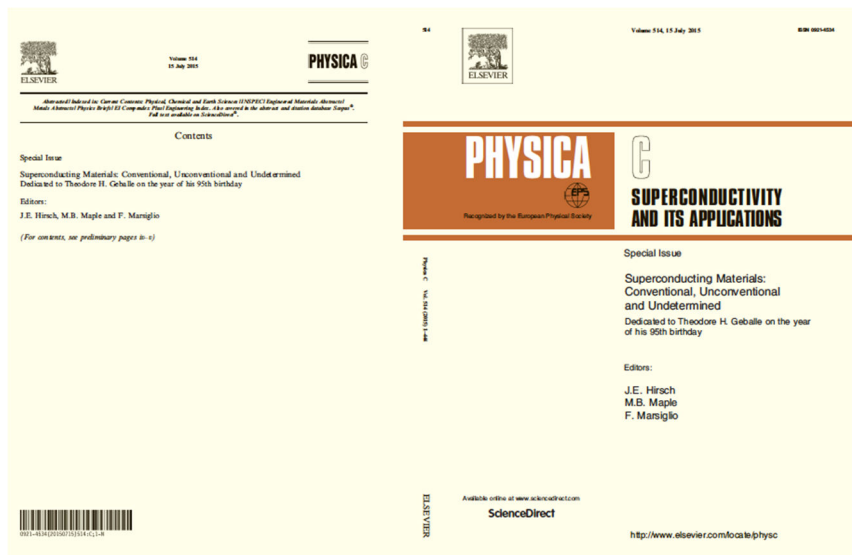


Figure 1: An assessment of the experimental facts for all known superconductors.

Electronic Orbital Order and Spin Nematicity in Iron-Pnictide High-Temperature Superconductors as Revealed by NMR

Guo-qing Zheng

Department of Physics, Okayama University, Japan

and

Institute of Physics, Chinese Academy of Sciences, Beijing, China

We report NMR results in hole- and electron-doped iron-pnictide superconductors $\text{BaFe}_{2-x}\text{Ni}_x\text{As}_2$ (Ref.1), $\text{NaFe}_{1-x}\text{Co}_x\text{As}$ (Ref.2), and $\text{LaFeAsO}_{1-x}\text{F}_x$ (Ref.3-4), and address the debating issues including spin and orbital nematicity, quantum critical phenomena, and coexistence of superconductivity and magnetism.

$\text{LaFeAsO}_{1-x}\text{F}_x$ ($x < 0.25$) is the first-discovered iron-pnictide high temperature superconductor⁵). By the high-pressure synthesis technique, we discovered a new dome with an even higher T_c than the originally-reported value⁵) which peaked at $x_{\text{opt}}=0.5$, where the electric resistivity shows a T -linear behavior but without magnetic fluctuations⁴). By NMR and transmission electron microscopy, we find that a C4 rotation symmetry-breaking structural transition takes place for large x which terminates at x_{opt} . Our results suggest the importance of nematic fluctuations and point to a new paradigm of high temperature superconductivity.

NaFeAs is a system where the structural transition temperature $T_s = 54$ K is well separated from Neel temperature T_N . We report NMR measurements on the electron-doped $\text{NaFe}_{1-x}\text{Co}_x\text{As}$ that revealed orbital and spin nematicity (in-plane anisotropy) occurring at a temperature well above T_s in the tetragonal phase²). We show that the NMR spectra splitting and its evolution can be explained by an incommensurate orbital order that sets in below T^* and becomes commensurate below T_s , which brings about the observed spin nematicity.

We will also present the NMR results on hole- and electron-doped materials^{1,3,6}) and discuss quantum critical phenomena and coexistence of superconductivity and magnetism.

This work was done in collaboration with R. Zhou, J. Yang, Z. Li, T. Oka, and S. Kawasaki.

References:

1. R. Zhou *et al*, Nature Commun. 4, 2265 (2013).
2. R. Zhou *et al*, Phys. Rev. B 93, 060502(R) (2016).
3. T. Oka *et al*, Phys. Rev. Lett. 108, 047001 (2012).
4. J. Yang *et al*, Chin. Phys. Lett. 32, 107401 (2015).
5. Y. Kamihara, *et al*, J. Am. Chem. Soc. 130, 3296 (2008).
6. Z. Li *et al*, Phys. Rev. B 83 140506(R) (2011).

Dynamical charge density waves rule the phase diagram of cuprates



S. Caprara^{1,2*}, C. Di Castro^{1,2}, G. Seibold³, M. Grilli^{1,2}

¹University of Rome Sapienza

²ISC-CNR and CNISM - Rome Sapienza

³Institut für Physik BTU Cottbus-Senftenberg

Email: * sergio.caprara@roma1.infn.it

Keywords: charge density waves, high T_c superconducting cuprates

In the last few years charge density waves (CDWs) have been ubiquitously observed in cuprates and are now the most investigated among the competing orders in the longstanding debate on high T_c superconducting cuprates. Different dome-shaped CDW onset lines in the temperature vs. doping phase diagram are detected by experiments with probes having different characteristic timescales. These lines are extrapolated at zero temperature to different quantum critical points (QCPs) in agreement with the theoretical prediction that CDWs are present in these systems and disappear with a QCP by increasing doping. This QCP is buried underneath the superconducting dome, in the optimal doping region (i.e., where the superconducting critical temperature T_c is highest).

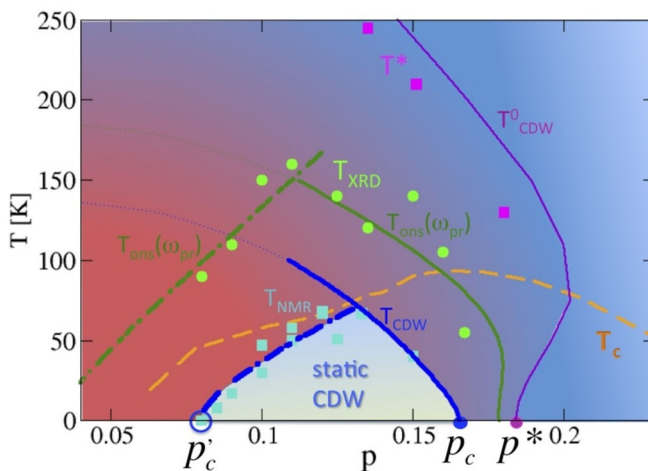


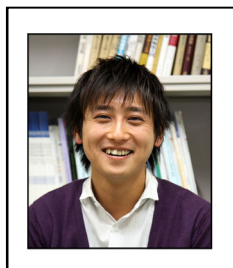
Figure 1: Overall phase diagram of YBa₂Cu₃O_y in the temperature vs. doping plane, including experimental points for the onset of CDW order (purple and green symbols) and its static realization (light blue symbols), with the corresponding theoretically predicted lines and QCPs. The superconducting dome is represented by the dashed orange line.

A wealth of new experimental data raise fundamental issues that challenge the various theoretical proposals. Here, we reproduce the complex experimental phase diagram and provide a coherent solution to all these problems based on the occurrence of dynamically fluctuating CDWs.

References

1. S. Caprara, C. Di Castro, G. Seibold, and M. Grilli, arXiv:1604.07852 (2016).

Development of VUV-laser-based ARPES system for higher spatial resolution and its application to Fermiology on high- T_c cuprates



Hideaki Iwasawa^{1*}, Eike F.Schwier¹, Yoshihiro Aiura²,
Kenya Shimada¹

¹*Hiroshima Synchrotron Radiation Center, Hiroshima University, Higashi-Hiroshima, Hiroshima 739-0046, Japan*

²*National Institute of Advanced Industrial Science and Technology, Tsukuba, Ibaraki 305-8568, Japan*

Email: *H. Iwasawa@hiroshima-u.ac.jp

Keywords: ARPES, high- T_c cuprates

Angle-resolved photoemission spectroscopy (ARPES) plays an important role for the investigation of the physical properties of solids. To realize higher spatial resolution, which is indispensable to obtain more intrinsic and reliable ARPES data, we have constructed a tunable VUV-laser-based ARPES system at Hiroshima Synchrotron Radiation Center (HiSOR), Japan. The tunable VUV-laser light source is composed of the commercial mode-locked Ti:sapphire laser, high-order harmonic generator, and focusing system, realizing high spatial resolution (Fig. 1) with ultimate energy and momentum resolutions. Here, we will report the recent developments of our VUV-laser-based ARPES system and its application to Fermiology on high- T_c cuprates.

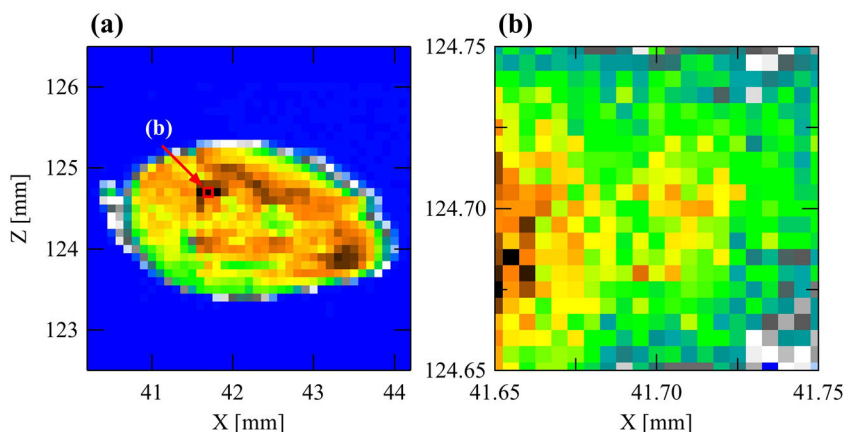


Figure 1: Spatial mapping of integrated nodal ARPES image of optimally doped $\text{Bi}_2\text{Sr}_2\text{CaCu}_2\text{O}_{8+\delta}$ in (a) entire region and (b) expanded region as indicated by the red box in (a). Those vertical and horizontal pixel sizes are $100 \times 100 \mu\text{m}$ and $5 \times 5 \mu\text{m}$, respectively.

ARPES measurements of Bi2212 thin-films in the presence of electrical current

Amit Kanigel^{1*}, Muntaser Nammneh¹

¹*Department of Physics, Technion, Haifa 32000, Israel*

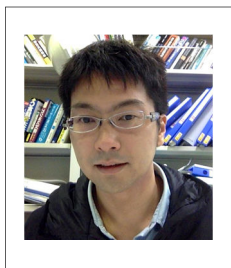
Email: amitk@physics.technion.ac.il

Keywords: high T_c, ARPES, Cuprates, PseudoGap

There are several different ways to turn a superconductor normal: Increasing the temperature, applying a large magnetic field or running a large current. The cuprate high T_c superconductors are unusual in the sense that experiments suggest that destroying superconductivity by heating the sample above T_c or by applying a large magnetic field result in different 'normal' states. Spectroscopic probes show that above T_c, in the pseudo gap regime, the Fermi-surface is partly gapped and there are no well defined quasiparticles. In contrary, transport measurements find quantum oscillations at high magnetic fields and low temperatures, suggesting a more usual Fermi-liquid state. Studying the electronic structure while suppressing superconductivity using current can hopefully shed new light on this problem. In type II SC, such as the cuprates, the resistive state created by the current is a result of vortex motion. The large dissipation in the flux-flow regime makes spectroscopic measurements in the presence of current challenging.

We performed angle resolved photoemission experiments in thin films of Bi2212 while running high current density through the samples. We find clear evidence for non-uniform flux-flow leaving most of the sample-volume free of mobile vortices and dissipation. The super-current changes the electronic spectrum creating quasi-particle and quasi-hole pockets. The size of these pockets as a function of the current is found to be doping-dependent; it depends both on the superfluid stiffness and on the strength of interactions.

Emergent Magnéli-type crystal phases and their mixture in pressurized sulfur hydride



Ryosuke Akashi^{1*}, *Wataru Sano^{1,2} Ryotaro Arita^{2,3},
Shinji Tsuneyuki¹
¹*The University of Tokyo, Japan*
²*RIKEN-CEMS, Japan*
³*JST-ERATO, Japan*

Email: * akashi@cms.phys.s.u-tokyo.ac.jp

Keywords: high T_c , hydrate, Magnéli phases, high pressure, first-principles calculation

The recent discovery of high-temperature superconductivity in sulfur hydride [1] has ignited people's attention to hydride systems as a possible stage to realize room-temperature superconductivity. First-principles studies have revealed the nature of the intriguing high- T_c phase, where H_3S phase emerges from the mother compound H_2S and it exhibits "extraordinarily conventional [2]" phonon-mediated superconductivity [3,4]. Also, the experimentally observed low- T_c phase is shown to be well explained with the H_2S metallic phases [5,6]. On this basis we next address a question: How the low- T_c phase transforms into the high- T_c phase under pressure?

Experimentally, the T_c of the system shows rapid and continuous increase with pressure when it is compressed at low temperature [1]. This suggests peculiar change of the electronic and lattice-dynamical properties through the low- T_c —high- T_c phase transformation. There have been numerous crystal phases which were shown to be (meta)stable according to first-principles calculations. However, up to now, any proposed structures have failed to yield clear explanation of this pressure dependence.

The current theoretical discussions on this issue appear to have focused too much on the possible understanding with a minimal number of distinct structural phases. Rather, we provide a different view: Not a single phase, but an infinite number of homologous series of phases are relevant [7]. Specifically, we find an infinite number of metastable crystal structures for variable stoichiometry H_xS ($2 < x < 3$). The newly found structures are long-period modulated crystals where slab-like H_2S and H_3S regions intergrow in a microscopic scale.

To understand these structures, we establish a unified theory based on the structural unit "interlaced H_2S ladders" [7]. The pristine H_2S phases ($P-1$ and $Cmca$) are formed by stacking the units of this type. The local H_3S -slab regions are then understood as the two-dimensional defects in the H_2S phases formed by edge-sharing bonding between the adjacent units. This formation mechanism is quite similar to those of the Magnéli phases [8] in the transition-metal oxides such as TiO_x and VO_x .

Finally, based on the first-principles calculations, we find that these "Magnéli" phases give a consistent explanation of the experimentally observed pressure dependence of

T_c . Extremely small formation enthalpy of the H_2S - H_3S boundary suggests that transformation through these phases can occur at low temperatures. The gradual increase of the H_3S stimulated by compression is expected to yield the increase of T_c . The newly found "Magnéli" phases thus gives a new insight into the superconductivity in sulfur hydride.

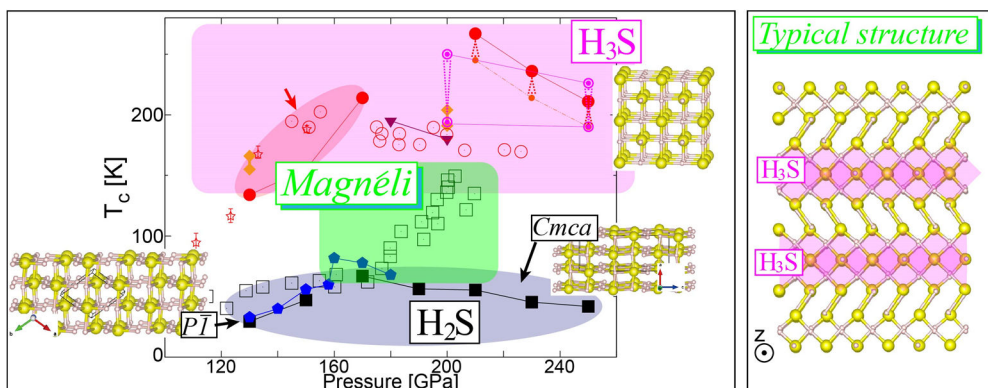
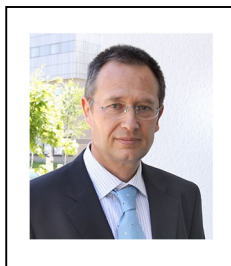


Figure 1: **(left)** Summary of the experimentally observed (open symbols) and theoretically predicted (solid symbols) T_c . The "Magnéli" phases explains the T_c in the green-shaded area. **(right)** A typical crystal structure belonging to the Magnéli type, where H_3S regions shaded in magenta emerge in the H_2S phase.

References

1. A. P. Drozdov, et al., Nature (London) **525**, 73 (2015). doi:10.1038/nature14964.
2. I. Mazin, Nature (London) **525**, 40 (2015). doi:10.1038/nature15203.
3. D. Duan, et al., Sci. Rep. **4**, 6968 (2014). doi:10.1038/srep06968.
4. I. Errea, et al., Phys. Rev. Lett. **114**, 157004 (2015). doi:10.1103/PhysRevLett.114.157004.
5. Y. Li, et al., J. Chem. Phys. **140**, 174712 (2014). doi:10.1063/1.4874158.
6. RA, et al., Phys. Rev. B **91**, 224513 (2015). doi:10.1103/PhysRevB.91.224513.
7. RA, et al., arXiv:1512.06680.
8. A. Magnéli, Acta Cryst. **6**, 495 (1953). doi: 10.1107/S0365110X53001381.

Relaxation and thermalization in many-body systems coupled to different bosonic degrees of freedom



J. Bonča^{1,2}

¹*Faculty of Mathematics and Physics, University of Ljubljana, Slovenia*

²*J. Stefan institute, Ljubljana, Slovenia*

Email: janez.bonca@ijs.si

Keywords: relaxation dynamics, correlated electron systems

In the first part I will briefly overview a fundamental study of the relaxation dynamics of a single hole in the two dimensional t - J model initially excited by a strong quench. Taking fully into account quantum effects we may follow the time-evolution of the system from a highly excited state until it reaches a steady state. Relaxation occurs on the time- scale of 10 fs due to inelastic scattering of a photo-excited carrier on spin excitations [1,2]. This mechanism can explain a finite raise of the scattering rate observed in ultrafast pump-probe experiments on cuprates [2].

In the second part I will discuss the primary relaxation process of a photo excited charge carrier coupled to quantum Einstein phonons [3]. If the pump pulse is sufficiently strong, the system relaxes after the primary energy redistribution towards a steady state. The one-particle density matrix computed in the steady state of a system described by a pure state overlaps with its thermal counterpart computed using the Gibbs state – thermal average over all states. The optical conductivity is as well independent of the initial state and resembles its thermal counterpart. Our results indicate that steady states are (quasi)thermal and the temperature can be read out from the optical conductivity. Therefore, secondary relaxation processes observed in time resolved ultrafast spectroscopy can be efficiently described by applying (quasi)thermal approaches, e.g., the many-temperature models.

Finally, I will compare relaxation mechanisms of a charge coupled to phonon degrees of freedom and hard-boson degrees of freedom. I will discuss the dependence of relaxation times of two systems on the pulse energy.

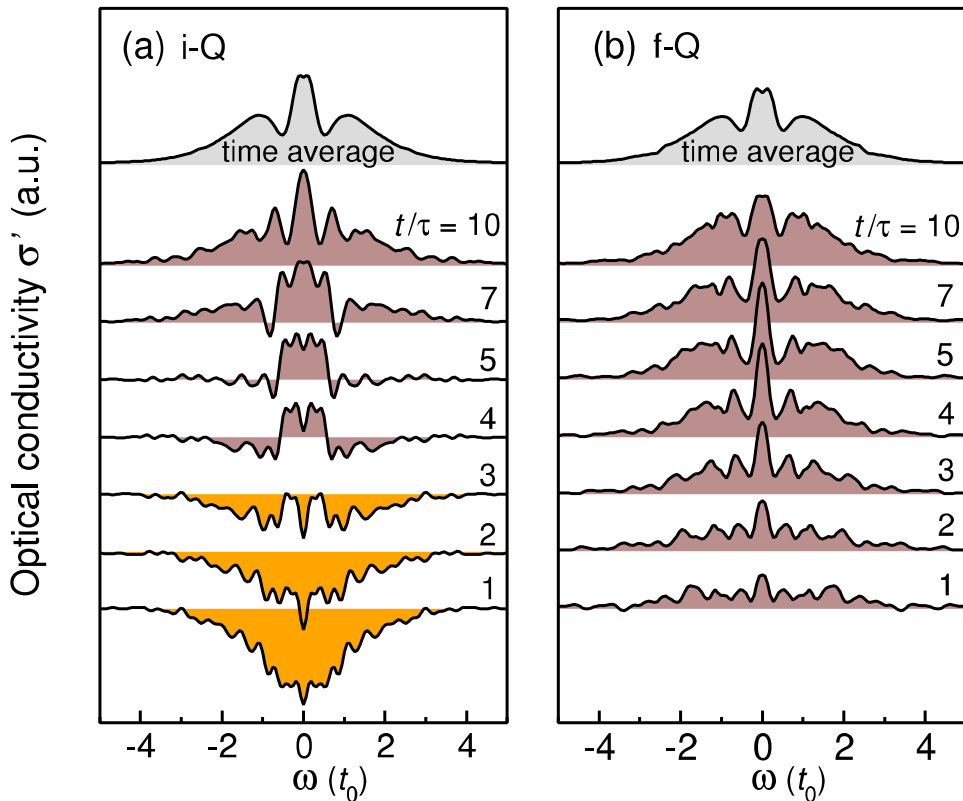


Figure 1: Time evolution of optical conductivity of a Holstein model starting from: **a)** a free electron solution initially positioned on the top of the conducting band with maximal kinetic energy then switching on electron-phonon coupling - an interaction quench and **b)** starting from the polaron ground state then driving the system with a constant external electric field up to the same total energy as in a). Picture taken from Ref.[3].

References:

1. D. Golež, J. Bonča, M. Mierzejewski, and L. Vidmar, *Phys. Rev. B* **89** 165118 (2014); M. Mierzejewski, L. Vidmar, J. Bonča, P. Prelovšek, *Phys. Rev. Lett.* **106**, 196401 (2011).
2. S. Dal Conte et al., *Nat. Phys.* **11**, 421 (2015)
3. J. Kogoj, L. Vidmar, M. Mierzejewski, S. A. Trugman, and J. Bonča, arXiv:1509.08431

Q=0 Magnetic order in the pseudogap state of cuprates superconductors



Ph Bourges^{1,*}

¹*Laboratoire Léon Brillouin CEA Saclay*

Email: * *Philippe.bourges@cea.fr*

Keywords: high T_c, magnetic structure

There has been a long-standing debate among condensed-matter physicists about the origin of the pseudo-gap state in high-temperature superconducting cuprates. Recent resonant ultra-sound measurements have provided evidence that the pseudo-gap phase is a symmetry breaking state, but the nature of the broken symmetry and the order parameter remain to be identified. Polarized neutron diffraction has revealed the existence of an ordered magnetic phase, hidden inside the pseudo-gap state of underdoped $\text{YBa}_2\text{Cu}_3\text{O}_{6+x}$, $\text{HgBa}_2\text{CuO}_{4+d}$ and $\text{Bi}_2\text{Sr}_2\text{CaCu}_2\text{O}_{8+d}$ [1]. Interestingly, the ordering temperature T_{mag} matches the pseudo-gap temperature T^* deduced from resistivity measurements. The magnetic order can be described as an Intra-Unit-cell magnetic order and it presents the symmetry predicted in the loop current theory of the pseudo-gap proposed by C.M. Varma [2]. In this theory, staggered current loops give rise to orbital-like magnetic moments within CuO_2 unit cell. Recently, we have shown the persistence of the magnetic order close to optimal doping but with finite-size planar magnetic correlation lengths of about ~ 7.5 nm [3]. Using the polarization analysis, we extract the moment components which display different temperature dependence.

References

1. P. Bourges and Y. Sidis, *C. R. Physique*, 12, 461, (2011);
2. Y. Sidis and P. Bourges, *J. Phys.: Conf. Ser.* 449, 012012 (2013)
3. C. M. Varma, *Phys. Rev. B* 73, 155113 (2006).
4. L. Mangin-Thro et al., *Phys. Rev. B* 89, 094523 (2014);
5. L. Mangin-Thro et al., *Nat. Comm.* 6:7705 doi: 10.1038/ncomms8705 (2015)

Long-range order and pinning of charge-density waves in competition with superconductivity



Yosef Caplan¹, Gideon Wachtel^{1,2}, Dror Orgad^{1*}

¹*Racah Institute of Physics, The Hebrew University,
Jerusalem 91904, Israel*

²*Department of Physics, University of Toronto, Toronto,
Ontario M5S1A7, Canada*

Email: orgad@phys.huji.ac.il

Keywords: CDW correlations, underdoped cuprates, competing orders

Recent experiments show that charge-density wave correlations are prevalent in underdoped cuprate superconductors. The correlations are short-ranged at weak magnetic fields but their intensity and spatial extent increase rapidly at low temperatures beyond a crossover field. Here we consider the possibility of long-range charge-density wave order in a model of a layered system where such order competes with superconductivity. We show that in the clean limit, low-temperature long-range order is stabilized by arbitrarily weak magnetic fields.

This apparent discrepancy with the experiments is resolved by the presence of disorder. Like the field, disorder nucleates halos of charge-density wave, but unlike the former it also disrupts inter-halo coherence, leading to a correlation length that is always finite. Our results are compatible with various experimental trends, including the onset of longer range correlations induced by inter-layer coupling above a characteristic field scale.

Exotic spin-orbital physics in hybrid d^4-d^3 and d^4-d^2 oxides



Andrzej M. Oleś^{1,2,*}, Wojciech Brzezicki^{1,3}, Mario Cuoco³,
Filomena Forte³

¹ Marian Smoluchowski Institute of Physics, Jagiellonian
University, prof. S. Łojasiewicza 11, 30348 Kraków, Poland

² Max-Planck-Institut FKF, 70569 Stuttgart, Germany

³ CNR-SPIN and Dipartimento di Fisica “E. R. Caianiello”,
Università di Salerno, 84084 Fisciano (SA), Italy

Email: * a.m.oles@fkf.mpg.de

Keywords: spin-orbital order – orbital dilution – orbital polarons – magnetic stripes

Strong Coulomb interactions in transition metal (TM) oxides lead to low-energy interactions between spins and orbitals in form of spin-orbital superexchange with entangled degrees of freedom [1]. Electronic states which arise under doping in such correlated insulators are very challenging and investigated only recently. For instance, charge defects in doped $Y_{1-x}Ca_xVO_3$ generate a soft kinetic gap within the defect band [2]. Here we investigate neutral defects arising when TM ions with active t_{2g} orbital degrees of freedom are replaced by TM ions with other valence, as for instance in doped ruthenate $Ca_2Ru_{1-x}Cr_xO_4$ where the magnetic and orbital transition temperature are modified and surprising negative volume thermal expansion is found [3]. To understand the consequences of such doping we investigate two cases: (i) *orbital dilution* realized by $3d^3$ impurities (Mn^{4+} , Cr^{3+}) in a planar ruthenate such as Ca_2RuO_4 (Sr_2RuO_4) [4], and (ii) *hole-doublon pairs* in case of $3d^2$ doping. The spin-orbital superexchange interactions concern host d^4-d^4 bonds and hybrid d^4-d^3 (d^4-d^2) bonds. We derive these interactions for both cases and show that the presence of hybrid d^4-d^3 (d^4-d^2) bonds modifies locally or even globally spin-orbital in a Mott insulator. In the first case shown in Fig. 1(a) the impurity acts either as a spin defect accompanied by the orbital vacancy when the host-impurity coupling is weak, or it favors doubly occupied active orbitals along the hybrid bond leading to orbital polarons [4]. This competition leads to rather rich and complex phase diagrams with frustrated magnetic interactions when antiferromagnetic and ferromagnetic host-impurity coupling compete. The spin-orbital order within the host is totally modified by double exchange at doping $x=1/4$ [5], with new spin-orbital stripes similar to orbital stripes [6]. We highlight the role of orbital quantum fluctuations [4] which modify quantitatively spin-orbital order imposed by superexchange. The case of hole doping represents a *doublon dilution*, see Fig. 1(b), which is even more challenging. The derived spin-orbital interactions on the hybrid bonds contain here $T_i^+T_j^+$ terms responsible for double hole-doublon excitations which provide more quantum fluctuations than in the case of orbital dilution – such terms are absent in the host. We investigate several distributions of d^2 impurities, from periodic to randomly distributed and show that such impurities may play a role for

magnetic stripes. Phase diagrams for single impurities and low doping are obtained and we demonstrate that again local and global modifications of spin-orbital order in the host may be induced by doping. The possible self-organization of defects is reminiscent of nano-striped magnetic puddles in high- T_c superconductors [7]. Our findings are expected to be of importance for future experimental and theoretical studies of $4d$ TM oxides with $3d$ impurities of different valence modifying the orbital order.

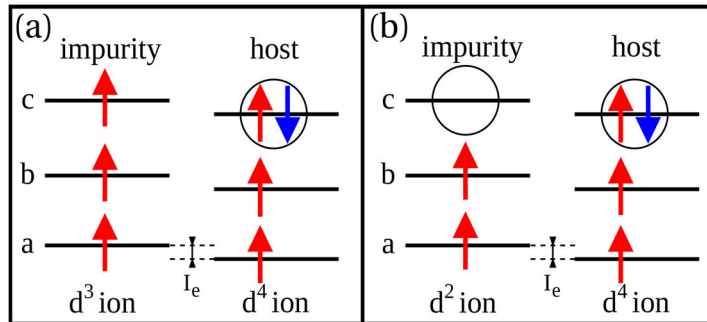


Figure 1: Transition metal impurities in a spin-orbital d^f system (ruthenate): (a) doping by d^3 ions (orbital dilution) [4,5], and (b) hole doping by d^2 ions

W. Brzezicki acknowledges support by the EC under Marie Skłodowska-Curie grant agreement No. 655515. Work supported by NCN Project No. 2012/04/A/ST3/00331.

References

1. M. Oleś, J. Phys: Condensed Matter **24**, 313201 (2012).
2. A. Avella, A. M. Oleś, and P. Horsch, Phys. Rev. Lett. **115**, 206403 (2015).
3. T. F. Qi, O. B. Korneta, S. Parkin *et al.*, Phys. Rev. Lett. **105**, 177203 (2010).
4. W. Brzezicki, A. M. Oleś, and M. Cuoco, Phys.Rev. X **5**, 011037 (2015).
5. W. Brzezicki, M. Cuoco, and A. M. Oleś, J. Sup. Novel Magn. **29**, in press (2016) doi:10.1007/s10948-015-3287-z.
6. P. Wróbel and A. M. Oleś, Phys. Rev. Lett. **104**, 206401 (2010).
7. A. Bianconi, J. Sup. Novel Magn. **27**, 909 (2011)

Superconductivity and unusual magnetic features in amorphous carbon and in other unrelated materials



Israel Felner
Institute of Physics, The Hebrew University, Jerusalem,
 91904, Israel

Email: israela@vms.huji.ac.il

Keywords: Amorphous carbon, superconductivity, peculiar magnetic behavior

Traces of superconductivity (SC) up to 65 K were observed by magnetic measurements in three different *inhomogeneous* sulfur doped amorphous carbon (a-C) systems: in (i) commercial and (ii) fabricated powders and in (iii) a-C thin films.

(i) The commercial (a-C) powder which contains 0.21% sulfur, reveals traces of *two* non-percolated superconducting phases at $\sim T_c$ 34 and 65 K. The SC volume fraction is enhanced by increasing the sulfur content. (ii) Pristine fabricated a-C powder obtained by pyrolytic decomposition of sucrose, is not SC down to 5 K. However, mixing of this powder with sulfur and heating the mixture at 400 °C (a-CS) for 24 hours, yields inhomogeneous products which shows traces of SC phases at $T_c = 17$ and 42 K. (iii) Non-superconducting a-C thin films were grown by electron-beam induced deposition. SC emerged at $T_c = 34.4$ K only after heat treatment with sulfur [1].

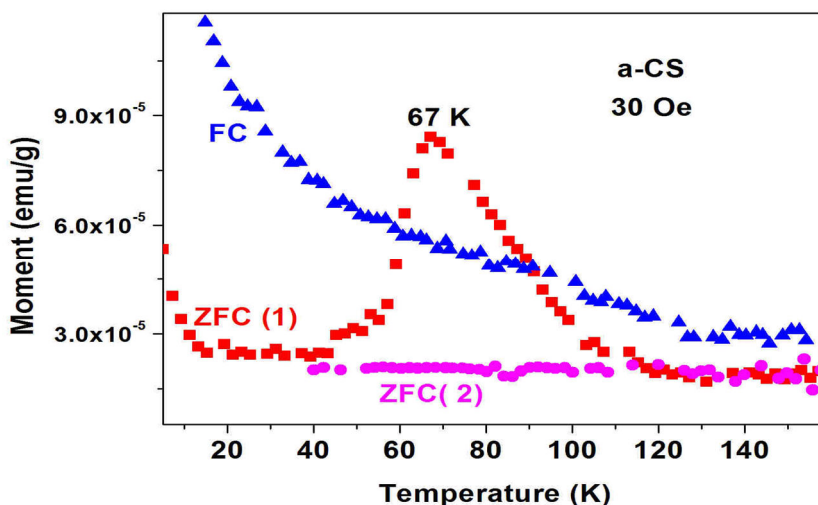


Fig. 1 Two ZFC and one FC plots of a-CS measured at 30 Oe. The ZFC(2) branch (in purple) was measured a few minutes after the ZFC(1) run (in red).

Other parts of the commercial a-C and/or pyrolytic a-CS powders, show unusual magnetic features (Fig. 1). (a) Pronounced irreversible peaks around 55-75 K appear in the *first* zero-field-cooled (ZFC) runs only. These peaks are totally suppressed in the second ZFC sweeps measured a few minutes later. (b) Around the peak position the field-cooled (FC) curves cross the ZFC plots (ZFC>FC). These two peculiar magnetic observations are connected to each other. All SC and magnetic phenomena observed are intrinsic properties of the a-CS materials [1].

It is proposed that the a-CS systems behave similarly to the high T_C curates and/or pnictides in which SC emerges from magnetic states. In addition, the a-CS system resembles the sulfur hydrides (H_3S) material which becomes SC at $T_C = 203$ K under high pressure (>200 GPa). In H_3S , SC is explained by the interaction between the electrons and the high frequencies hydrogen vibrations. This model may also be applied to a-CS. The relatively light carbon atoms and their high vibration frequencies as simple harmonic oscillators may induce SC even at *ambient pressure* with T_C as high as 67 K. Alternatively, it is possible that the a-CS powders contain small amount of hydrogen and that the observed SC states are pressed H_3S immersed or adsorbed in the a-C matrix.

References

1. I. Felner, Mater. Res. Express1, 16001 (2014).

Spin-orbit coupling and spin excitations in Sr_2RuO_4 and iron-based superconductors



Felix Ahn¹, Sergio Cobo¹, and Ilya Eremin^{1*}

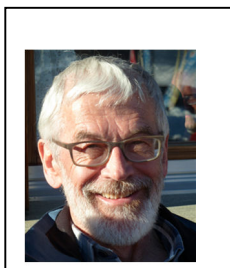
¹*Institut für Theoretische Physik III, Ruhr-Universität Bochum, 44801 Bochum, Germany*

Email: * Ilya.Eremin@rub.de

Keywords: unconventional superconductors, spin excitations, spin-orbit coupling

We analyze the magnetic excitations in Sr_2RuO_4 and iron-based superconductors in presence of spin-orbit coupling. Based on several tight-binding parametrizations of the 3d electron states we show how the spin-orbit coupling introduces the anisotropy of the magnetic excitations of paramagnetic states of both compounds. The orientation of the spin fluctuations is determined by the contribution of the xy, xz, and yz orbitals to the electronic states near the Fermi level. In iron based superconductors we find that within an itinerant approach the magnetic ordering is most favorable along the wavevector of the striped AF state. This appears to be a natural consequence of the spin-orbit coupling in the striped AF state where the ferro-orbital order of the xz and yz orbitals is only a consequence of the striped AF order. We further analyze the role of spin-orbit coupling for the Sr_2RuO_4 and contrast its behavior to the spin excitations in iron-based superconductors.

Variational results for the two-dimensional repulsive Hubbard model: The refined Gutzwiller ansatz



D. Baeriswyl and M. Menteshashvili
*Department of Physics, University of Fribourg,
 CH-1700 Fribourg*

Email: *dionys.baeriswyl@unifr.ch*

Keywords: Hubbard model, variational method, diagrammatic expansion, superconductivity

Gutzwiller's variational ansatz, introduced more than fifty years ago, has been quite successful in various respects. It takes into account electronic correlations in a very simple way, produces a link between a microscopic Hamiltonian and Fermi-liquid theory, can deal with various types of orderings, such as ferromagnetism, antiferromagnetism or superconductivity, and it has also been used for describing the Mott metal-insulator transition. More recently, the ansatz has been merged with *ab initio* techniques in the "Gutzwiller Density Functional Theory". In spite of all these successes, the Gutzwiller wave function has drawbacks, both at large values of the interaction parameter U , where it does not account for the strong binding of holons and doublons, and at small U , where it produces an unphysical increase in the Fermi step of the momentum distribution function. The large U problem has been cured by "inverting" the Gutzwiller ansatz [1]. A combination of the original Gutzwiller wave function and its inverse yields a refined ansatz, which we have used for exploring the possibility of a superconducting ground state, using a variational Monte Carlo method for U of the order of the bandwidth [2]. More recently, we have studied this refined wave function in the small U limit, using an expansion in powers of U [3]. We have found that the artefact of an enhanced Fermi step has disappeared, as shown in Figure 1 for a density of 0.67 electrons per site and a relatively small value of U . We have also studied superconductivity and antiferromagnetism as well as a possible coexistence between the two phases. While the antiferromagnetic ground state (at half filling) is found to agree well with previous variational Monte Carlo results, our findings related to superconductivity are quite puzzling, probably due to large finite size effects. Therefore at this time we cannot draw any definite conclusions about the evolution of the superconducting order parameter in the small U regime and even less so about the problem of coexistence. To circumvent this problem, we have started to study the effective interaction (technically the irreducible vertex) from the diagrammatic expansion of the refined Gutzwiller ansatz. Already at the lowest order attractive couplings appear, in a similar way as in studies based on the functional renormalization group or in other approaches inspired by the Kohn-Luttinger mechanism.

After a brief review of the Gutzwiller ansatz and its applications, this talk will be focussed on our current study of the refined Gutzwiller ansatz in the small U limit. The expansion in powers of U can be neatly visualized by diagrams, very much as in conventional perturbation expansions of quantum field theory. Results for the correlation energy, the momentum distribution, the effective interaction and the fate of superconductivity will be presented, together with an outlook on future studies along this line.

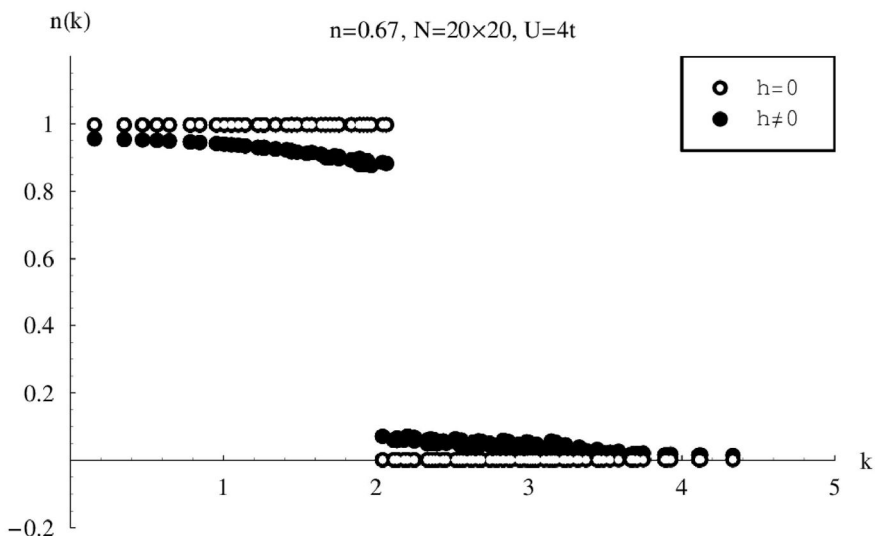


Figure 1: Momentum distribution along the diagonal of the Brillouin zone both for the original Gutzwiller ansatz ($h=0$) and for the refined wave function ($h \neq 0$).

References

1. D. Baeriswyl, *Solid St. Sciences* **69**, 183 (1987); *Found. Phys.* **30**, 2033 (2000).
2. D. Baeriswyl, D. Eichenberger and M. Menteshashvili, *New J. Phys.* **11**, 075010 (2009).
3. M. Menteshashvili and D. Baeriswyl, work in progress.

X-ray studies of complex materials for energy applications



Bernardo Barbiellini

Department of Physics, Northeastern University, Boston, Massachusetts 02115, USA

Email: * bba@neu.edu

Keywords: Lithium-ion battery, Cathode materials, x-ray spectroscopies.

We have studied Li_xFePO_4 olivine, $\text{Li}_x\text{Mn}_2\text{O}_4$ spinel and Li_xCoO_2 ceramic materials, which are used as cathodes in lithium-ion batteries. The transition metal oxidation number in Li_xFePO_4 and the nanoscale phase separation can be monitored with the L-edge x-ray absorption spectroscopy (XAS) [1]. In general, XAS reveals the electronic structure of unoccupied energy levels of the sample while x-ray emission spectroscopy (XES) gives the complementary information about the occupied energy levels [2]. All these spectra can be either predicted or verified by first-principles calculations. Moreover, the theory predicts that techniques based on inelastic x-ray scattering can be used to detect the elusive lithium. In particular, x-ray Compton scattering can directly image electronic orbitals associated with lithiation as demonstrated in recent studies of $\text{Li}_x\text{Mn}_2\text{O}_4$ [3,4]. So far, we have shown that x-ray spectra can be successfully predicted using first-principles. Thus, we have enabled a fundamental characterization of lithium battery materials involving spectroscopy and first-principles calculations. The detailed information we have obtained regarding the evolution of electronic states will be indispensable for understanding and optimizing battery and fuel cell materials [5].

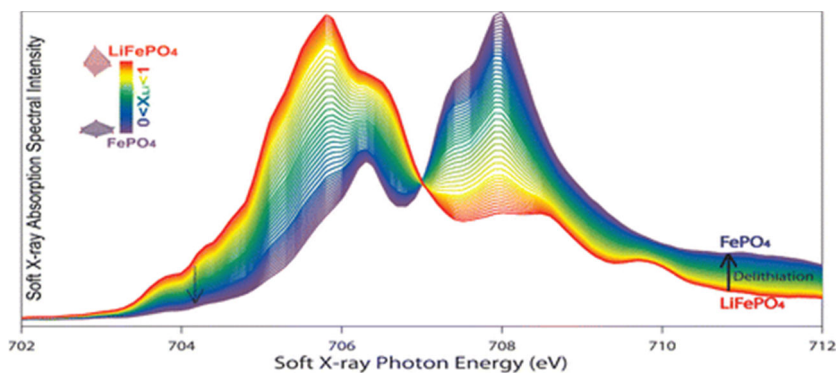


Figure 1: XAS data for Li_xFePO_4 . The spectra indicate nanoscale phase separation.

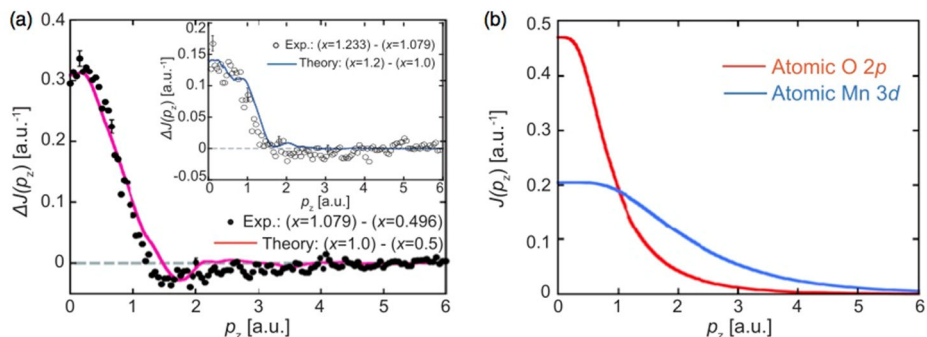


Figure 2: (a) x-ray Compton profiles differences for $\text{Li}_x\text{Mn}_2\text{O}_4$. (b) Compton profiles for selected orbitals.

References

1. Xiaosong Liu, Jun Liu, Ruimin, Qiao, Yan Yu, Hong Li, Liumin Suo, Yong-Sheng, Hu, Yi-De Chuang, Guojiun Shu, Fangcheng Chou, Tsu-Chien Weng, Dennis Nordlund, Dimosthenis Sokaras, Yung Jui Wang, Hsin Lin, Bernardo Barbiellini, Arun Bansil, Xiangyun Song, Zhi Liu, Shishen Yan, Gao Liu, Shan Qiao, Thomas J. Richardson, David Prendergast, Zahid Hussain, Frank M. F. de Groot, and Wanli Yang, *J. Am. Chem.* **134** (2012) 13708.
2. Xiaosong Liu, Yung Jui Wang, Bernardo Barbiellini, Hasnain Hafiz, Susmita Basak, Jun Liu, Thomas Richardson, Guojiun Shu, Fangcheng Chou, Tsu-Chien Weng, Dennis Nordlund, Dimosthenis Sokaras, Brian Moritz, Thomas P. Devereaux, Ruimin Qiao, Yi-De Chuang, Arun Bansil, Zahid Hussain and Wanli Yang, *Phys. Chem. Chem. Phys.* **17** (2015) 26369.
3. K. Suzuki, B. Barbiellini, Y. Orikasa, N. Go, H. Sakurai, S. Kaprzyk, M. Itou, K. Yamamoto, Y. Uchimoto, Yung Jui Wang, H. Hafiz, A. Bansil, Y. Sakurai, *Phys. Rev. Lett.* **114** (2015) 087401.
4. K. Suzuki, B. Barbiellini, Y. Orikasa, S. Kaprzyk, M. Itou, K. Yamamoto, Yung Jui Wang, H. Hafiz, Y. Uchimoto, A. Bansil, Y. Sakurai, H. Sakurai, *J. Appl. Phys.* **119**(2016) 025103.
5. Qingying Jia, Nagappan Ramaswamy, Hasnain Hafiz, Urszula Tylus, Kara Strickland, Gang Wu, Bernardo Barbiellini, Arun Bansil, Edward F. Holby, Piotr Zelenay, and Sanjeev Mukerjee, *ACS Nano* **9** (2015) 2496.

Zero and Finite-T Response of 2D Dipolar Bosons at Non-zero Tilt Angles



Khandker F. Quader*, and Pengtao Shen
Department of Physics, Kent State University, Kent, OH 44242, USA

Email: * quader@kent.edu

Keywords: Bose condensation, dipolar bosons, non-zero tilt angle, stripe phase, finite-T RPA

We study properties of dipolar bosons in 2D and quasi-2D geometry, with dipoles oriented at an angle to the direction perpendicular to the confining 2D plane. Starting from time-dependent Gross-Pitaevski equations, and Bogoliubov-de Gennes equations, we first calculate the $T=0$ excitation spectrum of the Bose-Einstein condensate, and explore possible instabilities of the system as the tilt angle, system density and the relative strength of the dipole-dipole interaction are varied. We then explore finite temperature response of the systems within the random phase approximation (RPA). We calculate the appropriate 2D finite-T pair bubble diagram needed in RPA, and explore ranges of density and temperature for various dipolar tilt angles. We find the system to exhibit a collapse transition and a finite momentum instability, signaling a striped phase. We construct phase diagrams depicting these instabilities and resulting phases; shown in Figure 1. We discuss how our results may apply to ultracold dense Bose gas of polar molecules, such as $^{41}\text{K}^{87}\text{Rb}$, that has been realized experimentally.

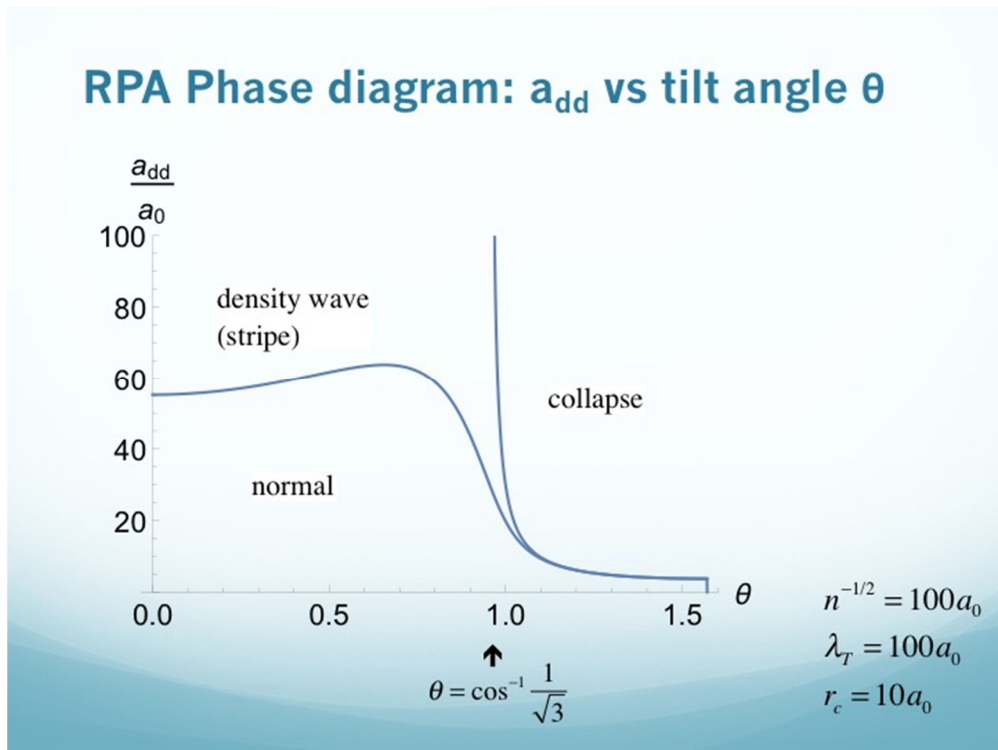


Figure 1: Phase diagram of 2D dipolar Bose gas constructed from finite-T RPA calculations: dipolar strength vs dipole tilt angle.

Time-resolved switching of magnetization in a multiferroic



E. M. Bothschafter^{1*}, M. Savoini², M. Porer¹, M. Buzzi¹, Y. W. Windsor¹, C. Dornes², L. Rettig^{1,2}, M. Ramakrishnan¹, A. Alberca¹, S.R.V. Avula¹, D. Schick³, N. Pontius³, C. Schuessler-Langeheine³, J. A. Heuver⁴, S. Mazten⁵, B. Noheda⁴, C. Piamonteze¹, S. L. Johnson², U. Staub¹

¹Swiss Light Source, Paul Scherrer Institute, Villigen, CH

²Institute for Quantum Electronics, Eidgenössische Technische Hochschule (ETH) Zürich, CH

³Helmholtz-Zentrum Berlin für Materialien und Energie GmbH, D

⁴Zernike Institute for Advanced Materials, University of Groningen, NL

⁵Institut d'Electronique Fondamentale, UMR CNRS, University Paris Sud, FR

Email: * elisabeth.bothschafter@psi.ch

Keywords: multiferroics, time-resolved dynamics, ferroelectric, optical switching

Understanding and controlling the magnetoelectric properties of multiferroic materials of type-II is of high interest, as these materials offer a unique direct coupling between magnetic order and ferroelectric polarization. In particular, the manipulation of these properties with ultrashort light pulses would allow new schemes for light-based data storage and manipulation.

Recent important advances in this field reported the observation of coherent spin dynamics by a controlled excitation of an electromagnon resonance [1]. Theoretical predictions show that a switching of the helicity of magnetic order by strongly exciting such an electromagnon resonance would simultaneously switch the ferroelectric polarization [2]. However, this process requires high electric field strength in the range of tens of MV/cm at terahertz frequencies. An alternative, very promising route towards ultrafast control of magnetization is the effect of all-optical switching which has been observed in multi-sublattice metallic alloys [3]. In order to simultaneously control magnetization and polarization by such a switching process, strong magnetoelectric coupling in a multiferroic is required.

Here we report on the magnetization switching of the insulating multiferroic CoCr_2O_4 using above band gap excitation with femtosecond laser pulses. The magnetization is probed by circularly polarized x-ray pulses, which allow for element-specific observation of the switching dynamics. The magnetization in both the Co and Cr magnetic sublattice is reversed up to 90% within tens of picoseconds. However, the optical excitation alone is not sufficient to initiate the switching of magnetization. The magnetization reversal only occurs in the presence of sufficient x-ray exposure. As the material is an insulator and x-ray exposure cannot act directly on the magnetization but enhance the conductivity of the material, this effect indicates that polarized spin currents and/or spin flip scattering play a significant role for the transfer of magnetic

moment in the all-optical switching process. Even more important is the observation of magnetic switching in the multiferroic phase of CoCr_2O_4 at low temperatures. The magnetization reversal is expected to simultaneously reverse the ferroelectric polarization as a result of strong magnetoelectric coupling [4]. Further investigation of the observed effect will provide insight into the microscopic origins of all-optical switching and the role of spin-polarized currents in the transfer of magnetic momentum between antiferromagnetically coupled sublattices. Our findings provide a new way of light-based control of ultrafast magnetization and polarization switching.

References

1. T. Kubacka, J. A. Johnson, M. C. Hoffmann, C. Vicario, S. de Jong, P. Beaud, S. Grubel, S. W. Huang, L. Huber, L. Patthey, Y. D. Chuang, J. J. Turner, G. L. Dakovski, W. S. Lee, M. P. Minitti, W. Schlotter, R. G. Moore, C. P. Hauri, S. M. Koohpayeh, V. Scagnoli, G. Ingold, S. L. Johnson, and U. Staub, *Science* **343**, 1333 (2014).
2. M. Mochizuki and N. Nagaosa, *Phys. Rev. Lett.* **105**, 147202 (2010).
3. C. D. Stanciu, A. Tsukamoto, A. V. Kimel, F. Hansteen, A. Kirilyuk, A. Itoh, and T. Rasing, *Phys. Rev. Lett.* **99**, 217204 (2007).
4. Y. Yamasaki, H. Sagayama, T. Goto, M. Matsuura, K. Hirota, T. Arima, and Y. Tokura, *Phys. Rev. Lett.* **98**, 147204 (2007).

A new approach to the growth of materials leading to macroscopic quantum coherence and high temperature superconductivity.



Philip Turner^{*}, Laurent Nottale^{2*},

¹*Edinburgh Napier University, 10 Colinton Road, Edinburgh, EH10 5DT, United Kingdom.*

²*CNRS, LUTH, Observatoire de Paris-Meudon, 5 Place Janssen, 92190, Meudon, France.*

Email: *ph.turner@napier.ac.uk.

Keywords: High temperature superconductivity, macroscopic quantum coherence, fractal networks.

We present a new evidenced based theoretical approach to the growth of structures exhibiting high levels of macroscopic quantum coherence, which has application in the development of high temperature super conductive materials.

The theory supports recent experimental work on the emergence of inorganic plant-like structures[1], dictated by controlling charge density (levels of protonation) directly linked to atmospheric CO₂ concentration. More detailed follow up work [2] has revealed that as levels of charge density increase beyond a critical point, dissipative systems driving fractal assembly and a fractal network of charges at the molecular scale leads to the emergence of a charged induced coherent bosonic field at macroscopic scales, i.e., a macroscopic quantum potential, which act as a structuring force during molecular assembly.

The strength of the coherent field determines the type of structure that emerges in diffusion based growth processes. Depending on the conditions, a wide range of structures associated with plants (e.g. crystals, tumors, ferns, fungi, stems, seeds, flowers pods, fruits, cells) can emerge. At the extremes, macroscopic spherical structures (Fig.1a) emerge at the highest levels of charge density, whilst dendritic structures (Fig.1b) signify the start of a macroscopic decoherence process which has its geometric equivalence in standard quantum mechanics. Full macroscopic quantum decoherence is reflected in pure crystalline structures in the same materials (Fig.1c).

Whilst the system is only partially coherent (i.e. only the bosonic fields are coherent), within these processes many of the phenomena associated with standard quantum theory are recovered, including quantization, non-dissipation, self-organization, confinement, structuration conditioned by the environment and environmental fluctuations leading to macroscopic quantum decoherence. The emerging processes can be described by macroscopic Schrödinger equations.

This work provides a strong case for the existence of quintessence-like behaviour [3], with macroscopic quantum potentials and associated forces having their equivalence in standard quantum mechanics. The forces driving these macroscopic quantum processes are directly analogous with macroscopic quantum coherence in high temperature super

conductivity [4]. We establish a testable hypothesis that structure emerging out of high-energy macroscopic potentials will lead to increased levels of T_c in HTSC materials. If the theory is confirmed it opens up a new first principles approach to the structural development of high temperature superconducting materials, with higher levels of macroscopic quantum coherence leading to higher values for T_c .

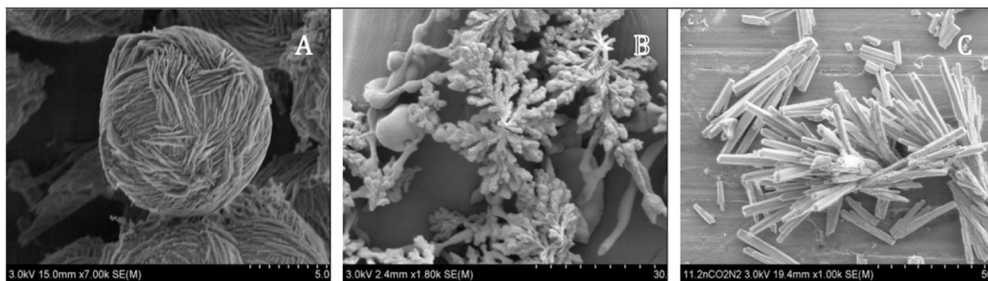


Figure 1. Emergent structure dependent on charge density [4] showing spherical (a), dendritic (b) and crystalline (C) structures.

References

1. Noorduyn. W. L, Grinthal. A, Mahadevan. L and Aizenberg.J. Rationally designed complex, hierarchical microarchitectures, *Science* 340 832-837 (2013). □
2. Turner. P and Nottale. L. The physical principles underpinning self-organization in plants. Submitted to *Science* (2016).
3. Witten. E. Comments on String theory. arXiv:hep-th/0212247v1 (2002). □
4. Turner. P and Nottale. L. The origins of macroscopic quantum coherence in high temperature super conductivity. *Physica C*. 515 15-30 (2015). □

Charge - orbital order and topological effects in presence of zig-zag magnetic textures in 4d – 3d hybrid oxides



Wojciech Brzezicki^{1*}, Mario Cuoco^{1*},
¹ *CNR-SPIN, IT-84084 Fisciano, Italy*

Email: *wbrzezicki@unisa.it*

Keywords: zig-zag, spin-orbit, Dirac points

The entanglement of spin, orbital and lattice degrees of freedom in correlated systems is known to lead to intricate quantum phenomena [1]. Correlated physics in transition metal oxides (TMO) traditionally emphasizes 3d materials because the more extended 4d-shells would a priori suggest a weaker ratio between the intra-atomic Coulomb interaction and the electron bandwidth. Nevertheless, the extension of the 4d- shells points towards a strong coupling between the 4d- orbitals and the neighboring oxygen orbitals, implying that these TMO have the tendency to form distorted structure with respect to the ideal one. Hence, the change in M-O-M bond angle often leads to a narrowing of the d-bandwidth, bringing the system on the verge of a metal-insulator transition or into an insulating state. The interplay between more localized 3d and more delocalized 4d states tunes the competition between correlated metallic and Mott-insulating states and, in turn, can significantly influence the strength and the hierarchy between the spin-orbital-lattice degrees of freedom. For instance the magnetic and orbital patterns in a uniform 4d host can be strongly modified by the inclusion of 3d impurities substituting the 4d ions [2]. After discussing the most suitable microscopic models for different types of 4d-3d hybrids, we determine the phase diagram assuming different conditions for the spin ordering in the metallic phase [3]. We demonstrate that the coupling between the impurity and the host, specific of the 4d-3d system, can generate a complex phase competition [3] and different types of orbital and charge orders can occur. For chosen striped spin orders in the metallic phase, i.e., zig-zags of the segment length $L_z=2,3$, see Fig. 1, we analyze the band structure of itinerant xz/yz electrons in presence of on-site spin-orbit coupling. We demonstrate that the spatial symmetries specific to the zig-zag pattern (see Fig. 1) can lead to single or multiple Dirac points that are topologically protected and whose nature and multiplicity depends on the zig-zag segment length L_z . We demonstrate topological phase diagrams for $z2$ and $z3$ zig-zag phases and identify topological invariants. Since ruthenates belonging to the Ruddlesden-Popper series represent a fertile 4d platform where to achieve different magnetic-orbital ordered states and metal-to-insulator transitions [4-6], a specific discussion of the Ru-oxides doped with Mn will be presented.

W.B. acknowledges support by the European Union Horizon 2020 grant agreements No. 655515.

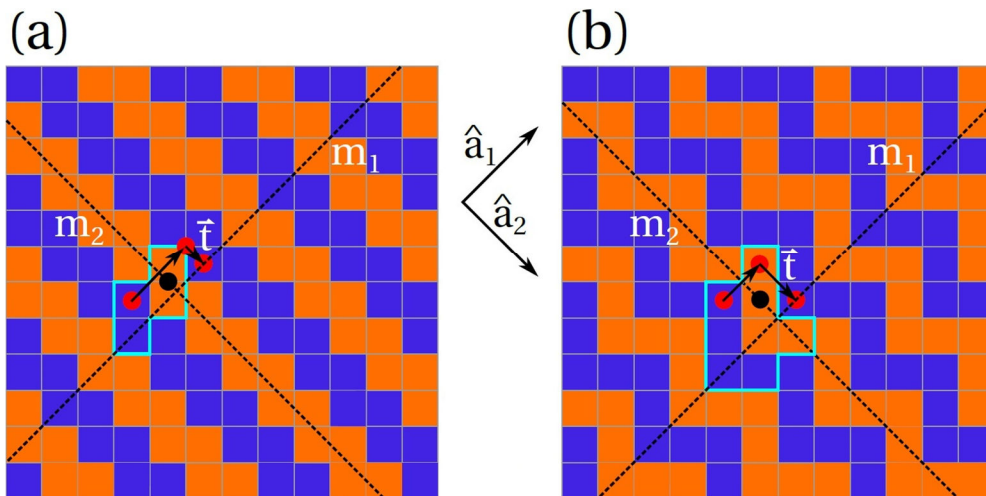
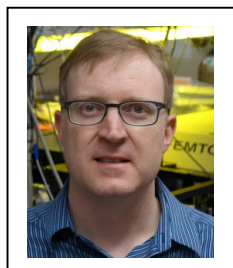


Figure 1: View of the classical zig-zag spin patterns; (a) zig-zag of the length $L_z = 2$ (z_2) and (b) zig-zag of the length $L_z = 3$ (z_3). The orange and blue fields symbolize spins up and down located in the center of each field. The unit cell is marked with a thick frame and $\hat{a}_{1,2}$ are the translation vectors. Dashed lines are the mirror planes m_1 or mirror planes m_2 being the part of the gliding symmetry. The action of gliding symmetry is shown with red dots and arrows; first the dot is subject to the reflection m_2 then it is translated by a vector \vec{t} parallel to the mirror plane m_2 . The black dots are the inversion centers.

References

1. Y. Tokura and N. Nagaosa, *Science* **288**, 462 (2000).
2. W. Brzezicki, A. M. Oleś, and M. Cuoco, *Phys. Rev. X* **5**, 011037 (2015).
3. W. Brzezicki, C. Noce, A. Romano, M. Cuoco, *Phys. Rev. Lett.* **114**, 247002 (2015).
4. C. Autieri, M. Cuoco, and C. Noce, *Phys. Rev. B* **89**, 075102 (2014).
5. M. Malvestuto, V. Capogrosso, E. Carleschi, L. Galli, E. Gorelov, E. Pavarini, R. Fittipaldi, F. Forte, M. Cuoco, A. Vecchione, and F. Parmigiani, *Phys. Rev. B* **88**, 195143 (2013).
6. F. Forte, M. Cuoco, and C. Noce, *Phys. Rev. B* **82**, 155104 (2010).

Stripes, phonons, and electronic dynamics: new views on ultrafast time scales



G. Coslovich¹, J. H. Buss¹, H. Wang¹, Y. Xu¹, J. Maklar¹, S. Behl¹, B. Huber¹, T. Sasagawa², C. Jozwiak³, A. Lanzara^{1,4}, H. A. Bechtel³, M. C. Martin³, and R. A. Kaindl^{1*}

¹Materials Sciences Division, Lawrence Berkeley National Laboratory, 1 Cyclotron Road, Berkeley, CA 94720, USA

²Materials and Structures Laboratory, Tokyo Institute of Technology, Kanagawa 226-8503, Japan

³Advanced Light Source, Lawrence Berkeley National Laboratory, 1 Cyclotron Road, Berkeley, CA 94720, USA

⁴Department of Physics, University of California at Berkeley, Berkeley, CA 94720, USA

Email: *rakaindl@lbl.gov

Keywords: charge order, nickelates, ultrafast spectroscopy, THz, photoemission

In complex materials, nanoscale and ultrafast phenomena are closely linked, motivating experiments that access these extremes to help understand the basic interactions and correlations. In particular, clarifying the complex and dynamic driving forces underlying the formation of quasi-1D stripes in transition metal oxides may be central to understanding high- T_C superconductivity. In the first part, we will discuss our recent experiments that track the initial steps of charge ordering in nickelates. The ultrafast mid-IR response of $\text{La}_{1.75}\text{Sr}_{0.25}\text{NiO}_4$ resolves charge localization and transient

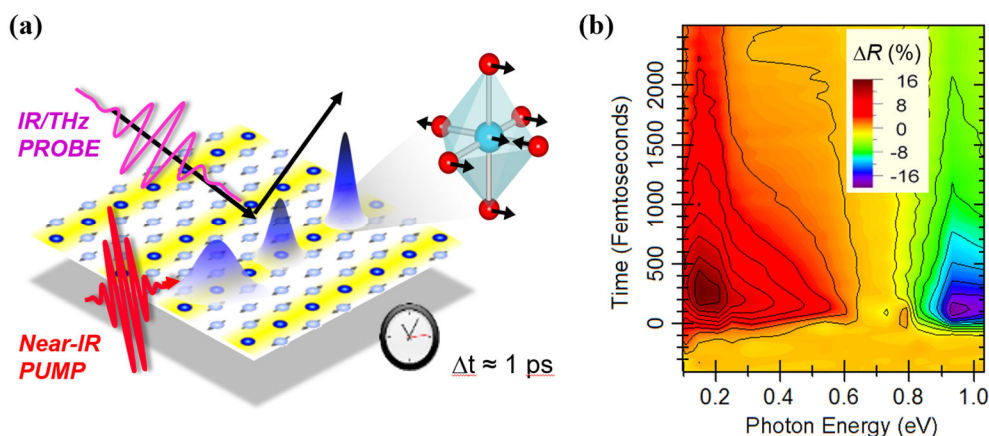


Figure 1: Ultrafast mid-IR probe of the initial steps of stripe-formation in $\text{La}_{1.75}\text{Sr}_{0.25}\text{NiO}_4$. [1] (a) Schematic illustration of charge localization and electron-phonon coupling. (b) Sub-picosecond dynamics of the pseudogap in the broadband optical conductivity.

electron-phonon coupling on femtosecond time scales, exposing their precursor role in stripe formation [1]. Here, the opening of a pseudogap at a crossover temperature T^* far above long-range stripe formation establishes the onset of electronic localization, which is accompanied by an enhanced Fano asymmetry of the Ni-O stretch vibrations. Ultrafast excitation triggers a sub-picosecond dynamics, revealing a synchronous modulation of electron-phonon coupling and charge localization. Moreover, the Ni-O bending vibration around 11 THz exhibits a splitting due to phonon zone folding, rendering lattice distortions at finite momenta accessible to electromagnetic detection. Here, transient multi-THz spectroscopy with high energy resolution provides access to both short and long-range ordering within a single THz pulse spectrum. Finally, we will discuss the development of a new table-top capability for time- and angle-resolved photoemission (trARPES) studies at high-repetition rates, which can provide complementary insight into the momentum-space signatures of atomic and nanoscale order. It is based on an efficient, high repetition rate (50-kHz) source of bright extreme-ultraviolet harmonics around 22 eV [2]. First experimental results will be discussed that utilize this novel femtosecond source to access the electronic structure dynamics in complex materials throughout momentum space with high energy and time resolution.

References

1. G. Coslovich, B. Huber, W.-S. Lee, Y.-D. Chuang, Y. Zhu, T. Sasagawa, Z. Hussain, H.A. Bechtel, M.C. Martin, Z.X. Shen, R.W. Schoenlein, and R.A. Kaindl, *Nature Comm.* **4**, 2643 (2013).
2. H. Wang, Y. Xu, S. Ulonska, J. S. Robinson, P. Ranitovic, and R. A. Kaindl, *Nature Comm.* **6**, 7459 (2015).

Fluctuating Superconductivity in the Strongly Correlated Organic Superconductors in κ -(BEDT-TTF)₂X (X = Cu[N(CN)₂]Br, Cu(NCS)₂) Studied by Polarized Femtosecond Spectroscopy



Koichi Nakagawa^{1*}, Satoshi Tsuchiya¹, Jun-ichi Yamada²,
Yasunori Toda¹

¹*Department of Applied Physics, Hokkaido University*

²*Graduate School of Material Science, University of Hyogo*

Email: * k.nakagawa@eng.hokudai.ac.jp

Keywords: organic superconductors, time-resolved dynamics, fluctuating superconductivity

Electronic properties of strongly correlated electron systems in copper oxide and organic superconductors have attracted much attention because of their exotic natures such as pseudogap (PG) phenomena, metal-insulating phase separation and unconventional superconductivity (SC). Especially in the organics, large Nernst signals were observed substantially above T_c , depending on effective electron correlation [1]. The result indicates that fluctuating superconductivity (FSC), which has finite Cooper pair density but no bulk coherence, is appeared and enhanced by electron correlation. Because the FSC will be one of the most intriguing interpretations of the PG formation in cuprates, it is important to explore its origin in terms of electron correlation. However, since the interpretation of Nernst effect signals in the FSC regime is still controversial, other measurements are required.

In this work, in order to investigate FSC in the organic superconductors κ -(BEDT-TTF)₂Cu(NCS)₂ (κ -NCS, $T_c \sim 10$ K) and κ -(BEDT-TTF)₂Cu[N(CN)₂]Br (κ -Br, $T_c \sim 12$ K), which has stronger effective electron correlation, we demonstrated a time-resolved pump-probe spectroscopy with different probe polarization. In the pump-probe measurements, photo-induced carrier relaxation dynamics of the FSC as well as a bulk superconducting state is detectable and the dynamics originating in different states such as SC and PG can be separated by differences of probe polarization anisotropy [2], relaxation time and excitation fluence dependence [3]. In the experiment, the pump and probe pulses are obtained from a cavity-dumped Ti:sapphire oscillator with a repetition rate 54 kHz whose pulse widths are about 120 fs centered at 400 nm and 800 nm, respectively. The two pulses are coaxially overlapped and irradiated perpendicular to the conducting plane. The probe polarization is rotated by a half-wave plate.

Figures 1(a) and (b) show the temperature dependences of anisotropic transient reflectivity $\Delta R/R$, respectively in κ -Br and κ -NCS, which were extracted by using the probe-polarization-angular dependence of $\Delta R/R$ fitted by a double sinusoidal function. Anisotropic $\Delta R/R$ seems to develop below ~ 70 K in both the salts with lowering temperature, implying the PG formation. Strikingly, we found that the long-lived component becomes more prominent at low temperatures in addition to the PG response in κ -Br as compared to κ -NCS. By assuming decay time of the long-lived

component is infinite, we decomposed the data into fast and slow decay components by fitting the data with the form $A_f \exp(-t/\tau_f) + A_s$, where A_f , A_s and τ_f are the amplitudes of the fast and slow components and the decay time of the fast component, respectively. As shown in Fig. 1(c), A_s starts to increase at ~ 40 K which is quite higher than T_c in κ -Br, whereas develops just below T_c in κ -NCS. A possible interpretation is that the long-lived components is attributed to quasiparticle relaxation of superconducting state and the emergence of A_s above T_c in κ -Br is ascribed to the FSC. At the conference, the data will be discussed in detail.

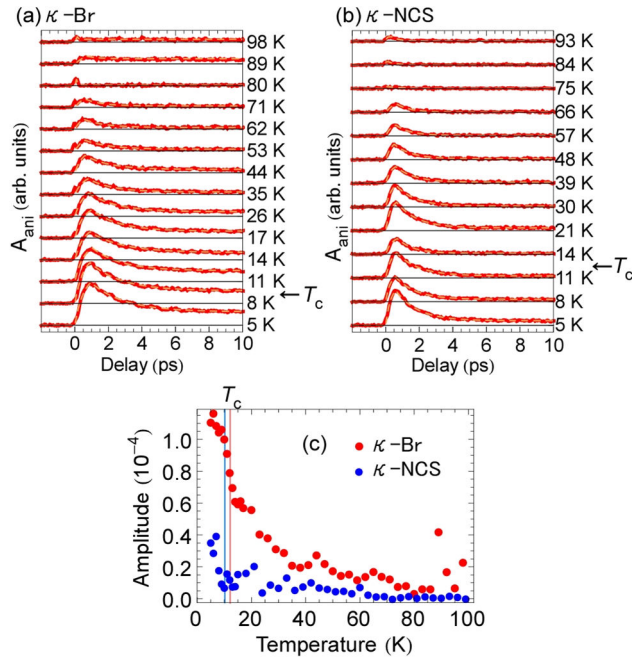


Figure 1: (a) and (b) Temperature dependences of anisotropic responses for the probe extracted from the probe-polarization-angular dependence of change of reflectivity $\Delta R/R$ in κ -Br and κ -NCS, respectively. (c) Temperature dependences of A_s extracted from (a) and (b).

References

1. Moon-Sun Nam *et al.*, Scientific Reports **3**, 3390 (2013)
2. Y. Toda *et al.*, Physical Review B **90**, 094513 (2014)
3. Y. Toda *et al.*, Physical Review B **84**, 174516 (2011)

Temperature dependent structural modulation in $\text{Ca}_{0.82}\text{La}_{0.18}\text{FeAs}_2$ pnictide superconductors

Boby Joseph^{1*}

¹*Eletra Sincrotrone-Trieste, S.S. 14, Km 163.5 in Area Science Park, Basovizza, Trieste 34012, Italy*

Email: * *boby.joseph@gmail.com*

Keywords: high T_c , x-ray diffraction, nano-scale manipulation

The iron based superconducting family continues to expand with several new families of compounds being discovered even recently. Not only the structurally complex compounds are being found, but also the structurally simple compounds like the new 112 family. Here, we present a comparative structural and local structure study of pnictide superconductors $\text{Ca}_{0.82}\text{La}_{0.18}\text{FeAs}_2$ (112-type, $T_c \sim 40$ K) and $\text{Ba}_{0.64}\text{K}_{0.36}\text{Fe}_2\text{As}_2$ (122-type, $T_c \sim 37$ K) using synchrotron x-ray diffraction [1] and x-ray total scattering [2]. The Fe–As superconducting active layer is found to be globally similar in both the systems consisting of edge-sharing $\text{FeAs}_{4/4}$ tetrahedra as in all the iron-pnictide superconductors discovered so far. Although optimally superconducting, the active layer in these compounds is found the active layer in these compounds is found to sustain a large local inhomogeneity. These results thus imply that a nanoscopic manipulation [3] of the Fe–As active layer, rather than its isotropic structural tuning, is the key parameter to control the superconducting properties of the iron-based systems.

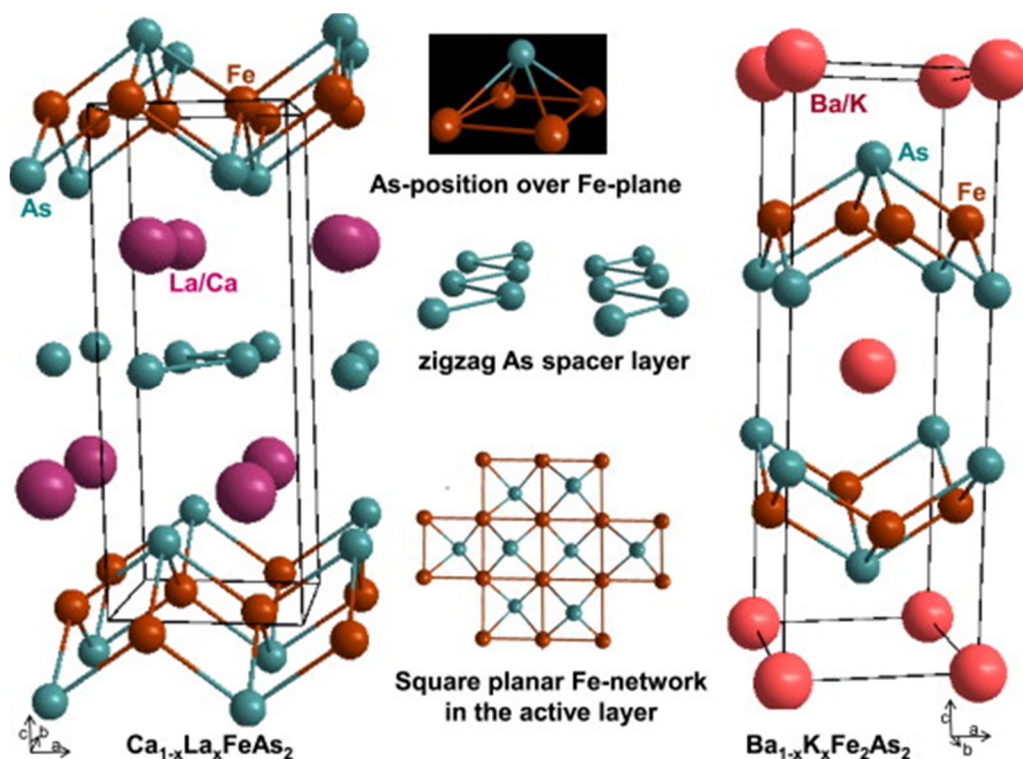


Figure 1: Structural models of $\text{Ca}_{1-x}\text{La}_x\text{FeAs}_2$ (left) and $\text{Ba}_{1-x}\text{K}_x\text{Fe}_2\text{As}_2$ (right). The a - b plane projection of the Fe-As active layer highlighting iron-square network and a view of the pnictogen position above the Fe-plane (common to both structures) and the peculiar As-As spacer layer in $\text{Ca}_{1-x}\text{La}_x\text{FeAs}_2$ are shown in the middle.

References

1. B. Joseph, et al., Superconductor Science and Technology 28, 092001 (2015). <http://dx.doi.org/10.1088/0953-2048/28/9/092001>
2. B. Joseph, et al., J. Phys. Chem.Solids 84, 24 (2015) <http://dx.doi.org/10.1016/j.jpcs.2015.03.022>
3. G. Campi, et al., Nature 525, 359 (2015). <http://dx.doi.org/10.1038/nature14987>

Orbital ordering as the unifying mechanism for both the structural and antiferromagnetic transitions in the Fe-based superconductors



Wei Bao^{1*}

¹*Renmin University of China, Department of Physics*

Email: * wbao@ruc.edu.cn

Keywords: iron based superconductor, orbital order, structural transition, antiferromagnetic transition

The breaking of the four-fold crystalline symmetry in the parent compounds of the 1111, 122 and 11 families of the Fe-based superconductor has generated active current interest in the origin of the structural and magnetic transitions which renders a two-fold crystalline symmetry. A spontaneous symmetry breaking of a Fermi liquid in the form of a nematic phase has been proposed and received a lot of attention.

We have investigated both the structural and antiferromagnetic transitions in 1111, 122, 11 and 245 families of the Fe-based superconductors using the capacity of neutron scattering in simultaneous measurements of the structural and magnetic orders [1-4]. The close relation between the expansion or contraction of the Fe pair distance with the antiferromagnetic or ferromagnetic exchange interaction [1-4] is very similar to our previous experience in investigations on classic transition metal oxides [5,6] for which such a close relation is shown to be a manifest of an underlying orbital order transition. Orbital ordering was initially invoked by Goodenough to explain rich magnetic phases discovered by Wolland and Koehler in their classic neutron scattering study on perovskite Manganites [7]. It is an indication of strong coupling between structural, magnetic and orbital degrees of freedom in transition metal compounds. Our neutron scattering works show that all three types of antiferromagnetic structures discovered so far in the Fe-based superconductors [1-4] can be attributed to two types of Fe bonds : contracting and ferromagnetic bond, and expanding and antiferromagnetic bond [8,1-4]. We attribute their difference in the different occupancy of the dxz and dyz orbitals as early as in 2008 [1]. Such an orbital ordering scheme can consistently explain all occurrences of the structural and magnetic transitions in 1111, 122, 11 and 245 families of Fe-based superconductors [8-10]. Therefore, the dxz/dyz orbital ordering is the essential physics process in the Fe-based superconductors, and the breaking of the four-fold symmetry of these compounds is a naturally expected consequence of the orbital ordering.

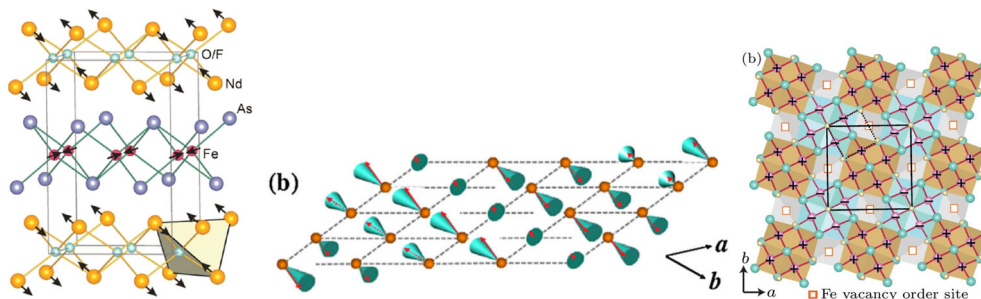


Figure 1: The antiferromagnetic structures of NdFeAsO(1111) [1], FeTe (11) [3] and K₂Fe₄Se₅ (245) [4]. The antiferromagnetic bond is expanded and the ferromagnetic bond is contracted in all three types of structural and magnetic transitions [8].

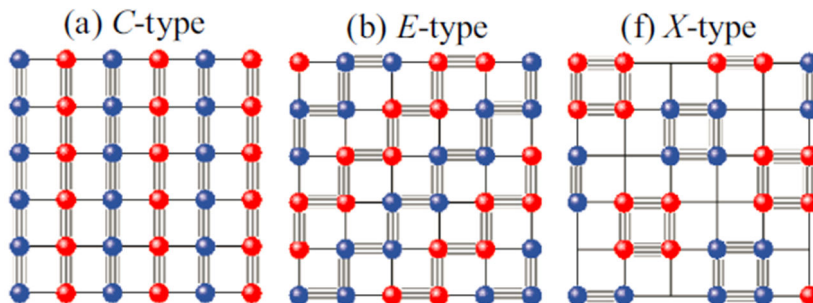


Figure 2: The corresponding ordered pattern of the two types of bonds for the three types of antiferromagnetic and structural orders in Figure 1 [10]. (b) refers to the commensurate limit of the 11 magnetic order in Fig. 1.

References

1. Y. Qiu, W. Bao*, Q. Huang et al., Phys. Rev. Lett. **101**, 257002 (2008).
2. Q. Huang, Y. Qiu, W. Bao* et al., Phys. Rev. Lett. **101**, 257003 (2008).
3. W. Bao*, Y. Qiu, Q. Huang et al., Phys. Rev. Lett. **102**, 247001 (2009).
4. W. Bao* et al., Chinese Phys. Lett. **28**, 086104 (2011).
5. W. Bao* et al., Phys. Rev. Lett. **78**, 507 (1997).
6. W. Bao* et al., Phys. Rev. Lett. **78**, 543 (1997).
7. E. O. Wollan and W. C. Koehler, Phys. Rev. **100**, 545 (1955); J. B. Goodenough, *ibid.* **100**, 564 (1955).
8. W. Bao, Chinese Phys. B **22**, 087405 (2013).
9. W. Lu et al., Phys. Rev. B **84**, 155107 (2011).
10. W. G. Yin et al., *ibid.* **86**, 081106 (2011).

Opening a diagonal gap by a dynamic spin density wave in lightly doped $\text{La}_{2-x}\text{Sr}_x\text{CuO}_4$

Amit Keren

Technion Israel Institute of Technology

Department of Physics

Technion City

320 00 Haifa

ISRAEL

Email: phkeren@gmail.com

The origin of the pseudogap in cuprates and its relationship with superconductivity in the cuprates remains vague. In particular, the interplay between the pseudogap and magnetism is mysterious. Here we investigate the newly discovered nodal gap in hole doped cuprates using a combination of three experimental techniques applied to one, custom-made, single crystal. The crystal is an antiferromagnetic $\text{La}_{2-x}\text{Sr}_x\text{CuO}_4$ with $x=1.92\%$, and the experimental techniques probe both its charge and spin properties. We performed angle resolved photoemission spectroscopy measurements as a function of temperature and find: quasiparticle peaks, Fermi surface, anti-nodal gap, and below 45 K a nodal gap. We also performed inelastic neutron scattering measurements and determined the thermal end temporal evolution of the commensurate and incommensurate magnetic order. Finally, we searched in vain, using soft and hard X-ray, for charge density wave (CDW). Our major finding is that a nodal gap opens at a temperature well below the commensurate ordering at 140 K, and exactly when dynamic incommensurate spin density wave fluctuations peak.

Finite-temperature localized state in superconducting films



Alexey Yu. Mironov^{1,2,3}, Daniel M. Silevitch⁴, Thomas Proslie⁵,
Svetlana V. Postolova^{1,2}, Maria V. Burdastyh^{1,2}, Anton K.
Gutakovskii^{1,2}, Thomas F. Rosenbaum^{3,4}, Valerii M. Vinokur⁵,
and Tatyana I. Baturina^{1,2,3,6*}

¹*A. V. Rzhanov Institute of Semiconductor Physics SB RAS,
630090 Novosibirsk, Russia*

²*Novosibirsk State University, 630090 Novosibirsk, Russia*

³*James Franck Institute and Department of Physics, The
University of Chicago, Chicago, Illinois 60637, USA*

⁴*Division of Physics, California Institute of Technology, Pasadena, California 91125,
USA*

⁵*Materials Science Division, Argonne National Laboratory, IL 60439, Argonne, USA*

⁶*University of Regensburg, 93053, Regensburg, Germany*

Email: * tatyana.baturina@physik.uni-regensburg.de

Keywords: superconductor-insulator transition, superinsulating state, long-range Cooper interaction

Zero-resistance in superconductors is protected at finite temperatures by the global phase coherence, which by virtue of the uncertainty principle guarantees the dissipationless flow of Cooper pairs. In two-dimensional critically disordered films dual superinsulating state can form [1,2]. In superinsulators coherent fluctuations of phase localize Cooper pairs leading to infinite-resistance at finite temperatures. Here we report an experimental observation of the magnetic field-driven superconductor-superinsulator transition in disordered thin NbTiN films, see Fig. 1. Perpendicular magnetic field breaks down superconductivity (Fig. 1a) and forms huge insulating peak in the resistance at $B = B_{\max}(T)$, see Fig. 1c. Appearance of the superinsulator is detected by the abrupt upturn from the Arrhenius-type temperature dependence of the resistance, evidencing formation of the zero-conducting state at finite temperature, see Fig. 1b,d. This phenomenon was first observed in TiN films [3] and was recently reported in InO [4]. At relatively low magnetic fields we have found the critical divergent behavior of the resistance characteristic to charge Berezinskii-Kosterlitz-Thouless (CBKT) transition, which is dual to the vortex BKT transition in superconducting state [2,5]. The divergence described by the expression $R \sim \exp\{\frac{b}{(T/T_{\text{CBKT}} - 1)^{1/2}}\}$, heralds the emergence of the superinsulating state where charges are fully localized at finite temperatures. We have found that the superinsulating state exists only at small fields, $B < B_{\max}$.

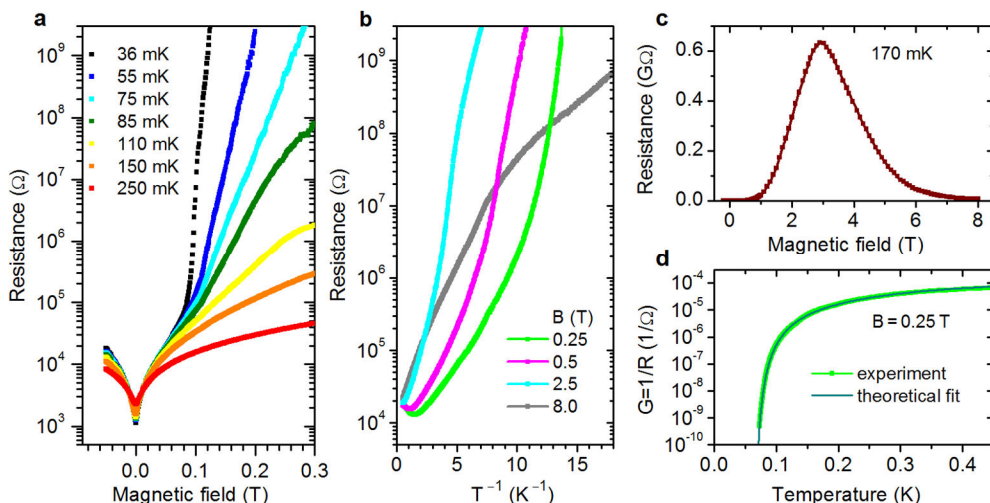


Figure 1: (a) Resistance isotherms at small magnetic fields in the logarithmic scale plotted as functions of the magnetic field. Abrupt upturns of magnetoresistance curves at temperatures below 150 mK mark transitions of the films into highly resistive state. (b) Arrhenius plots, $\log R$ vs. $1/T$, at different magnetic fields. At small fields the $\log R(1/T)$ demonstrates superactivation. At higher fields $\log R(1/T)$ (see the curve at $B = 8$ T) the growth of R slows down. (c) Exemplary B -induced insulating peak at $T = 170$ mK. Importantly, superactivation is found at fields below the peak. (d) Theoretical fit of the experimental temperature dependence of the conductance $G = 1/R$ illustrating the critical behavior characteristic to the CBKT transition at $B = 0.25$ T, with $b = 5.5$ and $T_{\text{CBKT}} = 63.5$ mK, and the emergence of the finite-temperature fully localized state.

References

1. Valerii M. Vinokur, Tatyana I. Baturina, Mikhail V. Fistul, Aleksey Yu. Mironov, Mikhail R. Baklanov, Christoph Strunk, *Nature* **452**, 613 (2008).
2. Tatyana I. Baturina, Valerii M. Vinokur, *Annals of Physics* **331**, 236-257 (2013).
3. T. I. Baturina, A. Yu. Mironov, V. M. Vinokur, M. R. Baklanov, C. Strunk, *JETP Lett.* **88**, 752 (2008).
4. M. Ovadia, D. Kalok, I. Tamir, S. Mitra, B. Sacépé, and D. Shahar, *Sci. Rep.* **5**, 13502 (2015).
5. Philip W. Anderson, in *Ill-Condensed Matter* (Eds. R Balian, R Maynard and G Toulouse, North Holland, Amsterdam, 1979), p 159-261.

Effect of disorder on the vortex Mott transition in array of superconducting islands



A. Yu. Mironov^{1,2*}, S. V. Postolova^{1,2,3}, N. Poccia^{4,5},
M. Lankhorst⁵, G. Bianconi⁶, V. M. Vinokur⁷, C. Strunk³ and
T. I. Baturina^{1,2,3}

¹*A. V. Rzhanov Institute of Semiconductor Physics SB RAS,
630090, Novosibirsk, Russia*

²*Novosibirsk State University, 630090, Novosibirsk, Russia*

³*University of Regensburg, 93053, Regensburg, Germany*

⁴*NEST Istituto Nanoscienze-CNR & Scuola Normale Superiore,
56127, Pisa, Italy*

⁵*MESA+ Institute for Nanotechnology, University of Twente, 7500, AE Enschede,
Netherlands*

⁶*School of Mathematical Sciences, Queen Mary University of London, London E1 4NS,
UK*

⁷*Materials Science Division, Argonne National Laboratory, IL 60439, Argonne, USA*

Email: * mironov@isp.nsc.ru

Keywords: phase transitions, vortex matter, superconducting array

We present the results of the study of low-temperature non-linear transport properties of disordered array of niobium (Nb) islands overlaid on the gold (Au) substrate. The substrate is 40-nm thick and harbors 58500 Nb islands 45 nm thick distributed randomly among 90000 nodes of the square lattice with the period around 250 nm. This number of islands corresponds to the filling factor of 65%. We investigated two samples S1 and S2 with the same lattice design but different sizes of the islands, 130 nm in sample S1 and 160 nm in sample S2, respectively. Increasing the island's size leads to broadening of the superconducting transition and increasing of the temperature at which the resistance starts to decrease. For both samples we observe the periodic dependence of the differential resistance upon the external magnetic field in the wide current region, with the period B_0 corresponding to the magnetic flux quantum per unit cell ($B_0 = \Phi_0/a^2 = 33$ mT). We find the vortex insulator-to-metal transitions where minima of the differential resistance dV/dI at rational frustrations $f = B/B_0$ reverse into maxima upon increasing the current, while magnetoresistances V/I maintain minima at rational f at any currents. These minima become shallower upon increasing current. The observed transition is similar to the vortex Mott insulator-to-metal transitions in regular arrays [1]. The transition threshold current I_t of sample S1 is lower than that of sample S2. Our findings evidence the robustness of the vortex Mott state with respect to the strength of coupling and large disorder.

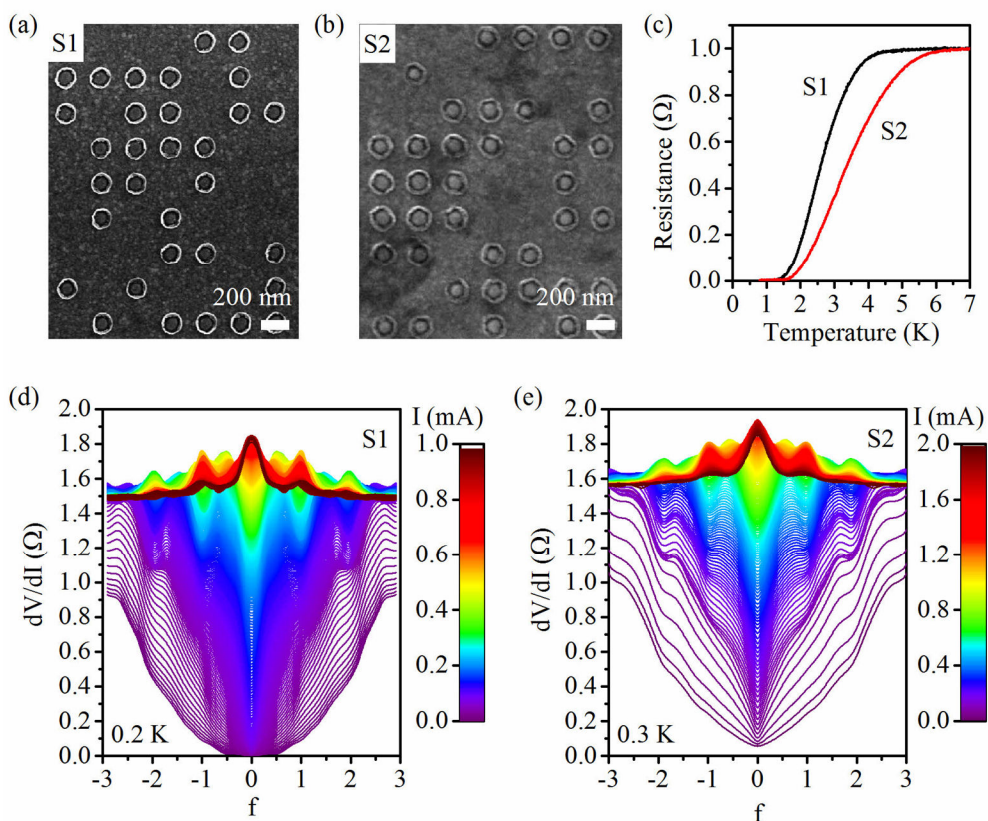


Figure 1: SEM images of the disordered arrays of Nb islands on Au – (a) sample S1 and (b) sample S2. (c) The temperature dependence of the resistance of the arrays S1 and S2. Differential magnetoresistance of the array S1 (d) and S2 (e) at different currents.

References

1. N. Poccia, T. I. Baturina, F. Coneri, C. G. Molenaar, X. R. Wang, G. Bianconi, A. Brinkman, H. Hilgenkamp, A. A. Golubov, V. M. Vinokur, *Science* **349**, 1202 (2015).

Hydrodynamic transport in high mobility graphene



Leonid A. Ponomarenko^{1,2*}, R. Krishna Kumar^{1,2}, D. A. Bandurin², I. Torre³, M. Ben Shalom², Tomadin³, A. Principi⁴, G. H. Auton², A. K. Geim², and M. Polini⁵

¹ *Lancaster University, Lancaster LA14YB, UK*

² *University of Manchester, Manchester M13 9PL, UK*

³ *Scuola Normale Superiore, I-56126 Pisa, Italy.*

⁴ *Radboud University, NL-6525 AJ Nijmegen, Netherlands*

⁵ *Istituto Italiano di Tecnologia, Graphene Labs, Via Morego 30, I-16163 Genova, Italy*

Email: * l.ponomarenko@lancaster.ac.uk

Keywords: graphene, hydrodynamic transport, electron-electron interaction

Graphene hosts a unique electron system in which electron-phonon scattering is extremely weak but electron-electron collisions are sufficiently frequent to provide local equilibrium above liquid nitrogen temperature. Under these conditions, electrons can behave as a viscous liquid and exhibit hydrodynamic phenomena similar to classical liquids [1]. Here we report strong evidence for this transport regime. We find that doped ultraclean graphene exhibits an anomalous (negative) voltage drop near current injection contacts, which is attributed to the formation of submicrometer-size whirlpools in the electron flow [2]. We describe a proper experimental geometry for studying the viscous electron liquid in transport experiment and explain how to distinguish hydrodynamic regime of electron transport from ballistic and diffusive ones. We also present a method for extracting the dynamic viscosity from resistance measurements. The viscosity of graphene's electron liquid is found to be of the order $0.1 \text{ m}^2 \text{ s}^{-1}$, an order of magnitude larger than that of honey, in agreement with many-body theory. The signature of hydrodynamic regime can be seen in the transport data in a broad range of temperatures, including room temperature opening a possibility to utilize this transport regime in electronic devices with new functionalities.

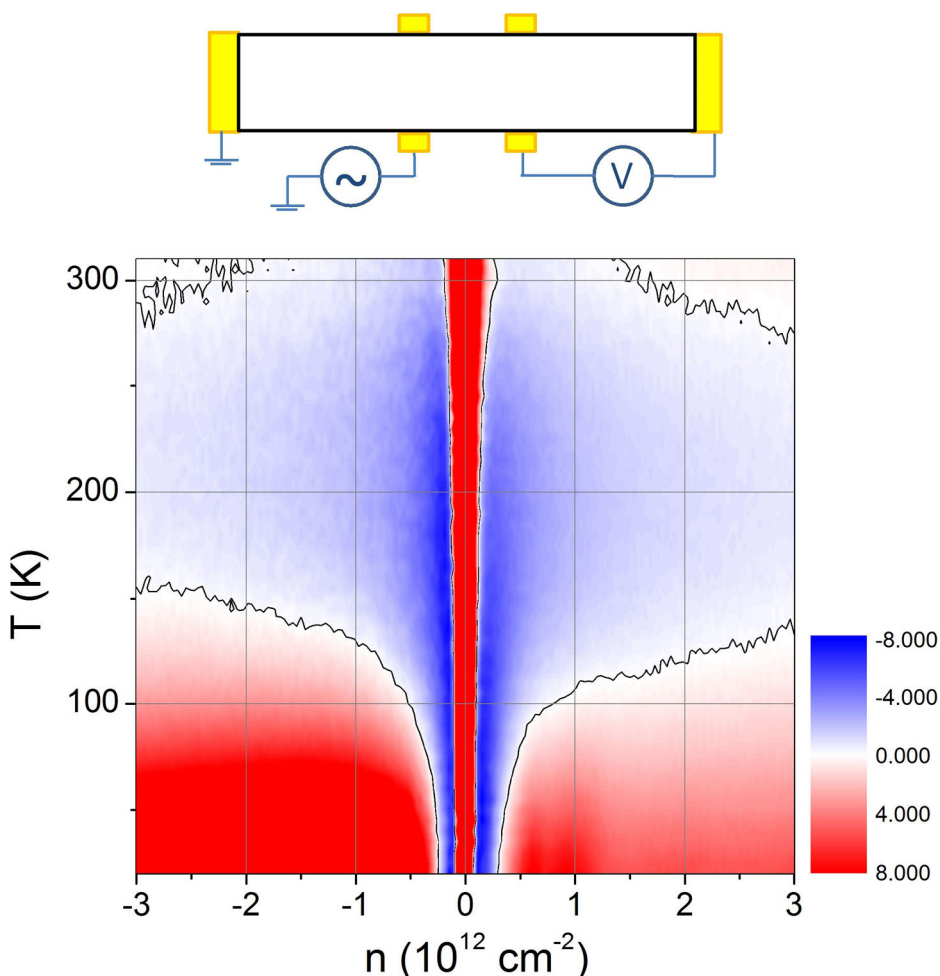


Figure 1: Top. Schematics of 4-probe resistivity measurements for observing hydrodynamic flow of electrons. Bottom. The resistance of a graphene device as function of the charge density and temperature. The colour change indicates the change of the sign of the resistance. Negative resistance is a “smoking gun” of the hydrodynamic regime, which extends to room temperatures.

References

1. R. N. Gurzhi, Hydrodynamic effects in solids at low temperature. *Sov. Phys. Usp.* 11, 255–270 (1968). doi:10.1070/PU1968v011n02ABEH003815
2. Bandurin et al., Negative local resistance caused by viscous electron backflow in graphene. *Science* 10.1126/science.aad0201 (2016).

2D B-C-O alloy: a promising electronic material



Si Zhou, Jijun Zhao

Key Laboratory of Materials Modification by Laser, Ion and Electron Beams, Dalian University of Technology, Ministry of Education, Dalian 116024, China

Email: sizhou@dlut.edu.cn

Keywords: graphene, boron, oxygen, mobility, band gap

Graphene, a superior 2D material with high carrier mobility, has its limitation in the electronic devices due to zero band gap.[1] In this regard, boron and nitrogen atoms have been integrated into the graphene lattice to fabricate 2D semiconducting heterostructures. [2] It is an intriguing question whether oxygen can, in replacement of nitrogen, enter the sp^2 honeycomb lattice and form stable B-C-O monolayer structures. Here we explore the atomic structure, energetic and thermodynamic stability, and electronic properties of various 2D B-C-O alloys using first-principles calculations. Our results show that oxygen can be stably incorporated into the graphene lattice by bonding with boron. The B and O species favor alternately patterning into the chain- or ring-like structures embedded in the pristine graphene regions. These B-C-O hybrid sheets can be either metals or semiconductors depending on the B:O ratio. The semiconducting $(B_2O)_n C_m$ and $(B_6O_3)_n C_m$ phases exist in the B- and O-rich conditions, and possess tunable band gap of 1.0~3.8 eV and high carrier mobility, retaining $\sim 1000 \text{ cm}^2 \text{V}^{-1} \text{ s}^{-1}$ even for half coverage of B and O atoms. These B-C-O alloys form a new class of 2D materials as promising candidate for the high-speed electronic devices.

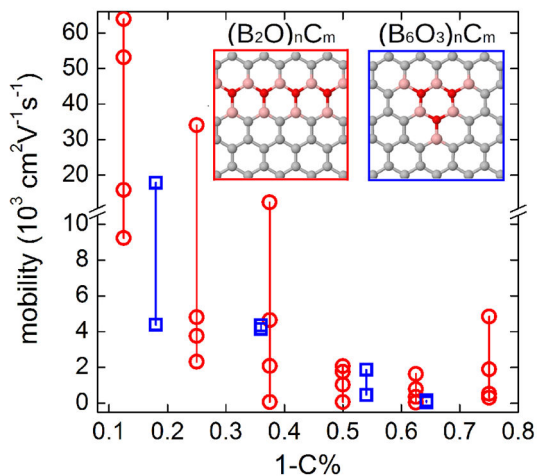


Figure 1: Carrier mobility of B-C-O 2D hybrid structures as a functional of doping level (1-C%).

References

1. N. M. R. Peres, Rev.Mod. Phys. 82, 2673-2700 (2010)
2. Y. Gong, G. Shi, Z. Zhang, W. Zhou, J. Jung, W. Gao, L. Ma, Y. Yang, S. Yang, G.You, R. Vajtai, Q. Xu, A. H. MacDonald, B. I. Yakobson, J. Lou, Z. Liu and P. M. Ajayan, Nat.Comm. 5, 3193 (2014)

Incipient Berezinskii Kosterlitz and Thouless transition in two-dimensional coplanar Josephson junctions



*B. Jouault*¹, *D. Massarotti*^{2,3}, *F. Tafuri*^{2,3}, *A. Tagliacozzo*^{3, 4}

¹*Laboratoire Charles Coulomb, UMR 5221 CNRS-UM2, Universit Montpellier 2, place Eugene Bataillon - CC074 F-34095 Montpellier, France*

²*Dip. Ingegneria dell'Informazione, SUN, I-81031 Aversa (CE), Italy*

³*CNR-SPIN, Monte S. Angelo-Via Cintia, I-80126, Napoli, Italy*

⁴*Dip. di Fisica, Universita` di Napoli Federico II, Via Cintia, I-80126 Napoli, Italy*

Email: arturo@na.infn.it

Keywords: Josephson effect, graphene, nanostructures

Graphene grown on SiC by Chemical Vapor Deposition (CVD) offers centimeter size monolayer areas on top of which contacts can be deposited with the desired patterning. We report on various submicrometer junctions that have been tested on the same flake with Al/Ti contacts in a planar quasi 2D junction, at low temperature in search for the Josephson effect. In samples with a graphene gap below 400 nm, we have found evidence of Josephson coherence in presence of an incipient Berezinski-Kosterlitz-Thouless transition. A remarkable hysteretic collapse and revival of the Josephson supercurrent is found when the magnetic field is cycled. Similar hystereses are found in granular systems and are usually justified within the Bean Critical State model (CSM). We show that the CSM, with appropriate account for the low dimensional geometry, can partly explain the odd features measured in these junctions.

References

1. B. Jouault, S. Charpentier, D. Massarotti, A. Michon, M. Paillet, J.-R. Huntzinger, A. Tiberj, A. Zahab, T. Bauch, P. Lucignano, A. Tagliacozzo, F. Lombardi, F. Tafuri, *J Supercond Nov Magn* (2016) 29:1145–1150
2. B. Jouault, et al. arXiv:1601.04552 and submitted

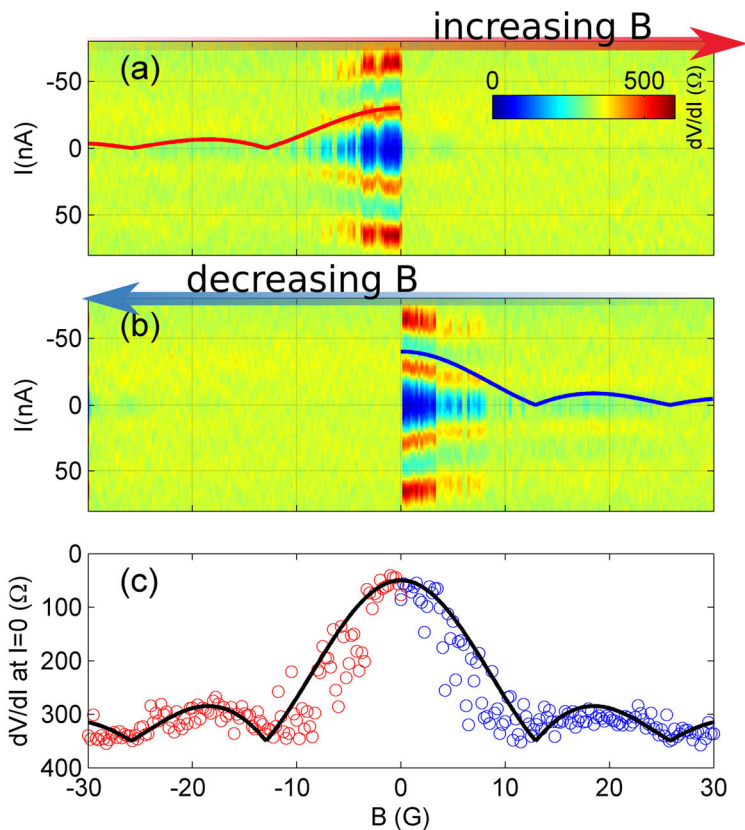


Figure 1: Colormaps of the differential resistance $dV/dI(H; I)$ evidencing a large hysteresis.
 a) The magnetic field is swept from -30 to 30 Oe.
 b) The field is swept from 30 to -30 Oe.
 The blue area corresponds to the low resistive region. The superposed blue and red curves are a Fraunhofer interference pattern, given as a reference, corresponding to a total area $S_{\text{eff}} = 1,6 \mu\text{m}^2$.
 c) Critical current as a function of the magnetic field (red open circles: sweep from -30 to 0 Oe ; blue open circles: sweep from 30 to 0 Oe). The black curve is the theoretical Fraunhofer pattern fit calculated using the RSJ model.

New evidences for in-plane entanglement of CDW in YBCO



C. Mazzoli^{1*}, A. Bombardi², M. Le Tacon³, G. Ghiringhelli⁴

¹*Brookhaven National Lab, Upton, US*

²*Diamond Light Source, Ltd, Chilton, UK*

³*Max Planck Institute, Stuttgart, Germany*

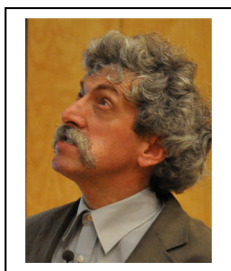
⁴*Politecnico di Milano, Milan, Italy*

Email: * cmazzoli@bnl.gov

Keywords: high T_c, CDW, YBCO, diffraction

We present an X-ray diffraction study on $\text{YBa}_2\text{Cu}_3\text{O}_{6.67}$ orthorhombic de-twinned single crystal. In the charge density wave phase we detected a new family of diffraction peaks, described by $\tau = (\pi, \pi, 1/2)$ propagation vector. Models of the structural distortion compatible with our data are discussed, together with the implications for charge arrangements on CuO_2 planes and CuO chains. Considerations on the role of the crystallographic structure in the $\text{YBa}_2\text{Cu}_3\text{O}_{6+\delta}$ series and of electronic interactions supporting the proposed model are drawn.

Phase separation in single crystals of iron-based superconductors



Roman Puzniak

*Institute of Physics, Polish Academy of Sciences, PL-02-668
Warsaw, Poland*

Email: puzni@ifpan.edu.pl

Keywords: high- T_c superconductors, iron based superconductors, nanoscale phase separation

Several years ago, a temperature dependent anisotropy was found in bulk iron based superconductors. It can be explained by inhomogeneity of the system.

The issues concerning the nature and the role of magnetic inhomogeneities in iron-based superconductors and their correlation with superconductivity are addressed. We have found that the sharpness of transition to the superconducting state in Fe-Te-Se is evidently inversely correlated with crystallographic quality of the crystals. Our data demonstrate a presence of nanometer scale hexagonal regions coexisting with tetragonal host lattice, a chemical disorder demonstrating non homogeneous distribution of host atoms in the crystal lattice, as well as hundreds-of-nanometers-long iron-deficient bands.

The most characteristic and distinct property of crystals of alkali metal intercalated iron selenides is an existence of an antiferromagnetic order. This order, with large magnetic moment of $3.3 \mu_B$ per Fe cation, exists below temperatures as high as ~ 560 K. It was stated that this magnetic order is mutually combined with defined iron vacancy order in the structure. Amazingly, the magnetic order does not hinder an appearance of superconductivity in these materials below ~ 30 K. This order can be influenced by an external magnetic field, making iron-based superconductors a fascinating template for magnetic-field tuned applications.

It is now commonly accepted that both magnetism and superconductivity can coexist, as a phase separation occurs in apparently single crystals. The majority phase of the composition $A_2Fe_4Se_5$ (245) is insulating, magnetic and shows ordered pattern of Fe vacancies in the structure. The second, minority phase of the composition $A_2Fe_4Se_5$ (122) is conducting/semiconducting and becomes superconducting below $T_c \sim 30$ K. An extended study of the superconducting and normal-state properties of various as grown and post-annealed $Rb_xFe_{2-y}Se_2$ single crystals is presented. Magnetization experiments evidence that annealing of $Rb_xFe_{2-y}Se_2$ at temperature well below the temperature of the onset of phase separation, T_p , neither changes the magnetic nor the superconducting properties of the crystals. In addition, annealing at temperature well above T_p suppresses the superconducting transition temperature T_c and leads to an increase of the antiferromagnetic susceptibility accompanied by the creation of

ferromagnetic impurity phases, which are developing with annealing time. However, annealing at $T \approx T_p$ increases T_c , sharpens the superconducting transition, increases the lower critical field, and strengthens the screening efficiency of the applied magnetic field.

This work was partially supported by the National Science Centre of Poland based on decision No. DEC-2013/08/M/ST3/00927.

Interplanar coupling-dependent magnetoresistivity in high-purity layered metals



N. Kikugawa^{1,2}, P. Goswami^{2,3}, A. Kiswandhi², E.S. Choi², D. Graf², R.E. Baumbach², J.S. Brooks², K. Sugii⁴, Y. Iida⁴, M. Nishio¹, S. Uji⁴, T. Terashima⁴, P.M.C. Rourke⁵, N.E. Hussey^{6,7}, H. Takatsu^{8,9}, S. Yonezawa⁹, Y. Maeno⁹ and L. Balicas²

¹*National Institute for Materials Science, Tsukuba, Ibaraki 305-0047, Japan.*

²*Condensed Matter Group, National High Magnetic Field Laboratory, Florida State University, 1800 East Paul Dirac Drive, Tallahassee, Florida 32310, USA.*

³*Condensed Matter Theory Center, University of Maryland, College Park, Maryland 20742-4111, USA.*

⁴*National Institute for Materials Science, Tsukuba, Ibaraki 305-0003, Japan.*

⁵*H.H. Wills Physics Laboratory, Q3 University of Bristol, Tyndall Avenue, Bristol BS8 1TL, UK.*

⁶*High Field Magnet Laboratory (HFML-EMFL), Radboud University, Toernooiveld 7, Nijmegen, The Netherlands.*

⁷*Institute of Molecules and Materials, Radboud University, Heyendaalseweg 135, 6525 AJ Nijmegen, The Netherlands.*

⁸*Department of Physics, Tokyo Metropolitan University, Tokyo 192-0397, Japan.*

⁹*Department of Physics, Graduate School of Science, Kyoto University, Kyoto 606-8502, Japan.*

Email: balicas@magnet.fsu.edu

Keywords: Quasi-two-dimensional metals, axial anomaly

The magnetic field-induced changes in the conductivity of metals are the subject of intense interest, both for revealing new phenomena and as a valuable tool for determining their Fermi surface. Here we will discuss a report¹ of a hitherto unobserved magnetoresistive effect in ultra-clean layered metals, namely a negative longitudinal magnetoresistance that is capable of overcoming their very pronounced orbital one. This effect is correlated with the interlayer coupling disappearing for fields applied along the so-called Yamaji angles where the interlayer coupling vanishes. Therefore, it is intrinsically associated with the Fermi points in the field-induced quasi-one-dimensional electronic dispersion, implying that it results from the axial anomaly among these Fermi points. In its original formulation, the anomaly is predicted to violate separate number conservation laws for left- and right-handed chiral (for example, Weyl) fermions. Its observation in PdCoO₂, PtCoO₂ and Sr₂RuO₄ suggests that the anomaly affects the transport of clean conductors, in particular near the quantum limit.

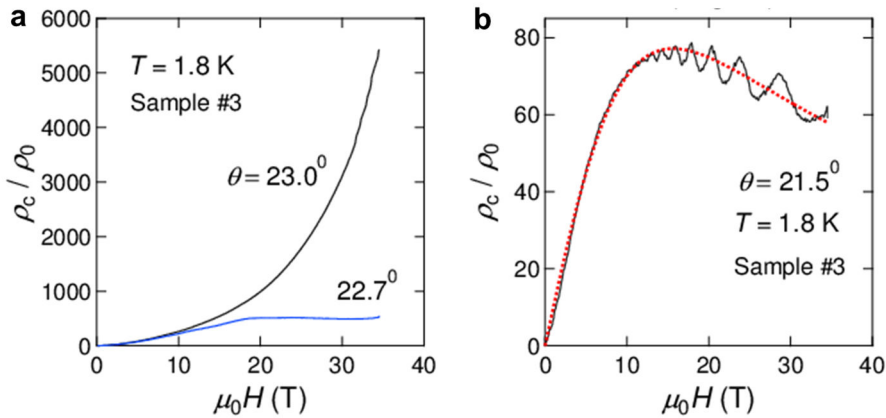
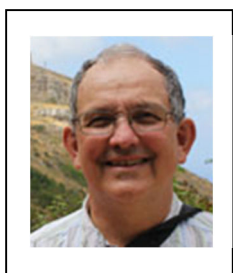


Figure 1: (a) Interplanar resistivity ρ_c for a PdCoO₂ single-crystal as a function of the field μ_0H at $T=1.8$ K and for two angles, that is, the Yamaji value $\theta_{n=1} = 23^\circ$ and $\theta = 22.7^\circ$. It is noteworthy how the pronounced positive magnetoresistivity observed at $\theta_{n=1}$ is strongly suppressed when μ_0H is rotated by just $\sim 0.3^\circ$, leading to magnetoresistance saturation. (b) ρ_c as a function of H under $T = 1.8$ K and for $\theta = 21.5^\circ$. It is noteworthy how ρ_c , after increasing by several orders of magnitude, displays negative magnetoresistivity at higher fields, thus indicating a clear competition between the orbital and another mechanism, which suppresses the magnetoresistivity. Dotted red line corresponds to a fit of $\rho_c = 1/\sigma_c^{-1} = (\sigma_0 + \alpha\mu_0H + \beta/\mu_0H)^{-1}$. The linear term is the orbital contribution to the magnetoresistivity of a system close to the quantum limit while the inverse field term corresponds to the contribution from the axial anomaly among chiral Fermi points in a quasi-one-dimensional dispersion. Fermi points and concomitant axial anomaly are suppressed at the Yamaji angle(s) thus leading only to positive magnetoresistivity

References

1. N. Kikugawa *et al.*, Nat. Commun. (2016) (in press)

The amplitude and origin of charge density wave in YBCO.



Y. A. Kharkov¹ and O. P. Sushkov¹

¹*School of Physics, University of New South Wales, Sydney 2052, Australia*

Email: sushkov@phys.unsw.edu.au

Keywords: high T_c, charge density wave

Discovered 4 years ago the charge density wave (CDW) in underdoped cuprates has attracted a great attention. In spite of intensive studies, the amplitude, the spatial pattern (s-wave versus d-wave), and the mechanism of the CDW formation remain undetermined and controversial. In the present work we perform combined analysis of experimental data on NQR [1, 2], RIXS [3, 4], phonon softening [5], and hard X-ray diffraction [6, 7]. We do not develop any microscopic theory/model, we just analyse the experimental data. We concentrate on ortho-II YBCO because the compound has least amount of disorder and hence narrowest ⁶³Cu and ¹⁷O NQR lines.

We come to the following conclusions.

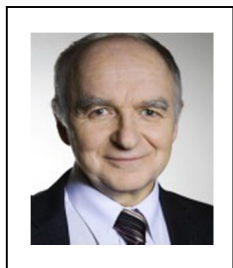
- Unambiguously there is the s-wave component of CDW. The amplitude of the component is $12 \cdot 10^{-3}$ in the strong magnetic field and $4 \cdot 10^{-3}$ in the weak magnetic field. This is in units of elementary charge per unit cell of CuO₂ plane.
- In the weak magnetic field there is the d-wave component of CDW. The d-wave is shifted by $\pi/2$ with respect to the s-wave. The d-wave amplitude is approximately equal to that of the s-wave component.
- The data allow us to separate between two scenarios of the CDW formation.
 - Scenario 1: the CDW is developed in electronic system and phonons are just spectators which follow electrons.
 - Scenario 2: phonons together with electrons are major players in the CDW instability.

We show that data point out in favor of the second scenario.

References

1. T. Wu et al, Nature 477, 191 (2011).
2. T. Wu et al, Nature Commun. 6, 6438 (2015).
3. G. Ghiringhelli et al, Science 337, 821 (2012).
4. R. Comin et al, Science 343, 390 (2015).
5. M. Le Tacon et al, Nature Phys. 10, 52 (2014).
6. J. Chang et al, Nature Phys. 8, 871 (2012).
7. E.M. Forgan et al, Nature Comm. 6, 10064 (2015).

Three-terminal system as a spin current source and heat to electricity converter



Karol I. Wysokiński

¹*Institute of Physics, M. Curie-Skłodowska University,
Pl- 20 031 Lublin*

Email: *karol@tytan.umcs.lublin.pl*

Keywords: Quantum transport, Performance characteristics of energy conversion systems; figure of merit

Three terminal devices with quantum dots connected to three normal or two normal and a superconducting electrode have been studied [1-3]. We are interested in their use as efficient heat to energy converters and/or spin current sources. The usefulness of the device as energy harvester is characterized by the Seebeck coefficient and thermoelectric figure of merit or the power factor. In the first case we study the geometry in which heat and charge currents in the device effectively flow in mutually perpendicular directions, allowing for their independent control. The energy flow from the hot electrode together with energy filtering provided by quantum dots leads to a voltage bias between the cold electrodes [1]. The presence of the superconducting electrode (case 2) allows to study the interplay between the crossed Andreev reflections and direct electron tunneling between two normal electrodes. This case is contrasted with the experimental data [4] on a similar planar structures. If external magnetic field is applied the three terminal hybrid system is a source of pure spin current which can be electrically controlled.

Our results are important from the theoretical point of view as well as for the practical implementation and control of the proposed devices.

(The work has been performed in collaboration with B.R. Bułka, T. Domański, G. Michałek, B. Szukiewicz and U. Eckern, and partially supported by the the National Science Centre – Poland- grant DEC-2014/13/B/ST3/04451)

References

1. B. Szukiewicz, U. Eckern, K.I. Wysokiński, *New J. Phys.* (2016)
2. G. Michałek, T. Domański, B. R. Bułka, K. I. Wysokiński, *Sci. Rep.* **5** 14572 (2015).
3. K. I. Wysokiński, *J. Phys. Cond. Matter* **24**, 335303 (2012).
4. S. Russo, M. Kroug, T. M. Klapwijk, A. F. Morpurgo, *Phys. Rev. Lett.* **95**, 027002 (2005).

Various metallic and insulating phases and their phase separations in charge ordered systems



Konrad Jerzy Kapcia^{1,*}, Adriano Amaricci², Stanislaw Robaszkiewicz³, Massimo Capone²

¹*Institute of Physics, Polish Academy of Sciences, al. Lotników 32/46, PL-02668 Warszawa, Poland*

²*International School for Advanced Studies (SISSA) and CNR-IOM Democritos, Via Bonomea 265, I-34136 Trieste, Italy*

³*Faculty of Physics, Adam Mickiewicz University in Poznań, ul. Umultowska 85, PL-61614 Poznań, Poland*

Email: * konrad.kapcia@ifpan.edu.pl; konrad.kapcia@gmail.com

Keywords: extended Hubbard model, dynamical mean-field theory, charge-orderings, metal-insulator transition

Charge orderings are relevant to a broad range of important materials, including manganites, cuprates, magnetite, several nickel, vanadium and cobalt oxides, heavy fermion systems (e.g. Yb4As3) and numerous organic compounds [1-4]. They have been also observed in two dimensional electron gases [5].

We present studies of the extended Hubbard model with both (i) the effective on-site interaction U and (ii) the intersite density-density interactions W (nearest-neighbors and next-nearest neighbors) [4-13], which is one the simplest models that capture the interplay between strong correlations and charge-ordering effects. In the analysis of the phase diagrams and properties of this model we have adopted the approaches, which treat the on-site interaction U term exactly and the intersite interactions within the mean-field approximation [5-8,10-12]. In particular, we studied the finite-bandwidth case of the model ($t > 0$, t -electron hopping) using the diagonalization method by the Lanczos algorithm within the dynamical mean-field theory [1,5-8].

Our investigation of the general case show that, depending on values of the interaction parameters and electron concentration/chemical potential, the system can exhibit not only several homogeneous charge ordered metallic and insulating phases, but also various phase separated states. We present the evolution of the ground state phase diagram from the weak-coupling limit ($U \ll t$) to the strong-coupling limit ($U \gg t$; or to the atomic limit: $t=0$) and discuss the phase transitions between phases found. The insulator-metal transitions between charge-ordered phases have been of our particular interest.

K.J.K. thanks SISSA for the hospitality during his six month research stay in Trieste. This work was partially supported by National Science Centre (NCN, Poland) - ETIUDA 1 programme, grant No. DEC-2013/08/T/ST3/00012 in years 2013-2015.

References

1. M. Imada, A. Fujimori, and Y. Tokura, *Rev. Mod. Phys.* 70 1039 (1998).
2. E. Dagotto, T. Hotta, and A. Moreo, *Phys. Rep.* 344, 1 (2001);
T. Goto, B. Lüthi, *Adv. Phys.* 52, 67 (2003).
3. J. van den Brink and D.I. Khomskii, *J. Phys.: Condens. Matter* 20, 434217 (2008).
4. H. Seo, C. Hotta, and H. Fukuyama, *Chem. Rev.* 104, 5005 (2004);
D. Jérôme, *Chem. Rev.* 104, 5565 (2004).
5. A. Amaricci, A. Camjayi, K. Haule, G. Kotliar, D. Tanaskovic, and V. Dobrosavljevic, *Phys. Rev. B* 82, 155102 (2010)
6. N.-H. Tong, S.-Q. Shen, and R. Bulla, *Phys. Rev. B* 70, 085118 (2004).
7. R. Pietig, R. Bulla, and S. Blawid, *Phys. Rev. Lett.* 82, 4046 (1999).
8. J. Merino, A. Ralko, and S. Fratini, *Phys. Rev. Lett.* 111, 126403 (2013).
9. F. Mancini and F. P. Mancini, *Phys. Rev. E* 77, 061120 (2008);
F. Mancini, E. Plekhanov, and G. Sica, *Eur. Phys. J. B* 86, 408 (2013).
10. R. Micnas, S. Robaszkiewicz, and K.A. Chao, *Phys. Rev. B* 29, 2784 (1984).
11. K. Kapcia and S. Robaszkiewicz, *J. Phys.: Condens. Matter* 23, 105601 (2011).
12. K. Kapcia, W. Klobus, and S. Robaszkiewicz, *Acta Phys. Pol. A* 118, 350 (2010);
K. Kapcia and S. Robaszkiewicz, *Acta Phys. Pol. A* 121, 1029 (2012).
13. T. Ayral, P. Werner, and S. Biermann, *Phys. Rev. Lett.* 109, 226401 (2012);
L. Huang, T. Ayral, S. Biermann, and P. Werner, *Phys. Rev. B* 90, 195114 (2014).

Mapping the spin-orbital texture of topological insulators in the energy, momentum spin and time domains.



Alessandra Lanzara

*Physics Department, University California, Berkeley
Materials Sciences Division, Lawrence Berkeley National Laboratory,
Berkeley*

The helical spin texture of surface electrons in topological insulator has attracted a great deal of interest in the past few years. Although this texture was predicted with the discovery of topological insulators and experimentally confirmed in few points in the momentum space, its full experimental verification has been non trivial because of the low efficiency of spin resolved experiments.

In this talk I will present new results on the spin texture in trivial and non-trivial topological insulators, obtained by using an innovative ultra-high efficiency spin-resolved photoemission instrument. Our results provide the first complete mapping of the spin texture both in momentum, energy spin and time space.

I will show that this texture can be fully manipulated by light and discuss the symmetry rules associated with it, revealing an intriguing relationship between the orbital and spin components and symmetry constriction.

I will finally extend the discussion to the time domain, presenting the first spin- time- and momentum mapping of a spin texture in any material, providing a compelling view of the co-evolution of surface states through a topological phase transition.

Poster Session

Detailed optical spectroscopy of the hybridization gap and the hidden order transition in high quality URu₂Si₂ single crystals



N. Bachar¹, D. Stricker¹, S. Muleady¹, J. A. Mydosh², Y. K. Huang³, D. van der Marel¹

¹ *Department of Quantum Matter Physics, University of Geneva, Switzerland*

² *Kamerlingh Onnes Laboratory, Leiden University, 2300RA Leiden, The Netherlands*

³ *Van der Waals-Zeeman Institute, University of Amsterdam, 1018XE Amsterdam, The Netherlands*

Email: * nimrod.bachar@unige.ch

Keywords: Heavy fermions, optical conductivity, hidden order

We measured the optical reflectivity of ac and ab -plane of high quality URu₂Si₂ single crystals. We demonstrate that the optical properties are very sensitive to strain in the sample surface, which may result from e.g. polishing. We obtained strain-free and stoichiometric ac-planes by vacuum annealing at 950°C, which allows measurement of the a-axis and c-axis optical conductivity. When the temperature is lowered below 75 K we observe a gradual reduction of the a-axis and c-axis optical conductivity in the frequency range from 10 to 50 meV, and a gradual emergence of interband transitions at 20 meV, which we interpret as a cross-over to a state where the narrow 5f bands become coherent. This temperature is higher than 30 K reported previously [1], as a result of aforementioned surface conditions. Below the hidden order transition at 17 K the low frequency optical conductivity shows two main components, namely a narrow (less than 1 meV) zero-frequency mode, and a fully gapped (6 meV) component. The spectral weight removed from the gapped region is transferred to the range just above the gap, which is reminiscent of a charge density wave. The gap size diminishes as a function of increasing temperature, and falls below the measured range as the hidden order temperature is approached from below. In contrast to recent reports [2,3] the optical conductivity just above the gap has a single-gap structure and the gap-feature is stronger, possibly due to higher homogeneity or cleaner surface conditions.

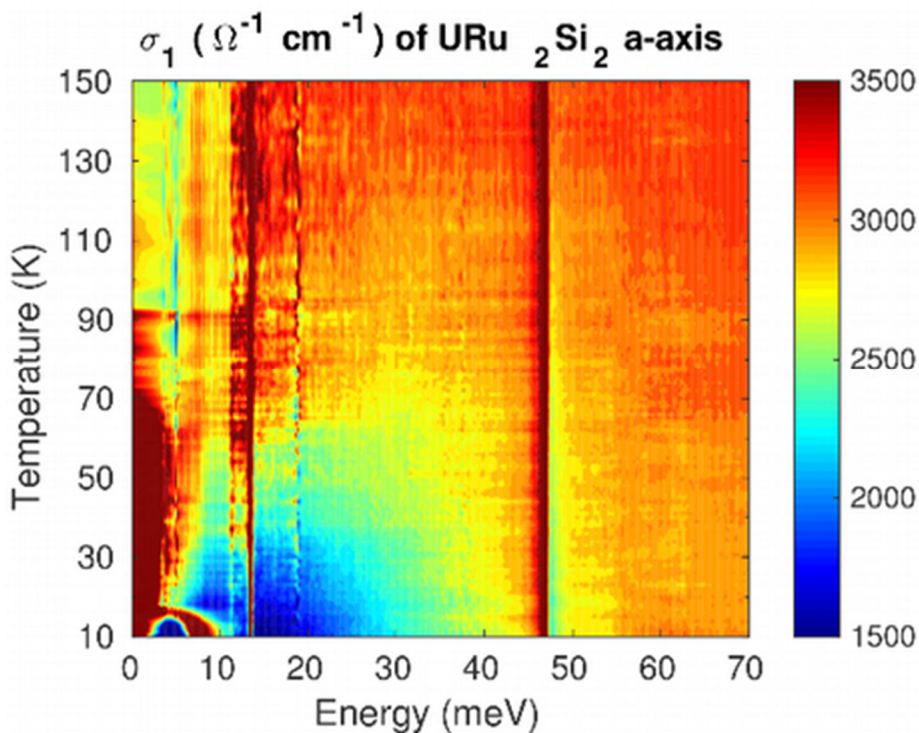


Figure 1: Real part of optical conductivity as a function of temperature and frequency in the a-axis of high quality URu₂Si₂ single crystal. A gradual reduction of the optical conductivity in the frequency range from 10 to 50 meV is observed below temperature of 75K. Opening of the hidden order gap is observed below 17K at the frequency of 6meV. The appearance of the bands hybridization and hidden order state are accompanied by the increase of the zero-frequency mode conductivity.

References

1. Levallois *et al.*, Phys. Rev. B **84**, 184420 (2011).
2. Hall *et al.*, Phys. Rev. B **86**, 035132 (2012).
3. Lobo *et al.*, Phys. Rev. B **92**, 045129 (2015).

BCS-Bose Crossover Extended with Hole Cooper Pairs



I. Chávez,^{1,*} L.A. García,¹ M. Grether,² M. de Llano.¹

¹*Instituto de Investigaciones en Materiales, Universidad Nacional Autónoma de México, 04510 Mexico City, MEXICO*

²*Facultad de Ciencias, Universidad Nacional Autónoma de México, 04510 Mexico City, MEXICO.*

Email: *israelito@ciencias.unam.mx

Keywords: high T_c ; BCS-Bose crossover; hole Cooper pairs

Within the generalized Bose-Einstein condensation (GBEC) formalism[1] we extend the BCS-Bose crossover[2] theory by adding hole Cooper pairs (2hCPs). From this we found a phase diagram[3] with two pure phases, one with 2hCPs and the other with electron Cooper pairs (2eCPs), plus a mixed phase with arbitrary proportions of 2eCPs and 2hCPs. One has a special-case phase when there is perfect symmetry (i.e., with ideal 50-50 proportions between 2eCPs and 2hCPs) and corresponds to usual BCS-Bose crossover. Explicitly including 2hCPs yields an *extended* BCS-Bose crossover which *predicts* T_c/T_F values for some well-known conventional superconductors (i.e., with electron-phonon dynamics) fitting reasonably well with experiment. To do this, we employ the BCS dimensionless coupling constant λ_{BCS} via the BCS gap equation and compare with the Bogoliubov upper limit[4] $\lambda_{\text{BCS}} \leq 1/2$.

The resulting phase diagram is shown below for the conventional superconductors mentioned, solving *two equations* for each phase; one gap-like equation and other for total number density of the system, these equations illustrates that the *extended* crossover theory *predicts* T_c/T_F vs the dimensionless charge-carrier number density $\Delta n \equiv n/n_f - 1$ where n is the total electron number density and $n_f \equiv n_f(T=0)$ the number density of unpaired electrons at zero temperature. In Figure 1 shows the experimental T_c/T_F (dots) associated with $\Delta n \neq 0$, i.e., with arbitrary proportions between 2e-CPs and 2h-CPs and is compared with theoretical curves associated with the extended crossover: i) the top pair of curves with $\lambda_{\text{BCS}} = 1/2$ (Bogoliubov upper limit) and ii) bottom pair of curves with $\lambda_{\text{BCS}} = 1/5$. The special case of perfect symmetry BCS-Bose holds at $\Delta n = 0$. The Inset table in Fig. 1 compares the experimental[5] T_c/T_F , BCS and the *extended* crossover theories. Here we used the BCS weak-coupling formula $T_c/T_F \approx 1.134(\hbar\omega_D/E_F)\exp(-1/\lambda_{\text{BCS}})$ (third column of Inset table) with $\hbar\omega_D$ the Debye energy and E_F the Fermi energy. Including 2hCPs enhances the critical temperature T_c by several orders of magnitude with respect to BCS.

Acknowledgment We thank G.C. Strinati for bringing first two papers in Ref.[2] to our attention.

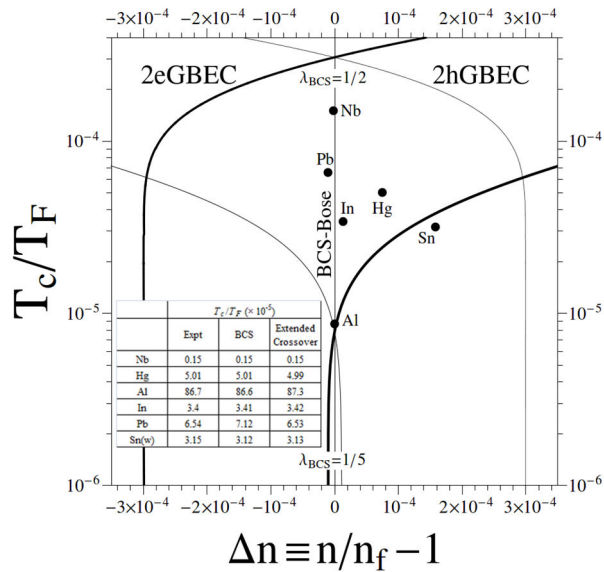


Figure 1: Phase diagram of the extendedBCS-Bose crossover theory for some familiar conventional superconductors, showing T_c/T_F vs $\Delta n \equiv n/n_f - 1$ where n is the total electron number density and $n_f \equiv n_f(T = 0)$ the number density of unpaired electrons at zero temperature. Thick curves refer to the pure phase of 2eCPs (here labeled 2eGBEC) and thin to a pure phase of 2hCPs (labeled 2hGBEC); blackdots locate experimental values[5] (second column of Inset table) of T_c/T_F are associated with $\Delta n \neq 0$. The T_c/T_F values of the *extended* crossover (fourth column in the Inset table) refer to perfect symmetry. Theoretical curves refer to $\lambda_{BCS}=1/2$ (Bogoliubov upper limit, top pair of curves) and $\lambda_{BCS}=1/5$ (bottom pair of curves). For theoretical curves with $\lambda_{BCS}=1/2$ we used $\hbar\omega_D/E_F = 0.002$ and for $\lambda_{BCS}=1/5$ we used $\hbar\omega_D/E_F = 0.001$.

References

1. V.V. Tolmachev, Phys. Lett. A **266**, 400 (2000); M. de Llano and V.V. Tolmachev, Physica A **317**, 546 (2003); M. de Llano and V.V. Tolmachev, Ukrainian J. Phys. **55**, 79 (2010); M. Grether, M. de Llano, and V.V. Tolmachev, Int. J. Quant. Chem. **112**, 3018 (2012)
2. L.V. Keldysh and Yu.V. Kopaev, Sov. Phys. Sol. State **6**, 2219 (1965); V.N. Popov, Sov. Phys. JETP **50**, 1034 (1966); J. Labbé, S. Barisic, and J. Friedel, Phys. Rev. Lett. **19**, 1039 (1967); D.M. Eagles, Phys. Rev. **186**, 456 (1969); A.J. Leggett, J. Phys. (Paris). Colloq. **41** C7-19 (1980); S.K. Adhikari, M. de Llano, F.J. Sevilla, M.A. Solís, and J.J. Valencia, Physica C **453**, 37 (2007)
3. I. Chávez, M. Grether, and M. de Llano, J. Supercond. and Novel Mag. **28**, 309 (2015)
4. N.N. Bogoliubov, Il Nuovo Cim. **3**, 794 (1958)
5. N.W. Ashcroft and N.D. Mermin, *Solid State Physics* (Saunders College Publishing, USA, 1976) pp. 38 and 729; C.P. Poole, Jr., H.A. Farah, R.J. Creswick and R. Prozorov, *Superconductivity* (Academic Press, Elsevier, New York, 2007) pp. 2-3 and 62

Onset of two-band superconductivity in superconducting-insulating superconducting tri-layer systems.



Mauro M. Doria^{1,2,3*}, Andrea Perali^{1,3}

¹*Dipartimento di Fisica, Università degli Studi di Camerino, Italy*

²*Instituto de Física, Universidade Federal do Rio de Janeiro, Brazil*

³*International MultiSuper Network*

Email: [*mauromdoria@gmail.com](mailto:mauromdoria@gmail.com)

web: <http://www.multisuper.org>

Keywords: shape resonance, thin film superconductor, Bogoliubov de Gennes equation

Since the pioneer work of Blatt and Thompson [1] more than fifty years ago thin film superconductors have been the subject of intense research in order to understand the effects of geometrical confinement in the superconducting state. Indeed lowering the dimensionality leads to shape resonances, namely, discontinuities in the density of states at the Fermi level caused by confinement to two-dimensional sub-bands and reconfiguration of the pairing interaction due to quantum size effects. Consequently interesting effects can occur in thin film superconductors, such as the dependence of the critical temperature according to the film thickness. This framework has been used as a model to understand high- T_c superconductors [2], as a super-lattice of quantum stripes, and as a model for the LaAlO_3 - SrTiO_3 interface [3]. To treat the discrete electronic levels defined by the geometrical confinement one needs to go beyond the standard BCS approach and consider the Bogoliubov de Gennes equations in order to cope with the series of two-dimensional sub-bands present in thin films. The simplest way to solve the Bogoliubov de Gennes equations is through the so-called Anderson approximation which assumes that the particle-like and hole-like quasiparticle wave functions are proportional to the single-electron wave functions. In this context we study here the superconducting-insulating-superconducting (SIS) tri-layer system. A thin layer of insulator is modelled through a repulsive delta function potential. This simple description is advantageous for the obtainment of analytical results describing the Cooper pair tunnelling between the two sides of the insulating barrier which are assumed to be symmetrical. As the condensate rests with the same phase in both sides, there is no supercurrent flowing from side to the other (Josephson effect). In this framework, we describe the shape resonances and the gap profile of the tri-layer system.

From this point of view the tri-layer is one of the simplest systems to naturally display multiband superconductivity because it can offer for special value of the potential barrier an absolute degeneracy between two energy sub-band levels. To understand it, consider the case where the chemical potential is such that only the lowest sub-band is occupied. Take the two extreme limits of the potential barrier, namely of no potential

barrier at all and of an infinite barrier. At a first glance these two limiting cases look alike with the only difference that in the former the film is twice as large as in the latter case. However a closer inspection reveals an important and fundamental difference: these two limiting cases are associated to distinct sub-bands. The fundamental state for the no barrier and for the infinite barrier cases corresponds to the symmetric and the anti-symmetric single-electron wave functions, respectively, as in the latter case the wave function must vanish at the insulating barrier. In conclusion, changing the potential barrier strength of a tri-layer system is a way to tune the two-band superconductivity. Here we report several properties of this superconducting-insulating-superconducting tri-layer system obtained in the framework of the Anderson approximation for the Bogoliubov de Gennes equations.

Mauro M.Doria acknowledges CNPq support from funding (014992/2015-39).

References

1. C. J. Thompson and J. M. Blatt, Phys. Lett. 5, 6 (1963); J. M. Blatt and C. J. Thompson, Phys. Rev. Lett. 10, 332 (1963).
2. A. Perali, A. Bianconi, A. Lanzara, and N. L. Saini, Solid State Commun. 100, 181 (1996).
3. A. Bianconi, D. Innocenti, A. Valletta and A. Perali, Journal of Physics: Conference Series 529, 012007 (2014).

Charge transfers and band dispersions in magnetic $\text{Nd}_{2-x}\text{Ce}_x\text{CuO}_4$

T. Jarlborg

DPMC, University of Geneva

CH-1211 Geneva 4, Switzerland

Email: *Thomas.jarlborg@unige.ch*

Keywords: high Tc, f-electrons, band structure

The electronic structure of Ce-doped $\text{Nd}_{2-x}\text{Ce}_x\text{CuO}_4$ (NCCO) is investigated through ab-initio density functional calculations for supercells. The effective electron doping, h , i.e. the additional electronic charge per Cu atom due to Ce doping, is found to be significantly smaller than x .

The explanation of this result is to be found in the hybridization of the CuO band with the Nd-f bands. This hybridization makes the Fermi surface break to occur at a larger k -vector than what is expected from the unhybridized band. The true band dispersion of the CuO band near E_F is different from what is seen in ARPES (1), which partly can be understood from calculations of relaxation energies in photoemission (2).

References

1. N.P. Armitage et al. Rev. Mod. Phys. 82, 2421, (2010).
2. T. Jarlborg et al. Phys. Rev. B 84, 045109(2011).

The interplay of long range interactions and electron density distributions in polar and strongly correlated materials

N. Kristoffel^{1*}, A. Pishtshev^{1**}, P. Rubin¹, M. Klopov²

¹*Institute of Physics, University of Tartu, Ravila 14c, 50411 Tartu, Estonia*

²*Department of Physics, Tallinn University of Technology, Ehitajate 5, 19086 Tallinn, Estonia*

Email: * kolja@ut.ee, ** aleksandr.pishtshev@ut.ee

Keywords: ferroelectrics, electron-phonon interaction, pnictides, multiband superconductivity

The dipole-active transverse optical (TO) vibrations play one of the key roles in polar and strongly correlated systems because they give rise the fundamental properties related to structural lattice instability, soft IR vibrational modes, dielectric function, etc. In the present contribution we summarize the recent theoretical results on the physics of the electron-TO-phonon (el-TO-ph) interaction in a number of actual materials. Within a first-principles microscopic approach, we show how to link the interaction of electrons with the long-wavelength TO phonons to the long-range dipole-dipole interaction. This interpretation establishes the fundamental macroscopic basis for the vibronic theory of ferroelectrics [1]. We suggest an universal parameterization of the el-TO-ph coupling compiled in terms of experimental material parameters, such as dipole oscillator strengths and a forbidden electronic gap. The parametrization provides us with a novel relation indicating how the dielectric behavior of the system is close to a ferroelectric instability. The relation may serve as a criterium especially useful in the applied context because it compares in the long-wavelength limit only three well-defined parameters: the zone-centre TO phonon frequency and its dipole oscillator strength as well as a dielectric constant. Further consideration is focused on an integrated analysis of charge, electronic and vibrational properties of iron-based narrow-gap systems FeAs₂ and FeSi. We show that similar to ferroelectrics there is a strong interplay of electronic and polarization degrees of freedom in these materials which is mediated by the dynamic hybridization [1] of the relevant frontier orbitals. Due to cooperative character of polarizable distortions of the electronic states there occurs a pairing channel of multiband origin that may provide an additional enhancement of superconductivity [2].

References

1. N. Kristoffel, P. Konsin, Phys. Status Solidi (b) 149 11 (1988)
2. N. Kristoffel, P. Rubin, J. Supercond. Nov. Magn. (2015). doi 10.1007/s10948-015-3321-1.

Effect of proton irradiation on the low-energy excitations of $\text{Ba}(\text{Fe}_{1-x}\text{Rh}_x)_2\text{As}_2$ superconductors



M. Moroni^{1*}, L. Bossoni^{1,2}, P. Carretta¹, M. H. Julien³,
H. Mayaffre³, P. C. Canfield⁴, W. P. Halperin⁵

¹*Department of Physics, University of Pavia, Italy*

²*Huygens-Kamerlingh Onnes Laboratory, Leiden University, The Netherlands*

³*Laboratoire National des Champs Magnetiques Intenses, CNRS, Grenoble, France*

⁴*Ames Laboratory US DOE, Iowa State University, Ames, Iowa, USA*

⁵*Department of Physics and Astronomy, Northwestern University,*

Evanston, Illinois, USA

Email: *matteo.moroni01@universitadipavia.it

Keywords: nematic phase, domain wall dynamics, proton irradiation

The understanding of normal phase excitations is a fundamental step towards the comprehension of the exotic pairing mechanisms at work in iron-based superconductors. In $\text{Ba}(\text{Fe}_{1-x}\text{Rh}_x)_2\text{As}_2$ Nuclear Magnetic Resonance (NMR) experiments reveal a marked increase of $1/T_2$ upon cooling already above T_c , suggesting the onset of unconventional very low-frequency activated dynamics [1,2]. By combining different spin-echo techniques, we demonstrated that the low-temperature increase in the transverse relaxation rate $1/T_2$ originates from an activated slowing down of the fluctuations rather than from an increase of their amplitude. Strikingly the correlation time derived by the $1/T_2$ measurement also accounts for the behavior of the spin lattice relaxation rate. We argue that these dynamics can be associated with activated motions of domain walls separating regions where $(\pi/a, 0)$ and $(0, \pi/a)$ nematic correlations develop.

Further insights on the nature of the fluctuations can be gained by studying the effect of proton irradiation (5.5 MeV protons, $3.2 \times 10^{16} \text{ cm}^{-2}$ and $6.4 \times 10^{16} \text{ cm}^{-2}$, total dose) on these systems. It was found that while T_c weakly changes by increasing the fluence [3], T^* , the characteristic temperature at which $1/T_2$ begins to increase, is markedly suppressed, suggesting that the proton induced defects are pinning the domain walls motions [4]. Even more interestingly, in the optimally doped $x=6.8\%$ sample, the NMR line width significantly increases with the fluence and its Curie Weiss temperature behavior indicates the onset of ferromagnetic correlations coexisting with superconductivity at the nanoscopic level.

References

1. L. Bossoni et al, Phys. Rev. B 88, 100503(R) (2013)
2. L. Bossoni et al, in preparation
3. Y. Nakajima et al, Phys. Rev. B Phys. Rev. B 82, 220504(R)
4. M. Moroni et al, in preparation

Syntheses and characterization of superconducting metal-doped LaOBiS₂



Saki Nishiyama^{1*}, Eri Uesugi¹, Hidenori Goto¹, Ritsuko Eguchi¹, Yoshihiro Kubozono^{1,2}

¹Research Laboratory for Surface Science, Okayama University, Okayama 700-8530, Japan

²Research Center of New Functional Materials for Energy Production, Storage and Transport, Okayama University, Okayama 700-8530, Japan

Email: * pjj24b1k@s.okayama-u.ac.jp

Keywords: superconductor, LaOBiS₂, two-dimensional layered material

LnOBiS₂ (Ln: lanthanide atoms) is one of two-dimensional layered materials. This material consists of conducting BiS₂ and insulating LnO layers. The superconductivity emerges in the LnO_{1-x}F_xBiS₂ material, in which O is partially replaced by F atom, owing to an electron-doping to BiS₂ layer [1]. In this study, we intercalated the metal atoms into LnOBiS₂ to induce the superconductivity. Since this method should donate electrons to BiS₂ layer, the superconductivity may be produced without any substitution of O atom.

The alkali-metal atoms were intercalated into LaOBiS₂ and CeOBiS₂ using liquid NH₃ technique. K_xLaOBiS₂ and Rb_xLaOBiS₂ showed the superconductivity with the superconducting transition temperature, T_c , as high as 3.7 K and 4.3 K, respectively. The shielding fraction was 12 and 10%, respectively, for the former and latter materials. The electric transport and magnetic behaviors were fully investigated for the metal-doped LnOBiS₂ under a wide pressure range. The crystal structures of these materials were investigated by powder X-ray diffraction.

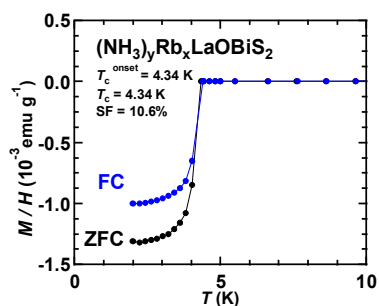


Figure 1: Temperature dependence of magnetic susceptibility in $(\text{NH}_3)_y\text{Rb}_x\text{LaOBiS}_2$.

References

1. Y. Mizuguchi et al., J. Phys. Soc. Jap. **81**, 114725 (2012)

Author Index

Adachi T.....	224
Aeppli G.....	235
Akashi R.....	310
Anahory Y.....	31
Andersen B. M.....	143
Annett J.....	237
Argyrou D. N.....	164
Arita R.....	297
Babaev E.....	33
Bachar N.....	204; 366
Baeriswyl D.....	321
Balakirev F.F.....	123
Balicas L.....	358
Bao W.....	341
Barbiellini B.....	323
Barisic N.....	261
Baron A. Q. R.....	62
Baturina T.....	345
Bauch T.....	55
Berciu M.....	288
Bianconi A.....	299
Bill A.....	206
Billinge S.J.L.....	156
Bonca J.....	312
Borisenko S.....	23
Bothschafter E.....	327
Bourges P.....	314
Bovensiepen U.....	72
Bozin S.....	160
Brazovskii S.....	200
Brinkman A.....	126
Brzezicki W.....	333
Bussmann-Holder A.....	302
Capone M.....	136
Caprara S.....	306
Carbone F.....	274
Chavez I.....	368
Conradson S.....	17
ContinentinoM. A.....	256
Cren T.....	218
Ćwik J.....	96
De Llano M.....	186
de Mello E.....	34
De Padova P.....	279
Dean M.....	158

Degiorgi L.	138
Dessau D.	214
Devereaux T.	236
Dobrosavljevic V.	258
Doria M.	183; 370
Eckstein M.	74
Efetov K.	66
Efremov D.	147
Egami T.	170
Eremets M.	291
Eremin I.	320
Eremin M.	64
Fatuzzo G.	122
Felner I.	318
Feng S.	216
Fine B.	125
Fink J.	162
Freeman P.G.	129
Freericks J.	75
Fujimori A.	111
Fujiwara N.	220
Gajda D.	153
Garcia-Garcia A. M.	81
Gastiasoro M.	145
Geck J.	52
Giraldo-Gallo P.	241
Glatz A.	166
Goncharov A. F.	294
Gray A.	20
Greene L. H.	234
Grinenko V.	289
Haase J.	195
Hackl r.	202
Hardy F.	208
Harrison N.	168
He S.	280
Hennel S.	251
Honercamp C.	140
Huang Z.	267
Iavarone M.	215
Inoue I. H.	222
Ishihara S.	77
Iwasawa H.	308
Jarlborg T.	372
Johnson R. D.	108
Joseph B.	339
Kaindl A.	335

Kanazawa I.....	69
Kanigel A.....	309
Kapcia K. J.....	362
Kartsovnik M. V.....	269
Kataev V.....	266
Katrych S.....	141
Keller H.....	19
Keren A.....	344
Khalyavin D. D.....	105
Khomskii D. I.....	238
Kirova N.....	151
Kontani H.....	28
Korshunov M. M.....	148
Kristoffel N.....	373
Krüger F.....	262
Ksenofontov V.....	42
Kubozono Y.....	135
Kuzmicheva T.....	190
Lanzara A.....	364
Lawler M. J.....	239
LeBoeuf D.....	58
Lemberger T. R.....	228
Li W.H.....	94
Liarokapis E.....	60
Lichtenstein A.....	260
Linscheid A.....	180
Lorenzana J.....	79
Luetkens H.....	44
Machida K.....	197
Mackenzie.....	131
Madan I.....	83
Maggio-Aprile I.....	240
Maier T.....	178
Manske D.....	210
Manuel P.....	106
Markovic N.....	98
Marsiglio M.....	304
Massarotti D.....	277
Mazzoli C.....	355
Menushenkov A. P.....	13
Mertelj T.....	85
Micnas R.....	182
Mihailovic D.....	70
Miletto Granozio F.....	278
Mironov Y.....	347
Moewes A.....	245
Moreo A.....	25

Moroni M.	374
Moskvin A.S.	102
Mukhin S. I.	286
Mustre de Leon J.	46
Nakagawa K.	337
Neilson D.	40
Nishiyama S.	375
Nissinen J.	217
Oda M.	59
Oles A.M.	316
Ord T.	189
Orgad D.	315
Ovchinnikov S.	26
Pan S. H.	173
Pelc D.	247
Pellicciari J.	50
Perali A.	176
Perfetti L.	89
Perring T.	36
Phillips P.	27
Ponomarenko L. A.	349
Popovic D.	254
Prassides K.	16
Pudalov V. M.	174
Pupillo G.	188
Purans J.	155
Puzniak R.	356
Qiu XG.	104
Quader K.	325
Radzihovsky L.	15
Renner Ch.	119
Reznik D.	120
Ricci A.	243
Ronnow H. M.	54
Salasnich L.	185
Samuely P.	276
Sanna S.	48
Schneider W.D.	283; 331
Schopohl N.	253
Seibold G.	124
Shen Dawei	230
Shengelaya A.	199
Shi Ming.	132
Shimizu K.	296
Simon P.	285
Soh Y. A.	231
Spivak B.	248

Stojchevska L.	87
Stornaiuolo D.	281
Streltsov S.	213
Strinati G.	118
Sunko D.	212
Sushkov P.	360
Szabo P.	101
Tabis W.	273
Tagliacozzo A.	353
Tajima S.	113
Takahashi H.	133
Tanner D. B.	115
Teitelbaum G.	30
Terashima.	271
Tohyama T.	68
Tokunaga Y.	264
Tortello M.	192
Tranquada J. M.	232
Tsuchiya S.	91
Turner P.	147; 329
Uemura Y.	172
Vargunin A.	194
Vinokourn V. M.	21
van der Marel D.	57
Wang N. L.	130
Watanabe T.	109
Wirth S.	38
Wu Shang-Yu.	150
Wysokiński K.	361
Yanagisawa T.	226
Yukalov I.	152
Zaikin A. D.	100
Zheng G.Q.	305
Zhigadlo N.	249
Zhou Si.	351
Zocco D.	127